Westinghouse Non-Proprietary Class 3

WCAP-16170-NP
Revision 0

November 2003

Diablo Canyon SG Alternate Repair Criteria Based On Limited Tube Support Plate Displacement

WCAP-16170-NP

Diablo Canyon SG
Alternate Repair Criteria
Based On Limited Tube Support Plate Displacement

November 2003

Westinghouse Electric Company LLC
P.O. Box 355
Pittsburgh, PA 15230-0355

© 2003 Westinghouse Electric Company LLC
All Rights Reserved

TABLE OF CONTENTS

LIST OF TABLES

LIST OF FIGURES

1.0 INTRODUCTION

This report provides technical support for implementing alternate repair criteria (ARC) for axial outside diameter stress corrosion cracking (ODSCC) based upon tube expansion at tube support plate (TSP) intersections for Westinghouse Model 51 steam generators (SGs) at the Diablo Canyon Power Plant (DCPP) Units 1 and 2 steam generators. The tube expansions to obtain mechanical locking of the TSPs provide a defense in depth or redundant backup to the locking provided by the dented and packed crevices in the DCPP SGs. Limited TSP displacements based on tube expansion are applied for hot leg TSPs 1-4 for DCPP and a 4.0 volt ARC is applied at these intersections. For hot leg TSPs 5-7 and all cold leg TSPs, the current 2.0 volt ARC is retained for ODSCC at these intersections.

With tube expansion, TSP displacements in a steam line break (SLB) event are limited to negligible levels and the axial tube burst probability is thereby also reduced to negligible levels. For very large bobbin voltage indications with a cellular corrosion morphology, it is possible for the axial pressure loads on the tube to cause axial tensile tearing of the indications. This condition establishes the structural limit for voltage repair limits and, based on current data, this limit is developed in this report and shown to be much higher than any indications reasonably expected at DCPP for the 4.0-volt repair limit recommended in this report. Thus any potential need for tube repair at < 4.0 volts at TSPs 1-4 with tube expansion would be primarily determined by the requirement to limit accident condition leakage to acceptable levels.

The evaluations of this report include hydraulic SLB analyses to obtain the time dependent pressure drop loads on the TSPs (Section 4). Analyses of a postulated SLB initiating from full power and from Hot Standby conditions were performed to determine the most conservative loads. Comparisons of RELAP5 and TRAC-M analyses of Model 51 steam generators are presented, along with studies to define the sensitivity of the loads to various modeling and computational options. For conservatism in the tube expansion design and supporting analyses, a factor of 1.5 increase in the RELAP5 code loads is applied to envelope the results of load sensitivity evaluations.

Structural analyses that apply the hydraulic loads to determine the tube locations requiring expansion to limit TSP displacements to acceptable levels are presented in Section 5. These analyses utilize the expansion joint stiffness demonstrated by the process development tests, Section 6. The structural model is specific to the DCPP steam generators, and accounts for the design features that provide support to the TSPs.

Section 6 provides the tube expansion process requirements, description, and supporting test and analysis results. A hydraulic expansion process with a sleeve stabilizer is applied to implement the required expansions at TSP intersections. This section provides the results of testing to determine the load capabilities of the expanded joints. Also included is an assessment of the potential for circumferential cracking in the expanded tubes in their plugged tube condition and considerations of TSP integrity for application of the expansion process.

Section 7 summarizes the results of tests to determine the leak rate for indications restricted from burst (IRB), that is, tube flaws that are constrained within the span of the TSPs. The IRB leak rate test data provide a bounding leak rate for indications at TSP intersections that would be predicted to be sufficiently large that they would burst if they occurred in the freespan of the tube, based on the ARC freespan burst

correlation. The limit of applicability for the IRB bounding leak rate, with respect to TSP displacement during a postulated SLB, is also presented based on the test data.

The analysis methods for SLB leak rate and tube burst probability assessments given in Section 3 are consistent with the requirements of NRC GL 95-05. An extension of the leak rate methodology is included for potentially overpressurized indications within the confines of the TSP (an IRB) and for leakage associated with potential free span bursts. This section also includes development of the voltage structural limit and burst probability for axial tensile tearing as the applicable structural limit with tube expansion. The GL 95-05 burst probability methodology is also extended to include potential axial rupture for indications within TSPs 1-4 with limited TSP displacement and increased voltage repair limits.

Because the predicted tube displacements depend on structural features such as tierods and wedges to support the TSPs, an inspection plan to verify the integrity of these features is presented in Section 9. This section also summarizes prior DCPP inspections performed on secondary side components including NDE analyses for tube support plate cracking.

The requirements on limiting TSP displacements to obtain negligible tube burst probabilities are developed in Section 10. This section integrates the analyses and tests performed, as presented in the prior report sections, to develop the alternate repair criteria with tube expansion for DCPP Units 1 and 2. Inspection and SLB analysis requirements are also given in Section 10.

2.0 SUMMARY AND CONCLUSIONS

This report documents the technical support for Alternate Repair Criteria with tube expansion at selected TSP intersections to limit TSP displacements in a SLB event for the Model 51 SGs at Diablo Canyon Units 1 and 2. A 4.0 volt ARC repair limit is proposed for hot leg TSPs 1-4 intersections and a 2.0 volt repair limit, according to the guidelines of GL 95-05, is proposed for hot leg TSPs 5-7 and for all cold leg TSP intersections. Mechanical locking of the TSPs by performing tube expansion at selected TSP intersections will be performed to ensure a locking mechanism is provided for the TSPs even though it has been shown in Reference 1 that the DCPP dented and packed tube to TSP crevices lead to tube to TSP contact forces sufficient to prevent significant TSP displacements in a SLB event. In fact, the DCPP crevice conditions would be able to prevent TSP displacement even if less than one percent of the TSPs (same percentage as will be expanded) have the expected contact forces. Reference 1 also shows that leakage would be negligible with the dented and packed crevices due to constraints on opening of the cracks with no tube to TSP gap. Despite the presence of the packed TSP condition at DCPP, the mechanical locking for TSPs 1-4 is provided under the very conservative assumptions of 100% open crevices to define the tube expansion requirements and that the crevices are open near the upper end of the original SG design clearances for leakage analyses.

The overall conclusions and recommendations for the ARC, and a summary of the technical basis for the ARC as presented in this report are provided in this section.

2.1 OVERALL CONCLUSIONS

Although TSP displacements up to 0.362 inch are adequate to restrict the total axial tube burst probabilities to a negligible 10^{-5} for TSPs 1-4 during a postulated SLB event, the tube expansion modification has been designed to obtain maximum TSP displacements of $\leq$ 0.15 inch with an associated tube burst probability of $<10^{-10}$ for a single throughwall indication extending outside the TSP. The 10^{-5} bounding tube burst probability has been obtained by the extremely conservative assumption that all hot leg TSPs 1-4 intersections have throughwall cracks exposed by the TSP displacements. Negligible TSP displacements for hot leg TSPs 1-4 are achieved with tube expansion by hydraulically expanding 30 tubes at 196 TSP intersections including some tubes with expansions at all hot and cold leg TSP intersections. The expansions at selected hot leg TSPs above TSP 4 and cold leg TSPs are included to limit the displacements at hot leg TSPs 1-4 considering interaction of the displacements between TSPs and to maintain existing tierod stresses within elastic limits. A sleeve stabilizer is expanded with the parent tube and functions to increase the stiffness of the expansion against TSP motion and to capture a severed tube end under the very conservative assumption that a circumferential crack at the parent tube expansion caused the tube to sever.

Since axial tube burst probabilities are negligibly small with tube expansion, repair limits to preclude burst at hot leg TSPs 1-4 are not required and tube repair requirements may be primarily based on limiting accident condition leakage to acceptable levels. At very high voltage levels for crack morphologies that include cellular corrosion, it is possible that the axial pressure loads on the tube could cause tensile tearing of an indication. This limit represents the structural limit applicable with tube expansion and, based on available data, is estimated to exceed 100 volts at the lower 95% confidence level for a $3\Delta P_{NO}$ structural margin guideline. Although voltage repair limits at least as high as 50 volts are justifiable with tube expansion, a 4.0 volt repair limit is proposed for the hot leg TSP intersections at DCPP Units 1 and 2.

For hot leg TSPs 5-7 and cold leg TSP intersections, the voltage repair limit is 2.0 volt, consistent with the requirements of GL 95-05 and the currently licensed ARC at DCPP.

For the postulated SLB event initiated from hot standby conditions, the required tube expansion matrix includes 30 tube locations with a total of 196 expansions to limit the TSP displacement to < 0.15 inch at all hot leg TSPs 1-4. The tube expansion matrix given in Table 2-1 identifies specific tubes for expansion, however, plant specific tubes can be selected from the nearby locations shown as darkened tube locations in Figures 2-1 and 2-2 for the hot and cold legs.

The inspection requirements with tube expansion are essentially the same as required for ARC inspections without tube expansion although supplemental inspections for expanded tubes are required as described in Section 2.2.8 below.

2.2 SUMMARY

2.2.1 Overall Approach to Tube Expansion ARC for DCPP Units 1 and 2

The approach applied to develop the tube expansion ARC is to:

- Define acceptable TSP displacements to achieve a negligible tube burst probability (a value of 10^{-5} is considered negligibly small compared to the NRC GL 95-05 reporting guideline of 10^{-2}).
- Utilize conservative SLB hydraulic loads on the TSPs (a 1.5 margin on the expected loads obtained from the RELAP5 code is used to envelope uncertainties).
- Limit TSP displacements to less than the displacements tested in the Indications Restricted from Burst (IRB) tests in order to utilize the bounding leak rate test results from these tests.
- Perform tests of prototypic TSP expansions to determine the required expansion diameter and the joint stiffness for the minimum required expansion diameter.
- Determine by structural analyses, the number and location of tubes for expansion to meet the TSP displacement goals.
- Expand the tubes at the TSP intersections determined by the structural analyses to be required to limit TSP displacements and confirm by NDE inspection that the minimum required expansion diameters have been achieved.

2.2.2 TSP Displacement for Negligible Probability of Burst

To obtain a negligible probability of burst, an acceptable TSP displacement of ≤ 0.362 inch was very conservatively developed by a) assuming that all TSPs 1-4 are uniformly displaced and b) by making the bounding assumption that these displacements exposed throughwall cracks at all hot leg TSPs 1-4 intersections (13,552 throughwall indications). At a uniform TSP displacement of 0.362 inch, the total probability of burst for a steam generator at a Δp of 2405 psi is less than 10^{-5}, which is negligibly small compared to the conservative limit on probability of burst of 10^{-2} given in NRC GL 95-05 for ODSCC at

the TSPs. Assuming a factor of 1.5 on the transient loads calculated using RELAP5 to envelope modeling and calculation uncertainties, expansions in 30 tubes results in maximum TSP displacements < 0.15 inch for all tube locations at all hot leg TSPs 1-4 for a SLB event initiated from hot standby conditions. At the goal TSP displacement of 0.15 inch, the probability of burst is significantly less than 10^{-10} for a single tube. Section 8 provides the basis for the probability of burst evaluations.

2.2.3 TSP Displacement to Utilize IRB Leak Rate Test Results

High temperature leak rate tests were performed to determine the leak rates for indications restricted from burst (IRB). Section 7 summarizes these tests. The bounding leak rate for the DCPP SLB pressure differential of 2405 psi, based on the PORVs for pressure relief, is 5.0 gpm. The bounding leak rate is based on tests with offsets (TSP displacements) up to 0.21 inch. The goal TSP displacement for the DCPP ARC was set at 0.15 to provide additional conservatism for the acceptable displacement of 0.21 inch for utilization of the IRB leak rate.

2.2.4 Tube Expansion Joint Process and Capabilities

The tube expansion at the TSPs is performed by a hydraulic expansion process that expands the parent tube and a sleeve stabilizer at the same time. Expansions are performed below and above each TSP intersection that requires expansion. The design requirement for the tube expansion process, as developed to restrain TSP displacement, is a minimum expanded tube stiffness of [ ]^{a,c,e}. The process development tests (Section 6) show that an expanded tube minimum diameter increase of [ ]^{a,c,e} provides a stiffness exceeding the required tube stiffness . The sleeve stabilizer expanded with the parent tube increases the expansion stiffness at a given diametral expansion and prevents lateral motion or adjacent tube damage for a postulated severed expansion. The design target range of [ ]^{a,c,e} for the expansion process leads to a low likelihood of circumferential crack at the bulges as described in Section 6.10. Axial cracking at the expansions also has a low likelihood of occurrence, but even if they do occur, they would not significantly affect the bulge stiffness since TSP displacements must compress or attempt to flatten the bulge (i.e., extrude the bulge) for which the required forces would not be significantly influenced by an axial crack in the bulge. After expansion of a tube in the field, bobbin coil profilometry is used to confirm that acceptable expanded tube diameters have been achieved and that the expansions are properly located relative to the TSP.

2.2.5 Hydraulic Load Analyses

Hydraulic loads on the TSPs for application to the TSP displacement analyses were obtained using the RELAP5 code for which the hydraulic loads bound those obtained using the TRAC-M code. The analyses show that the TSP loads are higher for a SLB event at hot standby operating conditions than for full power conditions. The hot standby loads are used for the tube expansion design even though only a small fraction of the operating cycle is spent at hot standby conditions. The reference hot standby loads are based on use of test-based support plate loss coefficients. The test-based loss coefficients generally compare well with, and are more conservative than, calculated loss coefficients. The RELAP5 modeling and analysis of the steam generators are discussed in Section 4.

Sensitivity analyses were performed to assess the dependence of the TSP loads on modeling and analysis uncertainties. When the potential modeling uncertainties or analysis options that could increase the TSP

hydraulic loads over the reference or expected base case results are combined, the TSP loads can be bounded by a factor of 1.5 increase over the reference loads. This factor of 1.5 increase on the reference hot standby loads was applied to obtain the design basis loads for tube expansion. Thus, the applied hydraulic loads are conservative.

2.2.6 Tube Locations and TSP Elevations Requiring Tube Expansion

The tube expansion length extends both above and below the tube support plates in order to permit the expanded tubes to act as additional supports, retarding the vertical displacement of the plates. The number and location of the tube expansions is expected to vary from plate to plate depending on the magnitude of the applied pressure loading. The TSP displacement analysis involves the preparation of a 180° tube bundle model that includes both the hot and cold leg sides of the tube bundle, consisting of the seven tube support plates, tierods, spacers, channel head, lower shell, wrapper, and tubesheet. Elements are also included to represent the expanded tubes and the expansion zone interfaces between the tubes and support plates. The WECAN computer code, a general purpose finite element code, is used to develop the model. It is the relative tube to support plate displacement that is of interest, with the tube and plate positions at the start of the SLB transient defined as the reference position. At hot standby, the TSP positions relative to cracks inside the TSP are essentially the same as at cold shutdown. SG cold condition inspections show outside stress corrosion cracks within the non-dented TSP with a trend towards being centered within the TSP. Therefore, the cold condition TSP location relative to the tubes is essentially the same as for the full power condition where the cracks formed, which is also the position during hot shutdown. These inspections indicate that there is little relative movement between the tubes and plates throughout the operating cycle. Thus, this analysis calculates relative tube/TSP motions based on the tube to plate positions at the initiation of the SLB transient. The dynamic analysis is performed assuming elastic response of the plate support structures. In order to support the displacement results, calculations are performed to demonstrate the applicability of the elastic analysis approach in determining the resulting displacements. These calculations consist of showing that the tierods/spacers remain elastic throughout the transient, that the expanded tubes remain elastic, that significant yielding of the tube support plates does not occur, and that the welds joining the vertical bars to the wrapper remain intact.

Based on the results of Section 5, the tubes summarized in Table 2-1 are concluded to provide sufficient support to limit relative tube to TSP displacement under SLB loads for the hot leg region of TSPs 1-4 to less than 0.150 inch. In addition, the stresses in the supporting structures for the tube support plates, and for the tube support plates themselves, are consistent with elastic analysis methodologies used to calculate the plate displacements.

2.2.7 Tube Repair Limits

Since tube expansion at TSPs 1-4 eliminates axial tube burst as a credible event at all TSP locations, guidelines for structural margins are inherently satisfied by the TSP constraint at both normal operating and accident conditions including a postulated SLB event. Consequently, tube repair limits are not required to satisfy tube burst margins, and tube repair would be required only as necessary to satisfy allowable leakage limits. At very high bobbin voltages corresponding to relatively large ODSCC indications compared to the GL-95-05 2 volt repair limit for 7/8 inch tubing, a structural limit based on axial tensile tearing of indications with cellular corrosion becomes applicable for the axial pressure differentials across the tube. Available pulled tube and laboratory specimen data on axial tensile tests

were used to estimate the tensile tearing structural limit. Based on a regression analysis of the axial rupture force to bobbin voltage, the tensile structural limit at the lower 95% confidence bound on the data, as adjusted for lower tolerance limit material properties at operating temperatures, is greater than 100 volts. With a conservative factor of two allowance for crack growth and NDE uncertainties (a factor of 1.5 to 1.75 is typical based on the ARC experience), the full ARC repair limit for tube expansion would be about 50 volts.

For DCPP, a tube repair limit of > 4.0 volts is conservatively applied for the hot leg TSPs 1-4 intersections. Bobbin voltage indications ≤ 4.0 volts can be left in service independent of RPC (or equivalent probe) confirmation as a flaw indication. Bobbin indications > 4.0 volts are repaired independent of RPC confirmation. For indications at hot leg TSPs 5-7 and at cold leg TSP intersections for which the limited TSP displacement ARC is not applied, the 2.0 volt tube repair limit for 7/8 inch diameter tubing is applied for the DCPP steam generators, consistent with NRC GL 95-05.

2.2.8 Inspection Requirements

The steam generator tube inspection requirements for applying the tube repair limits of this report are the same as those required by the NRC GL 95-05 with adjustment of the RPC inspection requirements for hot leg TSP intersections to reflect the higher tube repair limits with tube expansion. All hot leg TSPs 1-4 intersections with bobbin voltages > 4.0 volts will be inspected with an RPC (or equivalent) probe. In addition, a minimum sample inspection of 100 intersections with bobbin indications ≤ 4.0 volts will be applied at hot leg plates 1-4. The GL95-05 2-volt RPC threshold is applied for the TSPs 5-7 and cold leg TSP intersections. The RPC data shall be evaluated to confirm responses typical of ODSCC within the confines of the TSP. If one or more ODSCC indications at TSP intersections are found in the NDE inspection to extend beyond the edge of the TSP, the indications shall be evaluated for significance to safety and risk, and the results reported to the NRC prior to restart.

Additional inspections required for implementation and monitoring of expanded tubes include:

- Tubes selected for expansion will be inspected prior to performing the expansions. The selected tubes must have no circumferential indications in the WEXTEX expansion transition or W* length by +Point inspection. Any dented TSP intersections requiring expansion must have less than five volt dents and must be +Point inspected to confirm the absence of circumferential indications. TSP intersections requiring expansion must have no indications of TSP ligament cracking by the current bobbin inspection or historical database. TSP intersections requiring expansion must have bobbin coil voltages less than 2 volts for ODSCC or 3 volts for PWSCC and the indications must be confirmed by +Point inspection to be contained within the TSP.

- The TSP expansions in each of the expanded tubes will be inspected to verify that the minimum tube expansion has been achieved. Using bobbin coil profilometry, the inspection must confirm that an expansion diameter increase of [ ]^{a,c,e} has been achieved above and below the TSP.

- Following the expansion process, 100% of the expanded tubes in all four SGs will be +Point inspected at the TTS. If circumferential indications are found at the TTS in the expanded tubes, the potential need to expand additional tubes will be evaluated and the results of this evaluation reported

to the NRC prior to restart. The bases for not performing a +Point inspection of the expanded TSP intersections at this time are described in Section 10.5.3.

- If the SGS are not to be replaced at the outage following two complete cycles of operation after implementation of the locked TSP ARC, 20% of the TTS and expanded TSP locations in all four SGs will be +Point inspected. If circumferential indications greater than 100° are found at the TTS or above/below the tube support plate edges at TSP locations, the inspection will be expanded to 100% in any SG for which a circumferential indication >100° is found. The 100° crack size is less than the predicted near throughwall length for undetected circumferential indications left in the expanded tubes after two cycles of operation assuming growth rates for active tubes. If circumferential indications are found in the expanded tubes, the potential need for corrective actions will be evaluated and the results of this evaluation reported to the NRC prior to restart.

The minimum eddy current inspection of TSP ligaments at each scheduled outage shall include 100% bobbin coil with +Point confirmation for new bobbin calls and a 20% +Point inspection of TSP ligament indications previously confirmed by +Point inspections. The inspection of active tubes adjacent to expanded tubes shall include a bobbin coil examination for cracked TSP ligaments at expanded tube TSP intersections.

2.2.9 SLB Analyses

The SLB leakage and burst requirements for the NRC licensed 2.0 volt repair limit at DCPP per GL 95-05 continue to apply for implementation of the limited TSP displacement ARC with the following modifications:

- SLB leak rates evaluated as free span indications (Reference 2), except as modified by the provisions for leakage from indications restrained from burst (IRBs) at TSPs 1-4, shall be compared to the DCPP allowable SLB leakage limits for constrained indications. The freespan leak rate analyses shall include a large leak rate assigned to indications predicted to burst in a Monte Carlo simulation for the analyses. The sum of SLB leak rates from all DCPP ARCs shall satisfy the DCPP leakage limit.

- The SLB axial tube burst probability for cold leg TSP intersections and hot leg intersections at TSPs 5-7 when combined with the axial tube rupture probability for TSPs 1-4 shall be compared to the reporting value of 10^{-2} when summed with other DCPP ARCs. Due to the negligible burst probability for axial ODSCC indications at TSPs 1-4, analyses for axial burst are not required for these TSP intersections.

The leakage calculations for TSPs 1-4 include modifications to the freespan leak rate calculations to account for potentially overpressurized hot leg indications. The probability of an overpressurized condition is defined as the probability of a free span burst. With overpressurization, the flanks of the crack face can open until contact is made with the inside surface of the tube hole in the TSP. For this condition, the bounding IRB leak rate can be assigned to the leak rates associated with the overpressurized indications.

2.2.10 Steam Generator Internals Inspection

In addition to inspection of the tubes, inspection of the SG internals components is also necessary to verify the integrity of the structure to prevent TSP displacement greater than the results of the TSP displacement analysis. Section 9 provides the inspection plan for the SG structural components. Sampling visual inspections of the TSPs, tierods, wedges and support bars that support the TSPs will be performed to the extent that access to these components is available and radiation exposure and risk of foreign objects in the SG permit. The TSPs will be 100% inspected by EC to verify the absence of unacceptable TSP cracking. A sample of TSP wedges, support bars, tierods, spacers and nuts will be inspected in one of the SGs. These inspection, along with the results of prior inspections in both Units 1 and 2 will be used to verify the structural integrity of the SG internals to support the tube expansion ARC.

2.2.11 NRC Concerns Identified in South Texas-2 SER Affecting ARC Approval for More than One Cycle

In Section 2.5 of the safety evaluation for the South Texas 2 locked TSP ARC, the NRC identified six items that should be addressed before approval of the ARC for more than one cycle of operation. The six items, as summarized below, are addressed in Section 10 of this report.

a) The long term integrity and inspection of the SG internals, including the TSPs

b) The long term integrity and inspection plans of the expanded tubes

c) Combining the conditional probability of axial burst and axial tensile failures

d) The long term acceptability of the IRB leakage estimates

e) The effects on burst pressure of multiple indications extending outside the TSP

f) The methodology for combining the leakage estimates from the free span model and locked TSP model

2.2.12 References

1. WCAP-14707; "Model 51 Steam Generator Limited Tube Support Plate Displacement Analysis for Dented or Packed tube to Tube Support Plate Crevices," August 1996.

2. WCAP-14277; "SLB Leak Rate and Tube Burst Probability Analysis Methods for ODSCC at TSP Intersections;" (Rev 1), December 1996.

Table 2-1
Summary of Tube Expansion Locations

a,c

[ ]

a,c

Figure 2-1
Candidate Tubes for Expansion - Hot Leg

a,c

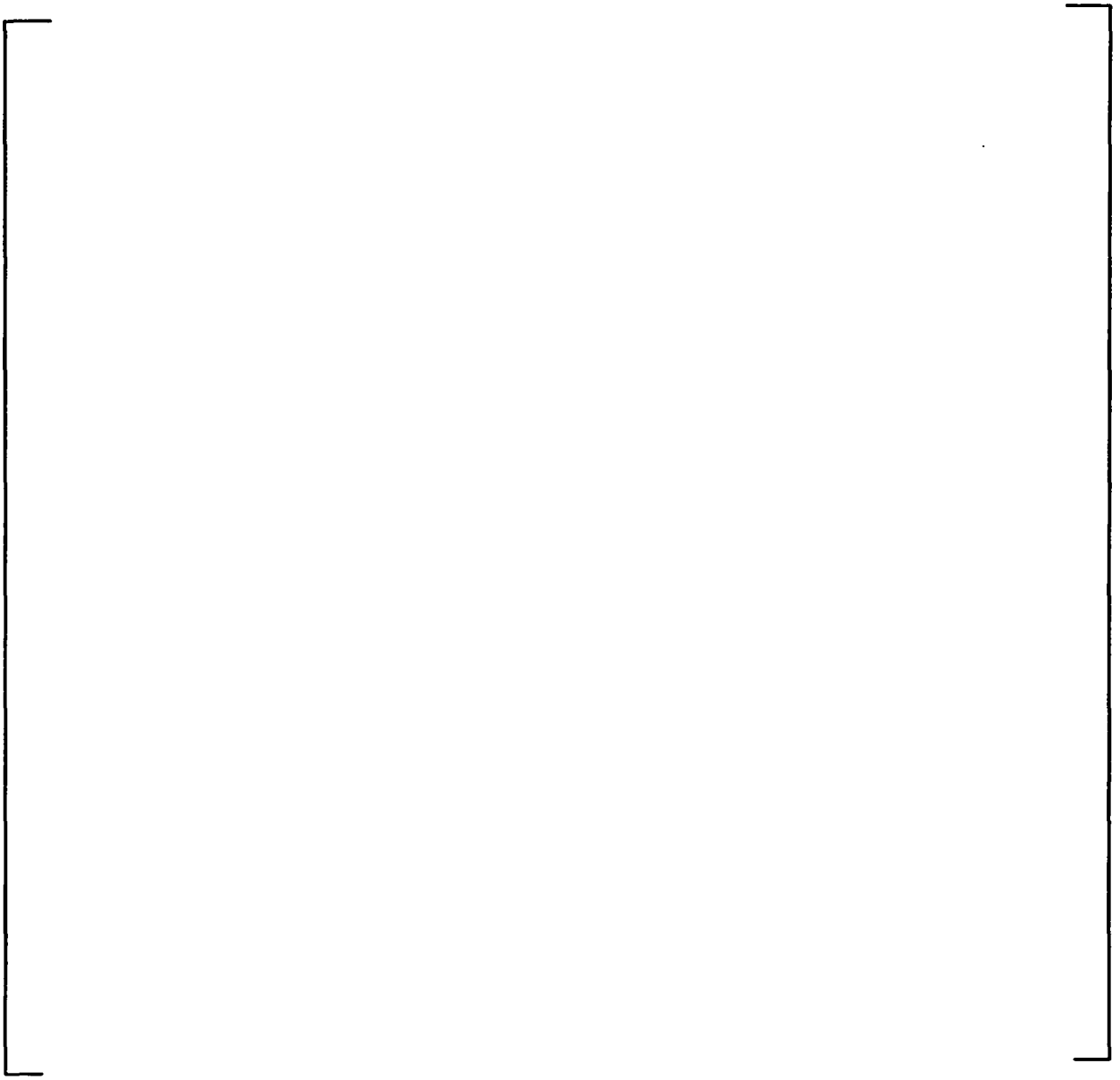

Figure 2-2
Candidate Tubes for Expansion - Cold Leg

3.0 MODEL 51 SG DESIGN DESCRIPTION

3.1 OVERALL DESIGN

The Diablo Canyon Units 1 and 2 steam generators are of the Westinghouse Model 51 steam generator design. Each steam generator (SG) contains 3388 mill-annealed Alloy 600 U-tubes, 0.875 inch OD x 0.050 inch wall, which provide 51,500 ft^2 of heat transfer area per SG. Figure 3-1 shows the steam generator layout. Primary coolant enters the hot leg channel head and passes through the U-tubes, which transfer heat from the primary side to water on the secondary side, where the water is converted to steam. The feedwater enters the SG through the feedwater nozzle, travels through a feedwater ring and is discharged into the upper plenum region. The feedwater mixes with the secondary water in the upper plenum, and then travels down the downcomer, which is the annulus between the shell and the wrapper surrounding the tube bundle region. At the bottom of the wrapper, which is 14 inches above the top of the tubesheet, the secondary fluid spreads out across the secondary face of the tubesheet and travels upward through the tube support plates and tube bundle. As the secondary fluid passes through the tube bundle, it is converted to a water/steam mixture that passes upward through the transition cone region of the SG shell, into the swirl vanes and moisture separators in the upper shell region. Water is separated from the steam before the dry steam exits the SG via the steam outlet nozzle. Water removed by the moisture separators flows into the upper plenum where it mixes with the incoming feedwater.

The SG tubes pass through tube support plates which provide lateral support to the tubes and contain circulation holes through which the water/steam passes upward through the tube bundle. During normal operation, a slight pressure drop exists across each TSP. If the tube to TSP crevices are assumed to be open, this pressure drop would cause a small displacement of the TSPs relative to the tubes during normal operating conditions. However, the DCPP SGs have dented and packed crevices, and the TSPs would not be displaced relative to the cold shutdown or hot standby condition under normal operating conditions. At hot standby conditions, there is no secondary flow or pressure drop across the TSPs, and the hot standby positions are the same as the full power and cold shutdown TSP positions relative to the tube due to the crevice conditions. However, during postulated accident conditions such as steam line break (SLB), pressure differentials across individual TSPs are assumed to displace the TSPs for development of tube expansion requirements in such a manner as to potentially uncover degradation within the TSP crevice.

3.2 TUBE SUPPORT PLATE DESIGN

The Model 51 steam generators at Diablo Canyon Units 1 and 2 utilize [ ]^{a,c} inch thick SA 285 Grade C carbon steel support plates with drilled (round) tube holes set on a square pitch of [ ]^{a,c} inches. The tube support plates also include flow circulation holes measuring [ ]^{a,c} inch in diameter, set on a square pitch of [ ]^{a,c} inches within the tube hole array.

3.3 TUBE SUPPORT PLATE SUPPORTS

The TSPs are supported vertically using a central tierod/spacer and four outer tierods/spacers located near the edge of the plate. The in-plane support for the TSPs is provided by the six tapered wedges located around the periphery of each plate. The manner in which the wedges are welded in place varies for

different steam generator models. For the Model 51 steam generators at Diablo Canyon, the wedges are welded to both the wrapper and tube support plate on both top and bottom surfaces. As a result of the wedges being welded to both the TSP and wrapper, the wedges also provide restraint to vertical motions of the support plates. Finally, there are two support bars welded between each TSP and wrapper, located 180° apart.

Section 5.2.1 provides a detailed description of the Model 51 SG TSP support system. A sketch of the wrapper / wedge / TSP and the wrapper / support bar / TSP interfaces is provided in Figure 5-2. The angular locations for the wedges and support bars are shown in Figure 5-3 for TSP 1 and in Figure 5-4 for TSPs 2-7. Additional details concerning the TSP support components, including the tierods, spacers, and wedge groups, are provided in Section 5.2.1.

a,c

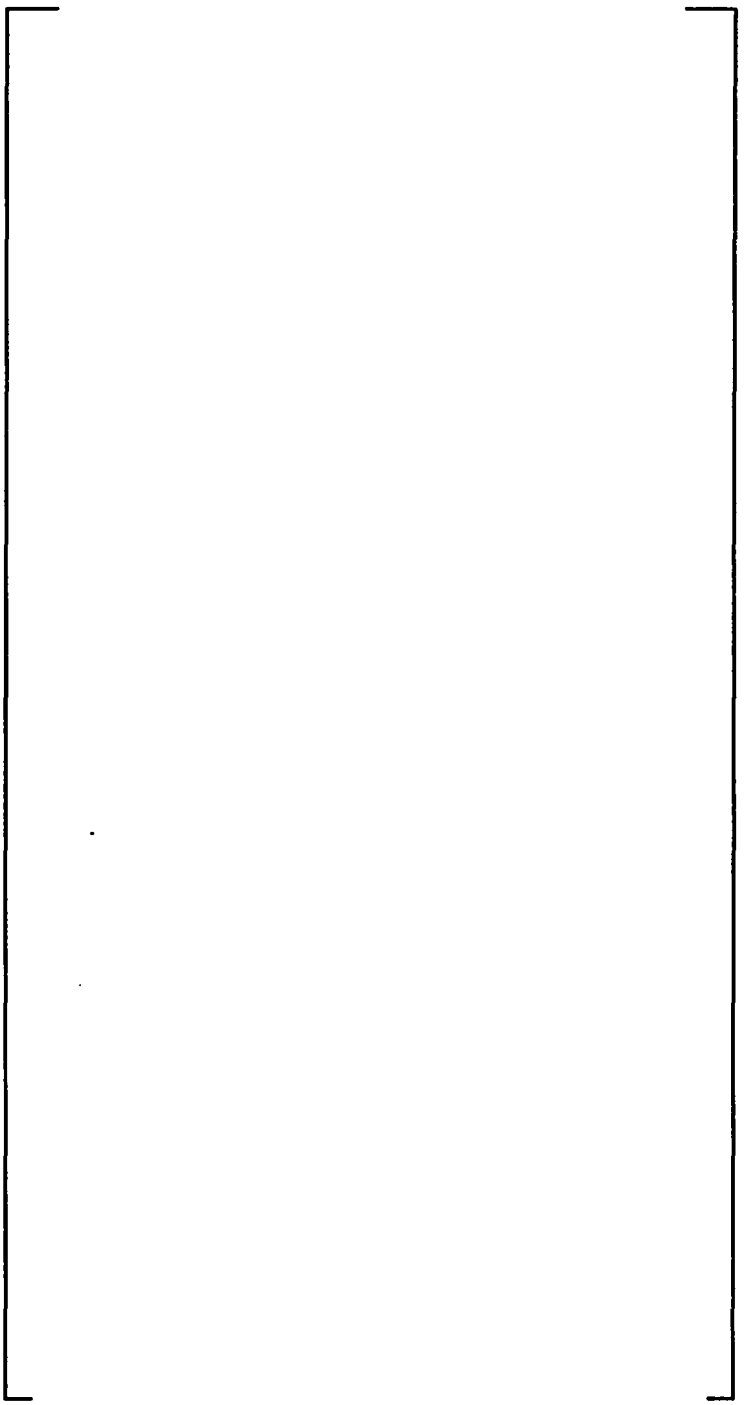

Figure 3-1
Model 51 Steam Generator Layout

4.0 THERMAL/HYDRAULIC ANALYSIS

4.1 STEAM LINE BREAK CHARACTERISTICS

A schematic of a Westinghouse Model 51 steam generator is shown in Figure 4-1. During a steam line break accident upstream of the flow restrictor, the steam nozzle limits the magnitude of the break flow. For a break downstream, the flow restrictor limits the break flow magnitude. In the top of the steam generator just below the steam line nozzle, there are several open volumetric regions in the flow paths with cross-sectional areas that vary between 75 times and 150 times the size of the flow area of the steam line with flow restrictor. These large flow areas act as accumulators that tend to absorb pressure fluctuations from the steam line and result in relatively low steam velocities near the top of the steam generator inside the main steam nozzle. In addition, there are two sets of steam separators that the steam flow must pass through prior to entering the steam outlet nozzle. These steam separators act in series and provide resistance to the steam flow as it approaches the main steam nozzle.

The water in the steam generator resides primarily in the region below the primary separators. When the steam generator is operating at power, the water in most of the tube bundle region is a two-phase mixture of steam and water with increased quality in the higher regions of the tube bundle. Typically, downcomer water with a subcooling of about 17 °F enters the tube bundle at the tubesheet. Heat transfer from the primary side of the tubes quickly brings the subcooled water to saturation conditions and a two-phase mixture of fluid and water forms. The flow in the bundle region will then be upwards due to natural convection effects arising from differences in density between the two-phase fluid in the heated tube bundle and the single phase water in the unheated downcomer. Water in the two-phase flow leaving the tube bundle is separated in the steam separators and is returned to the bundle via the downcomer annulus. The ratio of the total flow in the bundle to the steam flow exiting the main steam nozzle is known as the circulation ratio and is about 4.9 for the Model 51 steam generators at Diablo Canyon Units 1 and 2 at full power operating conditions. Consequently, at full power operating conditions, the upward flow in the tube bundle is about 4.9 times the steam flow that exits the main steam nozzle and the largest pressure drop across a tube support plate is less than 1 psi.

When a steam line break downstream of the flow restrictor occurs from full power operating conditions, the flow from the steam nozzle increases by a factor of approximately 2.3 until the flow restrictor chokes. Due to the resulting flow imbalance, a depressurization of the large volume at the top of the steam generator occurs. The decrease in pressure acts to disrupt the circulation flow as the flow in the downcomer slows down and reverses to help supply flow to the break. Consequently, when a steam line break occurs from full power operating conditions, there will be only a moderate increase in flow in the bundle itself that is directly attributable to the break. However, there is a secondary, more substantial contribution to flow in the tube bundle caused by the swelling of the fluid in the tube bundle region due to flashing of water as the steam generator pressure decreases.

This swelling effect in the tube bundle generates the peak loads on the tube support plates during the early part of a steam line break. Since the tube bundle region already contains substantial voids when the steam generator is operating, the amount of water in the tube bundle during power operation is much less than that during hot standby when only water is in the bundle. Therefore, the surge associated with swelling in the tube bundle from a steam line break at hot standby conditions will result in the worst case tube support plate loads for the steam generator.

4.2 METHODS

To determine the peak loads that could occur during a steam line break, two methods were employed to estimate the peak loads on the tube support plates that would occur as a result of the surge associated with depressurization of the steam generator due to a steam line break. These methods are (1) RELAP5 code, and (2) TRAC-M code.

4.3 METHOD AND RESULTS OF RELAP5

4.3.1 RELAP5 Code Description

The RELAP5 Code is an advanced thermal-hydraulic code which has been used as a tool to analyze transients for light water reactor systems (e.g., References 1 to 4). MOD3 is the third major variant of the code and MOD3.2 is the second revision of that variant.

The RELAP5/MOD3.2 Code equation set provides a two-fluid, non-equilibrium system simulation. The six equation set, continuity, momentum and energy equations for each phase, is used to solve for the dependent variables. These variables include local pressure for each phase, specific internal energy, void fraction and velocity. Constitutive models represent the interphase drag and mass transfer, flow regimes in vertical and horizontal flow, and wall friction.

The RELAP5/MOD3.2 Code has been used in calculating thermal hydraulic loads on tube support plates of steam generators during steam line break and feedwater line break transients (References 5 to 7).

4.3.2 Model 51 RELAP5 Models

Two fluid regions are modeled in RELAP5, the steam generator primary side and the steam generator secondary side. Heat slabs are used to model the heat transfer between the primary and secondary fluids.

Secondary Side Model

Nodalization for the RELAP5 model of the secondary side of the Model 51 SG is shown in Figure 4-2 that represents the general arrangement of nodes and node numbers in the RELAP5 model. The nodalization for the RELAP5 secondary side model is pictured in Figure 4-3. The elements which compose this model and their description are listed in Table 4-1.

Components 2 and 30 represent the tube bundle and tube bundle entrance respectively. In the RELAP5 model, Component 2 consists of 30 volumes and 29 junctions, while Component 30 has 1 volume and 2 junctions. The arrangement of these volumes and junctions is pictured schematically in Figure 4-4 with the elevations noted. In the RELAP5 model the downcomer has been incorporated into a single component, 35. The region outside the swirl vanes has been broken into two components, 33 and 53 for the RELAP5 modeling.

Primary Side Model

Figure 4-5 is a schematic representation of the primary side model. The model includes the following elements:

1. Pipe component consisting of 60 volumes and 59 junctions

2. Time dependent volume components, 100 and 101

For heat transfer between the primary and secondary fluids, there are 60 heat slabs. Each heat slab connects a primary side volume to a secondary side volume. The primary coolant flow through junctions 500 and 501 is assumed constant, 9149 lb_m/sec. Primary temperatures and pressures are also kept constant.

4.3.3 Analysis Plan for RELAP5

The hydraulic loads on the tube support plates in a steam line break event are calculated with the RELAP5/MOD3.2 computer code as described in Section 4.3.1. The RELAP5 analysis matrix is given in Table 4-2. Two cases for small break (SB) are called SB1 and SB2. SB1 is simulated with the non-equilibrium model and SB2 with the equilibrium model. Similarly, two cases for large break (LB) are called LB1 and LB2. Again, LB1 is for non-equilibrium and LB2 for equilibrium. The last case simulates a worst case by considering parameter uncertainty, and this case is called LB3. The uncertainty of input parameters to the simulation of the SLB hydraulic loads is to be evaluated later in Section 4.6, where an uncertainty factor is developed to scale the results for the structural evaluation.

An equilibrium RELAP model considers thermodynamic equilibrium between liquid and vapor phases, and thus there is neither temperature difference nor heat transfer between interfaces. A non-equilibrium RELAP model simulates thermodynamic non-equilibrium between liquid and vapor phases, and thus there is a temperature difference and heat transfer between the interfaces.

A set of RELAP5 analyses were performed and the results of these analyses are reported in this section. The RELAP5 analyses include two cases (i.e., SB1 and SB2) for a break downstream of the steamline flow restrictor with a 1.4 ft^2 throat area. Cases SB1 and SB2 were defined as "non-equilibrium" and "equilibrium," respectively.

For the non-equilibrium case (SB1), the potential for non equilibrium was permitted throughout the model. For the equilibrium case (SB2), the potential for non-equilibrium was limited to the regions outside the tube bundle and the tube bundle was assumed to be at equilibrium. The remaining runs (i.e., LB1 and LB2) were made with no flow restrictor. A guillotine break at the outlet to the steam generator nozzle is assumed with an area of 4.6 ft^2. One additional case (i.e., LB3) was run at the worst case initial conditions. Results of case LB3 confirm the 1.5 uncertainty multiplier developed from the sensitivity analysis, as evaluated in Section 4.6.

4.3.4 Results and Analysis of RELAP5 Small Break

The small break cases, SB1 (non-equilibrium) and SB2 (equilibrium) started from a typical hot standby condition and the modeled steam generator had an integral flow restrictor with a 1.4 ft^2 throat area. This is equivalent to the DCPP Model 51 steam generators with a break downstream of the flow restrictor, which is not integral to the steam generator. The TSP pressure drop traces vs. time from the break are plotted in Figures 4-6a, b, and c (non-equilibrium) and Figure 4-7 (equilibrium). The pressure drop traces for the non-equilibrium case are much more volatile than the equilibrium case. To improve the clarity of the non-equilibrium case, two figures were used, one that contained the odd numbered plates (Figure 4-6a) and one the even (Figure 4-6b). Figure 4-6c contains all of the plates with an expanded time scale.

In addition to the generally higher volatility, the non-equilibrium case is characterized by a single, very large pressure spike starting at 0.83 seconds. This spike appears to begin at TSP1, immediately followed by an extremely large spike (0.2 to 8.3 psi) in TSP4 which lasts a single time increment (0.01 sec). The disturbance then propagates to TSP's 5, 6 and 7. Figure 4-6c shows these pressure spikes with an expanded time scale between 0.8 and 0.9 seconds. Since this spike has no apparent generating mechanism, it is likely a product of the numerical solution and not a physical phenomenon. Table 4-3 tabulates peak pressure drop for Case SB1 with and without spike, and discussed below.

The equilibrium case, represented in Figure 4-7, shows pressure drop transients which are much more quiescent than the non-equilibrium case. Table 4-3 lists pressure drop peaks for the cases, SB1 and SB2. The peak pressure drop for each TSP is listed. Case SB1 is listed twice, once including the time interval of the spikes, 0.83 to 0.93 seconds and a second time excluding this interval. When the spike is excluded from the non-equilibrium Case SB1, the agreement with the equilibrium case (Case SB2) is more rational. RELAP5 shows pressure drops which are all positive, indicating an upward flow throughout the bundle. With this upward flow, RELAP5 generates higher TSP pressure drops for the lower tube support plates.

All RELAP5 pressure drops presented in this section have been adjusted to remove the static head component present in each TSP pressure drop over the nodal height of 12 inches (see Figure 4-4).

As discussed above, the non-equilibrium case (Case SB1) apparently involved numerical spikes in predicting pressure drop through TSPs. In view of this, results of the equilibrium case (Case SB2) are recommended for use in the TSP tube locking evaluation.

4.3.5 Results and Analysis of RELAP5 Large Break

The non-equilibrium (LB1) and equilibrium (LB2) cases for the 4.6 ft^2 break, without a flow restrictor, are pictured in Figures 4-8 and 4-9, respectively. Again the non-equilibrium case displays higher volatility than the equilibrium case. The peak pressure drops, however, are similar, reaching 9 psi for the 7th TSP. These peak pressure drops are significantly higher than those for runs assuming a flow restrictor (SB1 and SB2). This result is fully expected since the blowdown rate for the 4.6 ft^2 break is much higher than for the case where a flow restrictor is present. The higher blowdown rate results in higher bundle flow rates and higher TSP pressure drops. The blowdown rate, in terms of steam generator pressure is pictured in Figure 4-10.

4.3.6 Results and Analysis of RELAP5 Worst Case SLB Conditions

The final large break case, LB3, listed in Table 4-4, was run with the worst case SLB geometry and initial conditions. This run was made to confirm the adequacy of a 1.5 multiplier applied to the best estimate case to cover uncertainties (see Section 4.6 for detail). The key parameters which would increase TSP loads were a water level reduction and an increase in the TSP loss coefficient. Other parameters changed during the sensitivity study either had no effect or were already at worst case values. The LB3 case duplicates the worst case elements of Case 61 (see Section 4.6), including a reduced water level and TSP loss coefficients at their maximum values. The downcomer loss coefficient had no effect on TSP loads. LB3 is run with a full guillotine break at the outlet nozzle.

Table 4-4 compares peak pressure drops at each tube support plate for two cases, run LB3 and the reference LB1 case multiplied by the uncertainty factor of 1.5 developed from the sensitivity study (see Section 4.6). Both cases are non-equilibrium. The table shows that the peak pressure drops of the case (LB1), when multiplied by 1.5, bound the peak pressure drops of the worst case (LB3). This confirms that the 1.5 uncertainty multiplier will provide TSP loads that conservatively bound the loads that would occur for any range of SLB conditions.

4.3.7 Conclusions

Considering the above discussion, we can draw the following conclusions:

1. The large pressure spikes, occasionally present in non-equilibrium RELAP5 results, are artifacts of the numerical solution. The solutions with the equilibrium assumption in the tube bundle represent the best methodology for calculating SLB tube support plate loads.

2. The TSP pressure drops for a large break, without a flow restrictor are, as expected, significantly greater than pressure drops with a flow restrictor in place. The RELAP5 results with a flow restrictor are applicable to plants which have an integral flow restrictor or, such as DCPP, have special piping to reduce the likelihood of a steam pipe break between the steam generator and the flow restrictor. All SLB events outside containment, for which containment bypass of released radiation is possible, would have the break downstream of the flow restrictor. For this case, the lower loads are applicable.

3. A factor of 1.5, applied to the loads, bounds the uncertainty associated with defining the input parameters such as the TSP loss coefficient and water level.

4.4 RESULTS OF TRAC-M ANALYSES

Recently, Krotiuk (Reference 8) of the U.S. Nuclear Regulatory Commission (NRC) Office of Regulatory Research reported results for a Model 51 steam generator (such as the Diablo Canyon SGs) that was subjected to a small and a large steam line break using the NRC TH Code TRAC-M. The small break has a break area of 1.4 ft^2 and the large break has 4.6 ft^2, the same as the RELAP5 analyses discussed above.

Results of the calculation by the TRAC-M Code were read from the report entitled "Sensitivity Studies of Failure of Steam Generator Tubes during Main Steam Line Break and Other Secondary Side Depressurization Events," prepared by Majumdar (Reference 9). Table 4-5 tabulates the results read from Reference 9. As can be seen, the RELAP5 results bound the TRAC-M results for both the small and large breaks except at TSP 7.

4.5 HYDRAULIC LOADS DURING FEED LINE BREAK

In addition to the SLB, hydraulic loads to the TSPs were also calculated for a postulated feed line break (FLB) using the TRAC-M code. Table 4-6 tabulates results for the TRAC-M loads during a FLB at both hot standby and full power conditions together with the loads for a small SLB from both RELAP5 and TRAC-M (Reference 9). As can be seen, the RELAP5 results for a postulated, hot standby small SLB clearly bound the TRAC-M FLB results. Except for the first two plates for which the TRAC-M SLB results are very small, the small break SLB loads bound the FLB pressure drops. It is clear from Table 4-6 that for TSPs with significant pressure drops, the hot standby, small break SLB pressure drops bound the FLB pressure drops at both hot standby and full power conditions. Consequently, the small break SLB loads are the appropriate bounding loads for TSP displacement analyses.

4.6 SENSITIVITY EVALUATION OF SLB HYDRAULIC LOADS AND UNCERTAINTY FACTOR

The hydraulic loads on the TSPs during a SLB event were calculated for a small and a large break. A series of cases were run to assess the sensitivity of the TSP loads to the most influential input parameters including the break size for a limited break, the SG water level, the TSP pressure drop loss coefficient, the SG downcomer loss coefficient and the Moody discharge coefficient. The results of the sensitivity analyses are used to define a conservative uncertainty factor which is applied to the RELAP5 analyses pressure drops to obtain a bounding set of loads for the TSP displacement analyses.

The sensitivity analysis matrix is given in Table 4-7 and is described in detail in Reference 6. The sensitivity analyses were performed using the Westinghouse TRANFLO code using the node layout shown in Figure 4-11.

Sensitivity Analyses

The sensitivity analyses were performed to assess the influence of the principal input parameters, individually and collectively, on the TSP pressure drops. The more limiting hot standby SLB event was used to determine the TSP load sensitivity to the break size (guillotine versus 1.5 ft^2), water level (expected 490.5" versus lower uncertainty level of 478.5"), TSP loss coefficients (expected versus maximum values), downcomer loss coefficients (expected versus minimum values) and the Moody discharge coefficient (maximum 1.0 versus expected 0.84). These analyses, calculated using the Westinghouse TRANFLO code, are represented by Cases 51 to 55 in Table 4-7. From these analyses, it was determined that the reduction in water level, the increased TSP loss coefficients and the reduced downcomer loss coefficients resulted in an increase in the TSP loads.

The above three input parameter changes that increase the TSP loads were then combined, in Cases 61 and 62, with the most limiting SG guillotine break (with a Moody discharge coefficient of 1.0) to define a

bounding set of loads to develop an uncertainty adjustment factor for the reference analyses. The uncertainty factor is a constant factor on the loads obtained to reasonably bound the ratio of the peak pressure drop for each plate from the combined analyses of Cases 61 and 62 to the reference analyses of Cases 1 and 2. Note that there are four reference cases (i.e. Cases 1 to 4) for the reference analyses as tabulated in Table 4-7.

As discussed above, the most influential input parameters in the sensitivity of the TSP loads are: (1) the break size, (2) the water level, (3) the TSP pressure loss coefficient, (4) the downcomer loss coefficient, and (5) the Moody discharge coefficient. The percentage of tube plugging does not affect these five parameters, and therefore, the TSP hydraulic loads are not sensitive to the percentage of the tube plugging. Transient behaviors, including the TSP hydraulic loads during the SLB depend on water flashing into steam and the subsequent swelling motion. The percentage of tube plugging will not change the amount of the water mass in the secondary side, and therefore does not affect the TSP hydraulic loads.

Reference Analyses with Uncertainty Adjustment

Cases 61 and 62 combine all the worst case or most limiting input parameters, and thus they define the combined uncertainty factor for each plate. It is extremely conservative to combine all the collective worst case input conditions in a single TSP load analysis. A more realistic bounding analysis would collectively combine intermediate (between expected and worst case) values for the input parameters in a single run, or would combine the resulting TSP loads by the square root of the sum of squares since all worst case conditions would not be expected to act simultaneously. However, it is the intent of these analyses to develop a conservative set of bounding TSP loads, and the results of Cases 61 and 62 are used to define uncertainty factors. To further simplify the uncertainty factor approach, a constant uncertainty factor is developed based on the maximum ratio of the Case 61 to Case 1 and Case 62 to Case 2 pressure drops. As developed later in this section, this resulted in a multiplier of 1.5 for all reference case loads.

4.6.1 Reference Full Power and Hot Standby Loads

Case 1 is a reference analysis for SLB at hot standby with a guillotine break at the SG outlet nozzle. The water level is at the normal setting of 490.5 inches above the top of the tubesheet, and both TSP and downcomer loss coefficients are at nominal values. The Moody discharge coefficient for critical blowdown flow is set to be unity. Figure 4-12 shows the hydraulic loads through all seven TSPs. The peak pressure drops for each TSP, for this and succeeding cases, are tabulated in Table 4-8. Both peak pressure drop values and the values normalized to Case 1 are presented.

Case 2 is equivalent to Case 1, except the SLB is initiated from full power operation at a nominal water level of 506 inches. Figure 4-13 shows the hydraulic loads through all seven TSPs for Case 2. For the full power, peak pressure drops listed in Table 4-8, the initial pressure drop is subtracted from the maximum to calculate a peak SLB load change.

Case 3 is identical to Case 1, but the guillotine break at hot standby is assumed outside the containment building, with no flow restrictor. Figure 4-14 shows the hydraulic loads through all seven TSPs.

Case 4 is equivalent to Case 3 (still no flow restrictor), except it initiates from full power operation, not hot standby. Figure 4-15 shows the hydraulic loads through all seven TSPs.

For hot standby, a break at the SG steam outlet nozzle generally yields higher loads than a break outside containment assuming the same break size. This is also true for full power operation. This is expected because of the additional flow resistance due to extra piping of about 120 feet and three 90° elbows between the steam outlet nozzle and the containment penetration.

It is important to note that hot standby leads to higher loads on the TSPs than full power operation for all TSPs, except TSP 1. The higher load on TSP 1 for the full power case is related to flow split. In the lower tube bundle, flow splits into upward and downward directions. For hot standby, the split occurs between TSP 1 and TSP 2, and for the full power operation between TSP 2 and TSP 3. The downward flow at TSP 1 is higher for the full power case, resulting in a higher pressure drop. In both cases the pressure drops for TSP 1 are small and will not result in large loads.

Once an SLB event begins, it triggers a rapid depressurization, which leads to water flashing. The rapid water flashing generates water motion. Fluid velocity increases with an increase in the amount of water flashing. A higher water velocity will lead to a larger pressure drop across a TSP. In addition, when fluid moves in the tube bundle, water will exert a higher pressure drop across the TSP when compared to steam. Hot standby at zero power provides a solid water pool in the tube bundle, while power operation generates a steam and water mixture. Therefore, hot standby yields higher loads than full power operation.

4.6.2 Best Estimate Loads

As stated earlier, the hydraulic load varies with initial and boundary conditions of a SLB event. The reference cases described above were, as noted, slightly conservative. The best estimate case for a steamline break (Case 21 of Table 4-7) consists of the following:

- Break outside containment
- A limited break size of 1.5 ft^2
- A nominal water level of 490.5 inches at hot standby
- Nominal correlation constant for TSP loss coefficient
- Nominal downcomer loss coefficient
- A Moody discharge coefficient of 0.84.

For full power operation, the nominal water level is 506 inches.

A break size of 1.5 ft^2, about one third of the steam line flow area of 4.6 ft^2 is considered. Note that the throat area of the SG steam nozzle flow restrictor is about 1.4 ft^2 so that Case 21 bounds a break downstream of the flow restrictor at hot standby conditions.

TRANFLO uses the Moody model for calculations of break (or critical discharge) flow. Comparisons with measured break flows of pressure vessels have indicated the need to use a multiplier for the Moody

model. The multiplier is less than unity, and depends on the conditions of the two-phase flow and the geometry to and through the break. The multiplier can be as low as 0.55 and as high as 0.84.

The Moody model, like many critical flow models of two-phase flow discharge, considers one-dimensional flow; however, in fact, it is not one-dimensional flow. When two-dimensional flow is considered a multiplier of about 0.84 is needed to achieve agreement with measured data. As such, a multiplier of 0.84 is used as a best value for a SLB event.

Figure 4-16 shows pressure drops through TSPs for this best estimate Case 21. As expected, the best estimate pressure drops are smaller than those of Cases 1 and 3. The ratios to those of Case 1 range from about 0.6 to 0.75, depending on the individual TSP (see Table 4-8).

4.6.3 SLB Load Sensitivity Analyses

4.6.3.1 Break Size

To test the effect of break size, Case 51 was run with a limited break of 1.5 ft^2 at the exit of the SG steam nozzle. This represents an area of about one-third of the full pipe area, 4.6 ft^2, used in a guillotine break. The pressure drops through various TSPs are similar to those of Case 1, but smaller, as expected, for a limited break size. Table 4-8 presents ratios of the peak values of the pressure drops between Case 51 and Case 1; the peaks are about 10 to 20% smaller for the limited break than a guillotine break.

4.6.3.2 Water Level

A postulated steam line break (SLB) event results in blowdown of steam and water out of the steam generator. The fluid blowdown depressurizes the secondary side fluid, causing the fluid to move. Fluid motion leads to pressure drops and hydraulic loads across the TSPs. Depressurization triggers rapid water flashing, mainly across the water level during the early part of the transient. The rapid water flashing generates water and steam motion, and the closer the tube support plate is to the water level, the higher the flow rate and pressure drop.

For purposes of the sensitivity study, a water level of 478.5", one foot below the nominal level (490.5"), was chosen. For the minimum water level, Case 52, the pressure drops through the various TSPs are compared to those for the reference Case 1. Table 4-8 presents ratios of the peak value of pressure drops between Case 52 and Case 1. A lower water level leads to a higher pressure drop for TSPs 1 through 5, while slightly lower pressure drops result for TSPs 6 and 7.

4.6.3.3 TSP Loss Coefficient

The best value of the correlation constant for the loss coefficient correlation is 1.1 based on a regression analysis of test results (Reference 3). Its upper and lower bounds are [ ]^{a,b}, respectively. Reference analyses of Cases 1 to 4 use the best estimate of 1.1. The upper bound is applied to assess the sensitivity of the TSP loss coefficient on pressure drops. Use of the upper bound leads to higher pressure drops.

For the maximum TSP loss coefficient, Case 53, the TSP pressure drops are higher in value, as expected, than for Case 1. Table 4-8 presents ratios of peak value of pressure drops between Case 53 and Case 1; the peaks are about 15 to 30% higher for Case 53.

4.6.3.4 Downcomer Loss Coefficient

The loss coefficient of the downcomer consists of friction along the shell and wrapper, and form loss due to area changes and flow turns. The estimate of friction and form loss for the downcomer is straightforward, as it deals with single phase (water) flow, and simple geometry; but it can also be subject to uncertainty. Its total drop is only about 0.6 psi during full power operation.

For the sensitivity study, a decrease of about 0.3 psi, or a 50% decrease in the downcomer pressure loss was considered. This decrease is achieved by a decrease in the downcomer form loss coefficient. A decrease in downcomer loss will promote more tube bundle flow toward the tubesheet and into the downcomer.

For the minimum downcomer loss coefficient, Case 54, Table 4-8 presents ratios of peak value of pressure drops between Case 54 and Case 1; the ratios show that tube bundle flow is not sensitive to the uncertainty of the downcomer loss coefficient. This is expected because the downcomer loss is very small compared to the total loss through the whole bundle and separator.

4.6.3.5 Moody Discharge Coefficient

Pressure drop increases with an increase in flow rate, and vice versa. A decrease in break flow generally decreases the tube bundle flow and thus reduces the pressure drops across the TSPs. A Moody discharge coefficient of 0.84 reduces break flow compared to that of a coefficient of unity.

For the lower, 0.84 Moody discharge coefficient, Case 55, the pressure drops through various TSPs are lower. Table 4-8 presents ratios of peak value of pressure drops between Case 55 and Case 1; the peaks are up to about 20% smaller for Case 55 than for Case 1.

4.6.3.6 Combined Worst Conditions for Hot Standby

Combined worst conditions are given in Table 4-7; they are:

- Break at the steam outlet nozzle
- A guillotine break
- A lower water level of 478.5 inches
- An upper bound for the correlation constant of the TSP loss coefficient
- Minimum downcomer loss coefficient
- A Moody discharge coefficient of 1.0.

This is Case 61. Figure 4-17 depicts pressure drops through the TSPs. As expected, they are higher than those of Cases 1 and 3. Their ratios to those of Case 1 range from about 1.13 to 1.42, depending on the individual TSP (see Table 4-8).

4.6.3.7 Combined Worst Conditions for Full Power

The combined worst conditions for full power, Case 62, are identical to those for hot standby (see Section 4.6.3.6), except that water level was reduced by 21 inches from its nominal value. Figure 4-18 shows pressure drops through the TSPs. As expected, they are higher than those of Case 2 (see Table 4-8).

4.6.4 Adjusted Full Power and Hot Standby Loads

Sensitivity analyses of SLB loads are discussed in detail in Section 4.6.3. In these sensitivity studies, uncertainty considerations included water level, TSP loss coefficient, downcomer loss coefficient, Moody discharge coefficient, break location and break size. Based on these studies, the combined, limiting conditions are developed for hot standby (Case 61, see Table 4-7), and for full power (Case 62, see Table 4-7). Results of Cases 61 and 62 are presented in Table 4-8. This table includes the reference loads from Cases 1 and 2 for hot standby and full power, respectively.

An uncertainty adjustment factor of 1.5 on the reference loads for hot standby and full power conditions represents a conservative load adjustment factor that combines the uncertainties. The 1.5 adjustment factor bounds the uncertainties for all TSPs except the full power condition for TSP 1. TSP 1 has a very small pressure drop of 0.12 psi and thus is more sensitive to the uncertainties. However, due to the small pressure drop at TSP 1, this plate is not a significant concern for TSP displacements.

4.6.5 Conclusions

Considering the above discussion, we can draw the following conclusions.

1. A SLB at hot standby generates higher pressure drops across tube support plates than a SLB at full power operation. This trend is observed for all TSPs except TSP 1, which has a very low pressure drop for both hot standby and full power conditions (see Reference Cases 1 to 4 in Table 4-8).

2. The best estimate case (i.e., Case 21) for a hot standby SLB includes a limited break outside the containment and a Moody discharge coefficient of 0.84, and results in 25% to 40% lower pressure drops than the reference hot standby results of Case 1.

3. Sensitivity studies indicate that 1) a limited break is less severe in pressure drop than a guillotine break, 2) pressure drop increases with a decrease in water level, 3) an increase in TSP loss coefficient increases the pressure drop, 4) a decrease in downcomer loss coefficient has negligible effect on the pressure drop, and 5) a decrease in Moody discharge coefficient reduces the pressure drop.

4. Combined worst conditions were constructed from the sensitivity study. The sensitivity study has been applied to develop a bounding uncertainty factor on the TRANFLO TSP

pressure drops. The resulting uncertainty adjustment factors of 1.5, applied to the reference hot standby loads of Case 1, bounds the worst case loads, Case 61.

5. Results of TRANFLO simulation are similar to those of RELAP simulation, such as transient behavior of the pressure drop, and the drop being highest at the uppermost TSP and decreasing toward the lower TSPs. Therefore, the uncertainty multiplier of 1.5 should also be applicable to RELAP results.

4.7 HYDRAULIC LOADS STARTED FROM HOT STANDBY VS. FULL POWER

It is in order to compare hydraulic loads to the TSPs during the SLB started from hot standby vs. full power. As tabulated in Table 4-8. Case 1 represents the hydraulic loads started from hot standby and Case 2 from full power. Results of hydraulic loads on the TSPs at hot standby bound those from full power.

4.8 EFFECT OF STEAM LINE PRESSURE FLUCTUATIONS

The effects of a steam line break will diminish with time as the steam generator depressurizes and the flow out the break decreases. As long as the pressure in the steam generator is high enough and the break large enough to choke the flow restrictor, pressure fluctuations in the steam line downstream of the flow restrictor will not be able to propagate into the steam generator. If the area of the break is small enough (less than about 0.45 square feet or about 1/3 of the area of the flow restrictor), the break flow will be less than that normally experienced during operation. The internals of the steam generator should not be significantly affected since there is considerable operating experience at this level of flow. Nevertheless, it may be possible that for a medium sized break, for which the break area is smaller than the nozzle area, the break flow could exceed the full power operating flow and the flow restrictor may not be choked. Under these conditions, pressure fluctuations in the steam line could possibly propagate into the steam generator and affect the internals. However, the significant change in area and the presence of the compressible steam in the large volume at the top of the steam generator combine to act as an accumulator and will help to isolate the lower internals from the effect of sudden pressure changes in the steam line.

Additional isolation for the tube bundle region is provided by significant resistance that exists across the two levels of steam separators and the presence of large amounts of saturated liquid that can flash to maintain the pressure near saturation pressure. As a result, any sudden depressurization in the steam line leads to a much slower depressurization of the steam generator as a whole and relatively small pressure gradients would be expected inside the tube bundle. The pressure gradients that are established are primarily a result of "steady flow" rather than dynamic imbalance due to flow acceleration. In fact, the dominant loads on the tube support plates in the tube bundle result from the swell of the fluid trapped by the support plates as the steam generator begins to depressurize rather than from the propagation of sonic waves from the main steam nozzle.

To estimate the extent to which pressure fluctuations in the steam line could propagate into the tube bundle of the steam generator, a two-phase thermal-hydraulic analysis was conducted for which a sinusoidal pressure oscillation was imposed at the steam line boundary. The steam generator was assumed to be at hot standby. The pressure response in the tube bundle region was determined as a

function of the applied oscillatory pressure in the steam line. The analyses were run until steady state oscillating conditions were achieved. Several such analyses were conducted using several different frequencies for the pressure oscillations to determine the frequency transform for the pressure oscillations between the steam line and the tube bundle region.

4.8.1 Method

The steam generator was divided into control volumes that contain mass and energy. The control volumes are connected together by fluid connectors that transfer mass and energy between the control volumes. The integrated form of the momentum, mass, and energy conservation equations were solved for the control volumes and connectors to obtain transient pressures and flows. Computerized steam tables were used to represent the properties of the fluid and rigorous mass and energy conservation was imposed. Results from the technique have been compared to analytic solutions for wave propagation in piping systems with good agreement.

4.8.2 Results

Results were obtained from five separate runs with pressure oscillation frequencies between 10 and 50 hertz originated in a steam line of a Model E2 steam generator similar to the Model 51 (see Reference 7). Table 4-9 tabulates the relative response inside various parts of the steam generator. These results provide the relative amplitude of the calculated response of pressure at the inside of the steam nozzle, at the top of the tube bundle, and at the region just above the tubesheet as compared to the amplitude of the pressure oscillations imposed at the steam line boundary. At low frequency, the calculated amplitude of the pressure oscillations at the tubesheet is about 7 percent of the amplitude of the applied pressure oscillations in the steam line whereas the amplitude of the pressure oscillations at the U-bends is about 2 percent of the applied amplitude. There appears to be some frequency dependence for the response at low frequencies, particularly near the steam nozzle. This may indicate an acoustic resonance effect at the top of the steam generator since the response is about 90 degrees out of phase with the applied pressure. However, the response in the tube bundle remains low for all the analyzed frequencies. For frequencies above 30 Hertz, the calculated response in the tube bundle is negligible.

Figures 4-19 and 4-20 show the detailed transient pressures for 10 and 30 hertz. At low frequency, there is distortion of the signal between the applied pressure and the response. This may be due to resistances in the flow paths that tend to generate reflections in the pressure signal. These distortions disappear at the higher frequencies analyzed.

4.9 HEAT TRANSFER FROM THE PRIMARY COOLANT AND STORED HEAT IN THE METAL

For hot standby conditions, the temperature of the primary coolant and the metal in the steam generator will be the same as the temperature of the secondary fluid and heat transfer will be negligible. After the steam line break occurs, the secondary side will begin to depressurize and the temperature of the fluid will drop according to saturation conditions. Heat transfer from the primary coolant and the metal will increase due to the increasing temperature difference resulting in the transfer of additional energy to the secondary side fluid. Since the peak pressure drops across the tube support plates occur on initial flashing

of the secondary side early in the transient, these peak pressure drops will not be significantly affected by heat transfer when the steam line break occurs from hot standby.

The effect of heat transfer later in the transient results in two compensating effects. On the one hand, the additional heat transfer will tend to generate additional voids due to the increased energy. On the other hand, the increased energy will tend to maintain pressure that results in a slower rate of depressurization and the corresponding swell that accompanies it. This is one of the reasons why the steam line break from full power operating conditions is less severe than that from hot standby conditions. Preliminary calculations which incorporated the heat transfer from the metal by adding the appropriate term to the energy equation of the secondary fluid indicate the effect on tube support plate pressure drops is small.

4.10 POTENTIAL FOR WATER SLUG CONTRIBUTING TO TUBE SUPPORT PLATE LOADS

Water slug impacting on structures is usually associated with low pressure two phase flow conditions in constrained sections of horizontal piping. Slug flow is limited to low velocities under these conditions because higher velocities result in turbulent or annular flow regimes.

At low flow velocities, the possibility may exist that voids could coalesce in the tube bundle and form water slugs that might impact the tube support plates. Clearly discernable slug flow is rare in diabatic systems and is not considered to be a problem for the steam generator during normal operation due to the distributed formation of voids during the heat transfer process. Although a depressurization transient also forms distributed voids due to flashing of the hot fluid, due to lack of experience slug flow cannot totally be ruled out during the steam line break transient. Consequently, an estimate of the magnitude of the forces that would be involved is provided below.

For vertical slug flow, the terminal rise velocity is given by the following expression:

$$U_t = k_1 [\, g\, D_b\, (\varrho_l - \varrho_g) / \varrho_l \,]^{1/2}$$

Where: k_1 is an empirical constant and is equal to 0.345, D_b is conservatively taken as the diameter of the steam generator (about 10 feet), g is the acceleration of gravity, and ϱ_l & ϱ_g are the densities of the liquid and vapor phases.

The terminal rise velocity represents the relative velocity between voids and water slugs that could form and be present in vertical flow. As such, it is a good estimate of the peak slug velocities that could be obtained for unconstrained flow in the tube bundle. Since the rise velocity is proportional to the square root of the diameter of the water slug, the worst possible case would occur if a slug formed that fills the complete cross-section of the steam generator. At hot standby conditions of 1020 psia, the terminal rise velocity for such a slug will be about 6.0 feet/sec. The dynamic head associated with liquid flowing at this velocity will be about 0.17 psi. Similarly, at 600 psia the terminal rise velocity of such a slug will be about 6.1 ft/sec with a dynamic head of about 0.19 psi. Since the dynamic pressures associated with slug flow are small compared to the bounding pressure drop through TSPs, slug flow in the tube bundle is not considered significant for the tube support plates during a steam line break. The uncertainty multiplier of 1.5 is sufficient to absorb such a small effect.

4.11 CONCLUSIONS

Hydraulic loads on the tube support plates during the steam line break and feed line break were calculated and analyzed. These hydraulic loads on the TSPs were calculated using the RELAP5 Code for this report and loads using the TRAC-M Code were obtained from Reference 1. The hydraulic loads vary with different initial conditions. Generally, steam generators are in full power operation however, they can be in the hot standby state without power generation. Therefore, both hot standby and full power were considered in the load analyses. Since the hydraulic loads can vary with various input parameters and with the uncertainty of those parameters, a sensitivity study was conducted to derive an uncertainty factor for providing conservative loads for input to the structural evaluation.

Based upon the above evaluation, the following conclusions are drawn:

1. Hydraulic loads on the TSPs during the hot standby initiated SLB with both a small and large break calculated by RELAP5, bound those obtained with TRAC-M.

2. Hydraulic loads on the TSPs during the hot standby initiated small SLB bound those during the hot standby or full power initiated FLB for TSPs with loads large enough to be of concern for TSP displacement analyses (i.e., excluding the two lowest TSPs).

3. Hydraulic loads on the TSPs during hot standby initiated SLB bound those during full power initiated SLB.

4. Hydraulic loads on the TSPs during hot standby initiated SLB with large or small break bound those due to hot standby or full power initiated FLB.

5. A 1.5 uncertainty factor can be used to multiply the best estimate hydraulic loads to conservatively bound the hydraulic loads calculated with worst conditions of the various input parameters.

A steam line break downstream of the flow limiter is the limiting break flow area location based on a Leak Before Break (LBB) analysis performed using the guidance from NUREG-0800, Section 3.6.3 and NUREG-1061, Volume 3. These guidelines provide the NRC accepted LBB evaluation methodology and criteria for a LBB analysis. Consequently, the loads to be applied as the design basis for the limited TSP displacement ARC are the small break loads calculated by RELAP5 with a conservative factor of 1.5 applied for uncertainties in the load analyses. For TSPs 1 - 4 at which the limited TSP displacement ARC is applied, the RELAP5 small break loads are greater than a factor of 1.5 larger than obtained with the TRAC-M code. The factor of 1.5 applied to envelope analysis uncertainties provides additional conservatism for the hydraulic loads. The small break loads are based on a steam line break downstream of the flow restrictor which is located within the containment building.

4.12 REFERENCES

1. Steam Line Break Methodology for PWRs, XN-NF-84-93(P), Exxon Nuclear Company, November 1984.

2. Exxon Nuclear Company Evaluation Model Revised EXEM PWR Small Break Model, XN-NF-49(P) Revision 1, Supplement 1, Siemens Power Corporation, December 1994.

3. RELAP5/MOD2-B&W for Safety Analysis of B&W-Designed Pressurized Water Reactors, B&W Company, January 2000.

4. Mass and Energy Release and Containment Response Methodology, DPC-NE-3003-PA, Revision 1, Duke Energy Company, June 2002.

5. Technical Support for Alternate Plugging Criteria with Tube Expansion at Tube Support Plate Intersections for Braidwood-1 and Byron-1 Model D4 Steam Generators, WCAP-14273, Westinghouse Electric Corporation, February 1995.

6. Model 51 Steam Generator Limited Tube Support Plate Displacement Analysis for Dented or Packed Tube to Tube Support Plate Crevices, WCAP-14707, Westinghouse Electric Corporation, August 1996.

7. South Texas Unit 2; 3V Alternate Repair Criteria Application of Bounding Analysis and Tube Expansions, Addendum to WCAP-15163, Rev 1, Westinghouse Electric Company, January 2001.

8. Krotiuk, W. J., "Pressurized Water Reactor Steam Generator Internal Loading Following a Main Steam or Feedwater Line Break," SMSAB-02-05, Office of Nuclear Regulatory Research, September 2002.

9. Majumdar, S., "Sensitivity Studies of Failure of Steam Generator Tubes during Main Steam Line Break and Other Secondary Side Depressurization Events," NUREG/CR-xxxx, ANL-02/xx, To be published.

Table 4-1
RELAP5 Model Elements for Model 51 SG Secondary Side

Components	Type	# Volumes	# Junctions
2	Pipe	30	29
35	Pipe	3	2
19, 22	Separator	1	3
21, 30, 33, 53	Branch	1	2
34	Branch	1	1
17, 18, 20, 23, 32, 36, 38	Single Volume	1	0
519, 533	Single Junction	0	1
518	Valve	--	--

Table 4-2
RELAP5 Analysis Matrix

Case	Operating Conditions (All Hot Standby)	Analysis Conditions			
		Equilibrium in Tube Bundle	Break Size ft^2	Water Level, inch	TSP Loss Coefficient
Reference Analyses					
SB1	Flow restrictor, non-equilibrium	No	1.4.	490.5	Nom.
SB2	Flow restrictor, equilibrium	Yes	"	"	"
LB1	No flow restrictor, non-equilibrium	No	4.6	"	"
LB2	No flow restrictor, equilibrium	Yes	"	"	"
Worst Case Analyses					
LB3	No flow restrictor, non-equilibrium	No	4.6.	478.5	Max.

Table 4-3
Peak of Hot Standby TSP Pressure Drops in psi
During SLB with Small Break (1.4 ft^2)

Plate #	Case SB1 (Spike Included)	Case SB1 (Spike Excluded)	Case SB2
1	1.91	-0.95	1.12
2	-1.01 (+0.71 spike)	-1.01	1.25
3	0.25	0.25	1.23
4	8.25	1.18	1.35
5	3.20	1.31	1.56
6	3.94	2.11	2.14
7	2.91	2.37	2.26

Table 4-4
Peak of Hot Standby TSP Pressure Drops in psi
During SLB with Large Break (4.6 ft^2)

Plate #	Case LB1	Case LB3
1	1.76	1.76
2	5.66	1.52
3	9.38	12.77
4	9.63	11.08
5	9.44	10.89
6	9.32	11.50
7	8.69	12.70

Table 4-5
Peak of Hot Standby SLB TSP Pressure Drops in psi
By TRAC-M and RELAP5

Plate #	Small Break (1.4 ft^2)		Large Break (4.6 ft^2)	
	RELAP5	TRAC-M	RELAP5	TRAC-M
1	1.12	-0.05	1.76	-0.33
2	1.25	0.09	5.66	0.15
3	1.23	0.40	9.38	1.16
4	1.35	0.85	9.63	2.63
5	1.56	1.20	9.44	3.84
6	2.14	1.66	9.32	5.06
7	2.26	2.68	8.69	8.57

Table 4-6
Peak of Hot Standby and Full Power TSP Pressure Drops in psi
from FLB and from Hot Standby Small SLB

Plate #	Hot Standby FLB by TRAC-M	Full Power FLB by TRAC-M	Hot Standby Small SLB by TRAC-M	Hot Standby Small SLB by RELAP
1	0.020	0.19	-0.05	1.12
2	0.022	0.18	0.09	1.25
3	0.026	0.22	0.40	1.23
4	0.030	0.26	0.85	1.35
5	0.034	0.31	1.20	1.56
6	0.040	0.36	1.66	2.14
7	0.050	0.42	2.68	2.26

Table 4-7
TRANFLO Analysis Matrix

a,c

Table 4-8
SLB Peak TSP Pressure Drops and Ratio of Each Case to Case 1

a,c

Table 4-9
Results of Frequency Response Analysis
For Pressure Oscillations in Steam Line

Frequency	Relative Response in Percent		
	Inside Nozzle	U-Bends	Tubesheet
10	7.2	1.9	6.7
20	4.2	4.9	8.0
30	16.9	0.8	1.1
40	5.5	0.1	0.1
50	3.0	0.05	0.05

a,c

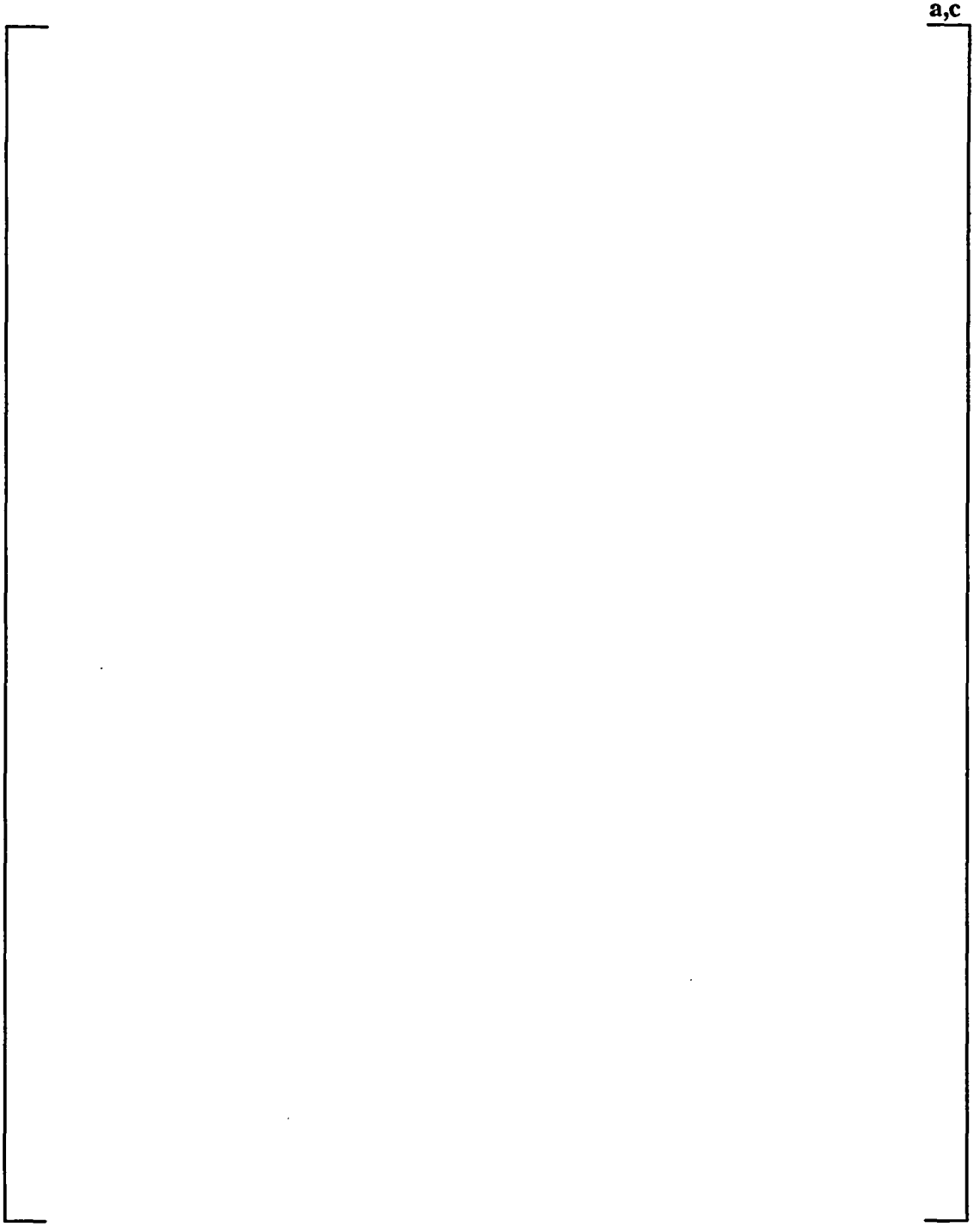

Figure 4-1
Schematic of Model 51 Steam Generator with Flow Paths

a,c

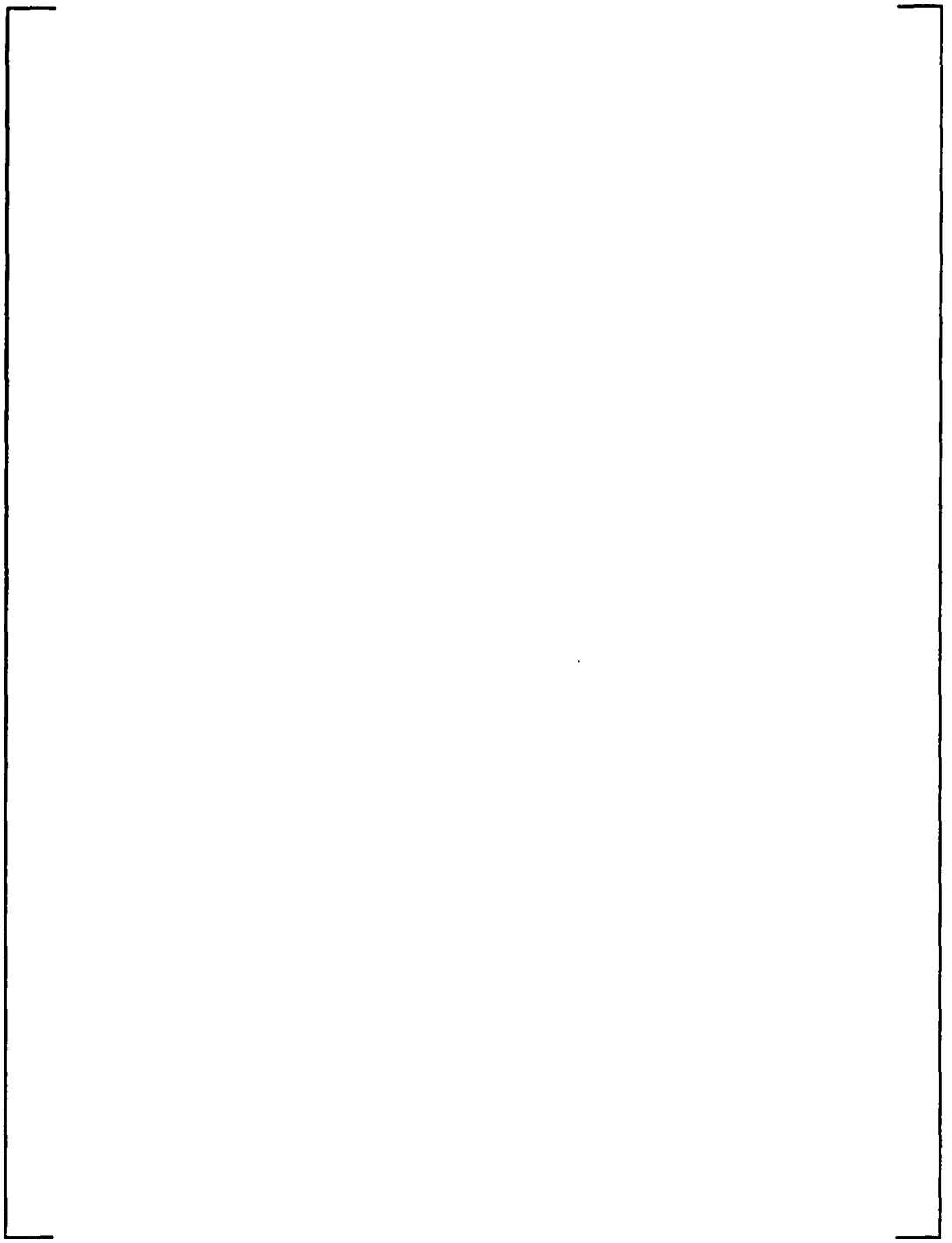

Figure 4-2
General Arrangement of Nodes
and Nodal Number of RELAP5 Model 51 SG

a,c

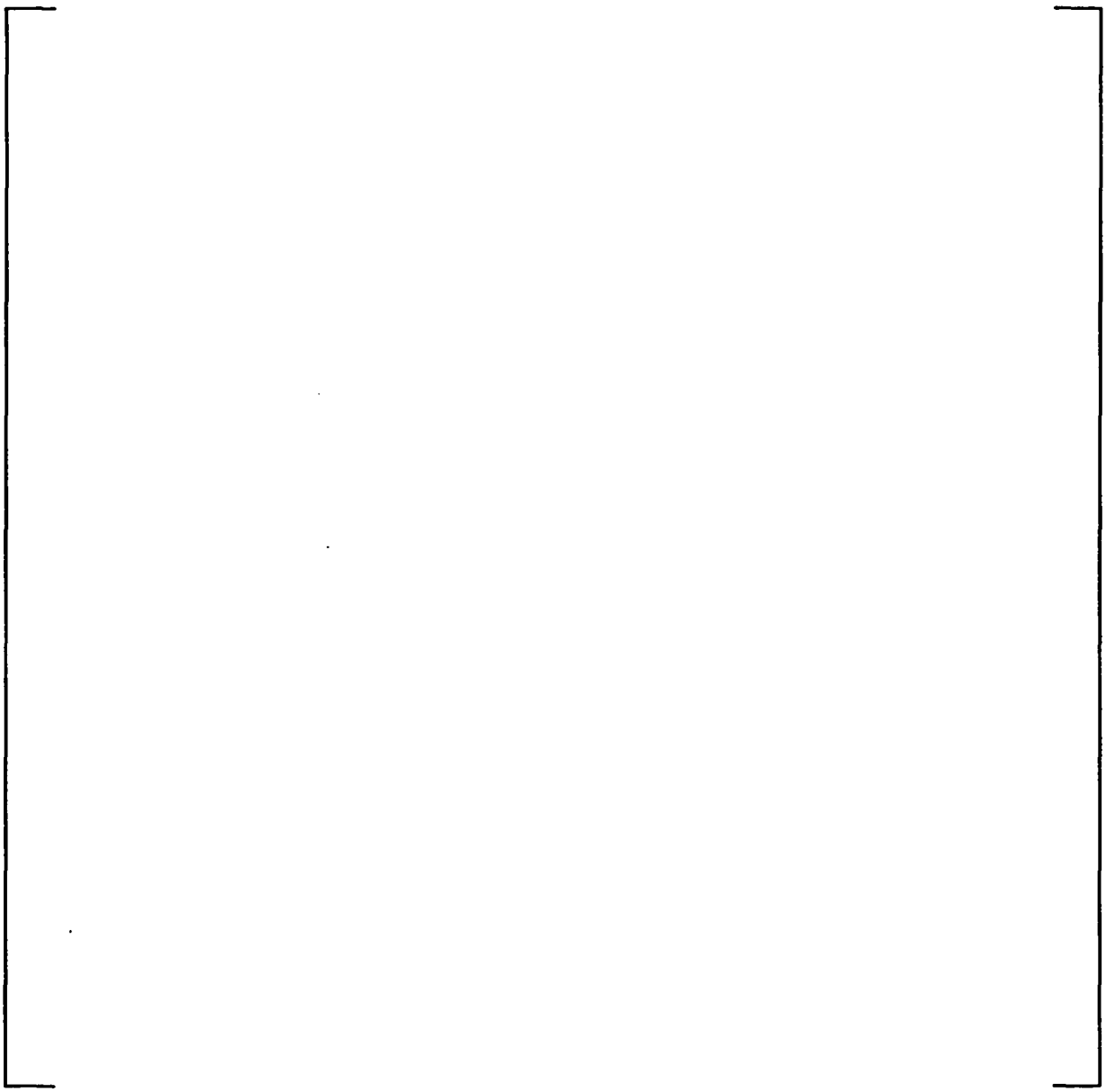

Figure 4-3
RELAP5 Model 51 SG Secondary Side Model

a,c

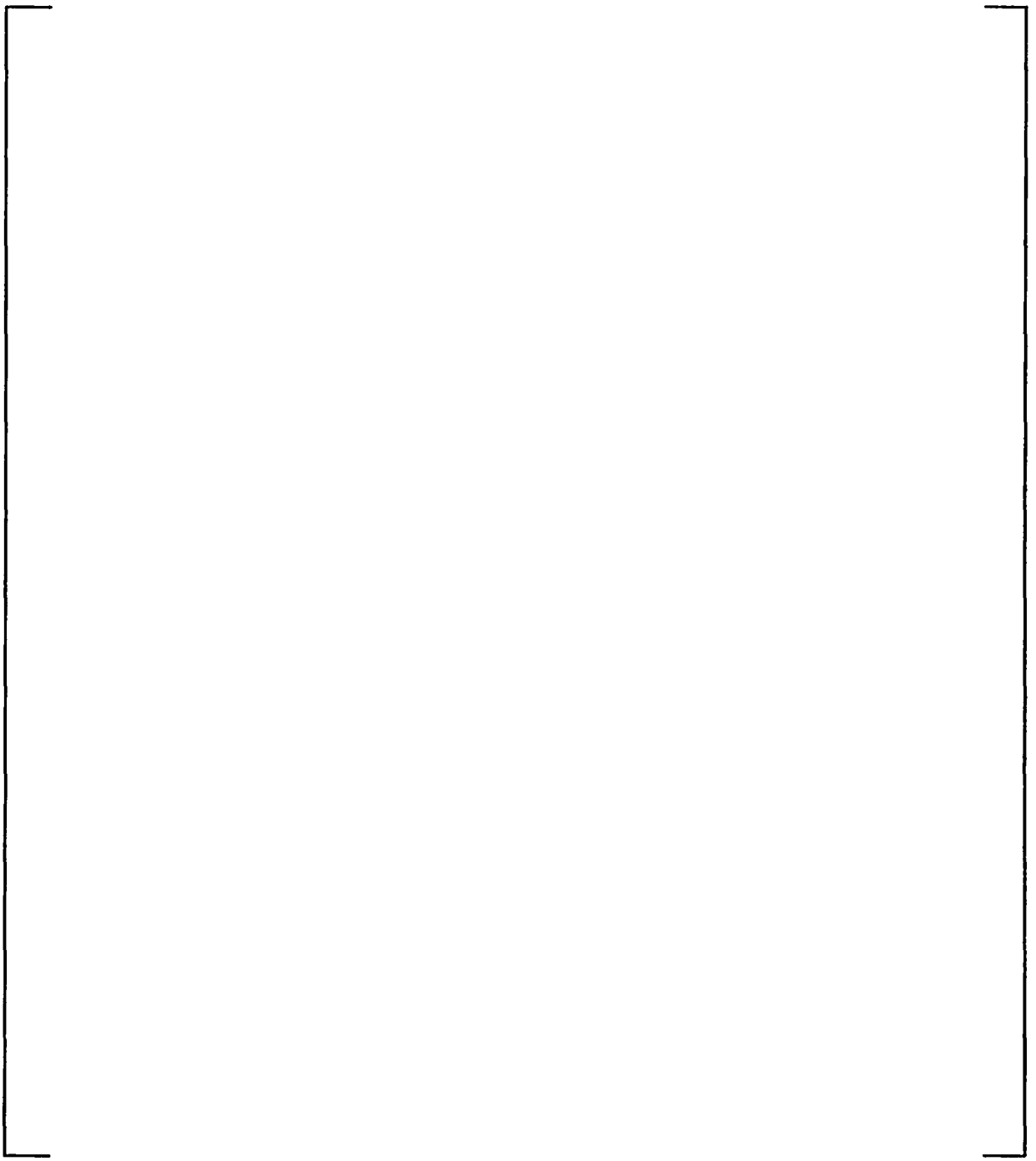

Figure 4-4
RELAP5 Tube Bundle Model

a,c

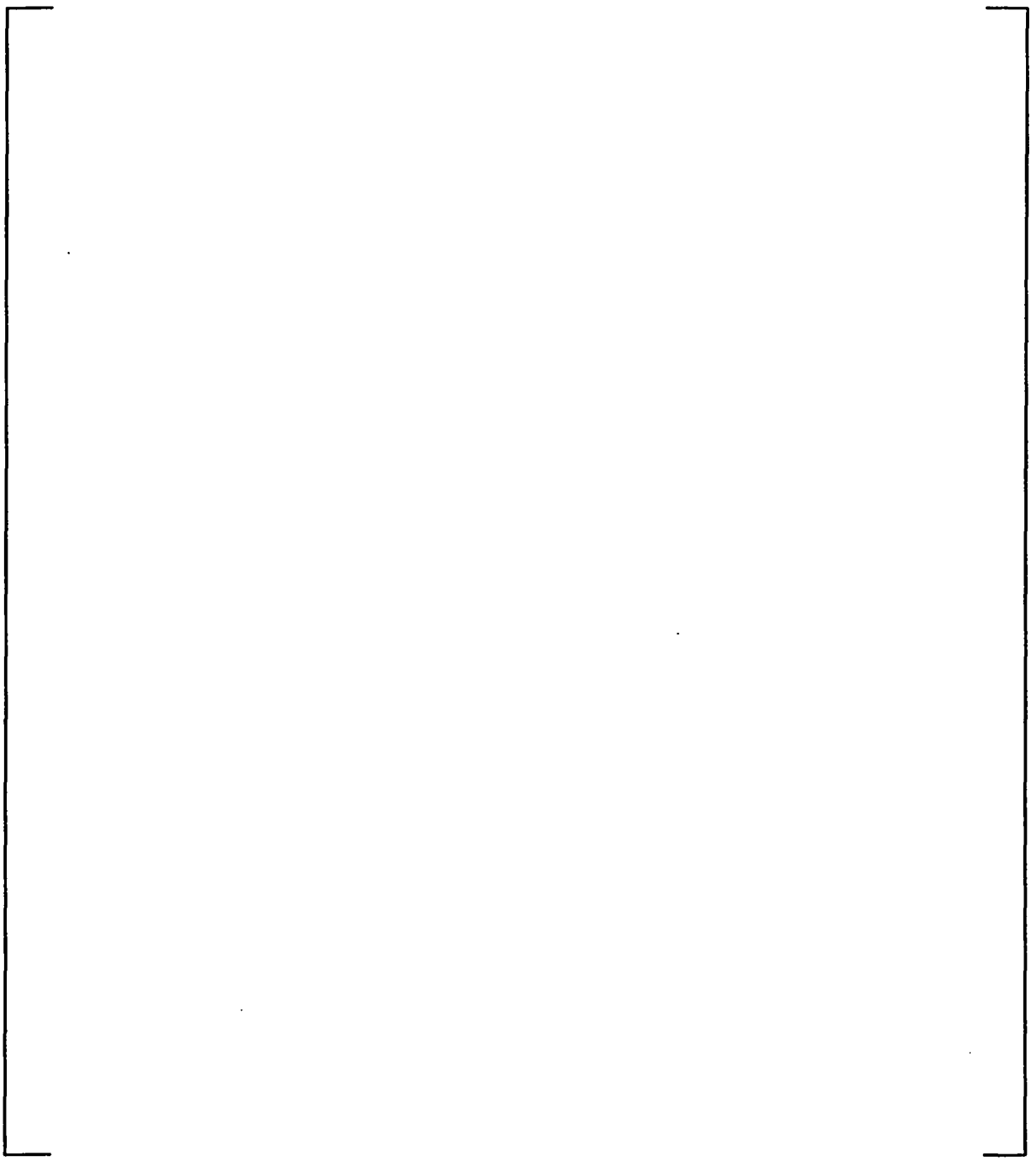

Figure 4-5
RELAP5 Primary Side Model

a.c

Figure 4-6a
Tube Support Plate Pressure Drops, Case SB1, 1.4 ft^2 Flow Restrictor
(Non-equilibrium. Odd numbered plates)

a,c

Figure 4-6b
Tube Support Plate Pressure Drops, Case SB1, 1.4 ft^2 Flow Restrictor
(Non-equilibrium. Even numbered plates)

a,c

Figure 4-6c
Tube Support Plate Pressure Drops, Case SB1, 1.4 ft^2 Flow Restrictor
(Non-equilibrium. Expanded Time Scale)

a,c

Figure 4-7
Tube Support Plate Pressure Drops,
Case SB2, 1.4 ft^2 Flow Restrictor (Equilibrium)

a.c

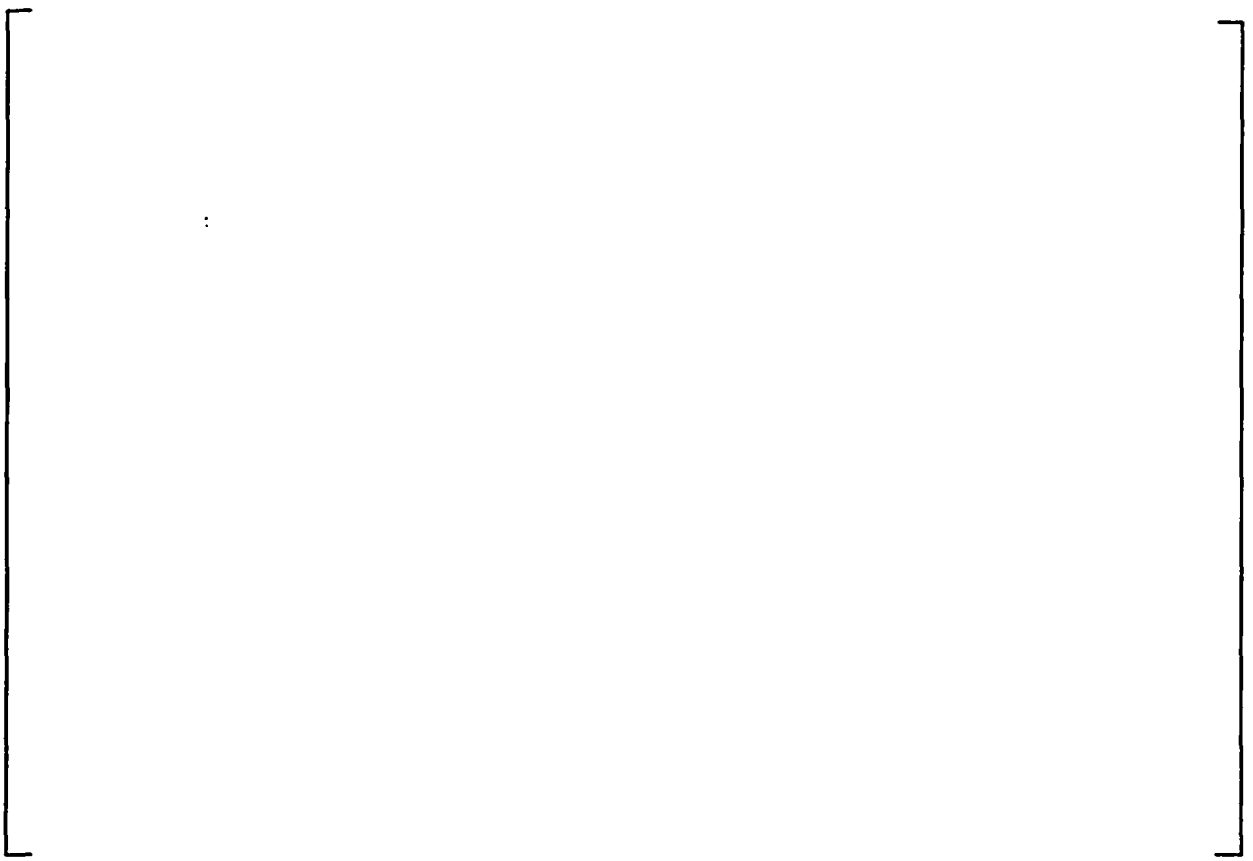

Figure 4-8
Tube Support Plate Pressure Drops,
Case LB1, 4.6 ft^2 Break Flow Area (Non-equilibrium)

a.c

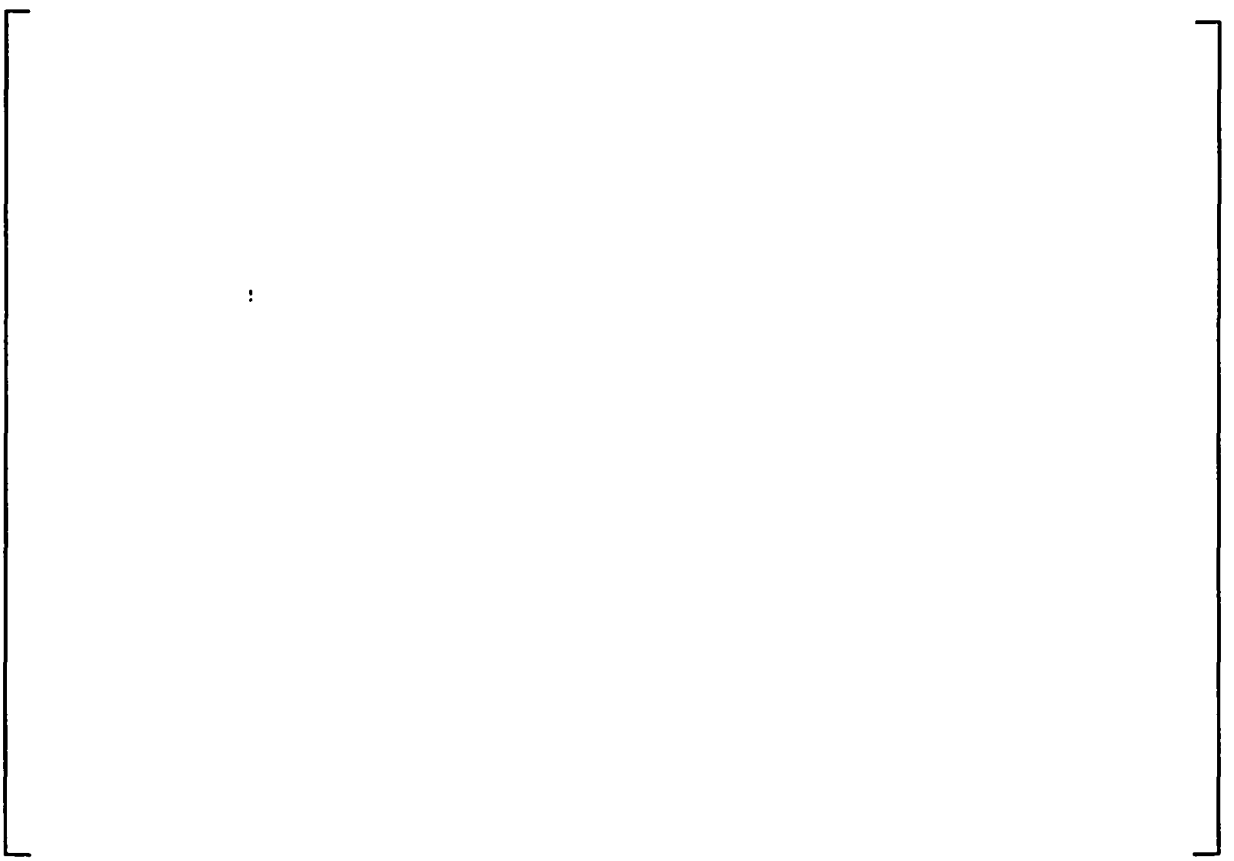

Figure 4-9
Tube Support Plate Pressure Drops,
Case LB2, 4.6 ft^2 Break Flow Area (Equilibrium)

a,c

Figure 4-10
Blowdown Flow Rate During SLB Event

a,c

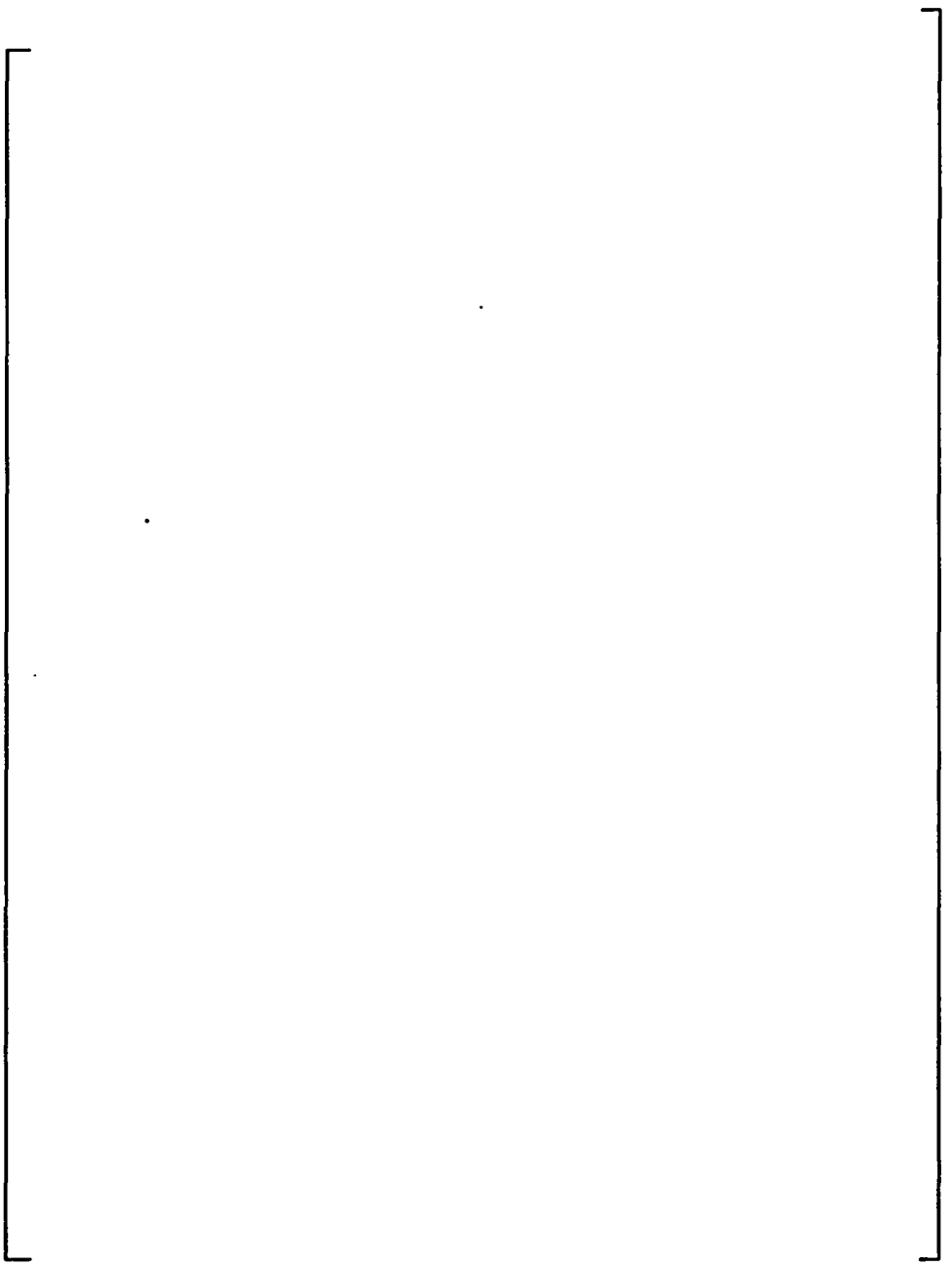

Figure 4-11
Node Layout for TRANFLO Model
of the Model 51 Steam Generator

a,c

Figure 4-12
Tube Support Plate Pressure Drops, Case 1

a,c

Figure 4-13
Tube Support Plate Pressure Drops, Case 2

a,c

Figure 4-14
Tube Support Plate Pressure Drops, Case 3

a,c

Figure 4-15
Tube Support Plate Pressure Drops, Case 4

a,c

Figure 4-16
Tube Support Plate Pressure Drops, Case 21

a,c

Figure 4-17
Tube Support Plate Pressure Drops, Case 61

a,c

Figure 4-18
Tube Support Plate Pressure Drops, Case 62

a,c

Figure 4-19
Attenuation of 10 Hertz Pressure Oscillations
Originated in Steam Line

a,c

Figure 4-20
Attenuation of 30 Hertz Pressure Oscillations
Originated in Steam Line

5.0 TSP DEFLECTION ANALYSIS

5.1 ANALYSIS OVERVIEW

This section summarizes the analysis to determine relative tube / tube support plate motions under steam line break loads for Diablo Canyon Units 1 and 2. The fundamental premise is that tube degradation that occurs inside the tube support plates (TSP) has limited leakage due to the presence of the tube support plates. However, it must be shown that under steam line break loads that the tube support plates do not displace relative to the tubes exposing the axial cracks in the tubes (more than an acceptance limit) and losing the benefit gained from the presence of the tube support plates in limiting burst and leakage. It should be noted that seismic loads on the tube support plates in the vertical direction are small in comparison to the steam line break pressure loads. As a result, this analysis only considers plate displacements resulting from steam line break.

It has been determined (Section 10) that relative tube / TSP displacements of up to 0.15 inch are acceptable without compromising the burst and leak requirements for the tubes. Due to the flexibility of the tube support plates for out-of-plane loads, the displacements of the plates will exceed 0.15 inch for the design configuration. In order to limit the plate displacements it is planned to expand a number of tubes such that the expansion length extends both above and below the tube support plates. In this way the tubes will act as additional supports, retarding the vertical displacement of the plates. The number and location of the tube expansions is expected to vary from plate to plate depending on the magnitude of the applied pressure loading.

The analysis involves the preparation of a 180° tube bundle model that includes both the hot and cold leg sides of the tube bundle, consisting of the seven tube support plates, tierods, spacers, channel head, lower shell, wrapper, and tubesheet. Elements are also included to represent the expanded tubes and the expansion zone interfaces between the tubes and support plates. The WECAN computer code, a general purpose finite element code, is used to develop the model. Modal calculations are performed to define applicable dynamic degrees of freedom (DOF). Once the DOF are defined, a global substructure is generated for the overall tube bundle. The dynamic response of the plates is then calculated using the special purpose computer program, *pltdym*.[1]

It is the relative tube / TSP displacement that is of interest, with the tube and plate positions at the start of the SLB transient defined as the reference position. At hot standby, the TSP positions relative to cracks inside the TSP are essentially the same as at cold shutdown. Every known SG cold condition inspection shows outside stress corrosion cracks within the TSP with a trend towards being centered within the TSP. Therefore, the cold condition TSP location relative to the tubes is essentially the same as for the full power condition where the cracks formed, which is also the position during hot shutdown. These inspections indicate that there is little relative movement between the tubes and plates throughout the operating cycle. Thus, this analysis calculates relative tube / TSP motions based on the tube / TSP positions at the initiation of the SLB transient.

---

[1] The Staff has reviewed and accepted the use of the computer code *pltdym* for predicting plate displacements under steamline break loads in Reference 1, page 10.

The dynamic analysis is performed assuming elastic response of the plate support structures. Thus, in order to support the analysis displacement results, calculations are performed to demonstrate the applicability of the elastic analysis approach in determining the resulting displacements. These calculations consist of showing that the tierods / spacers remain elastic throughout the transient, that the expanded tubes remain elastic, that significant yielding of the tube support plates does not occur, and that the welds joining the wedges and support bars to the wrapper remain intact.

5.2 DYNAMIC ANALYSIS PARAMETERS

5.2.1 Tube Support Plate Support System

The TSPs are supported vertically using several support mechanisms. A schematic of the tube bundle region is shown in Figure 5-1. The TSPs are supported vertically using a central tierod / spacer and four outer tierods / spacers located near the edge of the plate. The in-plane support for the TSPs is provided by tapered wedges located around the periphery of each plate. The manner in which the wedges are welded in place varies for different steam generator models. For the Model 51 steam generators at Diablo Canyon, the wedges are welded to both the wrapper and tube support plate on both top and bottom surfaces. As a result of the wedges being welded to both the TSP and wrapper, the wedges also provide restraint to vertical motions of the support plates. Finally, there are two bar supports welded between each TSP and wrapper, located 180° apart. Sketches showing the wrapper / wedge / TSP and the wrapper / support bar / TSP interfaces are provided in Figure 5-2. The angular locations for the wedges and support bars are shown in Figure 5-3 for TSP 1 and in Figure 5-4 for TSPs 2 - 7.

Regarding the tierods and spacers, the tierods are bars that are threaded into the tubesheet and run the full height of the tube bundle with a nut on the upper side of the top TSP. Note that the nut is welded to both the tierod and the top surface of the TSP. Around the outside of the tierods are spacers that are located between each of the support plates for positioning purposes. For the central tierod, the spacers are welded to each of the TSPs, with the exception of the spacer between the tubesheet and first TSP, which is not welded to the tubesheet. For the spacers located at the periphery of the TSPs, there are no rigid links between the spacers and the support plates.

The lack of a rigid link between the spacers and TSPs for the outer tierods / spacers results in a non-linear dynamic system. The TSP / spacer non-linearities are included in the dynamic solution. The tierods / spacers have different stiffness characteristics for upward and downward loads, and these differences are also incorporated into the model. For the up direction, the load path is through the spacers from the loaded plate to the one above it, up through the bundle to the top plate, where the load is transferred to the tierod and down to the tubesheet. For the down direction, the load path is through the spacers from the loaded plate to the one below it down through the bundle to the tubesheet. In general, the down load path is several times as stiff as the up load path.

5.2.2 Component Materials

A specification of component materials is contained in Table 5-1, with the corresponding material properties summarized in Table 5-2 through Table 5-7. The properties in these tables are taken from the 1965 edition of the ASME Code. The applicable editions of the Code for the Diablo Canyon steam generators are 1965-S66 and 1965-W65 for Units 1 and 2, respectively. Values for material density,

which is not specified in the ASME Code, are taken from open literature. It should be noted that although the properties are provided over the temperature range 70°F - 700°F, the average temperature during the SLB transient, based on the thermal hydraulic results, is ≈530°F. Since temperature dependent properties cannot be used in substructures, properties for the finite element model correspond to the values at 530°F. In addition, the material properties for the tubesheet and tube support plates must be modified to account for the tube penetrations and flow holes, and to account for added mass effects of the secondary side fluid. Additional details of the material property modifications are provided in Section 5.2.5.

5.2.3 Geometric Parameters

A summary of geometric parameters used in this analysis is provided in Table 5-8. Prior to the tube expansion effort, Diablo Canyon is planning to chemically clean both Units 1 and 2. As a result of the chemical cleaning material loss will occur for the carbon steel components. The upper bound material loss used to qualify the chemical cleaning process and the resulting component dimensions (used for this analysis) are provided in Table 5-9. Note that due to the presence of corrosion products in the tube-to-plate annulus, the chemical cleaning agents will not penetrate the crevice and the size of the tube hole is not affected by the chemical cleaning.

5.2.4 Expansion Zone Stiffness

A schematic of a typical expanded tube joint is shown in Figure 5-5. Recognize that although the sketch shows the axis of the tube to be in the horizontal direction, the tubes are oriented vertically in the steam generator. Under applied SLB pressures, the TSP will want to move vertically past the bulged region of the tube. The direction of the tube motion is a function of the pressure drop across the TSP, and whether the pressure drop is in the up or down direction. In order to determine the resistance (stiffness) of the tube to motion of the plate, a series of pull tests were run on prototypic expanded joints. Results of the tests are discussed in Section 6.5. Based on the results of the test program, the expansion zone stiffness selected for this analysis is [ ]^{a,c} lb/in.

5.2.5 Revised Material Properties

As noted earlier, the material properties for the tubesheet and TSP are modified to account for the tube holes in the tubesheet, and both the tube and flow holes in the TSP. The modified properties include Young's modulus, Poisson's ratio, and the material density. In the case of the TSPs, the density is additionally modified to account for the added mass of the secondary side fluid.

In establishing effective values for Young's Modulus and Poisson's ratio for the TSPs and tubesheet, separate formulations must be used due to the presence of flow holes in the TSPs, but not in the tubesheet. Also, because of the square penetration pattern, different properties exist in the pitch and diagonal directions. The equivalent Young's modulus for the overall plate is taken as the average of the values in the pitch and diagonal directions. Once an effective Young's modulus is calculated, the equivalent value for Poisson's ratio is determined using the relationship between Young's modulus and the shear modulus. For the tube support plates, the effective elastic constants are assumed to apply from the centerline of the first tube row out to the edge of the plate.

There are two aspects to revising the tube support plate density. The first is based on a ratio of solid plate area to the modeled area. The second corresponds to the plate moving through and displacing the secondary side fluid, creating an "added mass" effect. The resulting added mass is a direct function of the fluid density. Since the dynamic analysis cannot account for the change in fluid density with time, the analysis uses an average density value for the transient. Because the peak pressure loads occur over the initial 0.5 second of the transient, the average fluid density is calculated for this same time interval. The effective density for the tubesheet includes both the mass of the tubesheet and the mass of the tubes which are welded to the tubesheet bottom surface.

A summary of the resulting revised material properties for the tubesheet and tube support plates is provided Table 5-10.

5.2.6 Finite Element Model

The finite element model used to simulate the tube bundle response, shown in Figure 5-6, includes a 180° sector of the bundle. The model includes both the hot and cold leg sides of the tube bundle, consisting of the seven tube support plates, tierods, spacers, channel head, lower shell, wrapper, and tubesheet. Elements are also included to represent the expanded tubes and the expansion zone interfaces between the tubes and support plates. The tierods, spacers, and expanded tubes are modeled using three-dimensional beam elements, with the tubesheet, channel head, shell, and wrapper being modeled using three dimensional shell elements. The expanded tube expansion interface with the tube support plates is modeled using spring elements. In modeling the plates, the flow slots along the tubelane are modeled explicitly. In terms of material properties, equivalent properties are specified only in the tubed region of the plate. Actual plate properties are used along the tubelane.

A schematic of a typical expanded tube / TSP interface is shown in Figure 5-7. The expanded tube stiffness represents the action of pulling the plate up or down over the expanded region, or an extrusion process. Thus, this stiffness represents the interaction between the plate and tube, but is not in series with the plate above and/or below a given intersection.

5.2.7 Single Plate Model Analysis

Since the tube expansions are to be performed primarily on the hot leg side of the bundle, it is necessary to consider the effect of the plate response from the cold leg side of the bundle on the hot leg side. This requires a model that simulates the response of both the hot and cold legs of the bundle. In developing the finite element model of the tube bundle it is desired to utilize symmetry of the bundle as much as possible. In the case of the Model 51 tube bundle, geometric symmetry of the bundle exists about the tube bundle centerline that separates the left and right sides of the bundle. However, as shown in Figure 5-3 and Figure 5-4, the support system for the tube support plates is not symmetric about the bundle centerline.

Because a full 360° model of the tube bundle will result in a model size that exceeds the solution capability of the dynamics code, it is necessary to simulate the bundle response using boundary conditions that are representative of the actual configuration, and which are concluded to provide a bounding analysis for the actual support conditions. Thus, prior to performing the dynamic analysis of the bundle a preliminary set of calculations is performed using a single plate model to investigate the

effects of different support conditions for the plate. The finite element model used for the single plate evaluation to investigate the effects of different support conditions is shown in Figure 5-8. The element and node layout for the tube support plate is essentially identical to that used for the full bundle model, except that it has been duplicated and expanded to be a full 360° representation of the plate. Note that for the simplified model, the elements representing the tierods and expanded tubes are modeled above the plate. This is only for ease of viewing the model and does not affect the analysis results. Note that the expanded tube locations for the single plate analysis are based on preliminary calculations where hot leg only expansion was considered. However, the introduction of additional cold leg expansions will only enhance the symmetry aspect of the plate supports and deemphasize the significance of the offsets of the wedge supports. Thus, the use of the hot leg only expanded tube positions is considered a conservative representation of the final plate support system.

For the simplified model, the plate is represented using three-dimensional shell elements (the same as for the full model), while the tierods and expanded tubes are modeled using spring elements. A summary of the analysis cases considered using the single plate model is provided in Table 5-11. For each case, the plate is loaded with a 1.0 psi loading over the entire face of the plate. The plate is restrained against vertical motion along its outer edge at nodes corresponding to the wedge and support bar locations.

Referring to Table 5-11, Case 1 provides a reference set of displacements for the case without expanded tubes. A plot of the displaced geometry is shown in Figure 5-9. A second plot of the vertical displacement contours is provided in Figure 5-10. These plots show the effect of the non-symmetric wedge locations on the vertical displacement of the plate. While there is an asymmetry of sorts about the vertical centerline of the bundle, this cannot be effectively simulated with centerline boundary conditions. The effects of the expanded tubes on the displacement results are shown in Figure 5-11 and Figure 5-12. Again, there is a general symmetry about the vertical centerline. There is a noticeable variation in the deflection along the tubelane, particularly at the outer edge of the plate.

Due to the near symmetry conditions, Cases 3 and 4 calculated the plate displacement assuming symmetry about the plate centerline. Case 3 assumes the plate is constrained using the boundary conditions from Case 2 for the right side (+X) of the plate. Similarly, Case 4 assumes the plate is constrained using the boundary conditions from Case 2 for the left side (-X) of the plate. The displaced geometry plot for Case 3 is shown in Figure 5-13 with the displacement contour plot shown in Figure 5-14. Similar plots for Case 4 are provided in Figure 5-15 and Figure 5-16. Comparing the displacement contour plots in Figure 5-14 and Figure 5-16 with the displacement contours in Figure 5-12 shows that the assumption of symmetry along the vertical centerline provides a very good approximation of the full plate solution. The results also show, however, that neither of the support conditions provides a bounding set of displacements at all locations on the plate. Thus, the full bundle dynamic analysis with a 180° representation of the bundle must consider two support cases, one with the "right-side" wedge support locations and the second with the "left-side" wedge support locations.

5.2.8 Dynamic Degrees of Freedom

In setting up the global substructure, it is necessary to define the dynamic degrees of freedom for the structure. In this case, it is the dynamic degrees of freedom for the tube support plates. The channel head, shell, and wrapper are present primarily as support structures. In order to define dynamic degrees of freedom for the TSPs, two sets of modal calculations are performed. The first set of calculations

determines plate mode shapes and frequencies using a large number of degrees of freedom (approximately 75 per plate). The second set of calculations involves repeating the modal analysis, using a significantly reduced set of degrees of freedom (DOF). The reduced DOF are selected to predict all frequencies for a given plate below 75 hertz to within 10% of the frequencies for the large set of DOF. A frequency of 75 hertz is selected as a cutoff, as it is judged that higher frequencies will have a small energy content compared to the lower frequencies. Calculations are performed for both the left-side and right-side sets of boundary conditions.

As will be shown in Section 5.5, the same expansion locations are defined for TSPs 2, 3, and 4, and for TSPs 5, 6, and 7. Thus, three sets of modal calculations are necessary for selecting the DOF, one for TSP 1, one for TSPs 2, 3, and 4, and one for TSPs 5, 6, and 7. For the two groups of plates, TSP 4 and TSP 7 are selected for performing the modal calculations. Since the stiffness of the expanded tubes decreases with distance above the tubesheet while the magnitude of the load increases, TSPs 4 and 7 are expected to experience the highest deflections.

In calculating the TSP mode shapes and frequencies, each plate is considered separately. The channel head, shell, wrapper, and tubesheet are deactivated for the modal calculations. The tierods and spacers are included in the model as spring elements with an effective stiffness. Because the dominant loading for SLB is in the upward direction, an effective stiffness is calculated for the tierods / spacers for an upward load. Since each plate is considered separately for the modal runs, the plates are assumed to be coupled to the upper end of the tierods at the appropriate nodal locations. At locations corresponding to wedges and support bars, the nodes are constrained against vertical motions. Finally, for the expanded tube locations, the tubes are also represented by an effective stiffness.

The process to select the final set of dynamic DOF for each plate requires several iterations. An initial run is made with a large number of DOF, and then a series of runs is made with a reduced set of DOF until the mode shapes and frequencies for the reduced set of DOF are concluded to match the results for the large number of DOF. The frequencies are concluded to match if the frequencies for the reduced set are within 10% of the frequencies for the large set of DOF, and if the mode shapes for the reduced set of DOF are judged to match the mode shapes for the large number of DOF.

Calculations are performed for TSPs 1, 4, and 7 for both the right-side and left-side wedge positions. A summary of the frequency calculations comparing the large number of DOF with the reduced set is provided in Table 5-12. The final set of DOF selected for each plate is concluded to accurately predict the plate response for both sets of boundary conditions.

Plots showing the DOF locations for the tubesheet and TSP are provided in Figure 5-17 and Figure 5-18. The node numbers in these figures correspond to the tubesheet geometry. As noted earlier, it is the relative displacement between the tubes and plates that are of interest. Because the unexpanded tubes will move vertically based on tubesheet motions, dynamic degrees of freedom are defined for the tubesheet at the same planar locations as for the TSP. In addition, DOF are defined for the expanded tube nodes at locations where tube expansions are defined. Overall, there are 467 DOF defined for the analysis.

5.2.9 Displacement Boundary Conditions

The displacement boundary conditions for the substructure generation consist of the following:

1. Symmetry conditions along the "Y" axis for each of the components.

2. The base nodes for the expanded tubes are coupled to the corresponding tubesheet nodes for all degrees of freedom.

3. The plates are coupled to the wrapper consistent with the wedge and support bar locations. The plates are coupled to the wrapper for all six DOF at the wedge positions and the three translational DOF at the vertical bar locations. Preliminary results showed that the vertical bar welds will yield in bending forming a plastic hinge. Thus, only the translational DOF are coupled.

4. Constraint of the channel head at support locations.

Note that two different substructures are generated. One for the right-side support conditions and one for the left-side support conditions.

5.2.10 Integration Time Step / Structural Damping

The dynamic time step used in evaluating the SLB transient is 0.0001 second. Prior analyses of a similar nature have shown that a time step 0f 0.0001 second is sufficiently small to achieve a converged solution. In terms of damping, the analysis incorporates structural damping of 4%, which is judged to be a conservative value for the type of dynamic loading and response being considered.[2] That is, movement of the plates through the secondary fluid with a very large number of tube / TSP intersections that can introduce frictional loads that will tend to retard the plate displacement.

5.2.11 Application of Pressure Loads

The transient pressures are relative to the control volume for the thermal hydraulic analysis. The area over which the hydraulic pressure acts corresponds to the area inside the wrapper minus the tube area. Thus, the pressure drops are converted to loads on the TSP by multiplying the hydraulic loads by the corresponding area of the control volume, 54.22 ft^2. These loads are converted to pressures acting on the plates by dividing the total load by the model plate area for each of the plates. In addition, a factor of 1.5 is applied to the loads to account for uncertainties in the thermal hydraulic analysis. Plots of the final pressure time histories, as applied to each of the plates, are shown in Figure 5-19.

5.3 SELECTION OF TUBE LOCATIONS FOR EXPANSION

The process to select the number and location of the tube expansions is an iterative calculation. The process steps to arrive at the final set of expansions are as follows.

1. Based on the results of an analysis case without tube expansion, an initial set of expansions is selected and introduced to the finite element model.

---

2 The Staff has reviewed and accepted the use of 4% damping for evaluating plate displacements subject to steamline break loads in Reference 1, page 9.

2. Modal calculations are performed to determine an appropriate set of dynamic degrees of freedom to simulate the plate response with the increased stiffness due to the presence of the expanded tubes.

3. Using the resulting dynamic degrees of freedom, global substructures are generated to calculate the system mass and stiffness matrices.

4. Using the set of expansions from Step 1 and the mass and stiffness matrices from Step 3, the resulting plate displacements subject to the SLB transient are calculated. Due to the system non-linearities resulting from the plate / spacer interactions, the dynamic time history solution can be rather lengthy in compute time, up to a day or more of elapsed time. However, based on a review of the load time histories, where it is observed that the pressure loads on the plates occur at approximately the same time, it is expected that the spacers will be in compression during the majority of the transient. As such, an approximate linear solution is used, where the spacers for TSPs 3-7 are assumed to be linear.

5. Steps 1, 3 and 4 are repeated until the relative tube / TSP displacements are below the 0.15 inch displacement for the hot leg region of TSPs 1 through 4.

6. Checks of the following parameters are performed to determine if appropriate limits are satisfied.

   a. Check to determine that the tension / compression for the expansion zones is consistent with the value used to establish the tube expansion zone stiffness.

   b. Check the force in the expanded tubes to show that the tubes remain elastic during the dynamic transient.

   c. Check the stresses in the tierods and spacers to show that both components remain elastic during the dynamic response.

   d. Check the stresses for the hot leg of TSPs 1 through 4 to show that the average ligament stresses are less than yield.

   e. Check the stresses in the welds joining the wedges and support bars to the plates and wrapper to show that the welds remain intact during the SLB transient.

7. If any of the criteria of Step 6 are not satisfied, then additional tube expansions are incorporated in the system model and Steps 3- 6 are repeated until each of the criteria are satisfied.

8. Repeat the modal calculations of Step 2 to assure that the reduced set of dynamic degrees of freedom accurately predict the response of the system with the final set of expansions. (Note that the modal calculations in Section 5.2.8 are for the final set of DOF used in this analysis.)

9. Repeat the dynamic solution for a fully non-linear case to show that the linear assumption accurately predicts the plate response. If the linear solution is found to give acceptable results, then the final set of expansions is concluded to meet all of the necessary criteria.

5.4 ANALYSIS RESULTS

5.4.1 TSP Displacement Results

As discussed previously, this analysis calculates relative tube / TSP motions based on the tube / TSP positions at the initiation of the SLB transient. These displacements are calculated in two steps. First the relative tube / TSP displacement is calculated at each plate dynamic degree of freedom by subtracting the tubesheet displacement at a geometric position in line with the plate DOF from the plate displacement. (Note that it is conservatively assumed for this analysis that the tubes move as rigid bodies with the tubesheet. Axial strains in the tubes due to the increase in differential pressure, which tend to offset plate displacements, are not considered.) This subtraction process is conducted for each transient time point to arrive at the maximum variation during the transient. A relative change in displacement from the initiation of the transient is obtained by subtracting the relative tube / TSP displacement at time equal zero from the transient value at each time point.

Displacement results are provided for two sets of plate / spacer interactions, a pseudo-linear condition, and a fully non-linear solution. In addition, each of the plate / spacer interaction conditions are solved for both the right-side wedge supports and for the left-side wedge supports. A summary of the maximum relative tube / TSP displacement for each plate is provided in Table 5-13 for the pseudo linear case. Plots of the relative tube / TSP displacement for the right-side support conditions are provided in Figure 5-20 for TSPs 1-4 and in Figure 5-21 for TSPs 5-7. Plots of the relative tube / TSP displacement for the left-side support conditions are provided in Figure 5-22 for TSPs 1-4 and in Figure 5-23 for TSPs 5-7.

Comparison of the results for the pseudo linear case and the fully non-linear spacer case is provided in Table 5-14 and shows only small variation between the two sets of results. For TSP 1-4, the linear spacer case is shown to give slightly conservative results relative to the non-linear case. Thus, it is concluded that the results for the linear spacer condition provide an acceptable approximation of the non-linear condition.

5.4.2 Tube Support Plate Stresses

The displacement time history analysis is based on elastic response of the various structural members. Thus, it is necessary to show that the support structures remain elastic during the dynamic response. For this analysis, because the displacement limits only apply to TSPs 1-4, these are the plates where the stresses are evaluated. In addition, it is the hot leg region of the plates that is of concern. It is important to note that interaction between the unexpanded tubes and tube support plates due to rotation of the plates has been conservatively ignored in this analysis. If the plates should yield locally on the cold leg, the resultant effect would be increased plate rotations and contact with unexpanded tubes. Also, the interaction between the upper plates and TSPs 1-4 is through the tierods / spacers and through the expanded tubes. Yielding of the upper plates in the unsupported region of the plates would tend to relieve the load transferred to the lower plates, concentrating the deformation to the yielded portion of the plate. Thus, relative to predicting the relative tube / TSP displacements for TSPs 1-4, it is yielding of the hot leg

region of these plates that is of primary concern. Based on ASME Code minimum yield strength properties for SA 285 Grade C, the plate yield strength at a temperature of 530°F is 23.8 ksi.

The stresses in the tube support plates are calculated using the system finite element model. Based on the time history results, displacements for the dynamic degrees of freedom are extracted from the dynamic solution at times corresponding to the maximum plate displacements. Because the analysis is focused on limiting the displacements for the hot leg of the first four tube support plates, times for calculating the plate stresses are selected based on the response of these plates.

Displacements are extracted from the dynamic time history file at the selected times, and converted to displacement boundary conditions that are applied to the system model. In addition to the displacement constraints from the dynamic analysis, the boundary conditions discussed above for generating the system substructure are also applied, including the coupled nodes joining the various structural members.

The WECAN computer program is then used to solve for member stresses at the selected times. For the tube support plates, however, the calculated stresses represent equivalent plate values and do not provide the stresses in the plate ligaments. In order to develop a relationship between the equivalent plate stresses and peak ligament stresses, additional calculations were performed using two finite element models of the actual hole and ligament geometry for the Series 51 steam generators. One model is used to evaluate the plate response to applied loads in the pitch direction, and the second to evaluate loads applied in the diagonal direction. The orientation of the two models is shown in Figure 5-24 relative to the overall hole geometry. The pitch and diagonal model geometries are shown in Figure 5-25 and Figure 5-26, respectively. These models are used to calculate the ratio of maximum average ligament stress intensity for the perforated plate to an equivalent solid plate. Since it is the average stress across the plate ligament that will control the yielding of the plate, as opposed to peak stresses at the hole boundaries, the analysis calculates stress ratios based on the average ligament stress intensities. Because the plates are loaded out of plane by the steam line break pressure drops, the response is in terms of plate bending. Thus, the ligament models are analyzed subject to the application of edge moment loads.

Stress factors are calculated as a function of the biaxiality of the applied moments for ratios ranging from -1.0 to 1.0. The resulting ligament stress intensities are compared to the stress intensities for an equivalent solid plate subject to the same edge loads, and ratios of the stresses are calculated. The results of the calculations are summarized in Table 5-15, and show a maximum stress intensity ratio of 9.05.

Using the ratios of perforated plate stress to equivalent plate stress, the results file from the WECAN static analysis are scaled based on the stress biaxiality and a revised results file is generated. Using the revised stress results file, stress contour plots are then generated showing the distribution of stress for each of the first four plates. Typical sets of stress contour plots, one set for the right-side wedge supports and one set for the left-side wedge supports are shown in Figure 5-27 through Figure 5-36. In general, the stresses are below 5 ksi throughout the plate, with the highest stresses occurring at the locations where the wedges and support bars are welded to the wrapper. In these locations, the stresses can be as high as 24 ksi for the plate hot leg. However, it should be noted that the wedge regions of the plates do not have flow holes present, resulting in a significantly higher strength than for the remainder of the plate. This analysis has conservatively ignored the stiffening effect that occurs adjacent to the wedges. Based on the results for the local pitch and diagonal models (Figure 5-25 and Figure 5-26) for the stresses in the plate hole ligaments, a conservative estimate would be a factor of two on stress due to the absence of the flow

holes in this region, which would lower the plate stresses well below the ASME Code minimum yield stress.

Thus, the plate stresses are concluded to be acceptable relative to the elastic analysis methodology.

5.4.3 Tierod / Spacer Stresses

As with the tube support plates, the stresses in the tierods and spacers are compared to the applicable ASME Code minimum yield strength value. The applicable yield strength for both the tierods and spacers is 27.6 ksi. For the tierods and spacers, calculations are performed to calculate the end displacements (tension / compression) that occur during the transient. Note that, except for the spacers for the center tierods that are welded to the tube support plates, the spacers can only support compressive loads. Using the end displacements, the tensile / compressive stresses for the tierods and spacers are calculated. Knowing the length of the tierods / spacers, the differential displacements are converted to strains ($\varepsilon = \Delta L/L$) and then to axial stresses ($\sigma = E\,\varepsilon$). The resulting stresses are summarized in Table 5-16. The resulting stresses are well below the applicable yield stress (27.6 ksi) for the tierods and spacers.

5.4.4 Weld Stresses

As discussed in Section 5.2.9, the plates are coupled to the wrapper for all six DOF at the wedge positions and the three translational DOF at the vertical bar locations. As a result the welds are subject to vertical loads resulting from the SLB loads. In the case of the wedge welds, the welds experience both a vertical load and an overturning moment. For the vertical bar welds, only vertical forces result. The concern with the welds is that they maintain structural integrity (do not fail in shear) such that plate support is lost. For assessing the stresses in welds, an allowable stress consistent with ASME Code criteria under accident condition loads is used. In calculating the allowable stresses for the welds, weld quality factors for fillet welds with visual examination (ASME Code Section III, Subsection NG) are used. The factor for a single fillet weld (vertical bar) is 0.35, and the factor for a double fillet weld (wedge) is 0.40. Because the wedge welds are subject to both membrane and bending loads, a larger allowable stress is used. For the vertical bar welds the allowable stress is based on the criteria for membrane conditions only. In both cases, the allowable stress is a function of the stress intensity quantity, S_m, which for SA 285 Grade C at 530°F is 15.8 ksi. The resulting allowable stresses for the welds are as follows:

$$\text{Wedge Welds: } P_m + P_b = 2.4\ S_m \times 1.5 \times 0.40 = 22.75 \text{ ksi}$$

$$\text{Vertical Bar Weld: } P_m = 2.4\ S_m \times 0.35 = 13.3 \text{ ksi}$$

In order to calculate stresses in the welds, nodal forces are extracted from the static WECAN runs at the locations where the plates are coupled to the wrapper. The weld stresses are then calculated using conventional analysis methods. A summary of the stresses in the wedge and vertical bar welds is provided in Table 5-17.

The weld stresses are shown to be less than the allowable values stated above.

5.4.5 Expanded Tube Forces

A summary of the maximum axial forces in the expanded tubes as obtained from the dynamic solution are summarized in Table 5-18[3]. Based on the lower tolerance yield strength value for the tubes at 650°F (35.49 ksi), the force necessary to cause yield in the tubes is 4,600 pounds. Thus, the expanded tubes remain elastic throughout the SLB transient.

5.4.6 Tube Expansion Zone Extensions

The stiffness specified for the expanded tube expansion zone is a function of the differential displacement of the tubes and plates. Thus, it is necessary to show that the interface stiffness used is consistent with the differential displacements resulting from the dynamic analysis. A summary of the differential displacements for the tube expansion zones is provided in Table 5-19. These results show that the maximum differential displacement is [ ]^{a,c} inch.

The expansion zone stiffness used in the analysis, [ ]^{a,c} lb/in, is based on a series of pull tests of prototypic tube samples. As discussed in Section 6, for the bulge size to be applied at Diablo and a [ ]^{a,c} inch relative displacement the expansion zone stiffness is close to the [ ]^{a,c} lb/in value used in this analysis. The test data also show that there is little variation in joint stiffness between the minimum (50 mils) and maximum (150 mils) displacements. Thus, for the range of differential displacement observed in this analysis, only a small effect on joint stiffness would be expected. Overall, the [ ]^{a,c} lb/in joint stiffness is concluded to be applicable for this analysis.

5.5 EXPANDED TUBE LOCATIONS

A summary of the number and location of the tubes to be expanded is provided in Table 5-20. Note in Table 5-20 that the tube locations are identified by an arbitrarily assigned "tube group" number. Also note that there are tubes identified for expansion on both the hot and cold legs of the steam generator, as well as on both sides of the bundle, denoted as the nozzle and manway sides of the bundle. In cases where a tube is expanded on the cold leg side of the bundle, a single tube will be used for both the hot and cold leg expansion for a given tube location (row and column). Thus, although there are 40 expansions to be made for TSP 1, there are only 26 different tubes that will be affected. Initially, only hot leg expansions were considered. However, the "prying" action of the cold leg side of the plate on the expansions located adjacent to the tube lane resulted in displacements that exceeded the 0.150 inch displacement limit along the tube lane. Rather than taking additional tubes out of service (additional hot leg expansions), it was decided to expand a limited number of tubes (the same tubes as on the hot leg) near the tubelane. This provided a significant reduction in the hot leg displacements.

Plots of the candidate tubes for each tube group are shown in Figure 5-37 for the hot leg and in Figure 5-38 for the cold leg. It should be noted that the number of tubes listed in Table 5-20 for each tube group must be expanded at one of the locations indicated. For instance, a second tube cannot be selected from the tubes in Group 4-H as a substitute for the tube in Group 3-H.

---

[3] Note in Table 5-18 that the expanded forces are summarized for various "tube groups". The tube group designation refers to the various expanded tube locations on the hot (-H) and cold (-C) legs of the bundle. The location of the various tube groups is defined in Section 5.5.

5.6 THERMAL EXPANSION EFFECTS

5.6.1 Tube / Differential Expansion

In addition to the exposing of axial indications inside the tube support plate due to steam line break loads, the potential also exists for exposing cracks due to differential thermal expansion effects. The axial indications form in the tubes during full power operation. All available NDE exams show the indications to remain inside the tube support plates at cold shutdown conditions, with the cracks tending to be centered inside the plates. Thus, it is assumed that in cooling down from full power conditions to cold shutdown that the plates move with the tubes. However, following tube expansion it is possible, though unlikely, that active tubes may break free of the plates adjacent to the expanded tubes. Under these conditions, the plates will displace based on the thermal growth of the expanded tubes, with the potential to expose the axial indications in the active tubes that previously were located inside the plate.

At hot standby conditions, the steam generator is at a uniform 547°F. Thus, there will be no differential expansion between the active and expanded tubes in going from cold shutdown to hot standby conditions. However, at full power conditions, a thermal gradient will exist between the active and expanded tubes. A summary of the full power temperatures for the Diablo Canyon steam generators is summarized in Table 5-21[4]. The growth of the active tubes is a function of the temperature along the tube, with the primary side temperature being approximately linear along the tube from the hot leg inlet to the cold leg outlet. The tube wall temperature is calculated to be the average of the primary and secondary side temperatures.

A comparison of the axial growth of the active and expanded tubes in going from cold shutdown to full power conditions is provided in Table 5-22. The results show, as expected, that the active tubes will expand (grow axially) more than the expanded tubes. This would indicate that if the tubes with axial indications grow freely, that an axial indication could extend slightly above the tube support plate. However, under application of the SLB loads, the dominant motion of the plates is in the upward direction which would move the plates overtop of an exposed indication. There are times during the SLB transient when areas of the plates have a small downward movement. For the limiting downward movement, the combined displacements from thermal growth and SLB (for TSP 4) would be 0.124 inch, which is less than the 0.150 inch limit.

5.6.2 Expanded Tube Axial Loads

The steam line break analysis is based on the assumption that the tube / TSP annulus is clean for all tubes such that the unexpanded tubes provide no restraint to axial movement of the plates. However, based on eddy current analysis of the Diablo Canyon steam generators, the potential exists for a large number of tube / TSP intersections to be filled with magnetite material. In situations where the tube / TSP intersections are filled with magnetite, significant "breakaway" forces have been observed in situations where tubes have been removed from various plants and steam generators for metallographic examination. If it is assumed that a large number of tube / TSP intersections are packed with magnetite for tubes adjacent to an expanded tube, then the expanded tube may be subject to axial loads due to

[4] Note that the discussion and analysis results to follow would not be affected by a change in full power operating temperatures of a few degrees that could occur as a result of tube plugging.

differential thermal expansion between the active and expanded tubes. Based on the full power temperatures summarized in Table 5-21 and an assumption of rigid tube / TSP intersections, an axial stress of approximately 10 ksi can develop in an expanded tube if it is surrounded by packed tubes. This stress is well below the lower tolerance yield stress for the tubes of 35.5 ksi, and is judged to be acceptable.

It should be noted under such conditions, that the SLB load and thermal expansion load are not additive. That is, the stress in the expanded tubes due to SLB, which assumes clean intersections, and the stress due to differential thermal expansion, which is based on packed intersections, represent enveloping conditions for the expanded tubes. In the case where some tubes are packed and others are not, the net load on the expanded tube will be bounded by the above two limiting conditions.

5.7 ANALYSIS SUMMARY

Based on the combined results of Sections 5.4, 5.5, and 5.6, the tubes summarized in Table 5-20 are concluded to provide sufficient support to limit relative tube / TSP displacement under SLB loads for the hot leg region of TSPs 1-4 to less than 0.150 inch. In addition, the stresses in the supporting structures for the tube support plates, and for the tube support plates themselves, are consistent with elastic analysis methodologies used to calculate the plate displacements.

5.8 REFERENCE

1. NRC Staff Review of WCAP-14707/14708, "Model 51 Steam Generator Limited Tube Support Plate Displacement Analysis for Dented or Packed Tube-to-Tube Support Plate Cerevices" – Diablo Canyon Power Plant, Units 1 and 2 (TAC Nos. M99011 and M99012), 1/10/2000.

Table 5-1
Summary of Component Materials

a,c

[

]

Table 5-2
Summary of Material Properties
SA 216 Grade WCC

	Temperature - °F						
Property	70	200	300	400	500	600	700
Young's Modulus	27.90	27.70	27.40	27.00	26.40	25.70	24.80
Coefficient of Thermal Expansion	6.10	6.38	6.60	6.82	7.02	7.23	7.44
Density	0.283 7.324	0.282 7.303	0.282 7.287	0.281 7.269	0.280 7.252	0.280 7.234	0.279 7.215

Property	Units
Young's Modulus	psi x 10^{6}
Coefficient of Thermal Expansion	in/in/deg. F x 10^{-6}
Density	lb/in^3 $lb\text{-}sec^2/in^4$ x 10^{-4}

Table 5-3
Summary of Material Properties
SA 508 Class 2

	Temperature - °F						
Property	70	200	300	400	500	600	700
Young's Modulus	29.90	29.50	29.00	28.60	28.00	27.40	26.60
Coefficient of Thermal Expansion	6.10	6.38	6.60	6.82	7.02	7.23	7.44
Density	0.283	0.282	0.282	0.281	0.280	0.280	0.279
	7.324	7.303	7.287	7.269	7.252	7.234	7.215

Property	Units
Young's Modulus	psi x 10^{6}
Coefficient of Thermal Expansion	in/in/deg. F x 10^{-6}
Density	lb/in^{3}
	lb-sec^{2}/in^{4} x 10^{-4}

Table 5-4
Summary of Material Properties
SA 533, Grade A - Class 1

	Temperature - °F						
Property	70	200	300	400	500	600	700
Young's Modulus	29.90	29.50	29.00	28.60	28.00	27.40	26.60
Coefficient of Thermal Expansion	6.10	6.38	6.60	6.82	7.02	7.23	7.44
Density	0.283 7.324	0.282 7.303	0.282 7.287	0.281 7.269	0.280 7.252	0.280 7.234	0.279 7.215

Property	Units
Young's Modulus	psi x 10^6
Coefficient of Thermal Expansion	in/in/deg. F x 10^{-6}
Density	lb/in^3 $lb\text{-}sec^2/in^4$ x 10^{-4}

Table 5-5
Summary of Material Properties
SA 285 Grade C

	Temperature - °F						
Property	70	200	300	400	500	600	700
Young's Modulus	27.90	27.70	27.40	27.00	26.40	25.70	24.80
Coefficient of Thermal Expansion	6.10	6.38	6.60	6.82	7.02	7.23	7.44
Density	0.284 7.35	0.283 7.33	0.283 7.315	0.282 7.299	0.281 7.282	0.281 7.264	0.280 7.246

Property	Units
Young's Modulus	psi x 10^6
Coefficient of Thermal Expansion	in/in/deg. F x 10^{-6}
Density	lb/in^3 lb-sec^2/in^4 x 10^{-4}

Table 5-6
Summary of Material Properties
SA 106 Grade B

	Temperature - °F						
Property	70	200	300	400	500	600	700
Young's Modulus	27.90	27.70	27.40	27.00	26.40	25.70	24.80
Coefficient of Thermal Expansion	6.10	6.38	6.60	6.82	7.02	7.23	7.44
Density	0.284 7.35	0.283 7.33	0.283 7.315	0.282 7.299	0.281 7.282	0.281 7.264	0.280 7.246

Property	Units
Young's Modulus	psi x 10^6
Coefficient of Thermal Expansion	in/in/deg. F x 10^{-6}
Density	lb/in^3 lb-sec^2/in^4 x 10^{-4}

Table 5-7
Summary of Material Properties
SB 163 (Alloy 600)

	Temperature - °F						
Property	70	200	300	400	500	600	700
Young's Modulus	31.70	30.90	30.50	30.00	29.60	29.20	28.60
Coefficient of Thermal Expansion	6.95	7.13	7.27	7.43	7.59	7.71	7.83
Density	---	0.306	0.305	0.305	0.304	0.303	0.302
	---	7.923	7.905	7.886	7.867	7.847	7.828

Property	Units
Young's Modulus	psi x 10^{6}
Coefficient of Thermal Expansion	in/in/deg. F x 10^{-6}
Density	lb/in^{3}
	lb-sec^{2}/in^{4} x 10^{-4}

Table 5-8
Summary of Geometric Parameters

a,c

[

]

Table 5-9
Summary of Material Loss Due to Chemical Cleaning

a,c

[

]

Table 5-10
Summary of Equivalent Plate Properties

a,c

[ ]

Table 5-11
Summary of Analysis Cases
Single Plate Model

Case	Run Identifier	Description	Support Locations
1	static01	Static run - no expanded tubes	Prototypic
2	static02	Static run - with expanded tubes	Prototypic
3	static03	Static run - with expanded tubes Assumed symmetry about vertical axis	Prototypic - Right Side of Bundle
4	static04	Static run - with expanded tubes Assumed symmetry about vertical axis	Prototypic - Left Side of Bundle

Table 5-12
Comparison of Natural Frequencies
Full Versus Reduced DOF

a,c

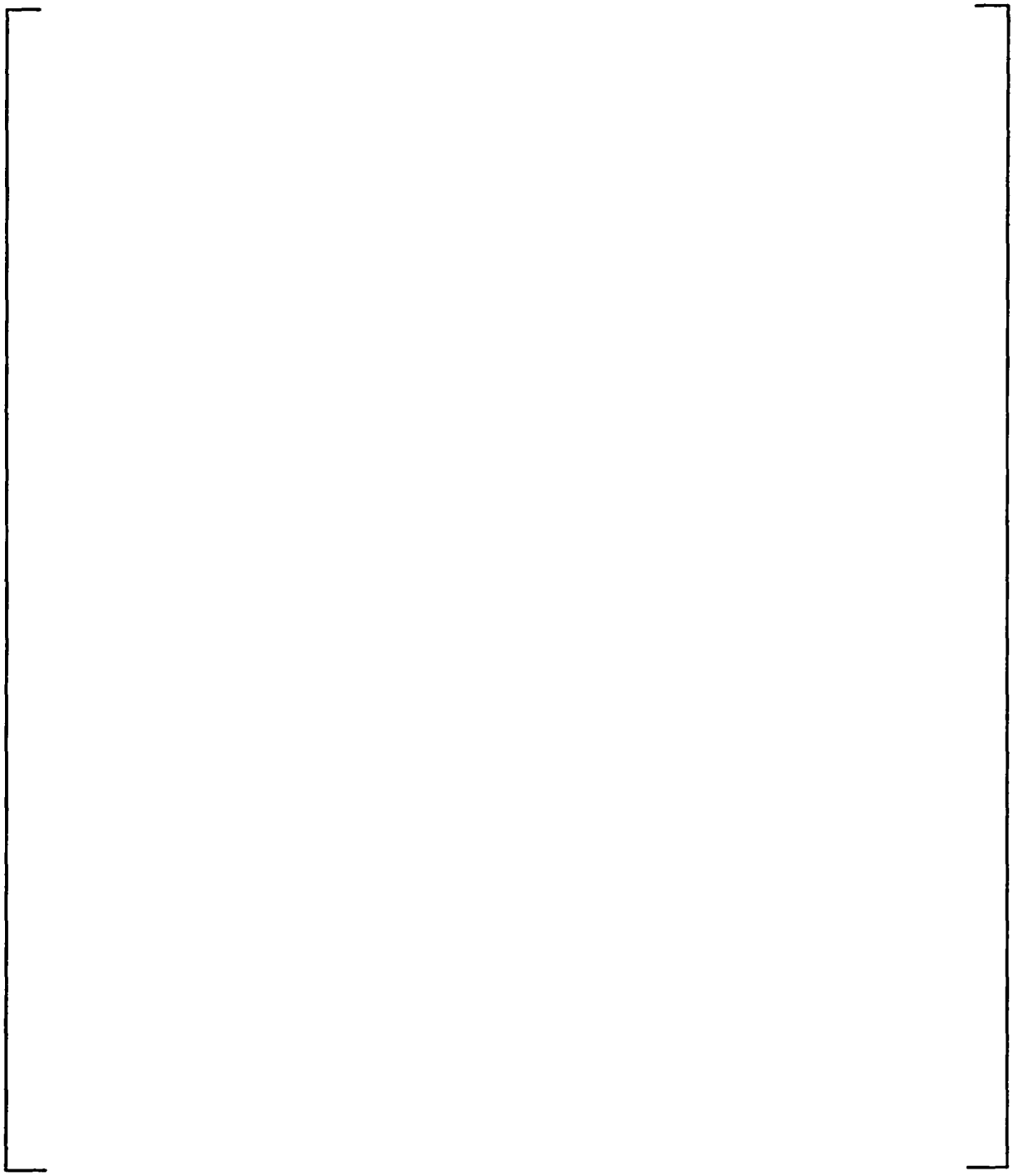

- Continued -

Table 5-12 (Continued)
Comparison of Natural Frequencies
Full Versus Reduced DOF

a,c

[

]

Table 5-13
Summary of Maximum Relative Tube / TSP Displacements
Pseudo Linear Plate / Spacer Interaction

a,c

Table 5-14
Comparison of Displacement Results
Linear versus Non-Linear Plate / Spacer Interaction

a,c

[

]

Table 5-15
Stress Intensity Factor as a Function of Biaxiality Ratio
Average Stress Intensity

a,c

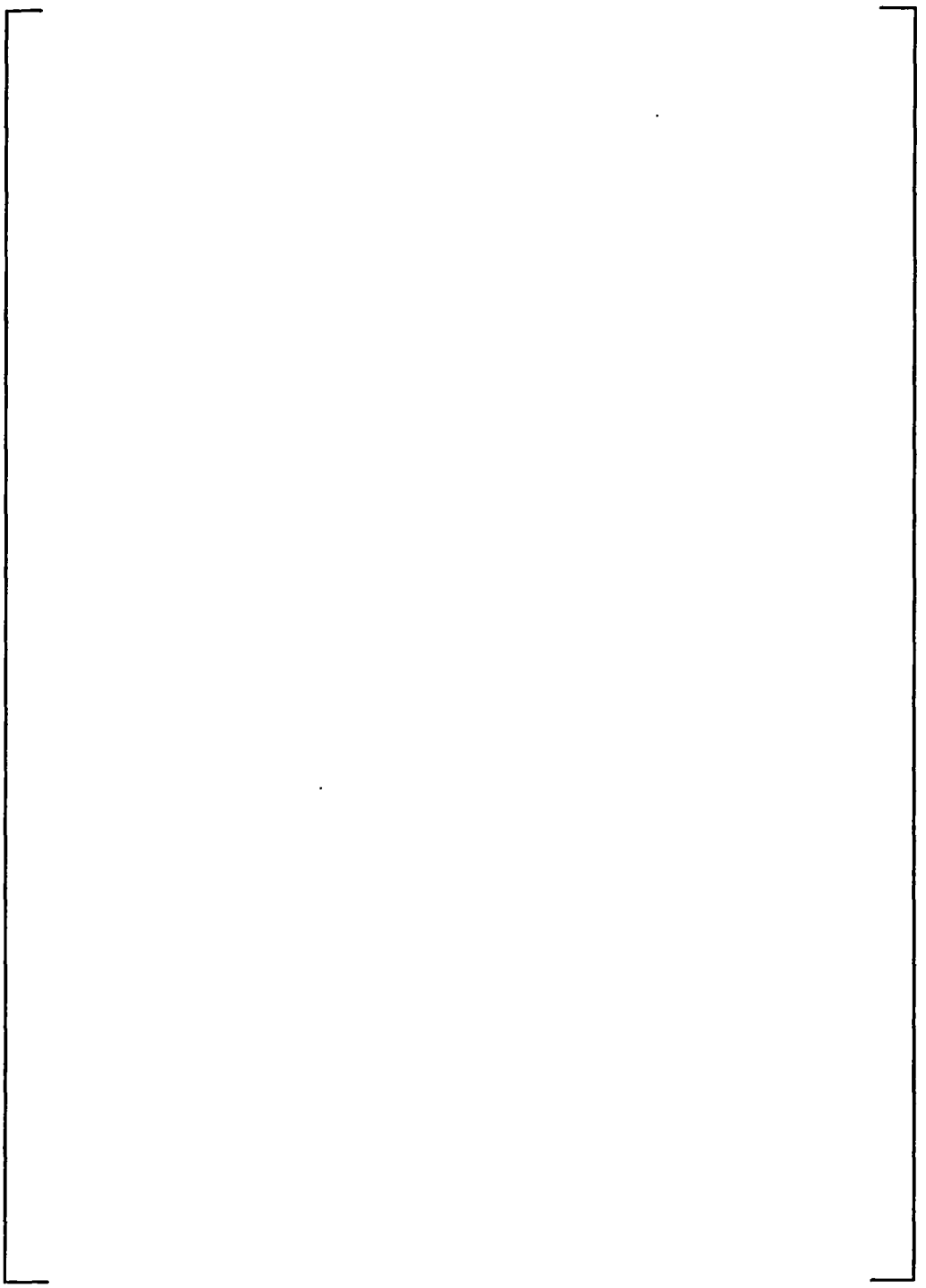

Table 5-16
Summary of Tierod / Spacer Stresses

a,c

[

]

Table 5-17
Summary of Weld Stresses

a,c

Table 5-18
Summary of Expanded Tube Forces

a,c

[ ]

Table 5-19
Summary of Expansion Zone Differential Displacements

a,c

[

]

Table 5-20
Summary of Tube Expansion Locations

a,c

[ ]

Table 5-21
Summary of Component Temperatures
Full Power Conditions

a,c

[

]

Table 5-22
Comparison of Thermal Growth
Active versus Expanded Tubes
Cold Shutdown to Full Power Conditions

a,c

[

]

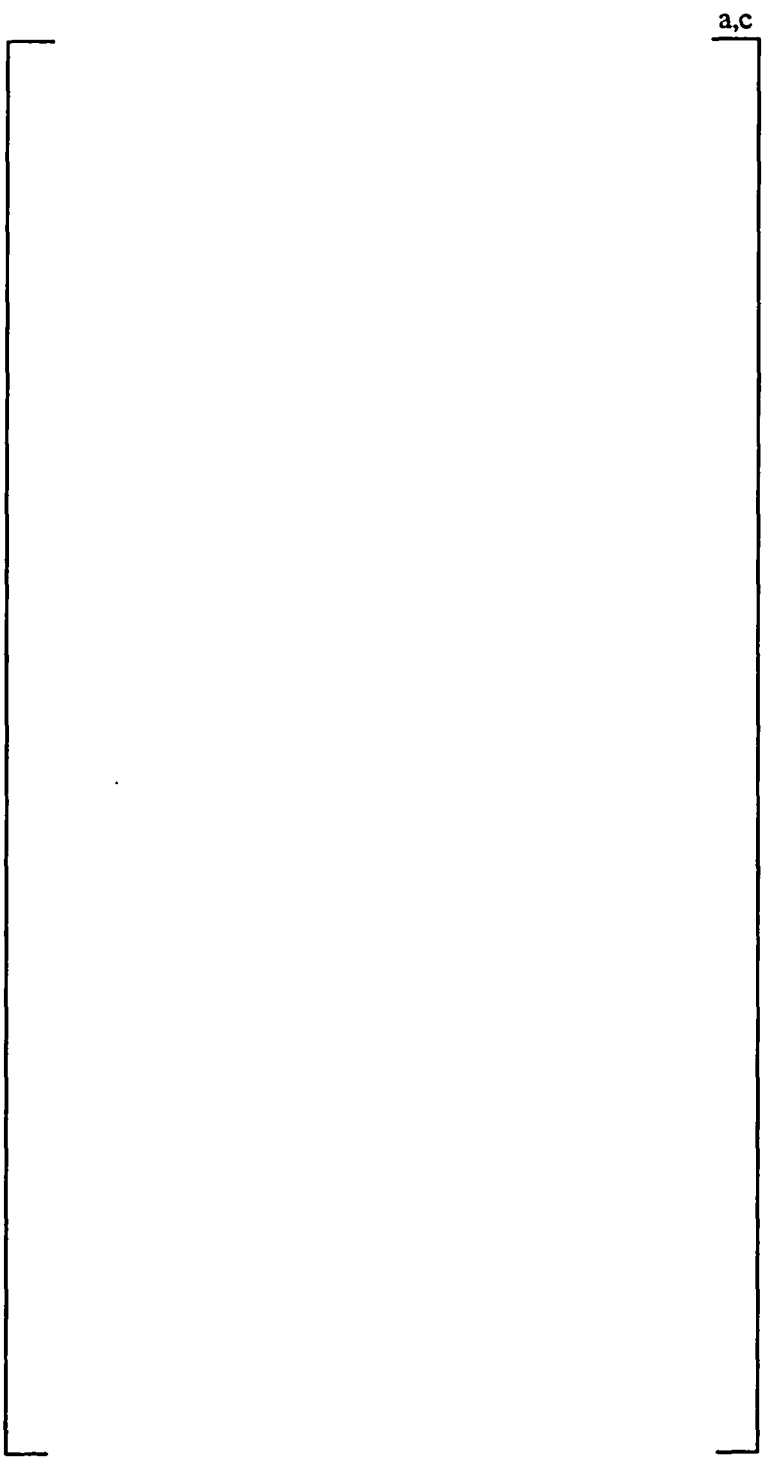

Figure 5-1
Model 51 Steam Generator Layout

a,c

Figure 5-2
TSP / Wrapper Support Configuration

a,c

Figure 5-3
TSP Support Locations
TSP 1

a,c

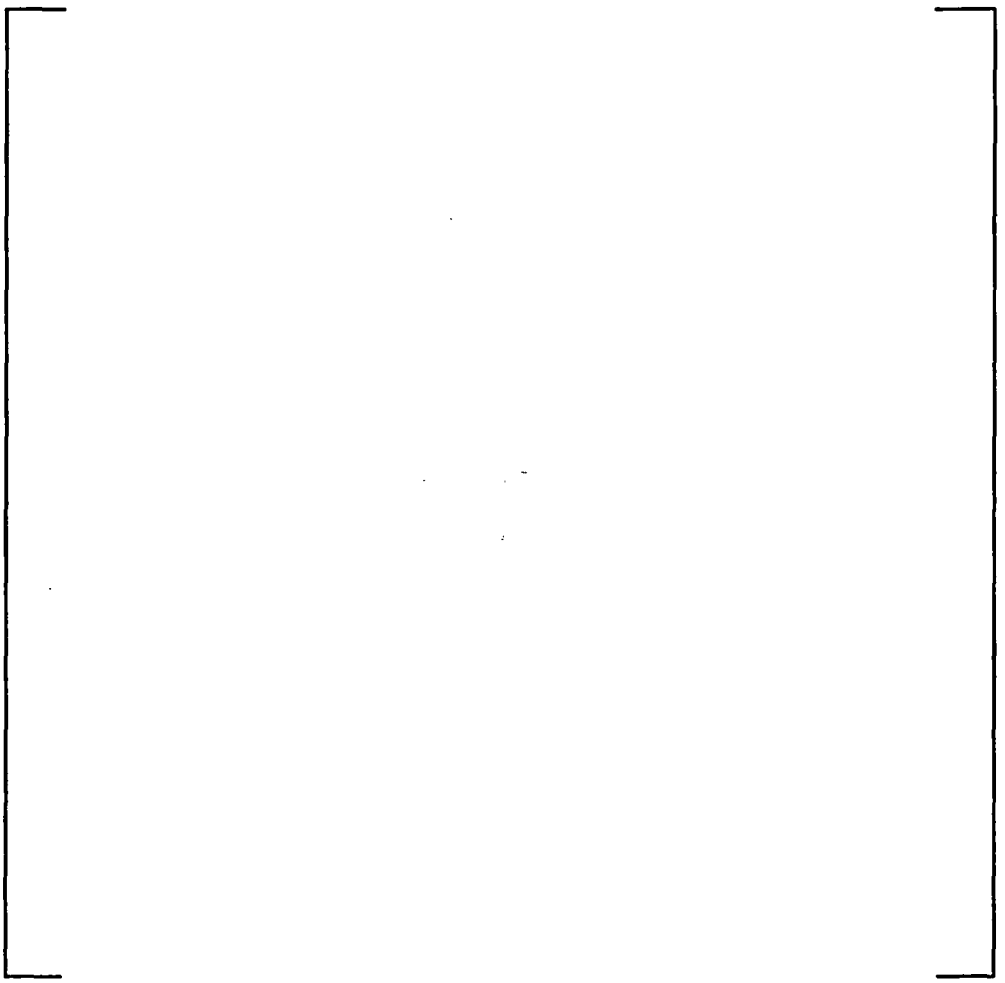

Figure 5-4
TSP Support Locations
TSPs 2-7

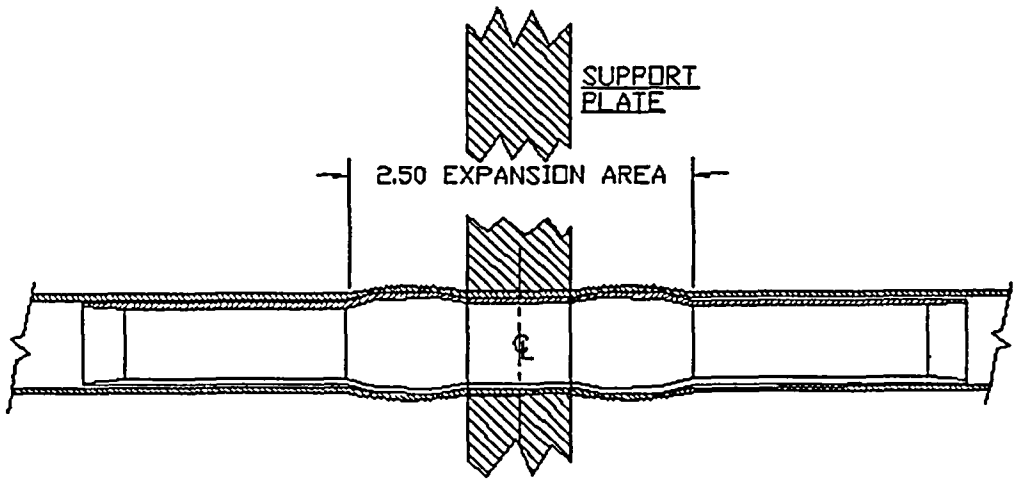

Figure 5-5
Expanded Tube Configuration

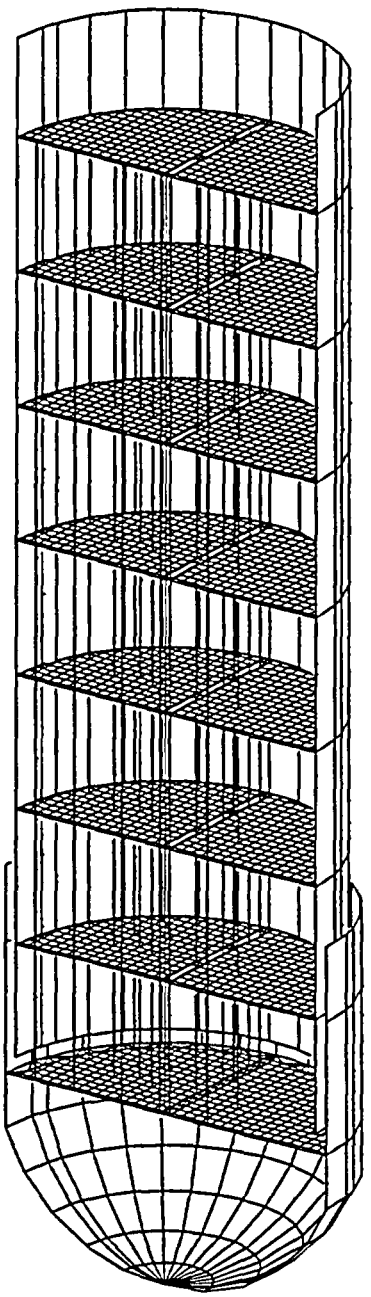

Figure 5-6
Finite Element Model

a,c

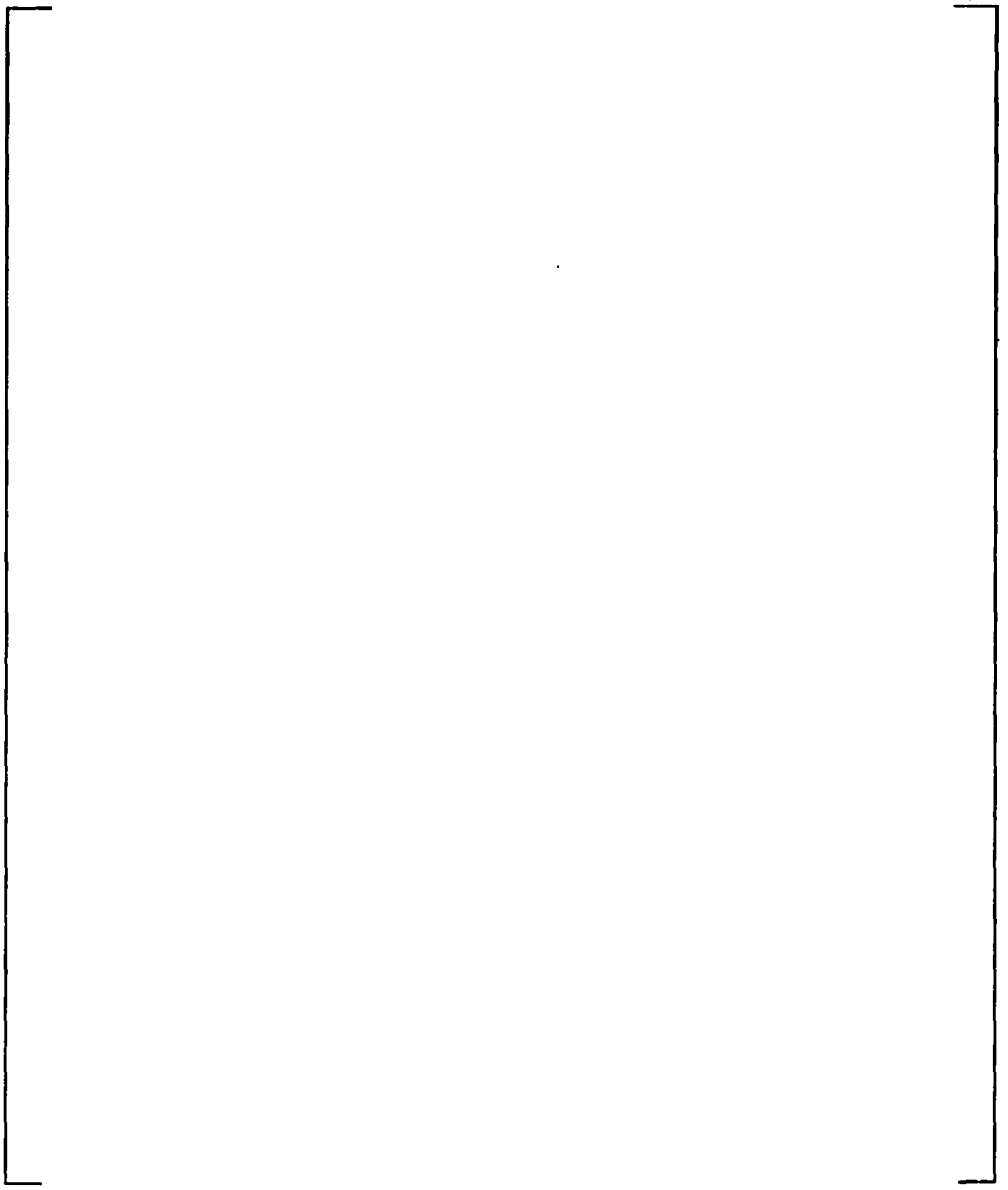

Figure 5-7
Model Representation of
Expanded Tube / TSP Interface

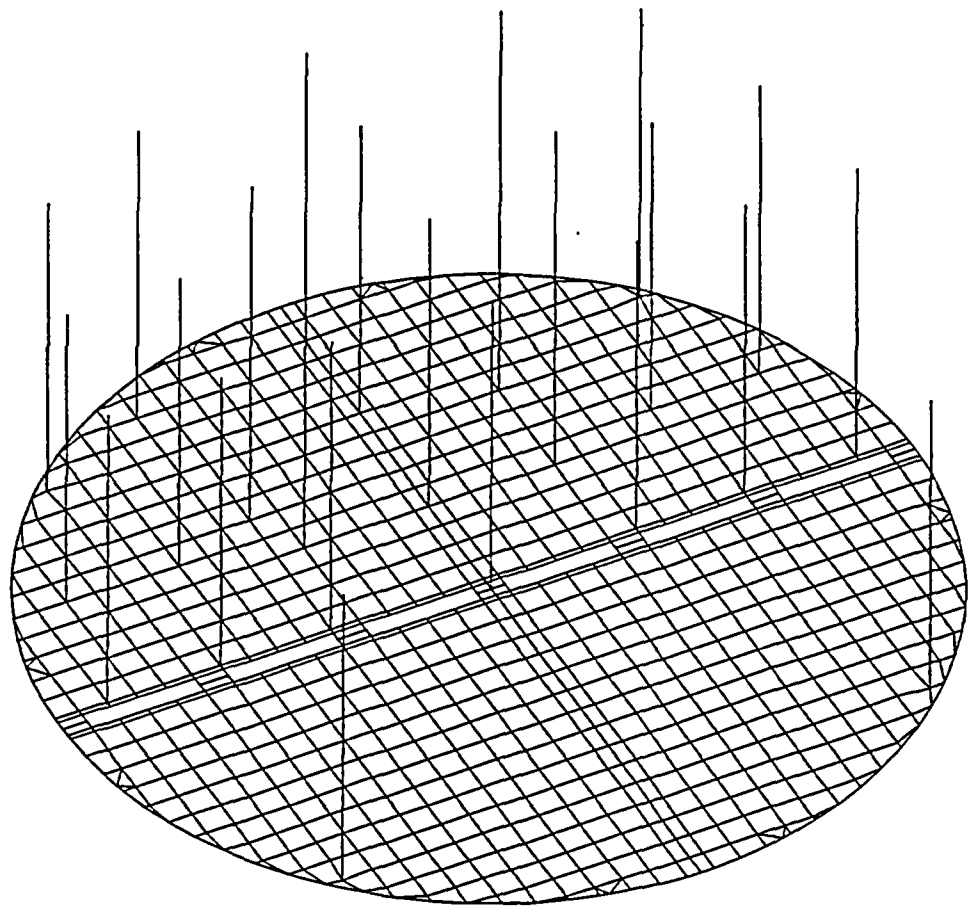

Figure 5-8
Single Plate Finite Element Model

a,c

Figure 5-9
Displaced Geometry – Single Plate Model
Case *static01*

a,c

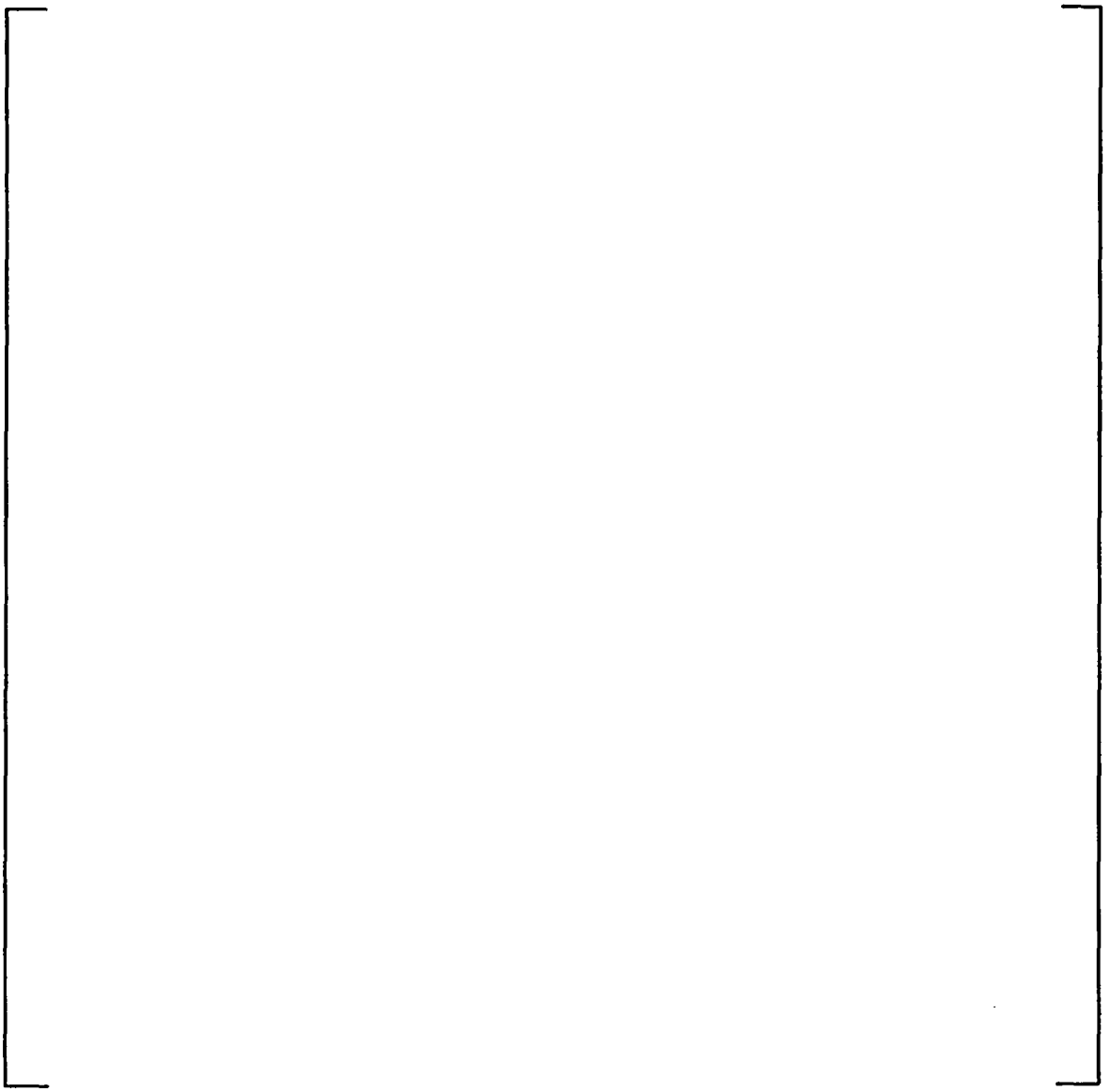

Figure 5-10
Vertical Displacement Contour Plot – Single Plate Model
Case *static01*

a,c

Figure 5-11
Displaced Geometry – Single Plate Model
Case *static02*

a,c

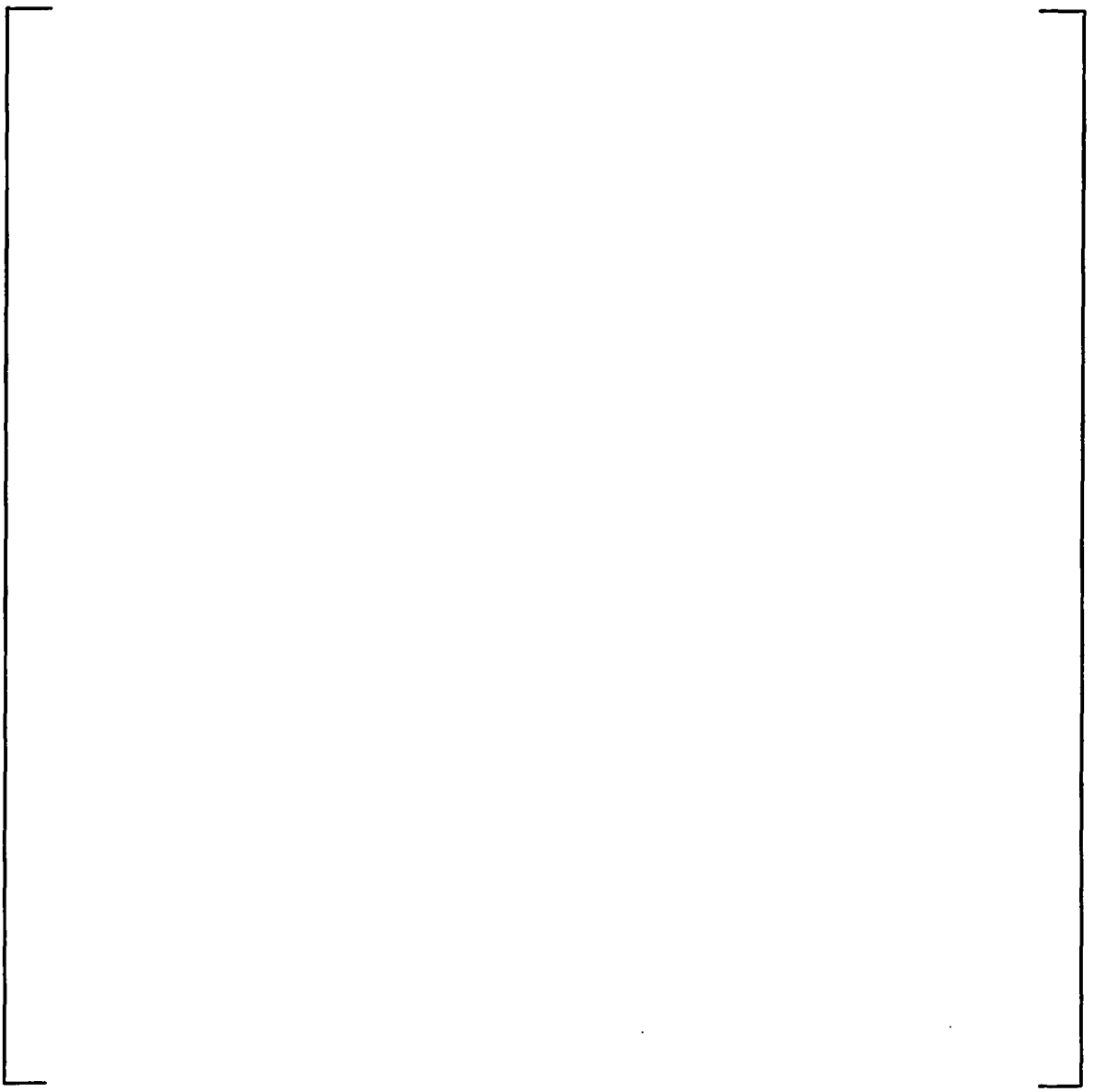

Figure 5-12
Vertical Displacement Contour Plot – Single Plate Model
Case *static02*

a,c

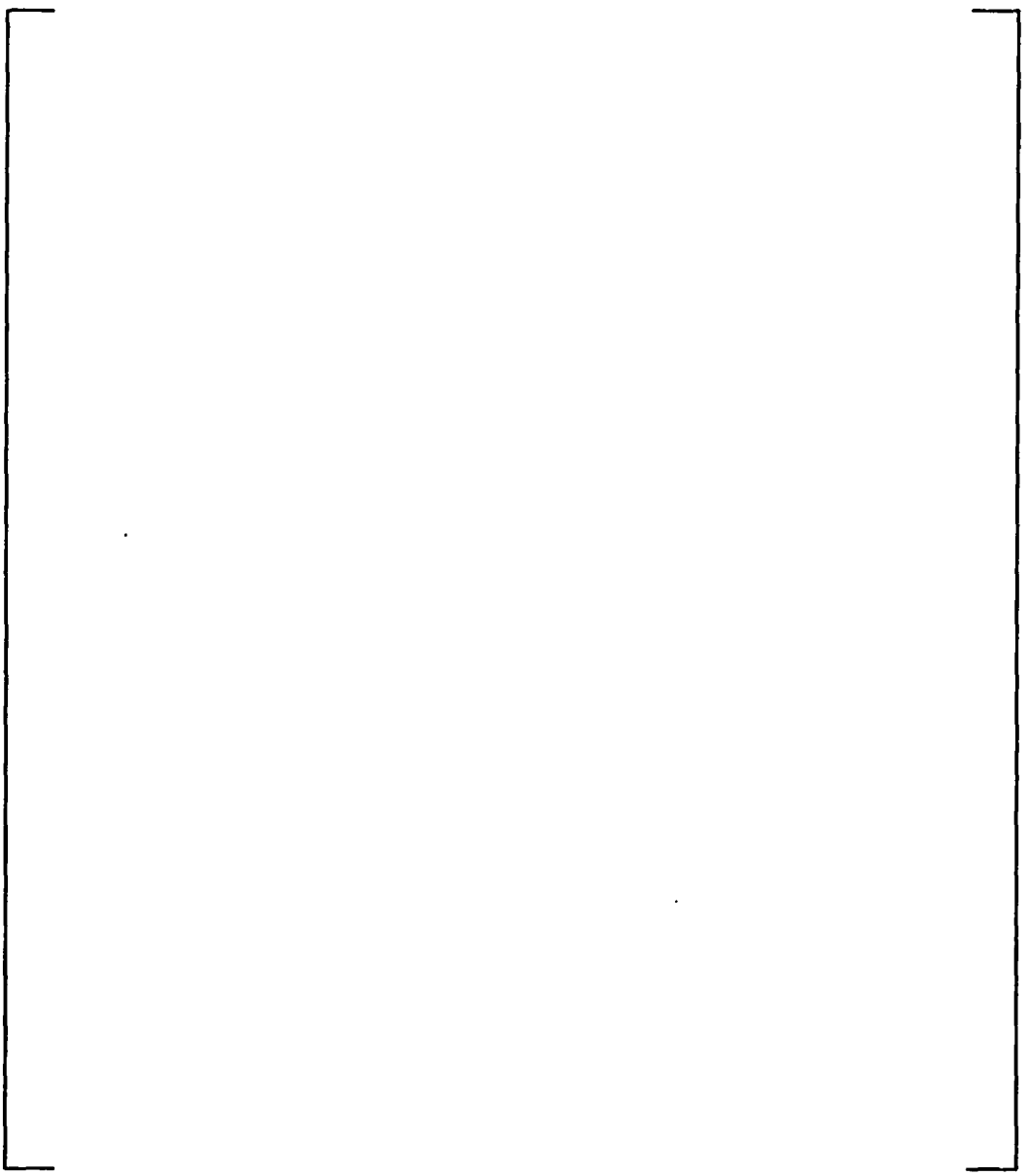

Figure 5-13
Displaced Geometry – Single Plate Model
Case *static03*

a,c

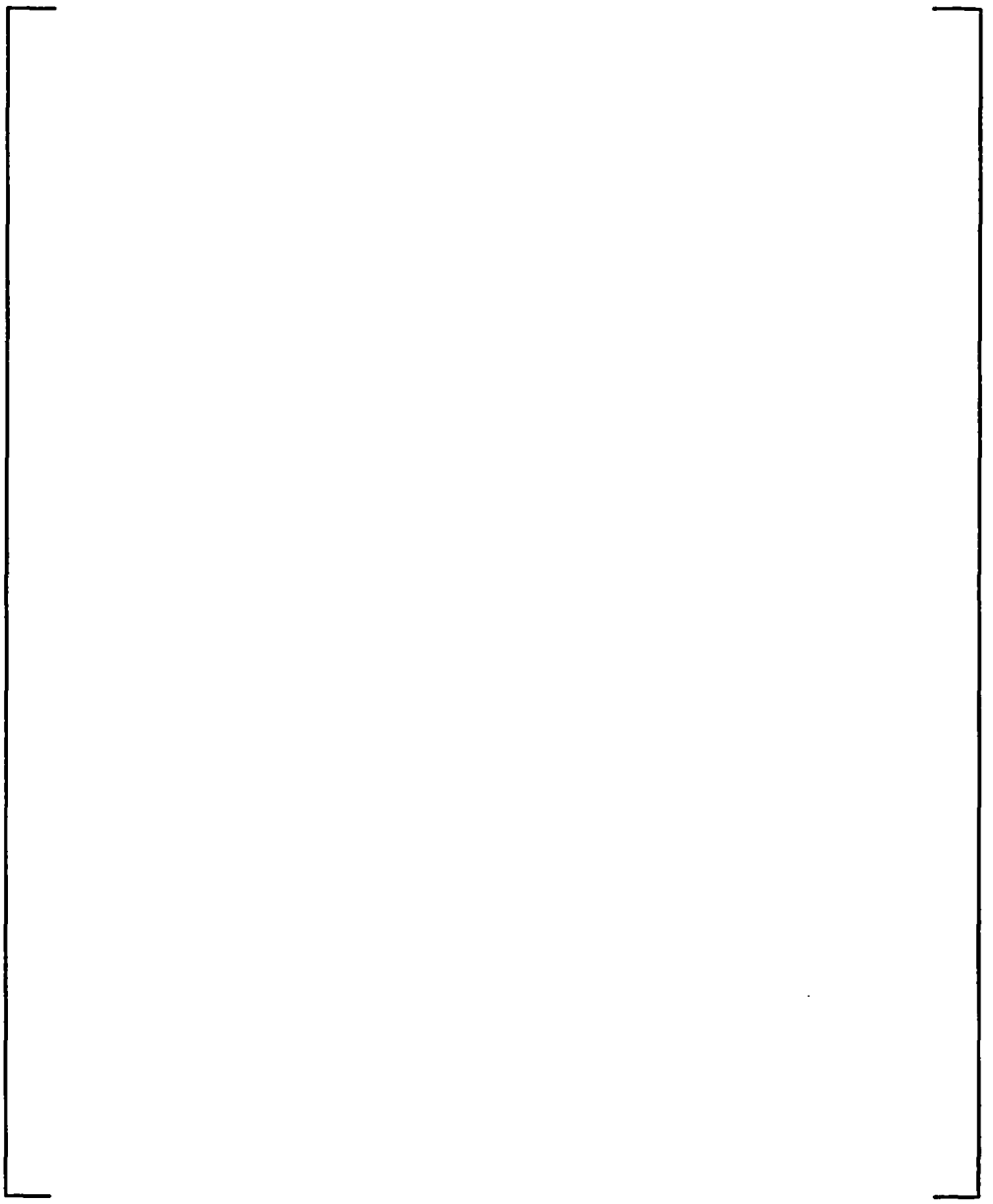

Figure 5-14
Vertical Displacement Contour Plot – Single Plate Model
Case *static03*

a,c

Figure 5-15
Displaced Geometry – Single Plate Model
Case *static04*

a,c

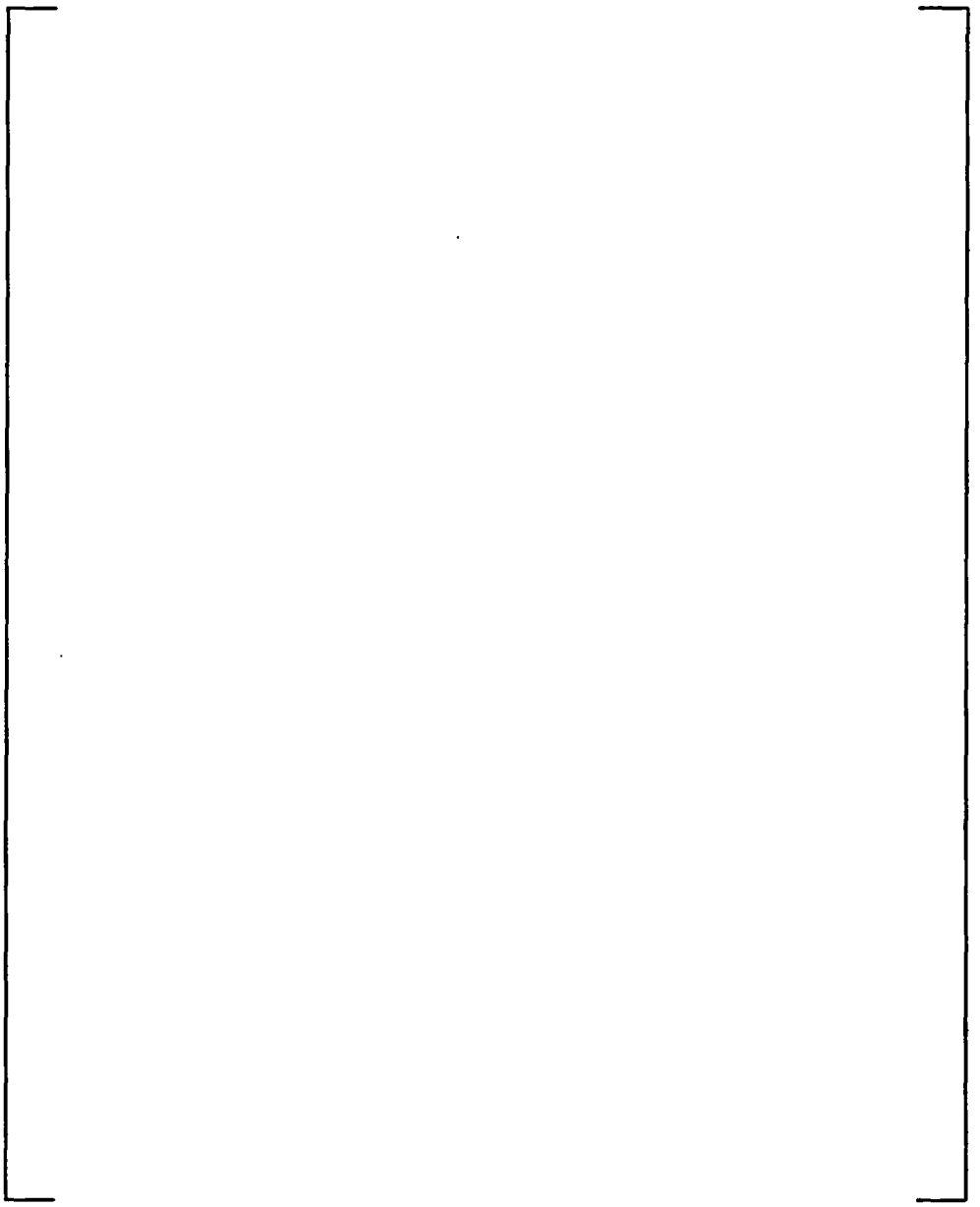

Figure 5-16
Vertical Displacement Contour Plot – Single Plate Model
Case *static04*

a,c

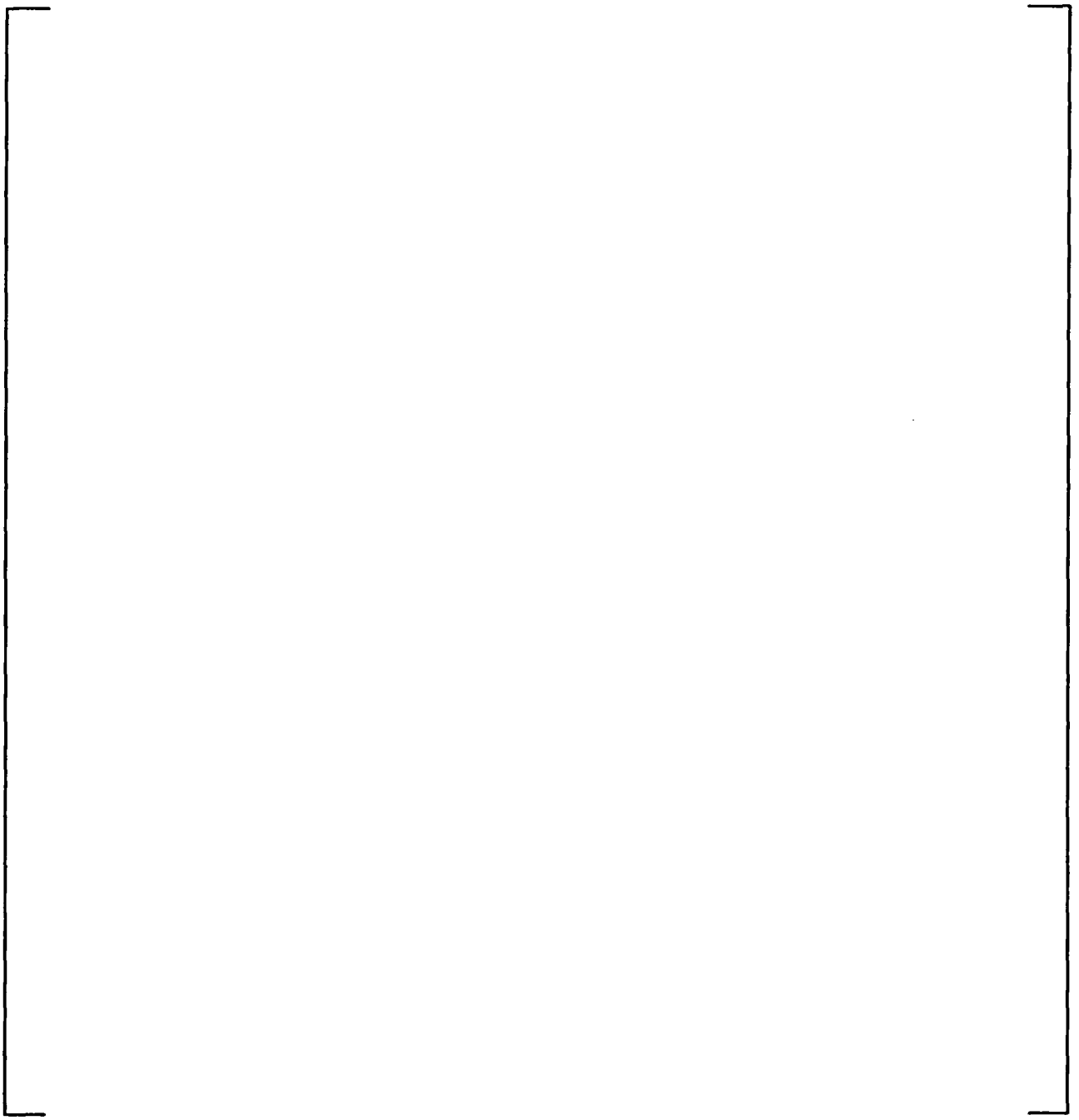

Figure 5-17
Dynamic Degrees of Freedom
Hot Leg

a,c

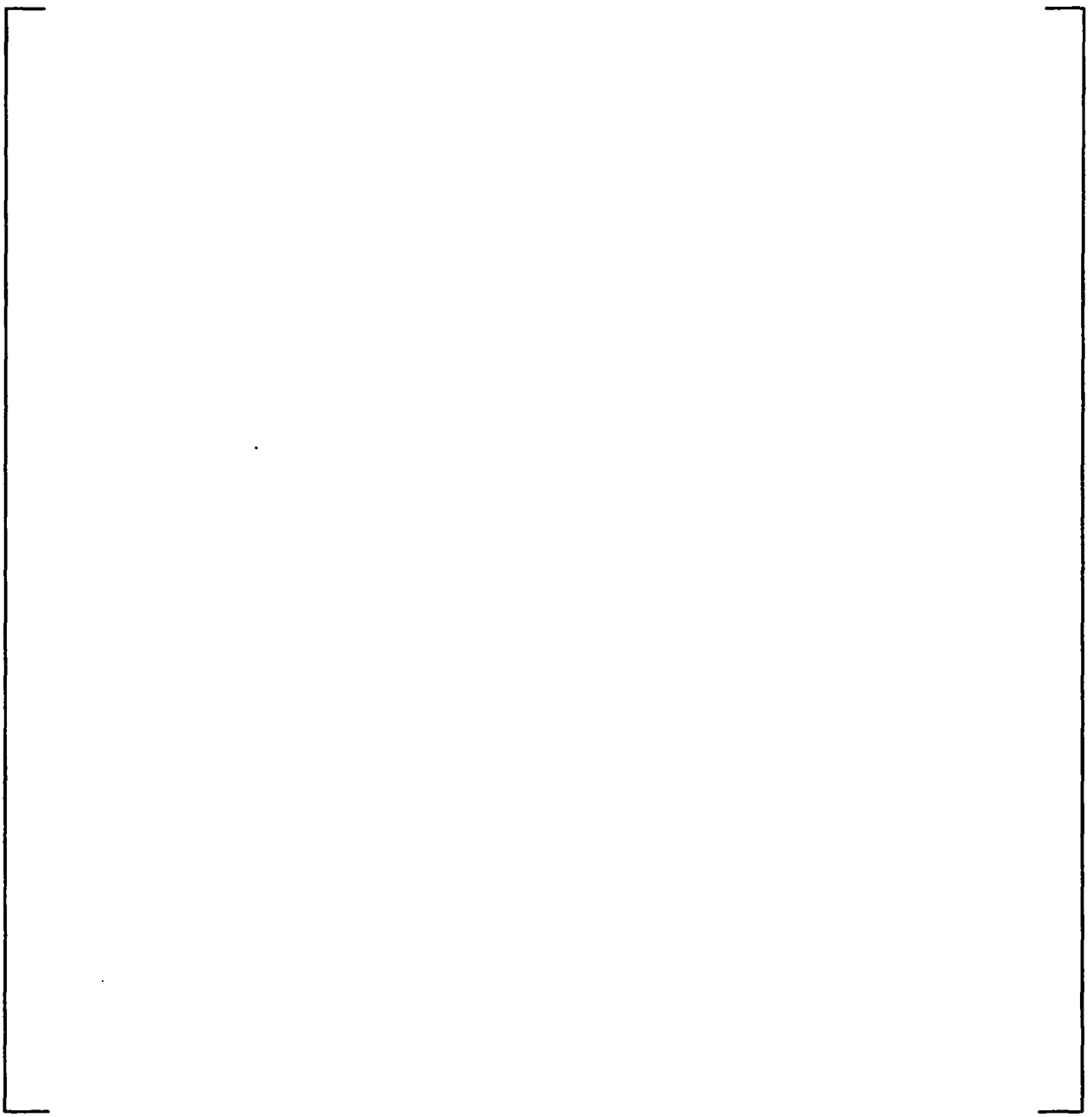

Figure 5-18
Dynamic Degrees of Freedom
Cold Leg

a,c

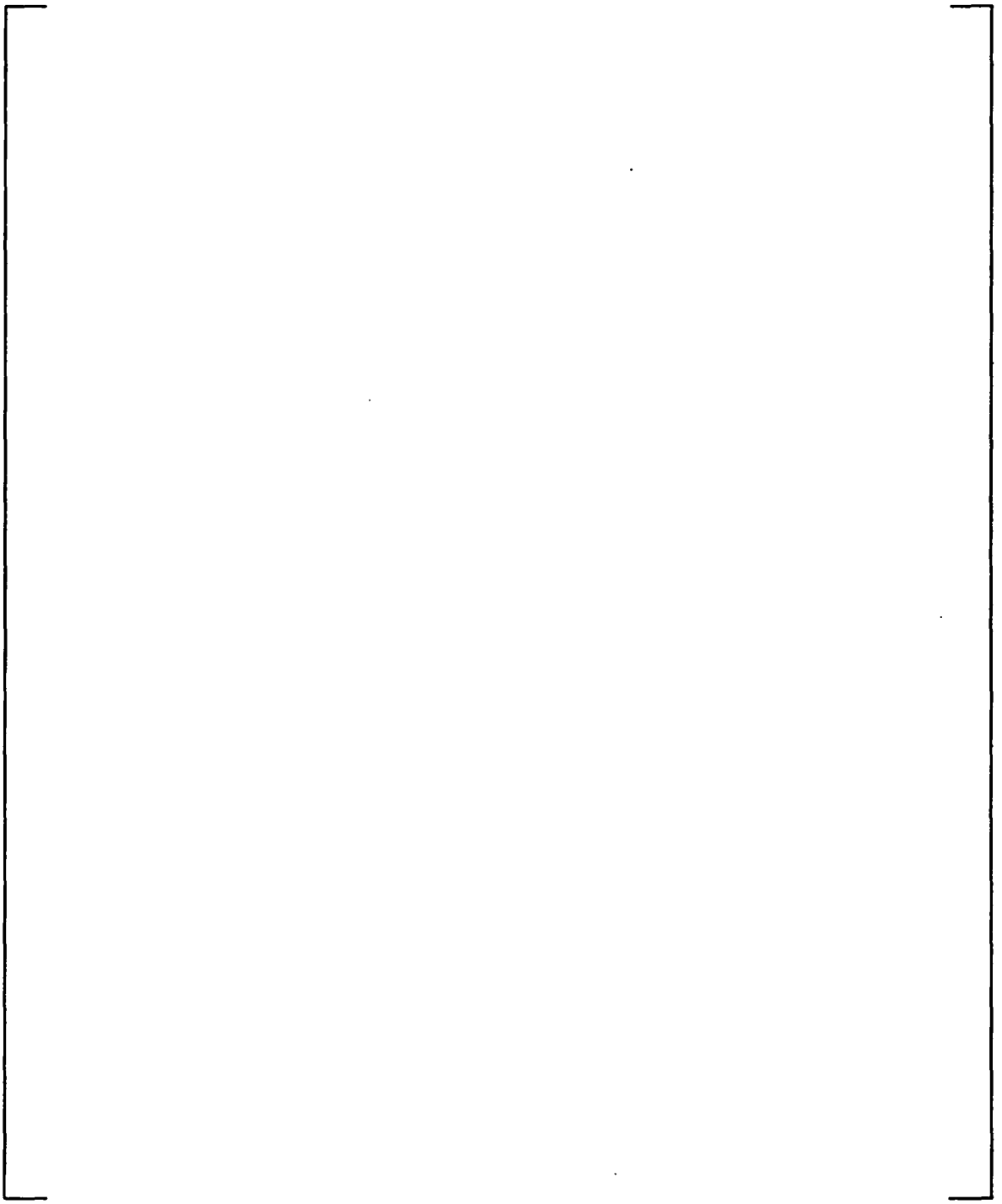

Figure 5-19
Steamline Break TSP Pressure Loads
Small Break – 1.5 Load Factor

a,c

Figure 5-20
Relative Tube / TSP Displacement versus Time
Right-Side Support Conditions
TSPs 1-4 – Hot leg

a,c

Figure 5-21
Relative Tube / TSP Displacement versus Time
Right-Side Support Conditions
TSPs 5-7 – Hot leg

a,c

Figure 5-22
Relative Tube / TSP Displacement versus Time
Left-Side Support Conditions
TSPs 1-4 – Hot leg

a,c

Figure 5-23
Relative Tube / TSP Displacement versus Time
Left-Side Support Conditions
TSPs 5-7 – Hot leg

a,c

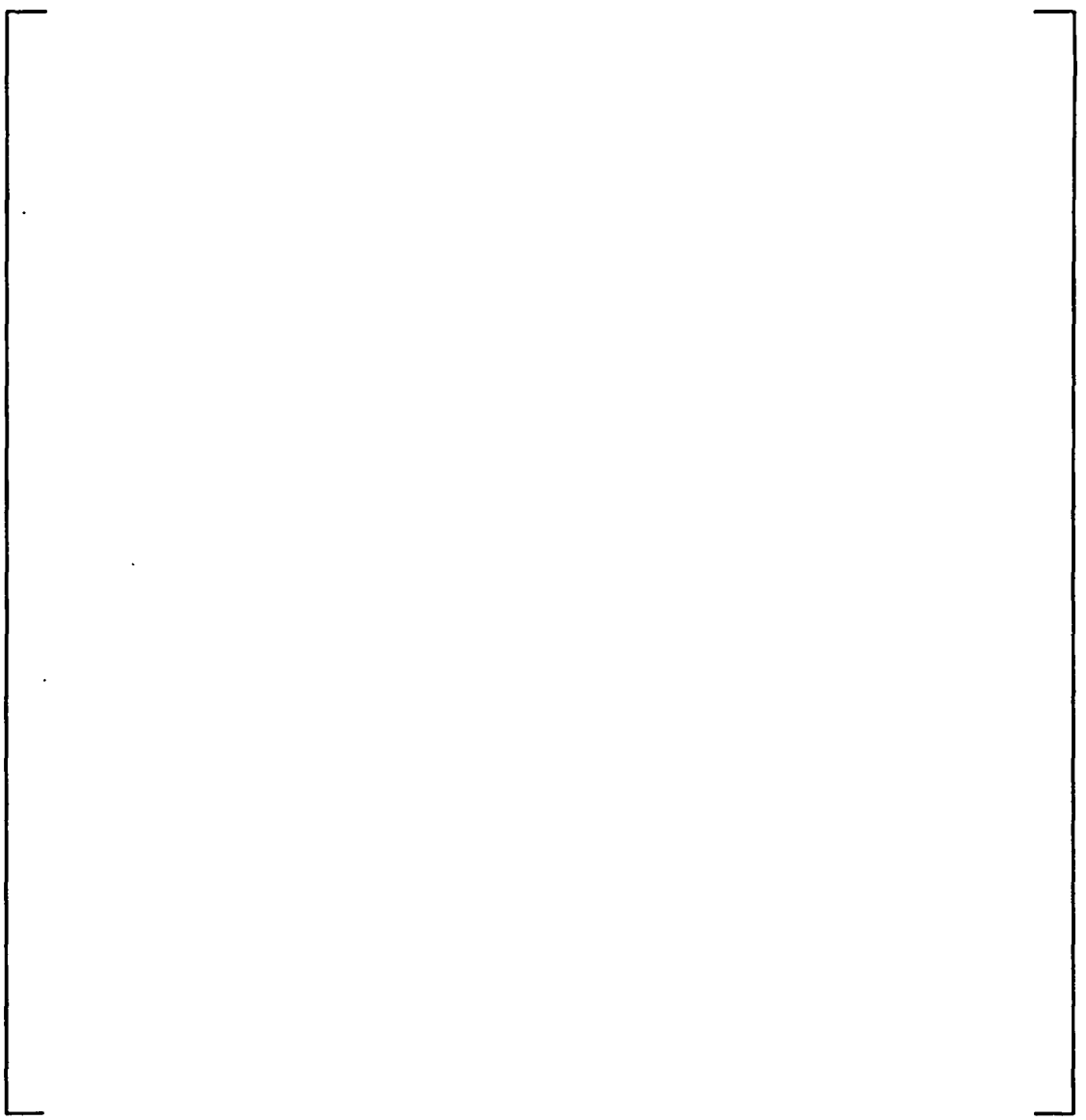

Figure 5-24
Tube Support Plate Hole Pattern

a,c

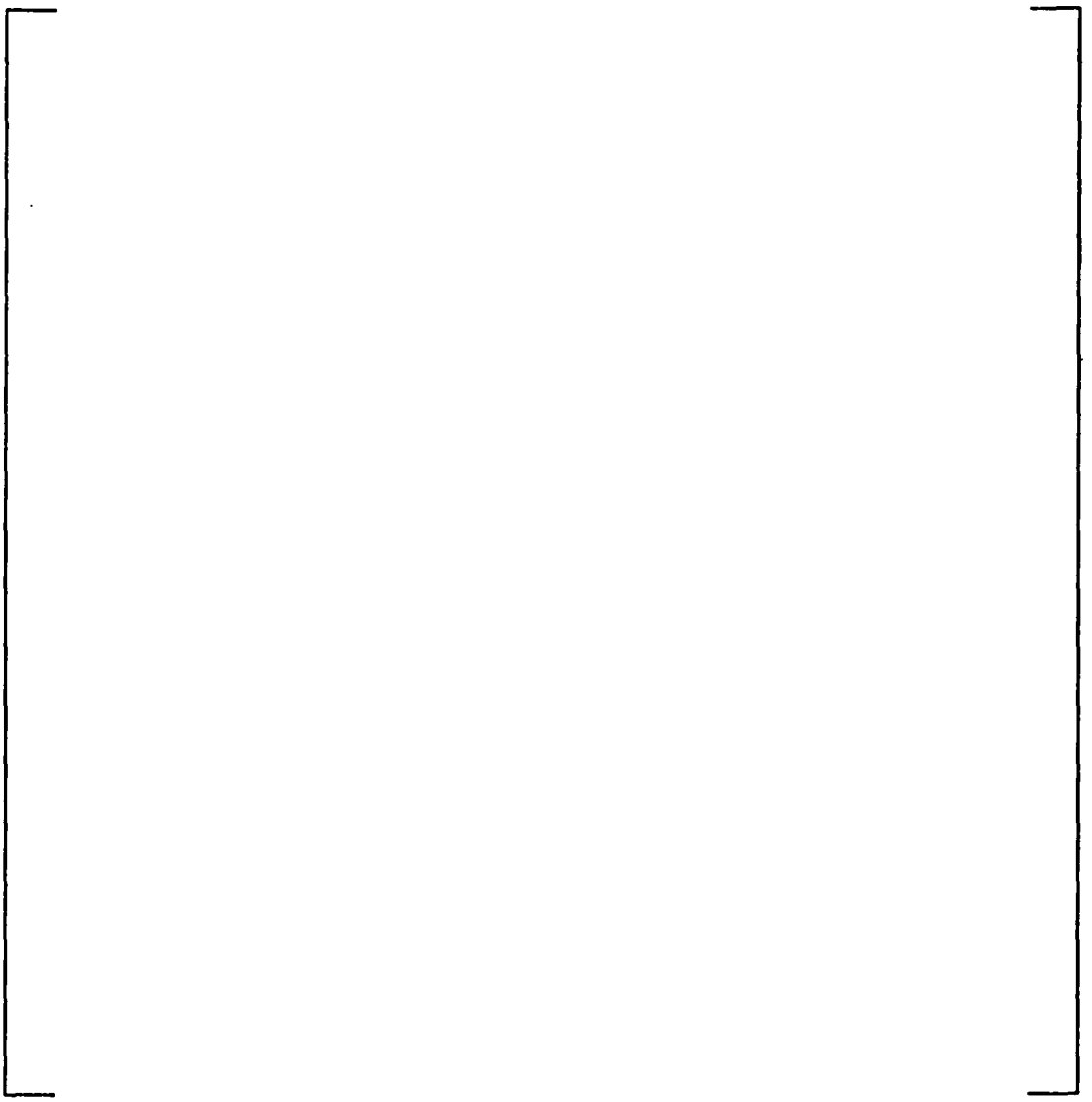

Figure 5-25
Pitch Model Geometry Plot

a,c

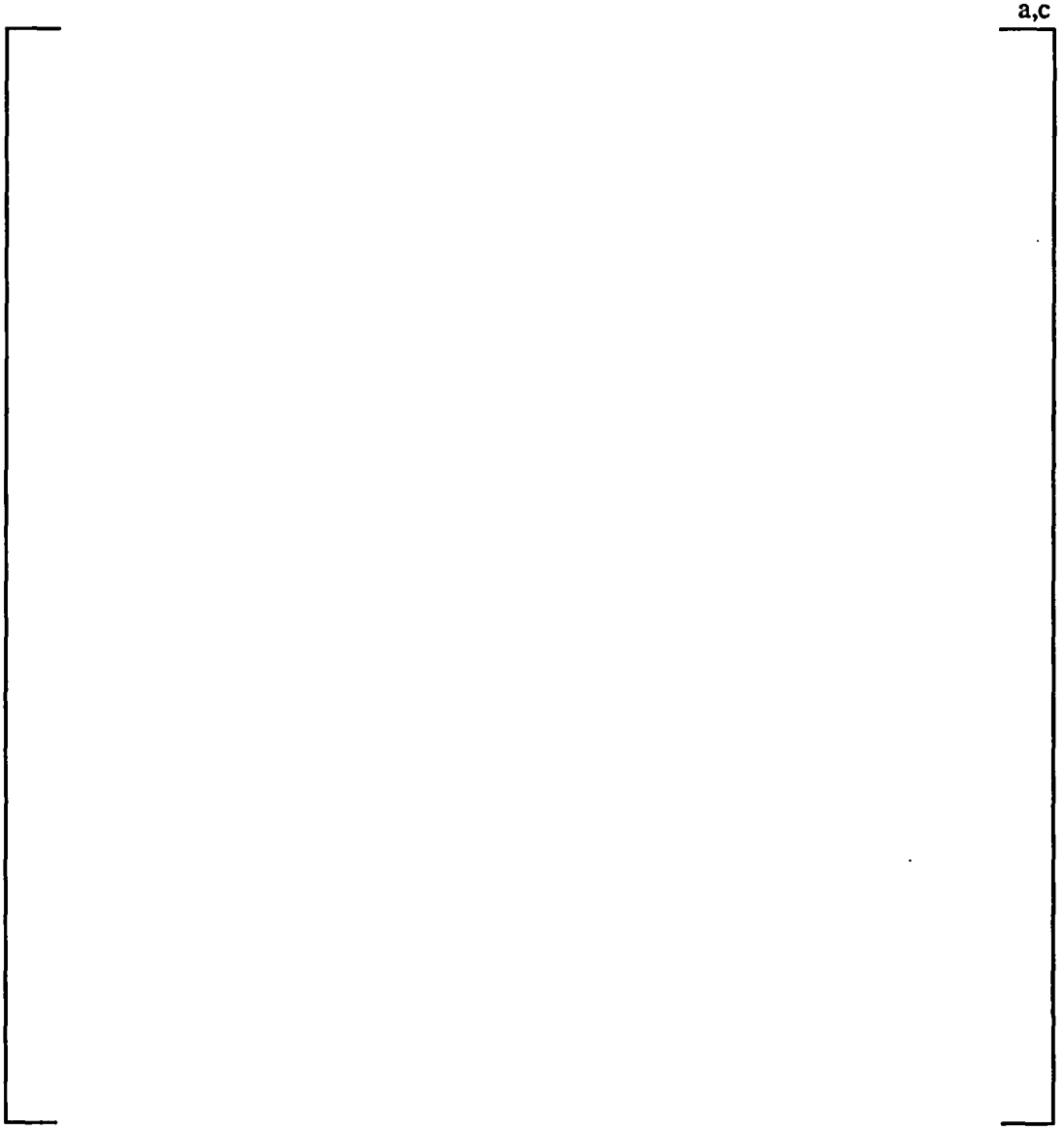

Figure 5-26
Diagonal Model Geometry Plot

a,c

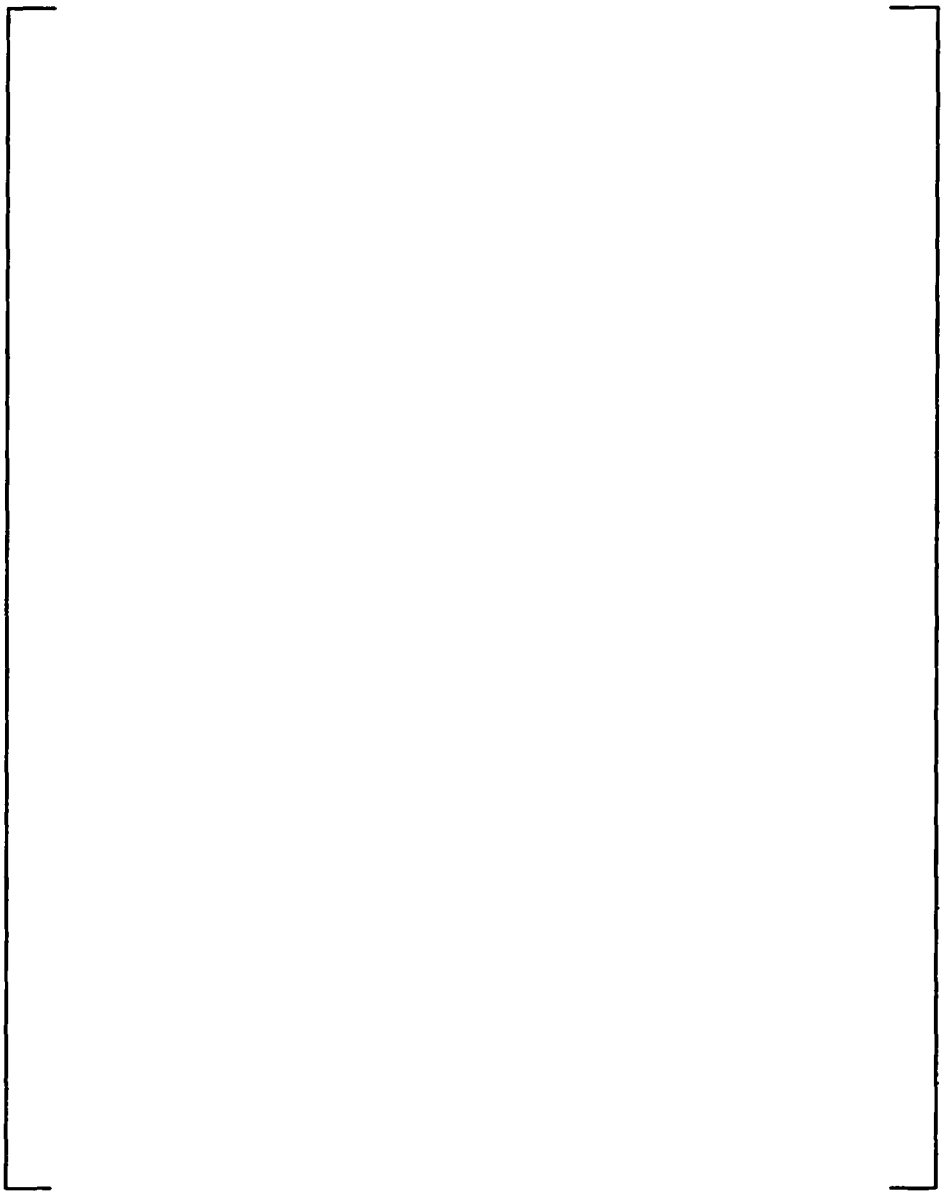

Figure 5-27
Stress Intensity Contour Plot
Right-Side Supports – Time = 0.260 sec
TSP 1

a,c

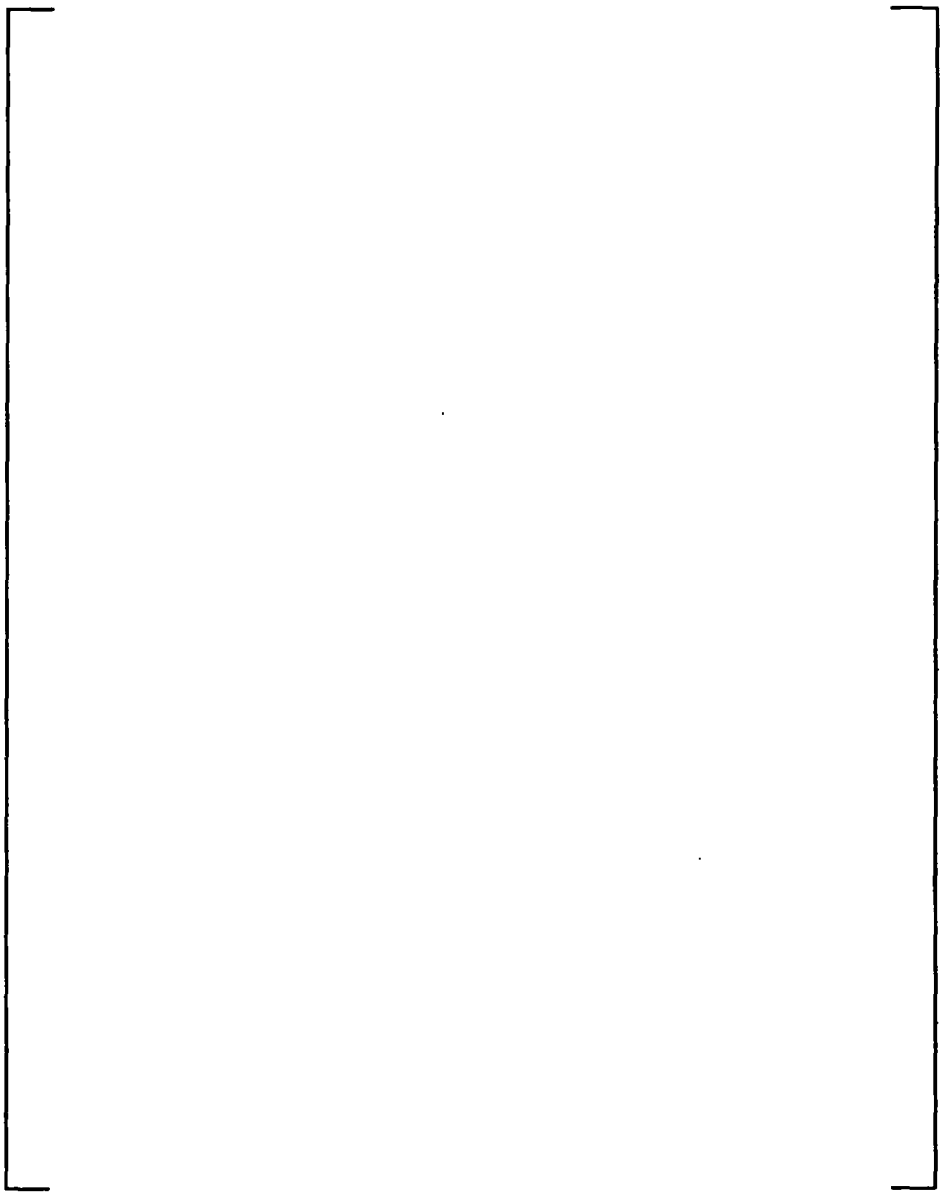

Figure 5-28
Stress Intensity Contour Plot
Right-Side Supports – Time = 0.260 sec
TSP 2

a,c

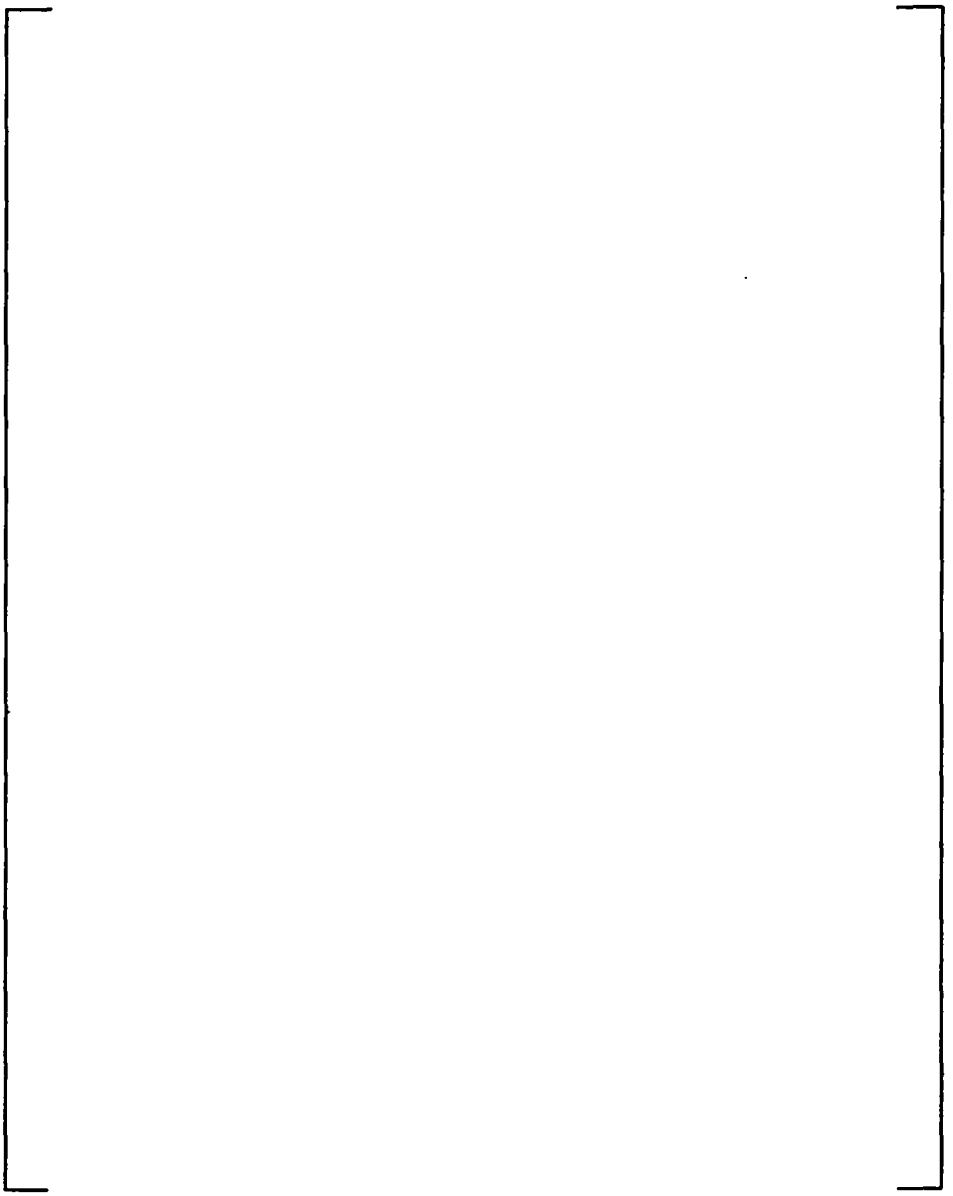

Figure 5-29
Stress Intensity Contour Plot
Right-Side Supports – Time = 0.260 sec
TSP 3

a,c

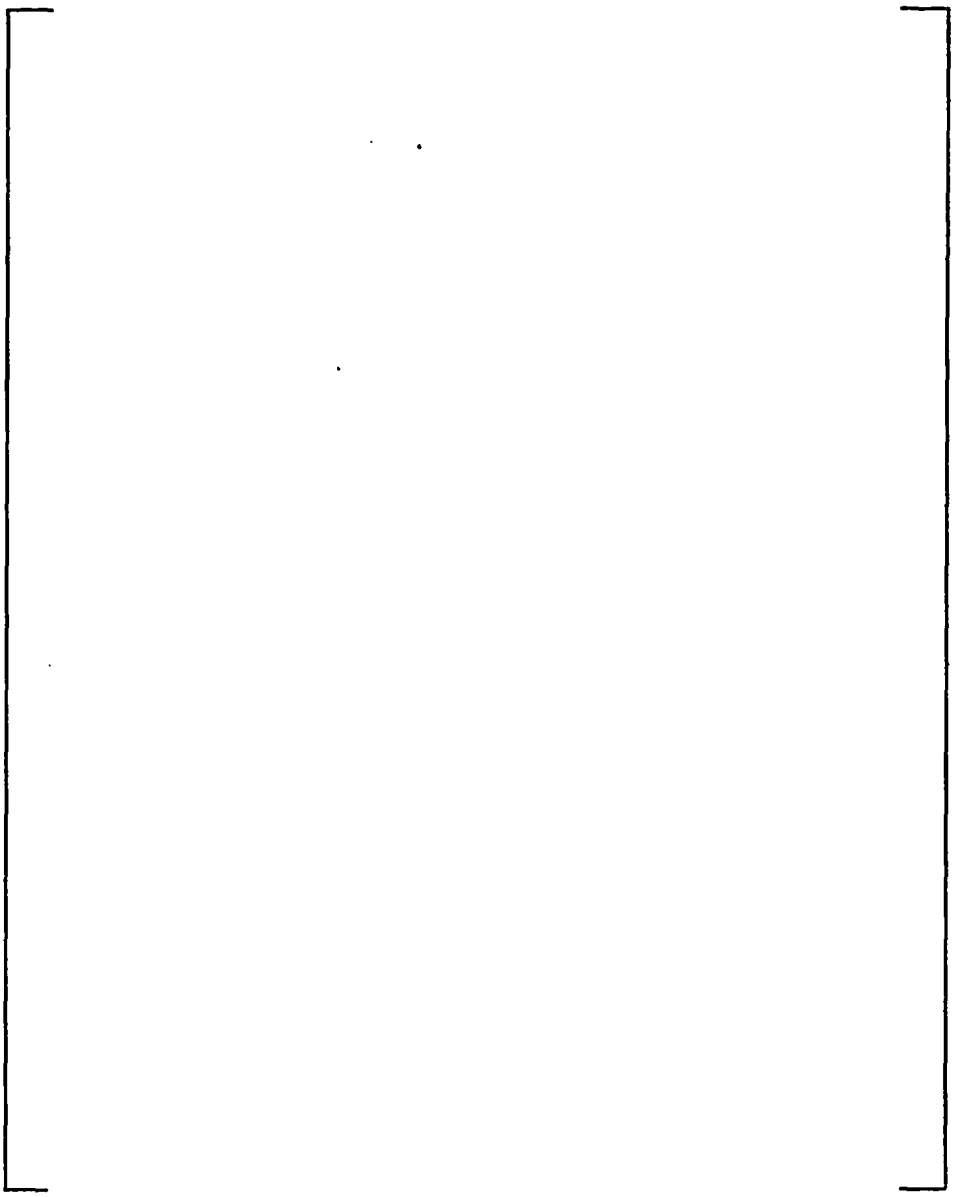

Figure 5-30
Stress Intensity Contour Plot
Right-Side Supports – Time = 0.260 sec
TSP 4

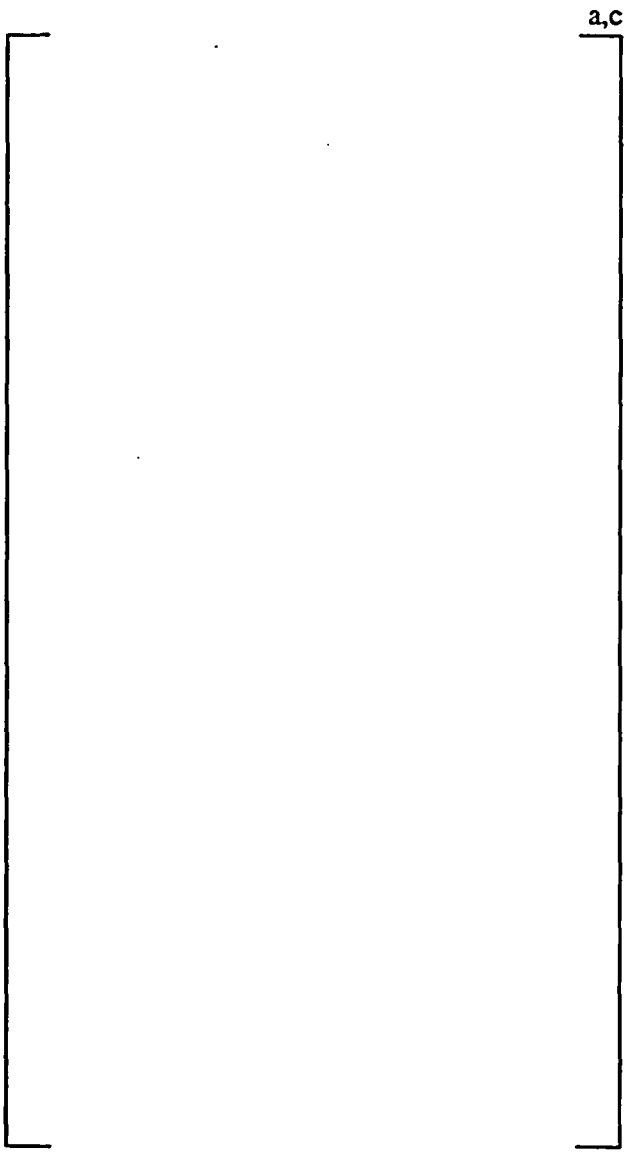

Figure 5-31
Displaced Geometry Plot
Right-Side Supports – Time = 0.260 sec

a,c

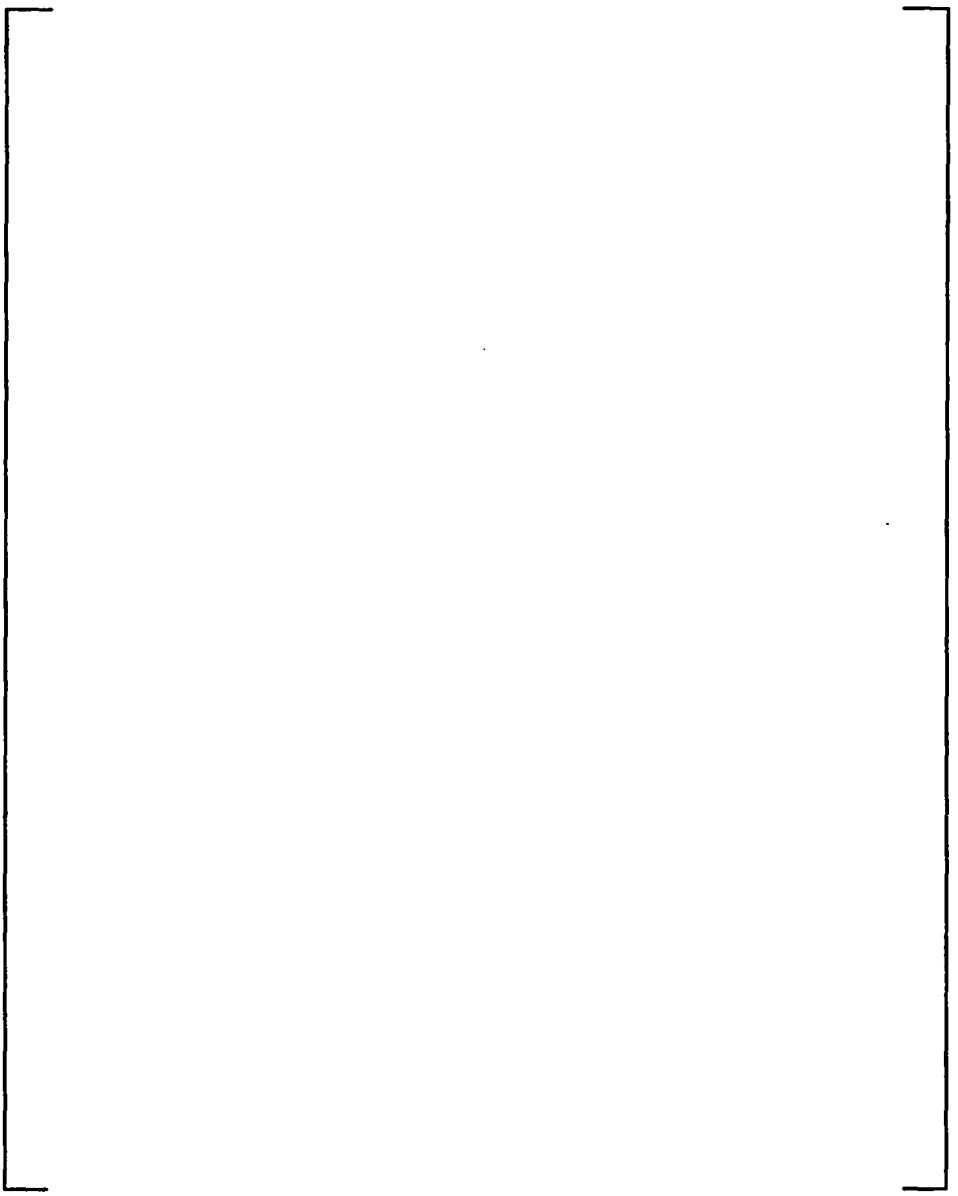

Figure 5-32
Stress Intensity Contour Plot
Left-Side Supports – Time = 0.265 sec
TSP 1

a,c

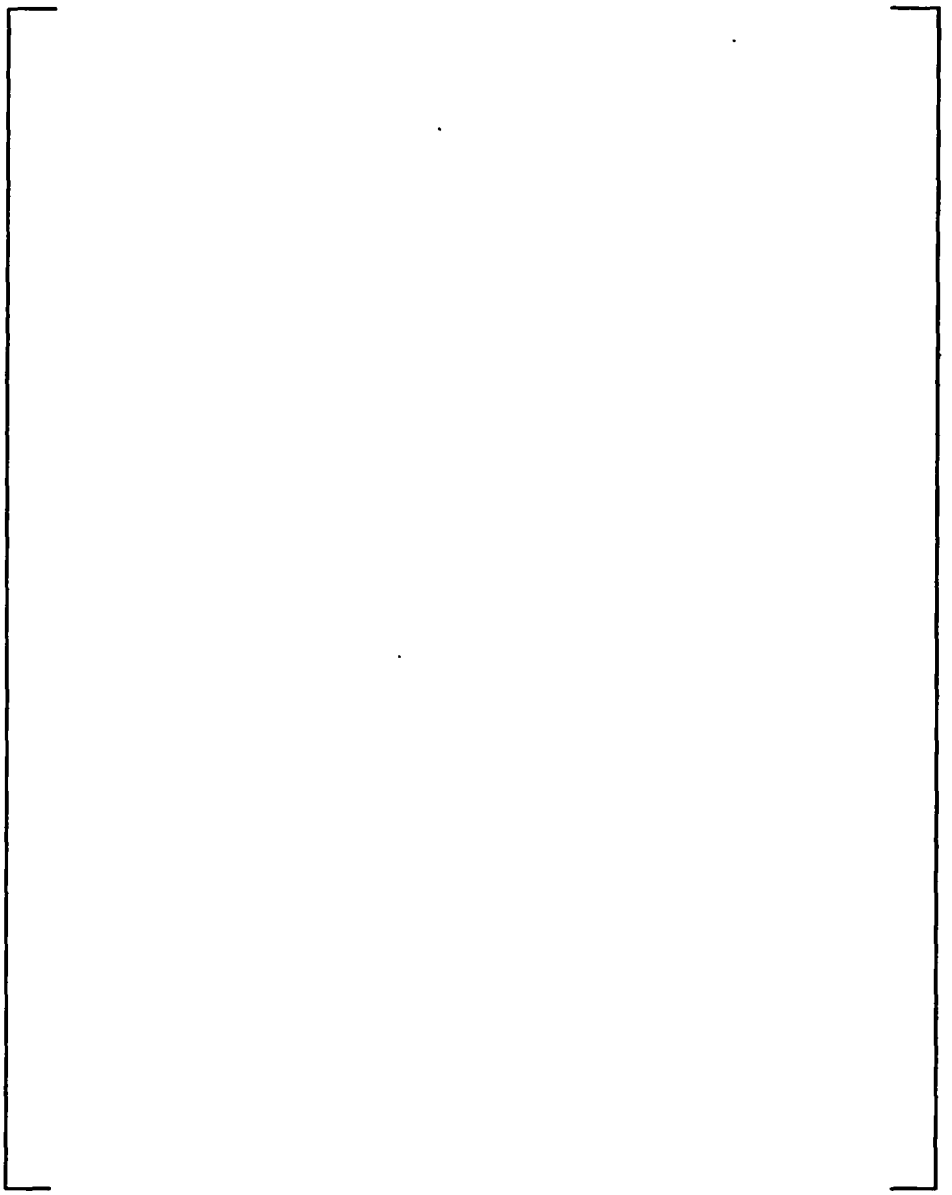

Figure 5-33
Stress Intensity Contour Plot
Left-Side Supports – Time = 0.265 sec
TSP 2

a,c

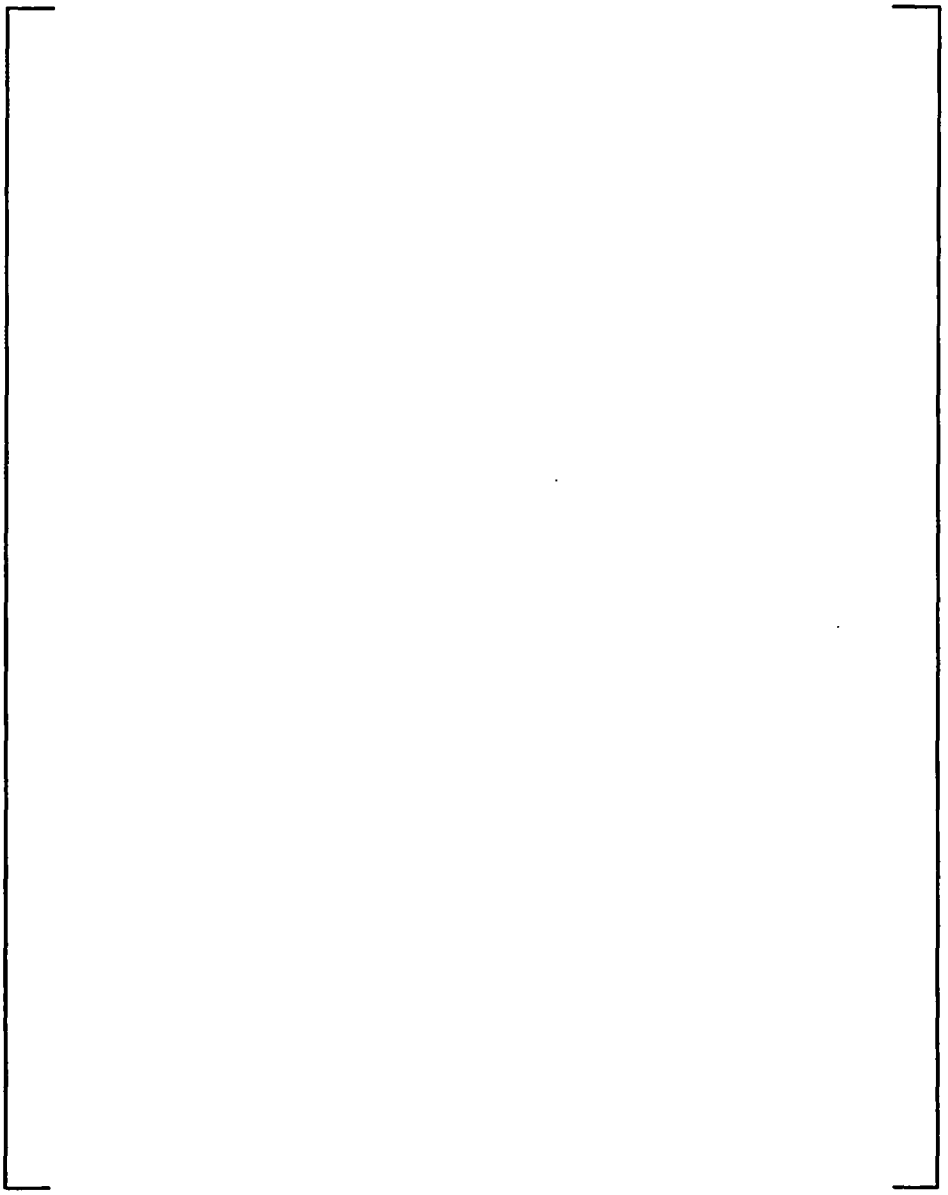

Figure 5-34
Stress Intensity Contour Plot
Left-Side Supports – Time = 0.265 sec
TSP 3

a,c

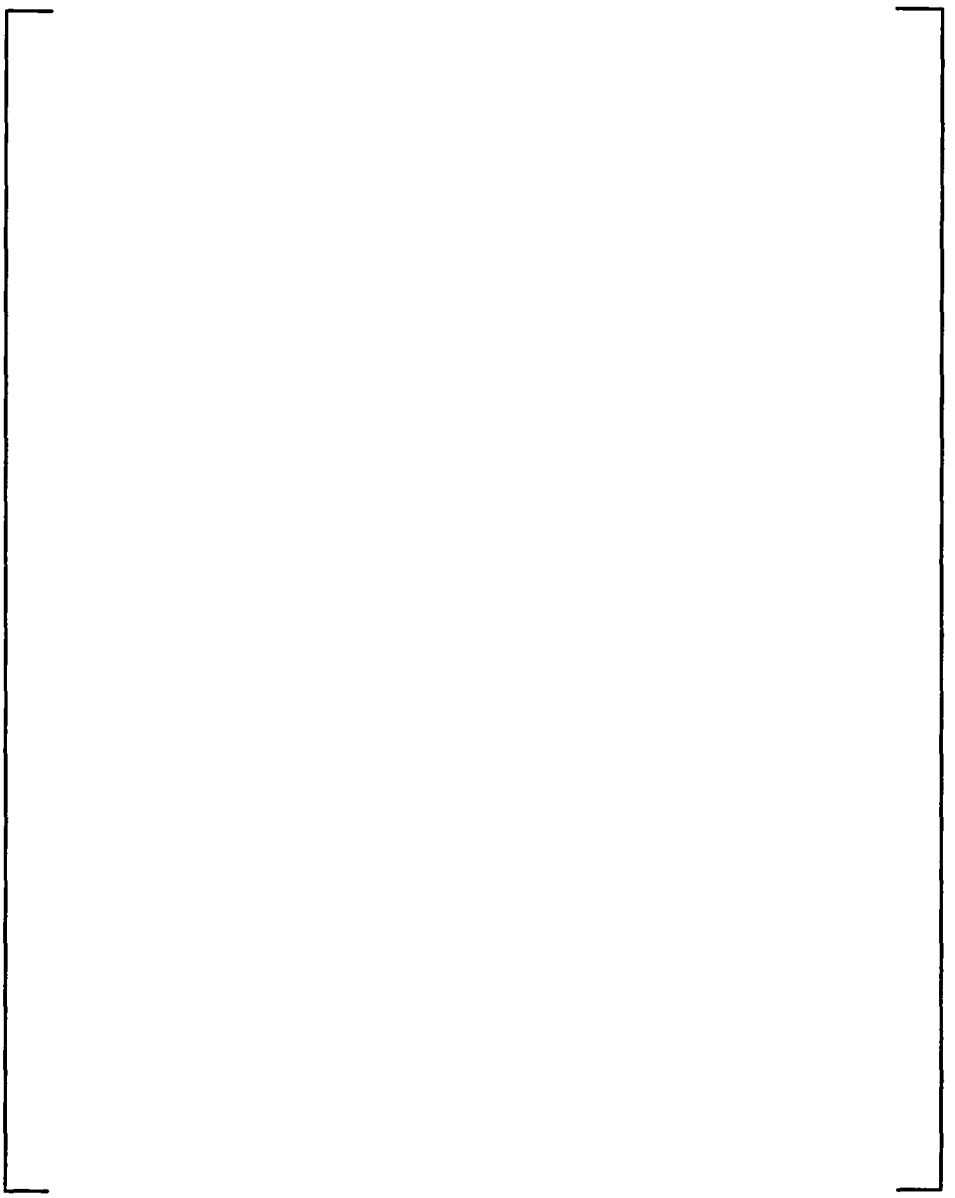

Figure 5-35
Stress Intensity Contour Plot
Left-Side Supports – Time = 0.265 sec
TSP 4

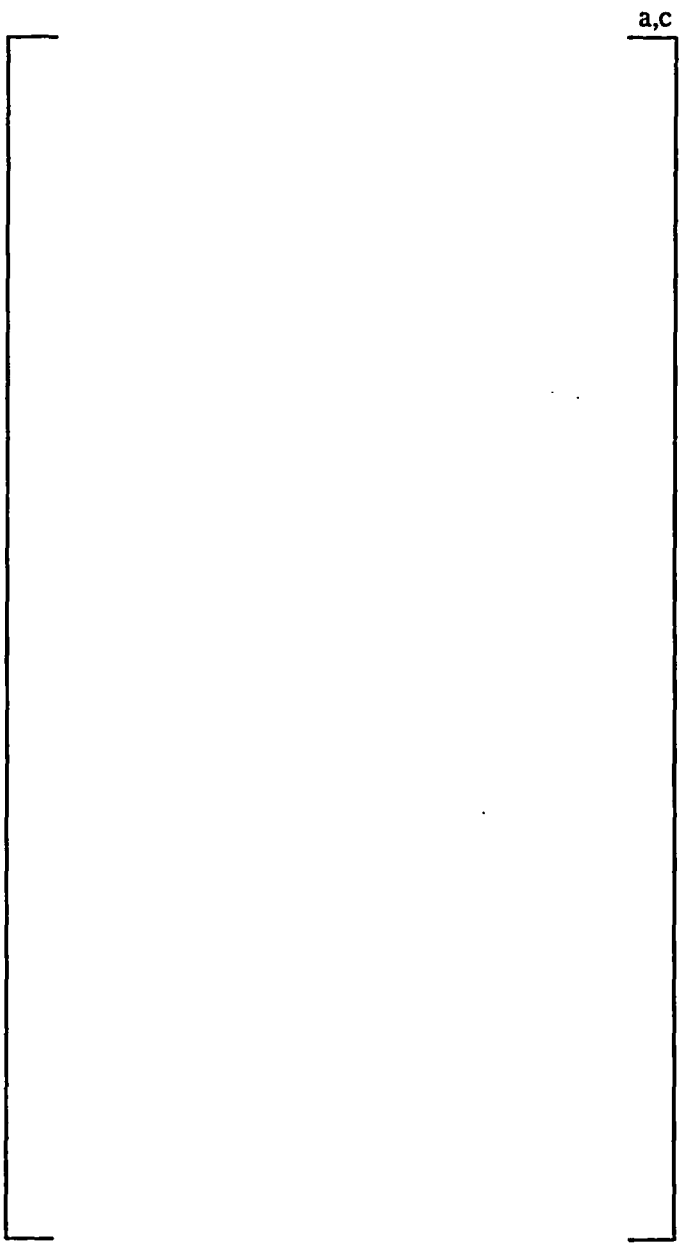

Figure 5-36
Displaced Geometry Plot
Left-Side Supports – Time = 0.265 sec

a,c

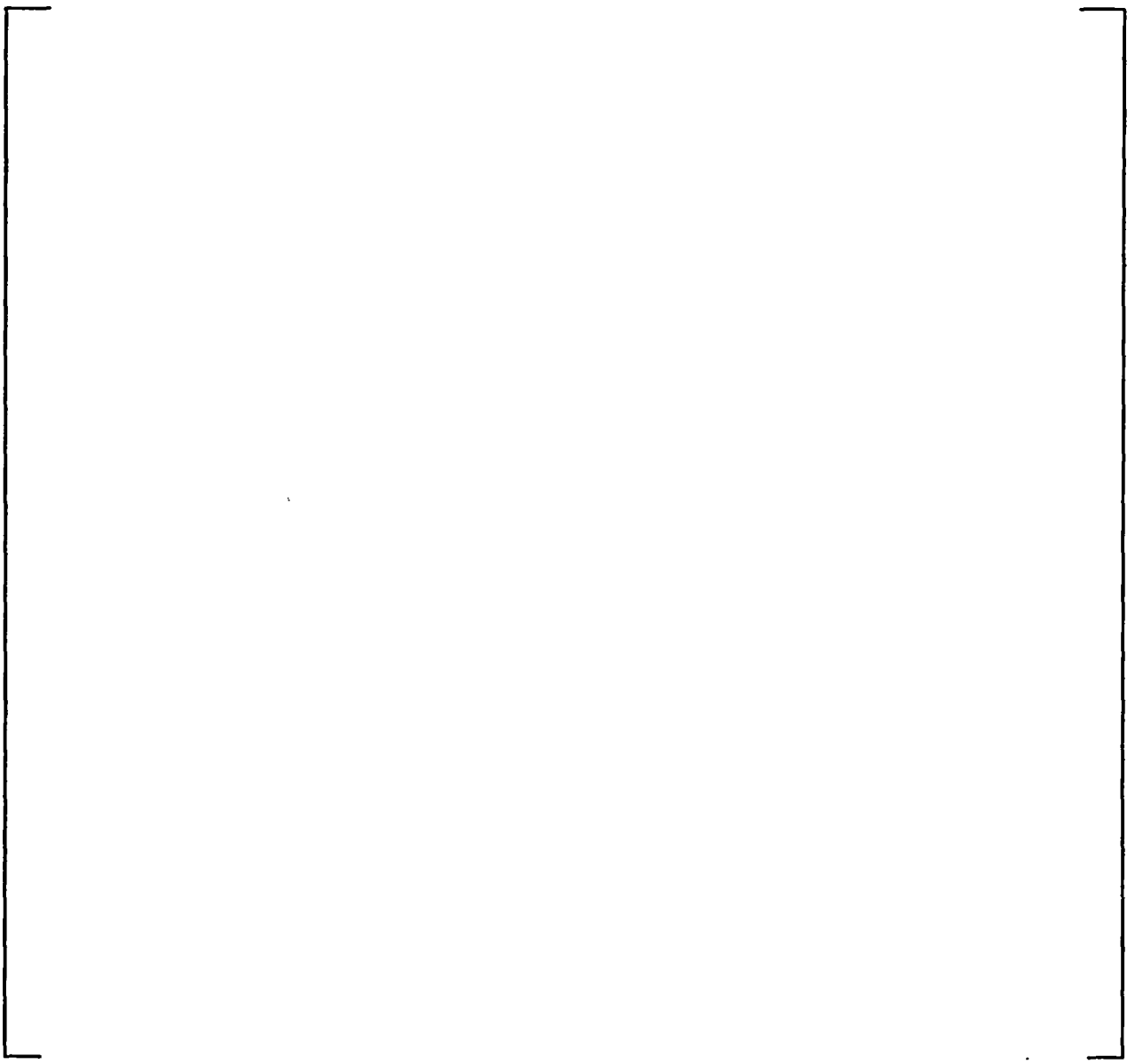

Figure 5-37
Candidate Tubes for Expansion
Hot Leg

a,c

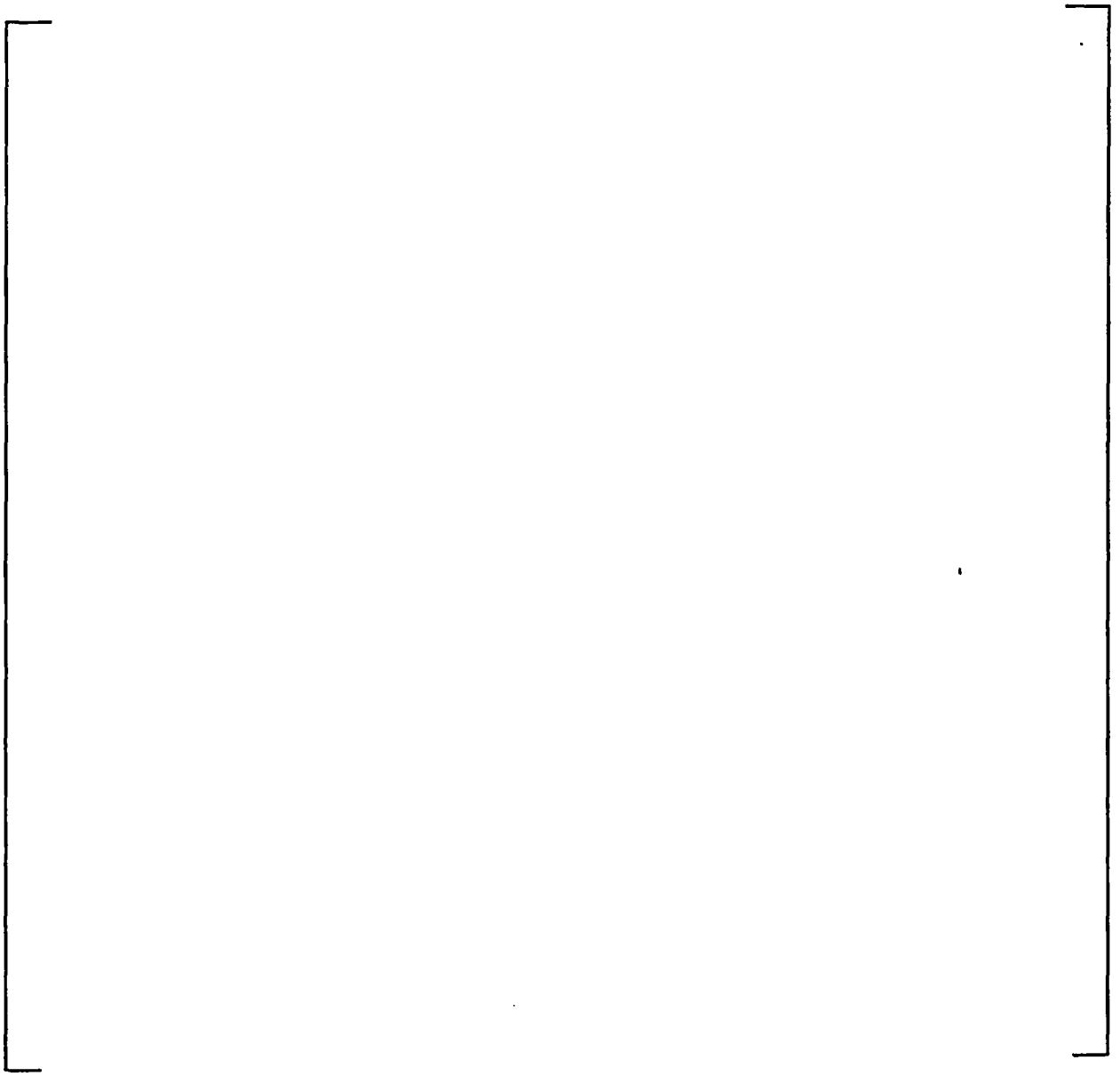

Figure 5-38
Candidate Tubes for Expansion
Cold Leg

6.0 TUBE EXPANSION PROCESS AND TEST SUPPORT

6.1 OVERVIEW

Since the TSPs do not undergo any displacement relative to indications developed within the TSPs during normal operation, tube burst at these locations is prevented by the TSP. Thus, the burst capability requirement of 3 times the normal operating differential pressure is obviated by the presence of the TSP, and the RG 1.121 requirement relative to $3\Delta P_{NO}$ is inherently met. If the TSPs did not undergo displacements during a postulated SLB event, the same would be true of the RG 1.121 requirement relative to $1.43\Delta P_{SLB}$. However, the TSPs are subjected to out-of-plane loads during a SLB resulting in vertical TSP displacements that could potentially expose cracks presumed to exist in the tube within the span of the TSP.

The principal requirement of the tube expansions is to limit TSP deflection to a value such that the probability of burst (POB) during a postulated SLB event is negligible. The design modification to accomplish this consists of expanding selected tubes, with an internal sleeve installed, into an hourglass shape at the elevation of the TSP, such that the TSP is captured by the tube/sleeve combination (Figure 6-1). Tubes selected for expansion will be plugged and removed from service.

Interaction of the expanded tube with the TSP will effectively cause the expanded tube assembly to act similar to a stayrod, significantly restricting the potential out-of-plane motion of the TSPs. To increase the load capacity of the expanded joint and to prevent the potential for tube-to-tube interaction in the unlikely event that an expanded tube experiences a circumferential separation in the expanded region, a surrogate sleeve is used. The expanded tube OD will be larger than the nominal tube OD by approximately [ ] [a,c] and larger than the TSP tube hole diameter by approximately [ ]. [a,c] A description of the design and testing of the expansion process is provided in this section. It should be noted that the Diablo Canyon SGs are scheduled to be chemically cleaned. The chemical cleaning will be implemented prior to the tube expansion such that the expansion joint will not be affected by the chemical cleaning.

An implicit requirement of the tube expansion modification is that the integrity of the expansions must be such that they perform their intended function for long periods of exposure to the secondary side environment. For Diablo Canyon, the period of performance is 2 to 3 cycles, or up to approximately 4.5 EFPY of operation, since SG replacement is planned for two cycles (about 3 EFPY) following the tube expansions.

6.2 REVIEW OF PRIOR APPLICATIONS

The tube expansion process has been previously applied at the Byron 1, Braidwood 1 and South Texas 2 plants. The process to be applied at Diablo Canyon differs from the Byron/Braidwood processes only in that the expansion bulge diameter is slightly smaller than that used at Byron/Braidwood and that standard thickness sleeves, as also applied at South Texas 2, will be used instead of thinned sleeves at the TSP expansions.

6.3 TUBE EXPANSION PROCESS REQUIREMENTS

The overall requirements for the application of tube expansion are summarized in Section 10 of this report. The following design requirements were established for the tube expansions. The actual performance of the tube expansions exceeds these design requirements as discussed later in this section.

1) The tube expansion at the TSP shall provide resistance to TSP motion with an associated stiffness of the expansion relative to plate motion of at least [ ] [a,c] when averaged over the initial 0.05" of TSP displacement as determined by TSP pull force versus displacement tests on expanded joints. As developed in Section 6.6, a minimum expanded tube diameter increase of [ ] [a,c] is required to achieve the minimum required joint stiffness of [ ]. [a,c]

2) The expansion shall be performed above and below the TSP by a hydraulic expansion process. A sleeve stabilizer shall be installed to extend above and below the parent tube expansion.

3) The expansion process shall be designed to achieve a maximum expanded tube diameter increase of approximately [ ] [a,c] when applied over the range of material properties (tubes and TSPs) and over the range of tube/TSP intersection dimensions. The limit on the expansion diameter is a design goal to limit residual stresses in the expanded tube; larger expansions are acceptable to meet the expanded tube stiffness and load requirements.

6.4 TUBE SUPPORT PLATE EXPANSION PROCESS DESCRIPTION

Figure 6-1 illustrates the TSP expansion configuration. The tube expansion is performed using hydraulic expansion equipment for Westinghouse 7/8" diameter tube sleeving and a modified sleeve delivery mandrel. The expansions are generated by supplying high-pressure water to an expansion mandrel/bladder system. The 2.5" long bladder used for sleeve expansion in the laser welded sleeving system is also used for the tube expansion process.

For development purposes, the tubes, sleeves, and TSP simulants were manually positioned. The sleeve sections used for the TSP expansions were cut to an overall length of 6 inches. Although the field applications of this process at Byron 1 and Braidwood 1 used sleeves thinned in the expansion region to accommodate tooling limitations, these limitations have been eliminated, and non-thinned sleeves are used for the Diablo Canyon application. The test samples used to determine the resistive load characteristics of the expanded assembly were configured with the sleeve centered at the axial center of the TSP simulant.

Field application will be performed using a Framatome based sleeving system, which includes the Search and Locate End Effector (SALEE), SALEE expansion mandrel, ROSA control computer, and standard sleeving system hydraulic expansion pressure unit. The Westinghouse mandrel has an integral eddy current coil that senses the center of the TSP and enables the tool to automatically stroke into the install/expansion position. The sleeve delivery mandrel has been modified to properly position the center of the sleeve, and consequently the center of the expansion bladder, adjacent to the center of the TSP. The

expansion process is computer controlled for consistency and repeatability. During the expansion process, the sleeve initially yields and contacts the tube. After the yielded sleeve contacts the tube, a volume controlled expansion is applied in which a predetermined piston stroke is monitored for confirmation of the required volume. This process leads to comparable bulge sizes for both low and high yield tubing.

6.5 TUBE EXPANSION PROCESS TEST RESULTS

Test specimens were prepared at various expansion pressures to establish a relationship between expansion pressure and projected tube OD and to establish a relationship between tube OD and resistive load capability at varying TSP deflection levels.

Test specimens were made using 12" long, Alloy 600 mill annealed, 0.875" OD x 0.043" nominal wall thickness tube sections and 6" long, Alloy 690 thermally treated, 0.740" OD x 0.040" nominal wall thickness sleeve sections. TSP simulants, Figure 6-2, were made from SA-285 Type C plate material, which is the same as the Diablo Canyon TSP material specification. The TSP simulants were ¾" thick, approximately 2.8" square sections with a center tube hole surrounded by 4 tube holes and 4 flow holes, with hole diameters, hole-to-hole pitches, and chamfers consistent with the SG manufacturing drawings. The ligament thickness at the edges of the TSP simulant was designed to be approximately half of the nominal ligament thickness. These simulants conservatively represented the in-plane stiffness of the TSPs since only a small portion of the plate pattern was used. It is expected that in-plane restraint provided by surrounding plate material will result in a stiffness over and above that considered in the tests. The tube yield strength, 43.1 – 56.3 ksi, and sleeve yield strength, nominally 48 – 50 ksi, represented the range of tube materials. For test purposes, SA-285 Type C plate with yield strength of 42.5 ksi was used for the TSP simulants. Sleeves were centered axially at the center of the TSP simulant, which was centered over the 12" tube length.

Samples were produced with a nominal fitup condition, that is, with the sleeve axially centered on the TSP, and with minor levels of sleeve/expansion mandrel axial mis-position relative to the center of the TSP. Samples were tested at room temperature by tensile loading in a MTS® tensile loading machine. The load testing setup is shown in Figure 6-3. One end of the sample was attached to the movable crosshead using self-adjusting tube OD gripper jaws. A fixture was bolted to the stationary base of the machine. This fixture is a stiff, box-like structure that restrains the TSP simulant while the movable crosshead essentially extrudes the expanded tube/sleeve assembly through the TSP simulant hole. Plate bending effects encountered during an actual SLB event, which would act to pinch the tube and further increase the resistive load capacity of the expansion, were not modeled into the test setup. Machine speed was set at a minimum of 0.25 ips. Previous testing, discussed in Reference 1, indicated that, at these speeds, the load response is independent of pull rate. The motion of the tube relative to the TSP simulant was accurately isolated by use of an extensometer, a precision testing device designed for such purposes, attached to the tube and the TSP simulant. Use of the extensometer eliminated the effects of potential gripper jaw slip and specimen elastic stretch during loading from influencing the load vs. displacement curve. Displacement of the upper head/gripper of the test machine was also confirmed on the test machine itself.

Resistive load versus TSP displacement curves were produced for each specimen. A sample of these curves is shown in Figure 6-4.

The expansion assembly stiffness was determined by calculating the stiffness coefficient over the first 50 mils, and then 100 mils, of TSP displacement. Table 6-1 provides the results of 31 tensile pull tests. The first set of samples was tested using the 3x3 hole TSP simulant shown in Figure 6-2. This group of tests includes samples 2-1 to 2-24 in Table 6-1. A second set of samples was tested with bulge sizes the same as for the first set, with the same tube and sleeve material heats, and a larger TSP simulant to represent an additional row of tube/flow holes (5x5 hole TSP). The 5x5 hole TSP simulant was approximately 4.6" square x ¾" thick. This set is labeled test samples 2-25 through 2-31 in Table 6-1.

Prior to performing the tests with the prototypic TSP pieces, an initial series of tests was run using a single hole, clamped TSP simulant. The expansions were initially performed in a 0.880 inch diameter hole. Following expansion, the TSP simulant was replaced with a clamped TSP with larger hole diameters to provide a general sensitivity to loss of TSP material following the expansion. The tests were performed to assess potential effects of chemical cleaning following application of the expansion process. However, since chemical cleaning will be applied for the Diablo Canyon SGs prior to the tube expansions, there will not be any change in the tube-to-TSP expansion joint following the tube expansions. In addition, any application of chemical cleaning at the Diablo Canyon SGs will not include process steps necessary to clean the TSP crevices. The results for these tests are summarized in Table 6-2, which includes the test conditions and average joint stiffness results for groups of three tests with common test conditions. The data of Table 6-2 are not applicable to the joint stiffness evaluations other than providing a general demonstration of the influence of TSP stiffness on the joint stiffness. For the single hole TSP simulant of Table 6-2, the joint stiffness results are on the order of [

]^{a,c}

The load vs. displacement test results show that the bulge size has a significant effect upon the resistive load developed as the TSP is pulled over the bulge, with the resistance being proportional to the degree of expansion. The test results are evaluated in Section 6.6 below to develop the required bulge size for the TSP displacement analyses of this report.

6.6 EVALUATION OF TUBE EXPANSION TEST RESULTS FOR JOINT STIFFNESS

This section develops the tube expansion bulge size requirements based on the test results of Table 6-1. The resulting bulge size requirement provides the associated joint stiffness applied in the TSP displacement analyses of Section 4.

6.6.1 TSP Displacements at Expansion Locations

The test results of Table 6-1 provide joint stiffness data as a function of bulge size for nominal tube to TSP displacements of 0.050 and 0.100 inch at the joint location. The TSP deflection analysis results of Section 5 were evaluated for relative tube to TSP displacements at the joint location. Figure 6-5 shows the distribution of TSP displacements at the joint locations resulting from the TSP displacement analyses described in Section 5. Figure 6-5 was obtained from the more limiting of two models applied in Section 5. The hot leg TSP displacements at the bulges are dominantly less than 0.05 inch. The cold leg expansions are applied to limit hot leg TSP displacements and no limited displacement requirements apply for the cold leg. In Section 5.4.6, it is noted that for the range of differential displacements observed in the TSP displacement analyses, variations in the joint stiffness would have only a small effect

on the displacements. Figure 6-6 compares the joint stiffness results for TSP displacements of 50 to 150 mils. The variation in joint stiffness between 50 mils, which spans most of the hot leg displacements, and about 125 mils, which bounds the cold leg displacements, is modest and the 125 mil data bounds the joint stiffness used in the displacement analyses of Section 5. Due to the fact that the displacements at the hot leg expansion locations are dominantly < 50 mils, the appropriate test results to apply for obtaining the bulge size requirements and associated joint stiffness are the Table 6-1 data for displacements of 0.050 inch.

6.6.2 Sensitivity of Joint Stiffness to TSP Stiffness

The forces required to displace the TSP relative to the tube are sensitive to the stiffness of the TSP. The TSP is a honeycomb structure with thin ligaments between tube holes. Test data were obtained for 3x3 and 5x5 TSP simulants as well as a non-prototypic single hole TSP as described in Section 6.5. The sensitivity of the joint stiffness to the TSP configuration is shown in Figure 6-7. The 5x5 hole TSP configuration is only slightly stiffer than the 3x3 hole TSP, and the Figure 6-7 results do not show significant differences for the joint stiffness between these two configurations with a small incremental difference in the plate lateral stiffness. Figure 6-7 also includes an example result for the single hole tests of Table 6-2 that shows a large increase in joint stiffness compared to the prototypic TSPs. Thus, the joint stiffness can be expected to increase with significant increases in the lateral TSP stiffness such as can be expected at dented TSP intersections. Based on the results of Figure 6-7, the data for the 3x3 and 5x5 TSP configurations can be combined to evaluate the joint stiffness.

The DCPP SGs have TSP crevices packed with magnetite formed by TSP corrosion and externally deposited magnetite with a significant number of dented TSP intersections. As a result of the essentially zero crevice gaps, the lateral stiffness of the TSP can be expected to be much higher than the TSP simulants with the crevice diametral clearance of about 15 mils used for the joint stiffness tests of Table 6-1. As a consequence of the expected increase in TSP stiffness, the joint stiffness test results of Table 6-1 are very conservative as further discussed in Section 6.6.3 below.

6.6.3 Sensitivity of Joint Stiffness to Tube Yield Strength

The joint stiffness can be expected to show some sensitivity to tube yield strength due to the deformation of the bulge required to displace the TSP relative to the tube. As shown in Table 6-1, tests results for joint stiffness were obtained for two yield strengths. The lower 43.1 and 45.5 ksi yield strengths are below the lower 90% confidence on the room temperature nominal value of 50.98 ksi for 7/8" tubing and only slightly above the nominal operating temperature yield strength of 41.89 ksi. The higher 56.3 ksi yield tubing included in the Table 6-1 test results corresponds to about the upper 90% confidence on the yield strength. Consequently, the yield strengths included in the tests can be expected to bound most of the DCPP SG tubes.

Figure 6-8 shows the joint stiffness sensitivity to the tube yield strength for TSP displacements at the joint location of about 50 mils. The results show modest sensitivity to yield strength for the range of yields used in the tests which span about the lower to upper 90% confidence levels on 7/8" tubing yield strengths. For bulge sizes of [ ]^{a,b,c}

The field expansion process to be applied at DCPP is described in Section 6.4. For the constant volume expansion process, the bulge size is approximately independent of the tube yield strength. The expansion pressure increases with the tube yield strength.

At normal operating temperatures, the material properties of the tubes, sleeves, and TSPs would be reduced by approximately 9% compared to room temperature conditions, and therefore, would be expected to result in a slight reduction in the resistive load capacity compared to the room temperature results. However, further evaluation of the operating performance characteristics of the expanded joint indicates that the room temperature data are conservative for application at operating conditions for the following reasons:

1) Out-of-plane bending of the plate during a postulated SLB would cause a bending lockup (cam-lock) condition between the tube/sleeve and TSP, and would act to increase resistive loads, compared to the room temperature tests that utilized flat plates to simulate the TSPs. This effect would be more significant at hot leg TSPs 5 to 7 and cold leg TSPs where TSP displacements and associated plate rotations are larger than the lower hot leg plates with limited displacement.

2) Interaction between the TSP and the tube OD results in a more severe galling condition at operating temperature than at room temperature. Galling would increase the joint stiffness. Previous testing related to structural integrity of hybrid expansion joint (HEJ) sleeve assemblies indicates that the extent of galling of Alloy 600 tubing and therefore, the galling forces, significantly increase at 600° F compared to room temperature. Because the geometry of an HEJ assembly and the TSP expansion assembly are similar; this result applies to the TSP expansions as well.

3) Crevice packing and dented TSP conditions will increase the lateral stiffness of the TSP with an associated increase in the joint stiffness as discussed in Section 6.6.2 above.

4) Crevice packing would limit the expanded diameter of the tube/sleeve assembly within the TSP, increasing the diameter difference between the expanded tube/sleeve assembly immediately above/below the TSP, and thereby increasing resistive load. The interaction angle between the tube OD and TSP hole diameter would become rotated towards the horizontal (plane of TSP), and this interaction angle would act to create increased resistive load by the extrusion action. Open crevices were used in the tests performed.

5) Thermal expansion effects would act to create a tighter joint at operating temperatures since the sleeve expands more than the tube due to the differences in thermal expansion coefficients between the tube and sleeve materials. The tube/sleeve assembly would also act to create a tighter fitup condition with the TSP assembly, as the thermal expansion coefficients of both Alloy 600 and Alloy 690 are greater than the expansion coefficient of the SA-285, Grade C TSP material. This would result in higher radial preloading between the tube/sleeve and TSP at operating and faulted conditions. This thermal expansion effect was not provided by the room temperature testing, and therefore, will add to the resistive load capacity of the expanded TSP joint at operating conditions.

It is concluded that it is reasonable and conservative to apply the room temperature joint stiffness values to SLB event conditions without adjustment for decreased material properties at elevated temperatures. Based on the above considerations, it is also reasonable and conservative to combine the low and high yield strength test results to develop the bulge size requirements.

6.6.4 Joint Stiffness Evaluation for TSP Displacement Analysis

Based on the discussions in Sections 6.6.1 to 6.6.3 above, the joint stiffness requirements are developed based on the following data considerations:

- Joint stiffness results for 50 mils TSP displacement adequately bound the relative tube-to-TSP displacements at the joint locations
- Combining data for the low and high yield strength test results and applying the room temperature test results for operating conditions adds conservatism, as described in Section 6.6.3, in evaluating the joint stiffness

Figure 6-9 shows the results of the regression analysis for the 50 mil TSP displacement data from Table 6-1 including the lower 95% confidence limit on the mean regression line. At the lower 95% confidence level, the data support a joint stiffness of [ ]^{a,c}

As discussed in Section 6.9, a maximum bulge size of [ ]^{a,c} is recommended to limit the residual stresses resulting from the expansion and the associated potential for circumferential cracks at the expansion joints. To provide flexibility on the bulge diameter for the field expansion process, the minimum acceptable bulge size is established at [ ]^{a,c} This bulge size results in a minimum joint stiffness for application in the TSP displacement analysis of [ ]^{a,c}

6.6.5 Considerations for Re-expansion of Undersized Expansions

The expanded tubes will be inspected following application of the process to verify that the expansion (proper bulge size) has been achieved. If the minimum acceptable bulge size has not been achieved either above or below the TSP, an additional tube must be selected for expansion. Due to the design of the expansion bladder, re-expansion of under-expanded joints is not feasible, since the increased sleeve to bladder gaps may cause bladder failure prior to complete expansion. Re-expansion should be attempted only if both expansions (above and below the TSP) are below the minimum acceptable value. This would be the case if a premature bladder failure occurred during the expansion process. The under-expanded tube will provide added margin against TSP deflection during a postulated SLB event. For tubes where expansions are performed at more than one TSP, if it is necessary to select an additional tube for expansions due to an unacceptable bulge size, expansions are required only at the TSP intersection(s) having bulge sizes less than the acceptance limit.

6.7 TSP STRESSES PRODUCED BY THE EXPANSION

A finite element (FE) structural analysis of the tube expansion process at DCPP was performed to assess the residual displacements, stresses and strains in the TSP ligaments. The FE model simulated the sleeve,

tube and the surrounding carbon steel TSP. Minimum specified yield strengths from the ASME Code were assumed as follows: 40 ksi for the TT Alloy 690 sleeve, 35 ksi for the MA Alloy 600 tube and 30 ksi for the SA-285 Grade C carbon steel TSP. As built actual yield strengths are expected to be higher, which would make the FE model conservative. Nominal initial geometric parameters were assumed, namely: tube outer diameter of 0.875 inch with a 0.050 inch wall; sleeve outer and inner diameters of 0.740 and 0.661 inch, respectively; TSP tube hole and flow hole diameters of 0.891 and 0.750 inch, respectively. These dimensions give a minimum TSP ligament at the flow hole of 0.085 inch for a 1.281 inch square pitch. Plane stress quadrilateral elements were employed to model the sleeve and TSP. The tube was modeled by plane strain quadrilateral elements to account for its relatively long length.

Unpacked conditions (i.e., wide-open crevices) in the surrounding tube-to-TSP interfaces were assumed because the structural properties of the hard magnetite are unknown. This assumption is judged conservative because packed tubes in the surrounding holes would provide additional in-plane stiffness to the TSP reducing the stresses in the TSP ligaments.

Compression-only contact elements were used to model the radial contact between the sleeve and the tube to be expanded. The initial radial gap at this interface before expansion is 0.0175 inch. The initial radial gap between the unexpanded tube and TSP hole is 0.008 inch. Two solutions were obtained by first assuming this gap is "unpacked" (i.e., a wide open 0.008 inch crevice before expansion), and then a second solution was obtained assuming hard magnetite fills the initial 0.008 inch gap (crevice). Since the structural properties of the magnetite are unknown, the "packed" interface is simulated in the FE model with stiff radial compression only elements that are assumed initially closed before expansion. This latter case approximates the "packed" condition. Again, in this latter case only the crevice between the expanded tube and TSP hole is assumed "packed." The surrounding tube holes in the FE model are assumed open in all cases.

An expansion pressure of 25 ksi is considered an upper bound for the process. Thus in both FE solution cases, the expansion pressure was applied to the inner surface of the sleeve incrementally up to a maximum of 25 ksi in the first load step. Next, in the second load step, the pressure was reduced incrementally back to zero to permit calculation of the residual stresses and strains in the TSP ligaments. Results calculated for both cases show that the peak residual plastic strains, due to the 25 ksi expansion pressure, are small (6% or less) and highly localized, confined to the minimum ligament between the expanded tube hole and adjacent flow hole. All other ligaments in the TSP essentially remain elastic. Even the minimum ligament between the expanded tube hole and the flow hole remains elastic for expansion pressures less than 15 ksi for the "packed" case and less than 18 ksi for the "unpacked" case. The permanent radial displacement, calculated for the 25 ksi maximum expansion pressure at the adjacent minimum ligament, is only about 9 mils for the "packed" case and less than 4 mils for the "unpacked" case. Such small residual displacements will not adversely affect the area of the adjacent flow hole. The expansion pressure of 25 ksi would only be approached for high yield stress tubing, for which the yield strength would exceed 55 ksi compared to the code value of 35 ksi used in the analysis. For the expected combinations of expansion pressures, tube yield strength and TSP yield strength, it is probable that there would be no plastic strain in the ligaments. Therefore, based on this FE analysis, it is concluded that no flow or TSP integrity issues would be expected due to the planned tube expansions.

6.8 NDE SUPPORT FOR TUBE EXPANSION

6.8.1 Determination of Expansion OD from ID Measurement

Post-expansion diameter verification of the expansions is required to ensure that the minimum stiffness requirements are met. Field measurements are made by NDE to define the ID of the actual bulge. The expansion joint load test basis is in terms of tube OD bulge. Due to the required IDs and non-expanded sleeve ID, mechanical measurement devices could not be inserted into the samples to determine the ID corresponding to the test OD. Therefore, a set of calculations was developed to predict IDs based on measured ODs, and ODs based on measured IDs. The range of acceptable tube IDs is based on these calculations.

To verify the adequacy of the OD to ID transfer calculation, several specimens were sectioned after expansion. The tube and sleeve pre-expansion dimensions were recorded, the specimens were assembled as TSP expansion samples, the expanded ODs were measured, and the specimens were sectioned at the maximum OD diameter of the bulges. The bulge IDs were measured with "Intrimiks" (special micrometers used for inspection of inside diameters) at the location of the maximum OD bulge diameter. Table 6-3 provides a summary of the calculated ID values and mechanically measured ID values for the sectioned samples. The sectioned samples used 7/8" tubes and sleeves. The calculation method is based on the measured sleeve wall thickness, assumed tube ID and wall thickness, and eddy current measured ID, which is used to calculate applied strains, and the amount of wall thinning due to the expansion process. The predicted IDs were nominally within 1 mil of the measured values. Similar results are obtained when the OD is predicted based on an ID measurement.

As part of the justification of eddy current ID measurement in the expansion region provided in Reference 2, 7 samples using 3/4" tubes and sleeves were prepared for verification of efficacy of the process. Following assembly of the test samples, the maximum OD bulge sizes were measured. The IDs in the expansion region were then calculated and compared to the values determined using eddy current methods. The average variance for the 7 samples (14 expansions) was -0.0008", with a standard deviation of 0.0018". The variance is defined as the eddy current measured diameter minus the calculated value. To verify these results, one of these samples was sectioned. The physically measured IDs were [ ]^{a,c,e}. The eddy current measured IDs were [ ]^{a,c,e}, respectively, while the calculated IDs were [ ]^{a,c,e}.

The required expansion ID dimensions will be established for each field expansion. Based on the excellent correlation between calculated and mechanically measured expansion IDs, a similar calculation can be performed to establish the resultant tube OD. Comparison of calculated and mechanically measured specimen IDs showed that in most cases the difference between the two values was less than 0.001". An accurate calculation of the expansion OD achieved can be performed, based on the known dimensions of the sleeve being used to calculate the sleeve hoop strain and the measured tube ID from the eddy current trace and the nominal tube wall thickness.

6.8.2 Bobbin Profilometry for Expansion Diameter Measurements

In the field, a standard bobbin profilometry probe will be used to determine the mean diameter of the expansion maxima (above and below the TSP). If the minimum bulge diameter requirements are not

achieved, additional tubes must be expanded. A detailed discussion of bobbin coil profilometry was presented in Reference 2. A summary is provided below.

The technique involves the use of a bobbin coil probe excited in differential and absolute modes at multiple frequencies, typically ranging form 10 kHz to 630 kHz. The lowest frequency penetrates outside of the sleeved tube and is used for steam generator landmark detection. The highest frequency has a very shallow depth of penetration and is used for the measurement of the diameter of the expansion. The bobbin probe integrates the signal response about the circumference of the tube and yields a mean diameter measurement at a given axial location.

A standard, with expansions of known diameter, is used to construct a calibration table that relates the diameter of the tube to the voltage of the eddy current response. The calibration standard for the process will include expansion bulge diameters that are close to the expected range of expansion process result in order to achieve the most accurate measurement possible.

Section 10.4 of Reference 1 shows the results of the evaluation of the expansions for both 7/8 and 3/4" diameter tubing along with the calculated bulge IDs based on the OD measurements and the expansion strain. These tables show that the eddy current measurement of the inner diameter, on the average, meets the expected value within ±0.002" ([ ]^{a,c,e}). This uncertainty on the bobbin profilometry results is acceptable and no adjustments are necessary to the bobbin data for field process applications. This shows that the tube ID can be reliably measured using eddy current methods. This measurement coupled with the knowledge of the strain experienced during the expansion process can be used to verify that the OD of the bulge falls within the desired process range.

6.9 TUBE STABILIZATION WITH AN EXPANDED SLEEVE

Adequate restraint is provided by the sleeve if circumferential cracking is postulated to occur in the original tube after it is expanded and plugged. For a crack that is postulated to form at the top edge of the TSP, the interaction between the tube and sleeve in the expanded area provides for a rigid link between the tube sections. Expanded specimens cut apart in the expansion region indicate intimate contact between the tube and sleeve. The expanded sleeve provides a rigid structure with the tube even if it is assumed that the tube is separated at the upper edge of the bulge. The tube at this point still acts as though it had a fixed support condition for tube vibration considerations due to the stiffness of the sleeve and the interaction of the tube and sleeve with the TSP.

The potential for fluidelastic vibration of the tube is negligible. If the tube is postulated to separate at the upper edge of the expansion, the tube end is effectively restrained by the sleeve above the bulged region. At the intersection between the tube and sleeve, the gap is zero. Lateral motion of the tube end is limited to the size of the gap, and the stiffness of the sleeve is sufficient to restrain further lateral motion of the tube, such that contact with adjacent tubes is precluded. The bending stiffness of the sleeve is sufficiently large that any operational loading due to flow effects is negated by the sleeve stiffness, and tube-to-tube contact will not occur. With the limited range of motion of the tube end, the end conditions are similar to a pinned connection when contact with the sleeve occurs. As long as some boundary condition fixity is provided, the potential for fluidelastic excitation is minimal.

In summary, the sleeve provides effective tube stabilization under the assumption that the parent tube is separated in the region of the expansion. The sleeve functions to essentially eliminate the likelihood of fluidelastic vibration of a separated parent tube and provides lateral restraint to prevent the assumed separated tube end from contacting adjacent tubes.

6.10 POTENTIAL FOR CIRCUMFERENTIAL CRACKING IN EXPANDED AND PLUGGED TUBES

6.10.1 TSP Region

6.10.1.1 Operating Experience for Circumferential Cracking

After one cycle of operation, all TSP expansions at Braidwood were inspected using the +Point coil. No indications were detected. The OD bulge diameters inspected at Braidwood included a maximum of 0.108", and 31 bulges greater than 90 mils, of which 5 were greater than 0.100". The target expansion for DCPP is a minimum of [ ]^{a,c}, compared to the target for Braidwood of [ ]^{a,c}. Since process improvements have been made to reduce the potential of axial misposition which, in turn, determines bulge variance and the potential for large bulges, the potential for having bulges greater than [ ]^{a,c} is greatly reduced.

No cracking has been found in the hydraulic expansions at TSP intersections in the preheater region of Model E and D4 SGs that include expansions up to about a 41 mil diameter increase in more than 10 years of plant operation.

Therefore, the likelihood of experiencing a circumferential crack in the parent tube at the TSP expansions is reduced for DCPP compared to Braidwood. Since no circumferential indications were detected in the TSP expansions at Braidwood after one cycle, and smaller bulges will be made at DCPP, circumferential cracking is not considered likely for the two to three cycles of operation planned for DCPP.

6.10.1.2 Potential for Circumferential Cracking

The potential for circumferential cracking in the hydraulically expanded and plugged tubes was evaluated in Reference 1. The operating temperature of the expansions in the plugged tube condition is between 522° F and 540° F, as determined by the secondary coolant temperature. Operating and laboratory experience for hydraulic expansions are reviewed in Reference 1. It was concluded that the low temperatures in plugged tubes with hydraulic expansions having [ ]^{a,c} lead to a low likelihood of circumferential cracking. The DCPP TSP tube expansions will have bulge [ ]^{a,c}; thus the likelihood of circumferential cracking is even further reduced.

6.10.2 Tubesheet Expansion Region

6.10.2.1 Operating Experience for Expanded Tubes

After one operating cycle following TSP expansions at Braidwood 1, the TTS regions in expanded tubes were inspected using the +Point coil, and circumferential indications were detected at the top of tubesheet region. The tube to tubesheet expansion process at Braidwood 1 was hard rolling. The EOC 6 inspection

(first inspection after implementation of the 3V ARC) was the first use of the +Point probe at Braidwood 1; prior TTS inspections were performed with the RPC probe. The results of the Braidwood 1 1997 inspection were discussed in a meeting between Commonwealth Edison (ComEd) and the NRC on 4/29/1997 (Reference 3). ComEd concluded that the top of tubesheet circumferential indications in the expanded tubes were likely undetected indications from the prior inspection that had grown to +Point detectable levels at EOC6. The signals of the circumferential indications were the same as circumferential indication signals in non-expanded tubes; thus, the indications in the expanded tubes did not represent a new degradation mechanism, but were, in fact, ODSCC at the roll transition. Subsequent evaluation indicated that the incidence of circumferential indications among the population of expanded tubes was independent of the number of expansions performed in a single tube. Consequently, the detected circumferential indications at Braidwood are considered to be independent of the expansions at TSP intersections.

6.10.2.2 Potential for Circumferential Cracking

DCPP Operating Experience For TTS Circumferential Indications

The DCPP SG tubes were explosively expanded in the tubesheet by the WEXTEX process. The industry operating experience has shown that explosive expansions are significantly less susceptible to circumferential cracking than hardroll expansions. There are small numbers of PWSCC and ODSCC circumferential cracks detected in the DCPP SGs.

Historically in the WEXTEX region, there have been 16 circumferential ODSCC indications (in 16 tubes) and 11 circumferential PWSCC indications (in 10 tubes) through the 1R11 inspection for Unit 1. One of the circumferential PWSCC indications is located below the W* length and the tube is in service under the W* ARC. Thus, a total of 25 Unit 1 tubes have been plugged due to circumferential WEXTEX indications. There have been 1 circumferential ODSCC indication (1 tube) and 12 circumferential PWSCC indications (in 11 tubes) through the 2R11 inspection for Unit 2. Thus, a total of 12 Unit 2 tubes have been plugged due to circumferential WEXTEX indications. Of the 40 circumferential indications detected in 38 tubes, 35 of the tubes were located in the central region of the SG (approximately radius of row 30 tubes) and 3 of the tubes with only PWSCC indications were in more peripheral regions.

Results from the most recent inspections are used to define a detection threshold. At the 1R11 inspection, there were 5 circumferential ODSCC indications and 1 circumferential PWSCC indication in the WEXTEX region (W* length), of which the largest measured crack angle was 42°. At the 2R11 inspection, there was 1 circumferential ODSCC indication in the WEXTEX region (W* length) with a measured crack angle of 78°. The small +Point voltages (< 0.35 volt) found for these indications implies that the cracks are both short and shallow.

Expansion Joint Design

The design of the TSP locking expansion was modified relative to the Braidwood operating experience. The objective was to reduce the residual stress in the tube due to expansion by reducing the required bulge diameter by about 0.010". To compensate for the expected loss of load carrying capability, a full wall thickness sleeve will be utilized for the DCPP process instead of the undercut sleeve utilized at Braidwood. The reduced expansion diameter reduces the residual stress in the tubes; thus the potential

for circumferential cracking is reduced. In addition, the span lengths between the TTS and 1st TSP and between TSPs is longer in the Model 51 SGs than the Model D4 SGs at Braidwood. The longer span lengths would help to reduce the residual stress in the tube from the expansions. In addition, the large contact forces between the tube and packed TSP crevices are likely to reduce the effect of multiple expansions in the tube on the residual tensile stress at the TTS. As noted in Section 6.10.2.1, the Braidwood incidence of circumferential indications among the population of expanded tubes was independent of the number of expansions performed in a single tube, and the detected circumferential indications are considered to be independent of the expansions at TSP intersections.

TTS Circumferential Crack Considerations

Based on the TSP displacement results of Section 5, the maximum SLB axial loads on the expanded tubes at the TTS are 1945 lbs for the hot leg and 2436 lbs. for the cold leg. The allowable throughwall crack lengths at the TTS to remain elastic under these loads are about 208° for the hot leg and 169° for the cold leg. Cold leg circumferential cracks have not been found in the DCPP SGs and would be very unlikely to be found in the expanded tubes. Thus, the significant criterion to remain elastic is a limiting throughwall crack length of 208°. A crack would have to grow from undetected to throughwall at this length to potentially influence the TSP displacements. Since the crack would have to grow from a short length at a shallow depth to a long throughwall length, growth of the crack as a result of heat up and cool down cycles for an expanded and plugged tube would also be small. Even if it is assumed that the crack was about 200° throughwall at the beginning of the third cycle. The crack would not grow to 208° by the end of the third cycle based on the number of cycles found for the DCPP SGs. The expanded peripheral tubes are subject to significant cross flow at the TTS for the flow entering from the downcomer. However, the peripheral tubes are expanded at the first TSP which provides a firm support such that tube vibration levels are small and the tube remains fluidelastically stable up to large throughwall crack sizes.

Since the expanded tubes are plugged, any potential circumferential crack initiation or growth would be ODSCC. The TSP circumferential crack detection threshold on depth developed for DCPP (WCAP-15573, Rev. 1 – Reference 4) is 35% for ODSCC. TSP circumferential crack growth rates are also developed in WCAP-15573, Rev. 1 – Reference 4, for which the upper 95% average depth and crack angle growth rates are estimated at 17.7%/EFPY and 29.4°/EFPY, respectively. These values bound all growth rates found at the last inspections for both units. Since more than 60% of the circumferential indications found in both units had crack angles < 40°, it is conservative to assume that the detection threshold in angle for depths > 35% is 40°. The growth in angle represents the growth in depth greater than the detection threshold of 35%. For DCPP Cycles 13 to 15, the longest two and three cycle lengths between both units are expected to be 3.13 EFPY for Unit 1 and 4.63 EFPY for Unit 2. By applying the 95% growth rates to the detection thresholds, the crack angle and average depth after 2 cycles would be 90% and 132° and the corresponding values after 3 cycles would be 100% and 176°. For these EOC crack sizes, growth due to heat up and cool down cycles would be negligible even for a peripheral expanded tube location. The largest number of TTS ODSCC circumferential cracks that have been found to date is 16 in Unit 1 or only 0.5% of the tubes. Thus, there is a low likelihood of an undetected circumferential crack in an expanded tube. Given the low likelihood of an undetected circumferential crack and that the projected throughwall crack angles even after three cycles of operation are less than the throughwall angle of 208° required to influence TSP displacements, undetected TTS circumferential cracks are not expected to impact TSP displacement predictions.

Summary

Circumferential cracking at the TTS tube expansions in the locked tubes at DCPP is not considered a meaningful issue for the following reasons:

1. Operation of the DCPP SGs with locked tubes will be limited to two to three cycles, followed by replacement of the SGs.

2. The DCPP SGs utilize WEXTEX tube expansions that are less susceptible to cracking than hardroll expansions, such as at Braidwood, as supported by the small number of circumferential indications found in the DCPP SGs

3. The design of the locking expansion was modified for DCPP application to reduce the residual axial stress in the expanded tube compared to Braidwood 1.

4. Since the TSP expansions would not be performed in tubes with WEXTEX circumferential indications, there is a low likelihood of a circumferential crack occurring in an expanded tube and growing to a length and depth that could lead to a throughwall crack length large enough to significantly influence the TSP displacements.

6.11 REQUIREMENTS ON LIMITING TUBE DENTING FOR TSP INTEGRITY

No requirements related to denting are required for the expansion process although limitations on dent size at expanded tube locations are applied for considerations of circumferential cracking as described in Section 10. The expansion process can be applied in a dented tube without adverse effects. In the event a dent is large enough to prevent insertion of the stabilizing sleeve, an acceptable alternate tube that does not affect the structural analysis results will be selected for expansion.

6.12 CONCLUSIONS

The process for tube expansion at the TSPs for DCPP is essentially the same process that was applied for the prior implementation of 3V ARC at Byron, Braidwood and South Texas.

A target expansion size of [ ]^{a,c,e} was selected for the TSP expansion. The computer volume controlled expansion program will produce expansions of this size range in both low and high yield strength tubing and will result in axial stiffness exceeding the minimum required stiffness of [ ]^{a,c,e} at the TSPs at a 90% confidence level.

As the tube to TSP interaction angle (with reference to the vertical axis) gets larger (for example, if the crevices are packed), the resistive loads increase. In the testing program the crevices were all open, resulting in smaller tube to TSP interaction angles. This causes the tube to be more easily pulled through the TSP as the angle decreases. Equal sized expansions in high yield tubing will result in greater stiffnesses than the minimum requirement.

In summary, the expansion process will be targeted toward obtaining a minimum of [ ]^{a,c,e} bulges in both low and high yield strength tubing.

6.13 REFERENCES

1. WCAP-14273; "Technical Support for Alternate Plugging Criteria with Tube Expansion at Tube Support Plate Intersections for Braidwood-1 and Byron-1 Model D4 Steam Generators;" W-NSD, February 1995.

2. WCAP-15163, Revision 1, "Technical Support for Implementing High Voltage Alternate Repair Criteria at Hot Leg Limited Displacement TSP Intersections for South Texas Plant Unit 2, Model E Steam Generators;" Westinghouse Energy Systems, March 1999.

3. Westinghouse Internal Memo NSD-RFK-97-017; "Com-Ed NRC Meeting on Braidwood 1 Inspection Results", 5/2/1997.

4. WCAP-15573, Revision 1, "Depth Based SG Tube Repair Criteria for Axial PWSCC at Dented TSP Intersections – Alternate Burst Pressure Calculation," Westinghouse Electric Company LLC, October 2001.

Table 6-1. Expanded Tube Test Results - Load versus Displacement and Joint Stiffness Data

a,c,e

Table 6-1. Expanded Tube Test Results - Load versus Displacement and Joint Stiffness Data a,c,e

Table 6-1. Expanded Tube Test Results - Load versus Displacement and Joint Stiffness Data

a,c,e

Table 6-2
Average Joint Stiffness for Expansions in Single Hole Clamped TSP with TSP Crevice Gaps Introduced Following Expansion

a,c,e

Table 6-3
Comparison of Calculated vs. Mechanically Measured IDs of Sectioned Samples

Calculated ID is based on Mechanical Measurement of Maximum Expansion Bulge Size

a.c.e

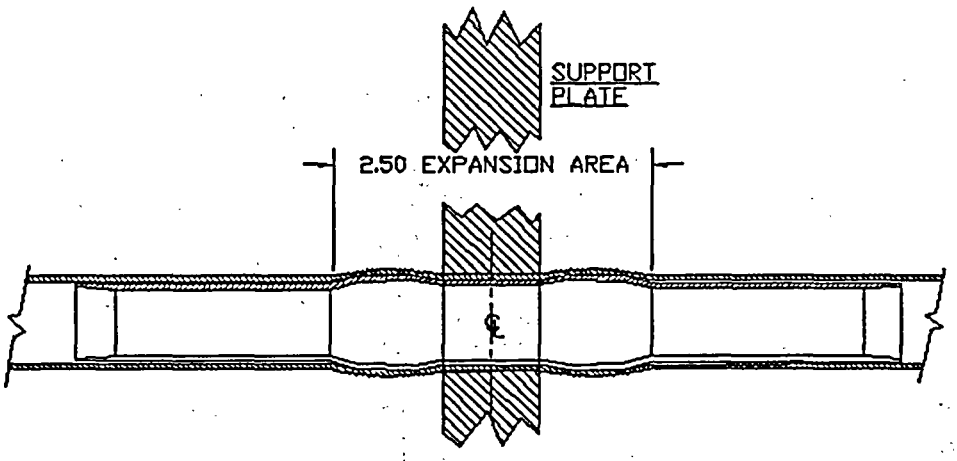

Figure 6-1
Tube Support Plate Expansion

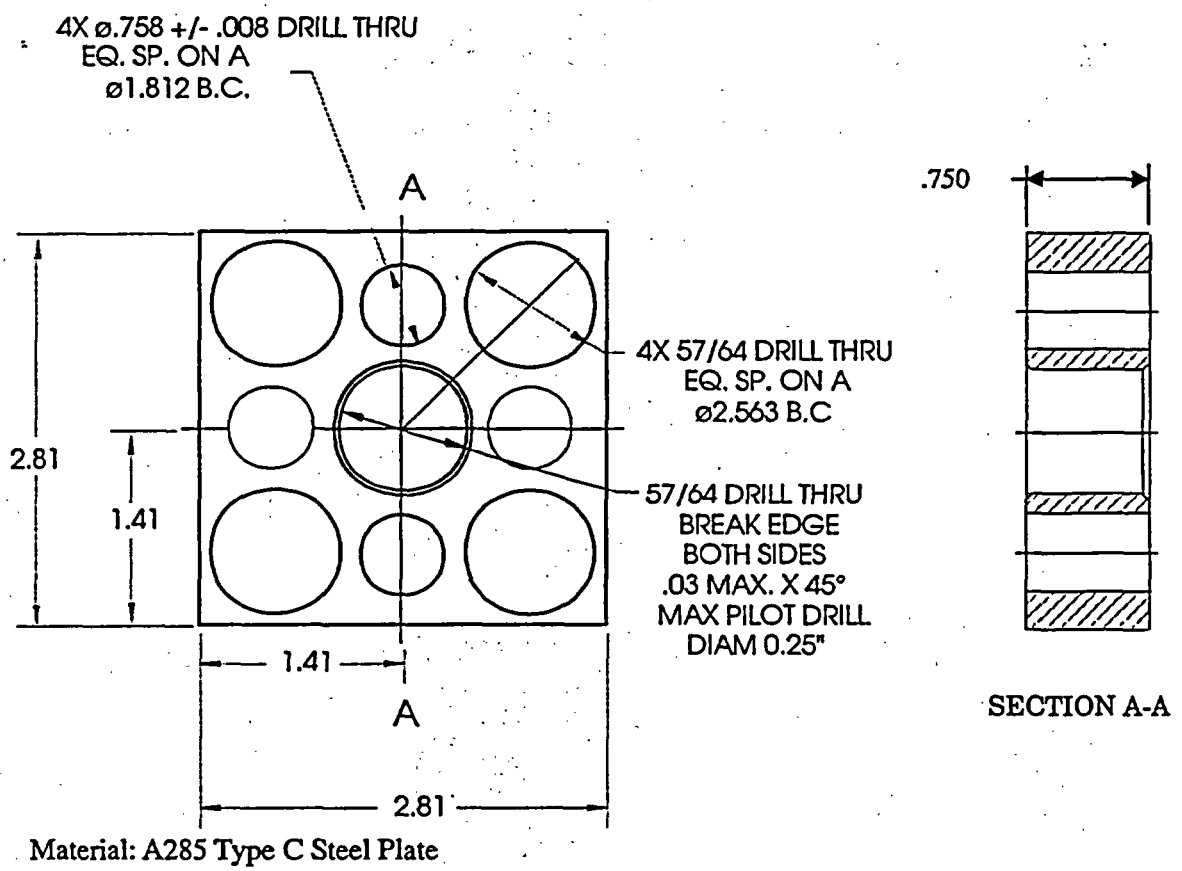

Material: A285 Type C Steel Plate

Figure 6-2
Tube Support Plate Simulant for Expansion Load Testing
(figure not to scale)

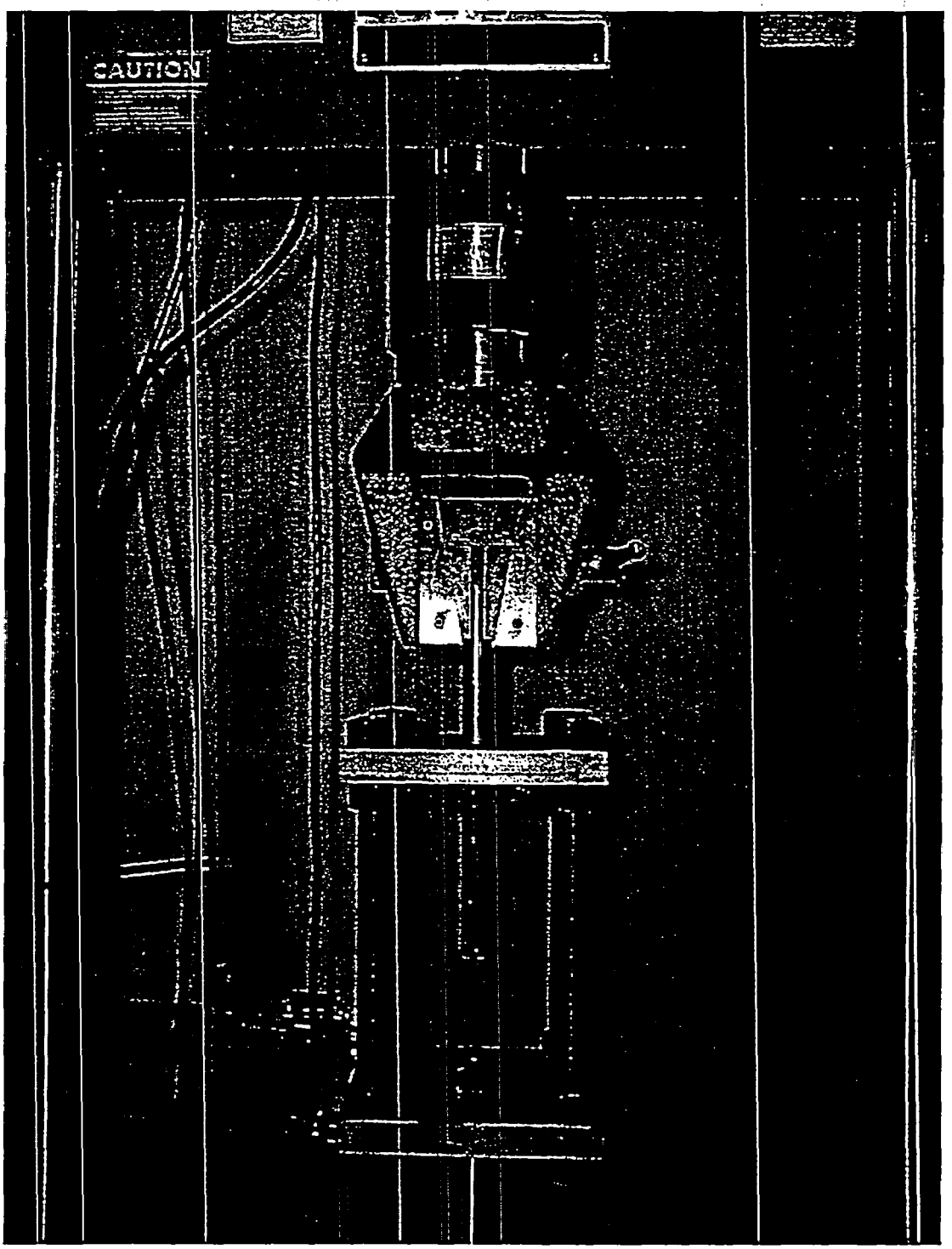

Figure 6-3
Expansion Joint Load Test Setup

a.c.e

Figure 6-4
Typical Bulge Resistive Load (lbs vs. inch) Tensile Loading Curve TSP Specimen (Test 2-30)

a.c.e

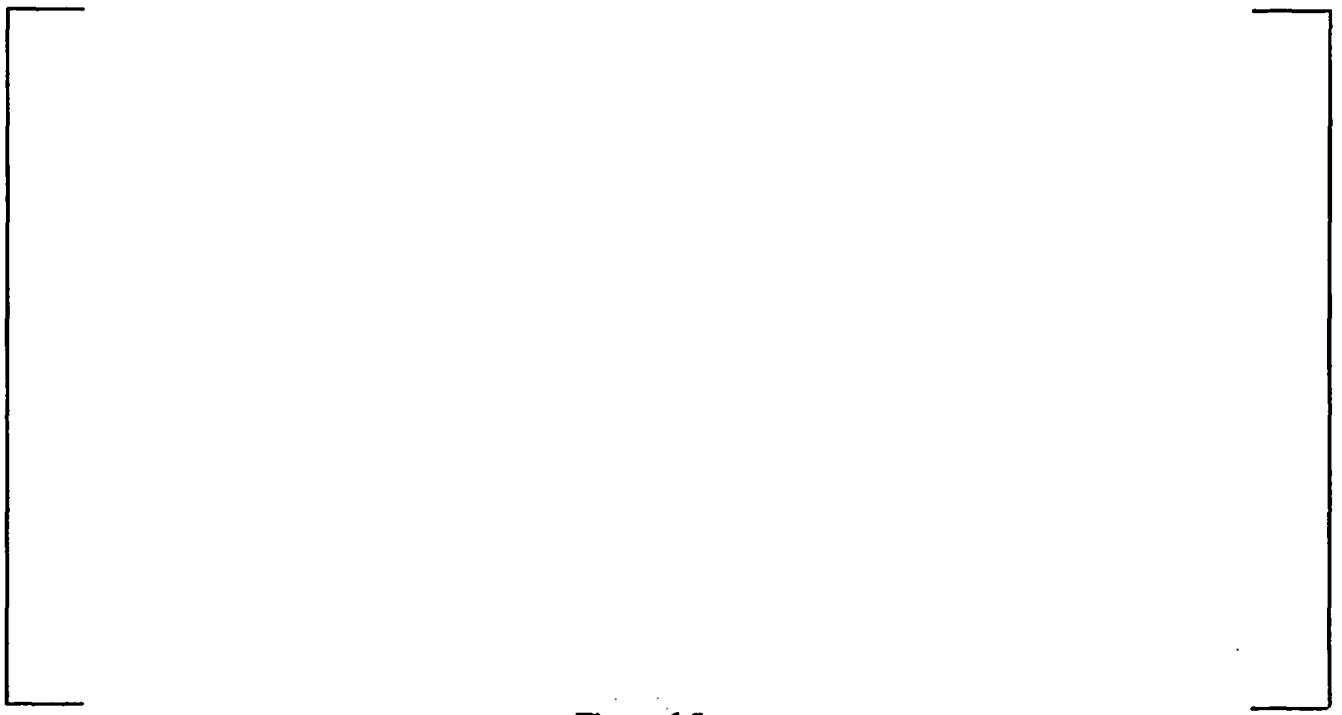

Figure 6-5
Distribution of TSP Displacements at Tube Expansion Locations

a,c,e

Figure 6-6
Sensitivity of Joint Stiffness to TSP Displacement

a,c,e

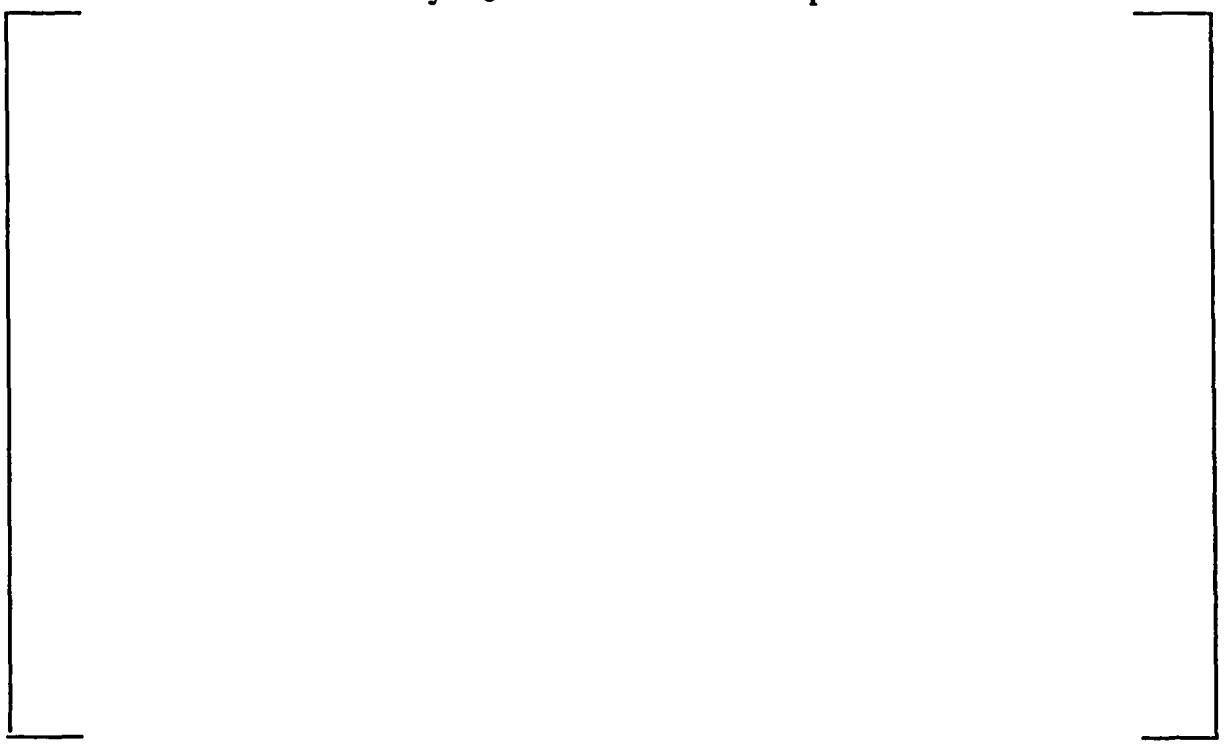

Figure 6-7
Sensitivity of Joint Stiffness to TSP Configuration

a,c,e

Figure 6-8
Sensitivity of Joint Stiffness to Tube Yield Strength

a,c,e

Figure 6-9
Bulged Tube Stiffness Evaluation Configuration/Stiffness

7.0 TEST DATA SUPPORT FOR LEAKAGE FROM CONSTRAINED CRACKS

7.1 INTRODUCTION

To support implementation of high voltage ARC for limited TSP displacement under postulated SLB conditions, a test program was completed to determine the bounding leak rate and its sensitivity to TSP displacement for throughwall indications restricted from burst (IRB) (Reference 1). The test program was performed under EPRI sponsorship.

An IRB is defined as a tube crack at the intersection of the tube with the support plate, of a size that could burst under SLB conditions if it were a freespan crack. The crack is restricted from burst by the TSP, and it is further demonstrated that the leakage flow from an IRB is limited by the presence of the TSP to less than the freespan leakage for a like crack. During a postulated SLB event, the depressurization of the SG causes the TSPs to deflect from their nominal position as discussed in Section 5, thus potentially partially exposing the cracks at the TSP intersections. The analysis results discussed in section 5 show that the maximum TSP displacement for the DCPP SGs is < 0.15 inch for locked TSPs 1-4 for which the IRB leak rate is applicable. The limited displacement of the TSPs permits an increase in the acceptable bobbin voltage for indications remaining in service.

It was the objective of this test program to establish a data base for leakage from cracks in prototypic steam generator tubing under prototypic pressure and temperature conditions to verify that the leakage from cracks left in service under a high voltage ARC will not result in unacceptable leakage during SLB accident conditions. SLB conditions are defined as 615°F primary coolant temperature and a pressure differential of 2560 psid. For DCPP, a SLB differential of 2405 psi may be applied based on operation of the PORVs to limit primary pressure. The bulk of the tests were performed in a high-energy steam test facility that is capable of flow rates of about 8 gpm at these conditions. A complete description of the high-energy leak tests facility and test operations is contained in Reference 1. The high temperature leak tests were augmented by tests performed in a room temperature, high-pressure leak test facility. Room temperature tests are much easier to perform; thus it was the objective of the room temperature tests to demonstrate the adequacy of the EPRI method for adjusting RT data to high temperature conditions.

A specific objective of the test program was to determine a bounding leak rate for an IRB for a crack size that exceeds any crack conservatively expected to occur at an end of cycle. GL 95-05 specifies that no indication extending beyond the span of the TSP may remain in service. The TSP thickness is 0.750 inch, thus the maximum indication is limited effectively to less than 0.750 inch for the packed crevice condition causing initiation and growth of the ODSCC indication. The critical throughwall crack length for a burst at the SLB pressure differential of 2405 psi in 7/8" diameter tubing at lower tolerance limit (LTL) material properties and 95% confidence on the throughwall burst correlation is 0.756 inch. At 95% confidence on material properties and the burst correlation, the critical throughwall length is 0.803 inch. Consequently, a burst at SLB conditions is very unlikely even for a tube with material properties as low as LTL values, which have not been found to crack in service due to improved grain structure. Cracks at, or less than, this throughwall length would not be expected to burst at the SLB pressure differential. Thus, the practical limit of cracks to be tested was set at approximately 0.750 inch, although

shorter cracks and one longer crack were also included in the test program to observe the structural and leakage trends of the cracks.

Fifteen specimens were tested as summarized on Table 7-1. The specimens were prepared from prototypic steam generator tubing material, mill annealed Alloy 600. Specimens were prepared by three processes: 1) accelerated corrosion, 2) accelerated corrosion followed by fatigue to increase the length of the crack, and 3) laser cutting. Eight of the specimens were 7/8" diameter specimens, and the remainder were 3/4" specimens. Cracks with different throughwall lengths in a range from 0.24" to 0.809" were tested. The tests simulated a cracked tube at a TSP, but, conservatively, with the maximum diametral clearance of 0.025" between the tube and the TSP. The tests were fixtured to provide a 0.025" gap at the side of the tube with the crack to minimize the restriction provided by the TSP.

The longest throughwall crack length tested, 0.809 inch was greater than any crack that could be formed at a TSP intersection, which is 0.750 inches thick. Also, throughwall cracks of significant length would have bobbin voltages well in excess of the repair limit proposed for the high voltage ARC.

Testing was performed with (a) the cracks completely contained within the span of the TSP with one end of the crack aligned with the edge of the TSP, and (b) with the crack tip intentionally positioned (offset) outside the TSP by a distance. The nominal offset of the crack tip from the TSP was 0.1" for the 3/4" diameter specimens and 0.15" for the 7/8" specimens. The actual range of offsets tested extended up to 0.210" for the total crack and 0.173 inch for the throughwall cracks based on in-process examination of the test specimens.

Following tests by pressurizing the ID of the tube and measuring the leak rate through the crack (Flow Pressurization Tests), the crack in the tube was opened by installing a bladder at the location of the crack, and pressurizing the bladder to the predicted freespan burst pressure (based on the length of the crack and the known material properties of the tube). Bladder pressurization was performed with the tube constrained within the TSP, but with the crack tip offset from the TSP. Following this, the bladder was removed, and additional leak tests were performed in both the non-offset and offset conditions. These tests are referred to as Bladder Pressurized flow tests.

Freespan leak tests were performed on some of the specimens to provide a comparison of IRB and freespan leak rates. Some of the specimens were tested at approximately room temperature conditions as well as prototypic elevated temperature conditions to provide a basis of evaluating analytical techniques for adjusting low temperature data to high temperature conditions. The method of adjusting the conditions of various tests to the standard SLB condition is described in Reference 3.

The burst pressure to bobbin voltage correlation results in very conservative burst pressures and burst probabilities when uncertainties are considered. A wide range of burst pressures occurs at a given voltage since different crack morphologies can result in comparable voltages. When a direct structural parameter such as throughwall crack length is correlated with burst pressure, correlation uncertainties are much smaller than for a voltage correlation. As noted above, the EPRI burst correlation (Reference 2) for throughwall axial cracks leads to a throughwall crack length of 0.756 inch at ΔP_{SLB} = 2405 psi for lower tolerance limit (LTL) material properties and lower 95% confidence on the burst correlation. Thus, the probability of burst at SLB conditions is negligibly small due to the requirement for a throughwall crack length equal to the thickness of the TSP. As noted later in Section 7.2, pulled tubes

with throughwall cracks near 0.5 inch long have had voltages between 13 and 22 volts, thus, a 0.75 inch throughwall crack could be expected to significantly exceed 22 volts. This demonstrates the conservatism in the burst /voltage correlation for which 16 volts corresponds to a 10^{-2} burst probability at 2405 psi.

The intent of the IRB test program was to develop a leak rate for an indication inside the TSP that could burst in freespan at 2560 psi. Since the ODSCC cracks formed in a TSP crevice do not exceed the 0.75 inch TSP thickness at any significant depth (none have been detected in approximately 50 ARC inspections), specimens could not be prepared that would burst at SLB conditions, since LTL materials were unavailable. Consequently, it was necessary to pressurize the cracked specimens with a bladder to the freespan burst pressure to simulate an attempted "burst" (IRB) inside the TSP. None of the indications, including a 0.81-inch throughwall indication, "burst" when tested at pressures near, or above, 2560 psid. The shorter throughwall indications (<0.6-inch) had to be pressurized to well above the SLB pressures; thus, the length and applied pressures are more conservative than the longest potential cracks for a SLB IRB. The following tests of Table 7-1 are most representative of IRB conditions: 1-1, 1-2, 1-6, 1-7, 11-1 and 11-2.

Since only cracks near 0.75-inch throughwall could burst at SLB conditions, a shorter crack length in a tube with a 0.75-inch crack would not significantly open, and its leak rate would not approach that of the "burst" crack. The potential for two cracks approaching 0.75-inch throughwall length to exist at a TSP is negligible since the associated bobbin voltage would be well above 22 volts. Thus, multiple cracks in a tube would not increase the bounding leak rate obtained from the tests at crack lengths exceeding 0.6 inch. When multiple shorter cracks are tested and the tube must be pressurized to more than 4000 psi to simulate an IRB, both cracks can open up and contribute to the leakage. However, this is a consequence of the artificially high pressurization and is not prototypic of an indication at a TSP intersection that could burst at SLB conditions. This applies to Test 12-1, which should not be applied to define the bounding IRB leak rate. For a SLB burst condition, the limiting crack would burst and potentially leak as an IRB, but any secondary cracks would not burst and would leak at freespan conditions in an assumed open crevice.

7.2 BOBBIN VOLTAGE FOR CRACK LENGTHS TESTED

The limiting leak rate and crack/TSP offset data were derived from tests of very long cracks with throughwall lengths approximately equal to the span of the TSP (0.750"). The leakage behavior of shorter cracks is essentially like that of freespan cracks regardless of offset, since the tests indicated negligible interaction of short cracks with the TSP. If longer cracks would be repaired on the basis of their bobbin voltages (i.e., such as the proposed ARC limit), the voltages for the test specimens should be consistent with projected EOC conditions which have operationally been bounded by about 12 volts.

Although EC data were not routinely acquired for the test specimens utilized in these tests, a few of the initial specimens were tested with a bobbin probe to determine the voltage range for the relatively large cracks being tested in this program. The laboratory specimens in this test program were generally cracked in doped steam and were not oxidized prior to bobbin voltage measurements. Prior work has shown that this results in bobbin voltages lower than found in pulled tubes due to the increased conductivity across the crack faces. In addition, other specimens that were not utilized for the leak and burst tests of this program were also examined with a bobbin probe and then were characterized for the

size of the crack for other purposes. Finally, a number of tubes have been pulled from operating SGs for which bobbin voltage data are available. Consequently, a small database exists for characterizing the bobbin voltage vs. the crack size (length of throughwall crack).

Among the specimens tested for which bobbin voltages are available (Table 7-2), the shortest throughwall length crack exhibited a bobbin voltage of 17.1 volts; however, the specimen included two separate cracks. A tested specimen with a 0.515 throughwall crack exhibited a bobbin voltage of 8 volts. The lowest voltage for any laboratory specimen for which there is bobbin data is 7.9 volts for a 0.15" throughwall crack. The longest throughwall cracks actually tested, for which there is a bobbin voltage, were 0.29 inch (0.600 in. total length) with a bobbin voltage of 11.4 volts, and 0.515 inch with a bobbin voltage of 8.0 volts.

Examples from the ARC database of pulled tubes with throughwall cracks are given in Table 7-2. DCPP-2 R44C45 had a 21.5 volt indication with a 0.374 inch throughwall crack. For 7/8" diameter pulled tubes, the lowest voltage is 3.35 volts for a throughwall crack of 0.197". The longest throughwall crack, 0.47 inch (0.67-inch total length) exhibits a bobbin voltage of 15.7 volts. The longest total crack, 0.81 inch (0.42 inch throughwall length) had a bobbin voltage of 13.55 volts. All of these throughwall lengths are much shorter than the 0.74 inch throughwall length of the specimen in Test 1-6 which strongly influences the IRB leak rate. Although no bobbin test was performed on the specimen for Test 1-6, it could be expected to have a bobbin voltage exceeding 25 volts.

Therefore, it is concluded that these tests are very conservative with respect to establishing the limiting leak rate of a crack offset from the TSP, since pulled tube throughwall lengths for indications up to 22 volts are a factor of 1.5 to 3 less than the throughwall crack length on which the limiting leak rate is based from these tests. It is judged that the IRB leak rate in this report corresponds to indications exceeding at least 25 volts.

7.3 BOUNDING LEAK RATE

The bounding leak rate for the limiting indication for which a high voltage ARC could be considered to apply was determined in these tests to be 5.5 gpm for a 2560 psid pressure differential, based principally on Test 1-6. The applicable pressure differential for DCPP is 2405 psi, based on the PORV setpoint plus uncertainties. For a 2405 psid pressure differential, the bounding leak rate is 5.0 gpm based on these tests.

Table 7-3 summarizes the leak rates, based on both flow pressurization and leak testing after bladder pressurization at the SLB conditions of 2560 psid, and an alternate pressure of 2405 for the PORV setpoint plus uncertainties for DCPP. The pre-test crack lengths are also shown. The SLB (2560 psid) leak rate from Test 1-6 for flow pressurization was 5.50 gpm and after bladder pressurization was 5.0 gpm.

For the DCPP accident pressure differential (2405 psid), the bounding leak rate is 5.0 gpm, based principally on Test 11-2 (5.0 gpm) and Test 1-6 (4.90 gpm). With the exception of three specimens with special circumstances noted below, all other tests had SLB leak rates less than the bounding leak rate of 5.0 gpm for both flow pressurization tests and post-bladder pressurization leak tests.

The bounding leak rate was determined based on the evaluation of the measured leak rate data for the average pressure during the tests. Therefore, the leak rate is conservative since the plastic crack opening is determined by the peak pressure differential at the start of the test, and this was up to 100 psi greater than the average pressure differential for which the bounding leak rate is evaluated. If the measured leak rates are evaluated against the peak pressure differentials, the 2560 psid bounding leak rate would be 5.0 gpm. For conservatism, the bounding leak rates for ARC applications are based on the average pressure drop and 5.5 gpm is applied for 2560 psid and 5.0 gpm for 2405 psid.

The bounding leak rate includes the effects of TSP offset, thus no additional consideration of offset is required. Test 11-2, a test of a 0.729 inch total length (0.630 inch initial throughwall) crack yielded a 2405 psi SLB leak rate of 5.0 gpm for both flow pressurization (0.208" offset, 0.173" TW) and bladder pressurization (0.180" offset, 0.150" TW) of the specimen. After bladder pressurization, this specimen had a throughwall length of 0.707 inch. The large offset and associated throughwall lengths contribute to the larger leak rates for this specimen. The offset lengths for this test exceed the 0.150 inch maximum TSP displacement for the ARC.

Test 1-6 utilized a specimen with a total crack length of 0.760 inch and an initial throughwall crack length of 0.740 inch. For Test 1-6, the offset was established at 0.091" for the crack tip, which included a throughwall length of 0.070". After bladder pressurization, this specimen had a throughwall length of 0.773 inch. This test conservatively helps to establish the bounding leak rate because the throughwall portion (0.740" at beginning of test) of the crack is essentially the full span of the TSP (0.750"). The throughwall lengths for both of these specimens exceed any found in operating SGs including European plants which operated with no repair limits.

The bounding leak rate from Tests 11-2 and 1-6 is supported by the following additional tests:

- Test 11-1, a test of a 0.710-inch total length (0.600 inch throughwall) crack yielded 2405 psi SLB leak rates of 4.35 gpm for offset flow pressurization and 4.5 gpm after bladder pressurization. This 7/8-inch diameter specimen had offset lengths of 0.185 inch with an exposed throughwall length of 0.15 inch for both tests.

- Test 12-1, a test of a specimen with two cracks, 90° separated, of total length 0.607 inch and 0.465 inch. The initial throughwall lengths of these cracks were 0.518 inch and 0.360 inch respectively. The 2405 psi SLB leak rates of this specimen were 3.0 gpm for offset flow pressurization and 5.6 gpm after bladder pressurization. After pressurization for the bladder pressurization tests, the larger crack had a throughwall length of 0.645 inch with a total length of 0.658 inch based on fractography and the smaller crack throughwall length was 0.411 inch based on in-process measurements. The bladder pressurization tests for two throughwall cracks are not representative of SLB conditions. The specimen was pressurized with a bladder to 4850 psi which significantly opened the second crack width beyond that expected for a non-burst tube at 2405 psi. Multiple cracks with 90° separation lead to maximum leak rates inside a TSP, since crack openings that interact with the TSP hole diameter are approximately independent of each other. This specimen was a 7/8" diameter specimen.

Three tests are excluded from consideration for defining the bounding leak rate for an IRB that would be conservatively considered for implementation of a high voltage ARC.

- Test 11-7 was a test of a crack that was significantly longer than the span of the TSP, and would therefore not be considered in the population of IRBs that would be considered for implementation of the ARC. This specimen included a crack of 0.813-inch total length and 0.809 inch throughwall length. Following pressurization the throughwall length was 0.854 inch. The specimen length exceeds the TSP thickness of 0.75 inch which provides the crevice environment for crack initiation and growth. However, this test supports the bounding leak rate discussed above by demonstrating that cracks that extend beyond the TSP under normal operating conditions do not lead to a significant increase in the SLB leak rate with SLB TSP displacement. This conclusion is true even if the crack is pressurized to its freespan burst pressure.

- Test 2-8 was a test of a specimen with a laser cut flaw, to evaluate if these easily prepared specimens are good simulations of corrosion cracks for leak testing. Laser cut flaws, and machined flaws in general, are characterized by smooth-walled, uniform opening slits, that do not simulate the tortuosity of corrosion cracks. This leads to much higher leak rates for the machined flaws compared to similarly sized corrosion cracks. Similarly, the fatigue cracks used in these tests do not simulate the corrosion crack tortuosity and have higher leak rates. Further, the ends of the machined slits have a radius instead of the sharp crack tips of corrosion or fatigue cracks, which causes the slit ends to behave like plastic hinges instead of tearing like corrosion/fatigue cracks. The resulting crack opening under pressurization is much greater than for the corrosion cracks. Consequently, machined flaws were rejected as suitable simulants of corrosion cracks for these leak tests, and the measured leak rate for this test is non-representative of the IRBs addressed by the proposed ARC.

- Test 12-1 resulted in a leak rate of 5.6 gpm at 2405 psi after bladder pressurization to the predicted freespan burst pressure for both the zero-offset and the offset tests. This specimen included two cracks, separated by 90°, 0.607 inch (0.515 inch TW) and 0.465 (0.360 inch TW) long, respectively. For flow pressurization to 2680 psid, the offset SLB leak rate from this specimen was 3.2 gpm. After bladder pressurization to 3310 psi, the offset SLB leak rate was 4.2 gpm. Up to this point, post-tests inspection showed that the secondary crack had not opened, and the primary crack had opened to about 0.005 inch width. After bladder pressurization to the predicted freespan burst pressure (4850 psi), the primary crack opened to 0.022 inch width and the secondary crack also opened to about 0.005 inch. Thus, for the flow pressurization tests exceeding the SLB pressure differential, this specimen with two moderately long cracks had a leak rate about 60% of the bounding leak rate. After bladder pressurization about 90% greater than SLB pressure differential, this specimen had a leak rate only about 10% greater than the bounding leak rate. The influence of a typically shorter second crack is an artifact of the high bladder pressurization applied to simulate an IRB. At SLB pressure differentials, shorter cracks would not open sufficiently to significantly increase the leak rate above that of the larger crack that could burst at SLB conditions.

7.4 APPLICABLE RANGE OF OFFSET

The data from the IRB leak tests conservatively bound a minimum TSP offset of 0.15 inch. Offset is defined as the length of the total crack outside of the span of the TSP. The maximum offsets tested were 0.210 inch (Test 1-2), 0.208 inch (Test 11-2) and 0.185 inch (Test 11-1) for flow pressurization, and 0.185 inch (Test 11-1) and 0.180 inch (Test 11-2) for leak tests after bladder pressurization. Two of these tests, Tests 11-1 and 11-2, are principal supporting tests for the bounding leak rate; thus the maximum offsets are represented in the bounding leak rate.

The offset tests were initially set up based on total crack length outside the TSP, nominally 0.10 inch for 3/4" diameter tubes and 0.15 inch for 7/8" diameter tubes. Later offset tests were conservatively set up based on the throughwall length outside the TSP, thus much longer total crack lengths outside the TSP were actually tested. The offset setup based on total crack length outside the TSP simulates the actual condition of TSP deflection during a postulated SLB.

During pressurization, both the total crack length and the throughwall crack length increased; thus, the offset lengths actually tested were frequently greater than the setup offsets. The maximum offsets noted above were the post-test measurements, based on in-process measurement techniques; thus, the measured and bounding leak rates include the effects of the offsets.

Fractographic examination of a number of the specimens was performed after all leak testing had been completed. The results of this examination showed that the in-process measurement techniques were conservative. The crack tips were often tight and could not be observed by the visual methods employed during the IRB tests, even with the aid of a toolmaker's microscope. Similarly, the method of determining throughwall length, using a back-lighting technique, is limited to a crack opening about 0.001 inch that is also approximately normal to the plane of vision. Therefore, the crack length measurements that define the applicable crack offset, either total crack or throughwall crack, are conservative, and the enveloping offset, based on the IRB testing, is 0.21 inch (Tests 11-2 and 1-2).

An IRB leak test was also performed on a pulled tube from Plant AA-1 (Reference 4). This test was set up like the test specimens tested in the IRB leak test program (Reference 1). The pulled tube tested, R28C24, had a total crack length of 0.688", with a throughwall portion of 0.260". The crack was offset from the simulated TSP 0.20" based on post-test destructive examination. The leak rate results from the tests performed in the offset condition were the same as the result from tests with the crack completely contained within the span of the TSP.

For the maximum acceptable crack length of 0.750 inch, a limiting offset was defined based on the observations during the IRB test. The maximum contact length between the crack flanks and the TSP in the IRB tests was estimated at 0.3 inch. The crack opening behavior was observed to be symmetric about the axial and longitudinal crack centerline. Therefore, the length of the crack not in contact with the TSP was half the difference between the total length and the length in contact with the TSP, or 0.23-inch. This defines the maximum offset for the limiting crack. An offset less than this distance will not increase the available flow area of the crack, and therefore, the leak rate would not significantly increase up to this offset.

7.5 BOUNDING LEAK RATE SENSITIVITY TO TSP OFFSET

The bounding leak rate conservatively includes the effects of offset, and is insensitive to offset for crack lengths nearly equal to or longer than the TSP thickness of 0.75 inch.

The offset leak rates were essentially the same as the zero-offset leak rates for the range of crack lengths tested. Figure 7-1 provides a comparison of the leak rates correlated to crack length for the offset tests and for the zero offset tests. Figure 7-1 shows that the slope of the correlation for offset tests is slightly greater than for the zero-offset tests, indicating that there may be a small effect of the offset on the leak rate. However, the leak rate at the limiting crack length, 0.750 inch, is the same for both offset and zero offset tests. Further, the bounding leak rate is based on the offset test results. Therefore, offset is a negligible factor on the bounding leak rate for the range of offsets tested for which many tests exceed the ARC limit of 0.15 inch offset.

7.6 LEAK RATE SENSITIVITY TO TUBE SIZE

The leak data from the tests of 3/4" diameter specimens and 7/8" diameter specimens are equally applicable for both tube sizes.

The leak rates were correlated to the crack properties, length and limiting throughwall area, and were found to have strong correlations in both crack length and area. Figure 7-2 shows a correlation of the leak rates for all of the tests, including 3/4" and 7/8" diameter tubing and both offset and zero-offset tests for flow and bladder pressurization. No difference in the data scatter was observed, based on the tube diameter, for the leak rate as a function of crack length, the principal correlation parameter.

7.7 EFFECT OF A SECOND CRACK ON THE BOUNDING LEAK RATE

The bounding leak rate does not need to be adjusted for potential multiple throughwall indications. Leakage from a tube with two cracks is dominated by the principal crack with the longest throughwall length. Similarly, the structural behavior of a specimen with two cracks is dominated by the principal crack. At SLB conditions, only the limiting crack would burst and open up to be an IRB. The second crack would leak at its normal SLB leak rate, which would be much smaller than the bounding IRB leak rate applied for the ARC.

The leak rate from a crack is an exponential function of the throughwall length of the crack, neglecting any TSP interaction. Thus, if a tube has a longer crack together with a shorter crack, the leak rate is dominated by the longer crack, and the shorter crack contributes only slightly to the leak rate. The combined leak rate from the principal and secondary cracks is much less than the leak rate from a single crack whose length is the sum of the lengths of the principal and secondary cracks. This observation is supported by pulled tubes from plants AA and AB with indications in the 10-11 volt range, and model boiler test data, both of which show that the secondary crack is much shorter than the principal crack. An exception to this rule is manifested in a tube pulled from Plant S with a 22.9-volt indication that had a principal crack of 0.50 inch and a secondary crack of 0.41 inch. No leak tests were performed on this tube; however, calculations for this tube showed that the principal crack would have a leak rate three times that of the secondary crack.

Test 12-1 of the IRB tests included two cracks comparable in length to the tube pulled from Plant S, in planes about 90° apart. In-process measurements showed that the secondary crack did not open until the specimen was pressurized with a bladder to greater than 70% of the predicted freespan burst pressure for this specimen. Consequently, leakage from the second crack following bladder pressurization is not representative of SLB conditions. Based on flow pressurization only to 2405 psi, the leak rate was 3.0 gpm and increased to 5.6 gpm following bladder pressurization. Thus, this specimen confirms that the SLB leak rate is dominated by the principal crack in a specimen with two cracks, and the bladder pressurization steps lead to unrealistically large leak rates from the secondary crack.

The probability of multiple throughwall cracks occurring at the location of the maximum TSP offset is extremely low. The largest TSP offset occurs only at a localized area on the highest loaded TSP. Therefore, it is extremely unlikely that the incidence of multiple cracks will coincide with the location of maximum TSP offset.

Pulled tube data confirm that the location of throughwall cracks is not near the edge of the TSP. Among the sixteen available pulled tubes from Plant AA and AB with bobbin voltages of 1-16 volts, 1 tube included an indication located ~0.1 inch inboard from the edge of the TSP, 12 tubes included an indication located ~ 0.2 inch inboard from the edge of the TSP, and the remainder included an indication near the center of the TSP. DCPP pulled tubes R44C45 and R35C57 both had throughwall lengths more than 0.15 inch from the edge of the TSP. Therefore, it is concluded that indications do not occur at the edge of the TSP with significant frequency, further reducing the likelihood of multiple indications increasing the SLB leak rate due to TSP offset.

7.8 LEAK RATE UNCERTAINTIES

The bounding SLB (2405 psid) leak rate, 5.0 gpm, is a conservatively high value. Evaluation of the uncertainties of the IRB tests identified four sources of potential uncertainty. These, and their range of uncertainties, are:

1) Fluctuation of leak rate during the tests (±3.1%)

2) Use of the test maximum Δp vs. the use of the test average Δp for the reported leak rates (-10%)

3) Leak rate adjustment procedure for SLB conditions (negligible)

4) Test loop calibrations (+0.1%)

The combined uncertainty for these four sources of uncertainty varies from -7% to -10%, based on the upper and lower limits of the individual uncertainties. The negative values indicate that the test-based bounding leak rate is conservatively high, that is, the uncertainties would reduce the stated leak rate.

As shown in Table 7-1, the IRB leak rate tests were performed at prototypic hot conditions with the exception of a few tests with short crack lengths that do not contribute to defining the bounding leak rate. The leak rate adjustment procedure is applied only to interpolate the measured pressure differentials to the reference SLB pressure differentials. The cold tests were performed primarily as supplemental tests

to help verify the leak rate adjustment procedure for cold to hot adjustments using common test conditions for both hot and cold tests.

7.9 SUMMARY

- Based on the IRB tests, the bounding leak rate for a 2405 psid pressure differential, based on the PORV setpoint plus uncertainties for DCPP, is 5.0 gpm.

- The IRB tests demonstrate that the bounding leak rate applies for TSP offsets up to 0.21 inch including throughwall offsets up to 0.17 inch, which conservatively bound the limiting maximum displacement of 0.15 inch for the high voltage ARC.

- The bounding leak rate data include the effects of offsets, hence, the bounding leak rate does not need to be adjusted for offset.

- The bobbin voltages of the limiting crack lengths that define the bounding leak rate (Tests 11-2 and 1-6) are expected to exceed 25 volts due to throughwall lengths of 0.63 and 0.74 inch. The indications can be confidently expected to exceed any end of cycle indication following implementation of the limited TSP displacement ARC.

- The limiting offset for the limiting TSP length crack of 0.75 inch is estimated at 0.23 inch. This is the offset at which the bounding leak rate would be expected to increase with greater offset as a consequence of reducing the burst opening contact length within the TSP.

- Cracks longer than the TSP limiting crack length of 0.75 inch continue the leak rate trends demonstrated for cracks up to this length and do not result in a step increase in leakage.

- The measured leak rates do not depend on tube size; thus the combined data for both 3/4" diameter and 7/8" diameter tubes can be applied equally for both tube sizes.

- The bounding leak rate does not need to be adjusted for the potential of multiple indications.

- The bounding leak rate is conservative due to the conservatively large tube/TSP gap used in these tests. The gap used was 0.025 inch, which is the 95% confidence bound on the expected steam generator tube/TSP gap and the cracks were oriented within the TSP to locate the full gap opposite the crack in order to maximize the crack opening area. For DCPP, the tube to TSP gaps are essentially zero at operating temperatures due to dented and packed crevices. The DCPP crevice conditions would prevent crack opening and limit leakage to negligible levels compared to freespan leak rates and, particularly, the bounding IRB leak rate of 5 gpm.

- The bounding leak rate is conservatively high by 7% to 10%, based on evaluation of the tests and analysis uncertainties.

7.10 REFERENCES

1. EPRI TR-107625,"Steam Generator Indications Restricted from Burst (IRB) Leak Rate Tests", (Draft) April 1998.

2. W-NSD, SG-95-03-010, "Burst Pressure Correlation for Steam Generator Tubes With Throughwall Axial Cracks", March 1995.

3. EPRI NP-7480-L, Revision 2, "Steam Generator Tubing Outside Diameter Stress Corrosion Cracking at Tube Support Plates - Database for Alternate Repair Limits", August 1996.

4. W-NSD SG-98-01-007, "Plant AA-1 Steam Generator Steam Tube Examinations", April 1998.

Table 7-1
Test Matrix for Indications Restricted from Burst (IRB) - As Tested

Test No.	Tube Dia.	Specimen Type, No.	Throughwall Crack Length (in.)			Free Span Leak Test[1]	Crack to TSP Offset[1] (inch)						Bladder Press. Applied	Test Offset Flow and Bladder Pressurization
							Flow Press.			Bladder Press.				
			.25-.45	.45-.60	.60-.75		0.0	0.10	0.15	0.0	0.10	0.15	(psid)	(inch)
1-1	7/8	Corr./Fatg. 8161G			0.62"	H	H		H	H		H, C	4250	0.152 Flow 0.147 TW 0.150 Bladder 0.147 TW
1-2	7/8	Corr./Fatg. 8161E			0.62"	H	H		H	H		H, C	4080	0.210 Flow 0.145 TW 0.150 Bladder 0.085 TW
1-6	3/4	Corrosion 2008E			0.74"	H	H	H		H	H, C		3035	0.091 Flow 0.070 TW 0.094 Bladder 0.070 TW
1-7	3/4	Corr./Fatg. 2051A			0.60"		H	H		H	H		2970	0.103 Flow 0.091 TW 0.100 Bladder 0.100 TW
2-1	7/8	Corr./Fatg. 8161A		0.515"		H	H		H	H		H, C	4500	0.150 Flow 0.134 TW 0.150 Bladder 0.132 TW
2-4[3]	7/8	Corrosion 4C218	0.29"			H	H		H, C	C		C, H	4125, 5550	0.150 Flow 0.150 Bladder
2-7	3/4	Corr./Fatg. 2051E		0.577"		C	C	H		H	H, C		2800, 3950	0.101 Flow 0.100 Bladder
2-8	3/4	Laser Cut IRB-LC-2		0.55"		H	H	H, C						0.107 Flow 0.104 TW
2-10[3]	3/4	Corrosion 2051B	0.425"			H	H	H, C		H	H, C		3850, 4960	0.100 Flow 0.106 Bladder

Table continued next page.

Table 7-1 (Continued)
Test Matrix for Indications Restricted from Burst (IRB) - As Tested

Test No.	Tube Dia.	Specimen Type, No.	Throughwall Crack Length			Free Span Leak Test	Crack to TSP Offset[1] (inch)						Bladder Press. Applied	Test Offset Flow and Bladder Pressurization
							Flow Press.			Bladder Press.				
			.25-.45	.45-.60	.60-.75		0.0	0.10	0.15	0.0	0.10	0.15	(psid)	(inch)
4-1	7/8	Corrosion 4B214	0.24"							C		C	5800, 6900, 7725, 8900, 10120	0.167 Bladder 0.112 TW
11-1	7/8	Corr./Fatg. 5B403			0.71		H		H	H		H	3670	0.185 Flow 0.150 TW 0.185 Bladder 0.154 TW
11-2	7/8	Corr./Fatg. 8161B			0.63		H		H	H		H	2940, 4075	0.208 Flow 0.173 TW 0.180 Bladder 0.150 TW
11-7	3/4	Corr./Fatg. 2008A			0.809		H	H		H	H		2900	0.111 Flow 0.102 TW 0.109 Bladder 0.100 TW
12-1	7/8	Corr./Fatg. 8161C		0.515[4] 0.360			H		H	H		H	3310, 4850	0.158 Flow 0.105 TW 0.165 Bladder 0.151 TW
12-7	3/4	Corr./Fatg. 2008D		0.580[5]			H	H		H	H		2800, 6200	0.104 Flow 0.100 TW 0.116 Bladder 0.100 TW

Table continued next page.

Table 7-1 (Continued)
Test Matrix for Indications Restricted from Burst (IRB) - As Tested

Notes:

1. H is hot test at operating temperatures, C is a room temperature test
2. Test sequences include pressurizing with a bladder typically to the free span burst pressure. Test 4-1 includes incremental increases in bladder pressure beyond that equivalent to a free span burst. Tests 2-4, 2-10, 11-1, 11-2, 12-1 and 12-7 include bladder pressurizations below and at the free span burst pressure. Bladder pressurization is performed to open the crack beyond that obtained within the pressure capability of the facility.
3. Leak tests in small leak test facility prior to bladder pressurization and large facility after pressurization. All other tests in large leak test facility.
4. Specimen has two throughwall cracks 90° apart.
5. Two essentially co-planar cracks (0.012" circumferential offset) separated by a ligament at 0.365" from the end of the longer segment.

Table 7-2
Voltage Characteristics of Large Cracks

Specimen/ Tube	Tube Diameter	IRB Test No./ Plant	Bobbin Volts	Total Crack Length	Throughwall Crack Length	Remarks
Laboratory Specimens						
4C218	7/8"	2-4	11.4	0.600" (1)	0.290" (1)	Two cracks in Specimen
4B214	7/8"	4-1	17.1	0.670" (1)	0.24" (1)	Two cracks in Specimen
4B276	7/8"	2-1	8.0	0.62" (2)	0.515" (2)	
4C220	7/8"	not tested	7.9	0.59" (1)	0.15" (1)	
4B272	7/8"	not tested	8.0	0.72" (2)	0.38" (2)	
Pulled Tubes						
R44C45	7/8"	DCPP-2	21.5	0.70	0.374"	Ref. 2
R35C57	7/8"	DCPP-2	5.09	0.519	0.217"	Ref. 2
R34C53	7/8"	Plant A-2	6.73	0.612"	0.282"	Ref. 1
R2C85	7/8"	Plant A-1	13.55	0.81"	0.42"	Ref. 1
R15C62	7/8"	Plant P-1	5.30	0.68"	0.252"	Ref. 1
R12C45	7/8"	Plant W-2	3.35	0.625"	0.197"	Ref. 1
R16C31	3/4"	Plant E-4	15.70	0.67"	0.47"	Ref. 1
R26C34	3/4"	Plant E-4	8.55	0.67"	0.24"	Ref. 1
R28C41	3/4"	Plant S	11.8	0.80"	0.45"	Ref. 1
R33C20	3/4"	Plant S	9.8	0.47"	0.33"	Ref. 1
R42C43	3/4"	Plant S	22.9	0.75"	0.50"	Ref. 1; Two cracks
R41C65	3/4"	Plant AA-1	8.93 (3)	0.698"	0.268"	Ref. 1
R28C24	3/4"	Plant AA-1	6.08 (3)	0.688"	0.260"	Ref. 1

Notes:
1. Based on dye penetrant measurement prior to any testing
2. Based on UT measurements

References:
1. EPRI NP-7480-L, Addendum 5, 1996 Database Update
2. 51-5027436-00, Examination of Diablo Canyon Unit 2 SG Tubes – Final Report, Framatome ANP

Table 7-3
Summary of SLB Leak Rates (2560 psid and 2405 psid)[1] and Crack Length Data

Test	Specimen	Initial Crack Lengths		Offset Tests				Zero Offset Tests		
		Total	TW	TW Length	Offset TW Length	2560 psi Leak Rate (gpm)	2405 psi Leak Rate (gpm)	TW Length	2560 psi Leak Rate (gpm)	2405 psi Leak Rate (gpm)
Flow Pressurization Tests										
2-4	7/8,4C218	0.600	0.290	0.330	0.000	0.37	0.22	N.M.	0.37[8]	0.22[8]
2-10	3/4,2051B	0.551	0.425	0.425	0.000	1.70	1.0	N.M.	1.70[8]	1.0[8]
2-1	7/8,8161A	0.640	0.515	0.504	0.134	1.65	1.28	0.230	0.93	0.73
2-7	3/4,2051E	0.660	0.577	0.636	0.088	4.10	4.05	0.515	N.R.[2]	N.R.[2]
2-8	3/4,IRB-LC2	0.553	0.550	0.558	0.104	6.10	6.10	0.525	N.R.[2]	N.R.[2]
1-1	7/8,8161G	0.626	0.620	0.595	0.147	3.70	3.0	0.494	2.30	2.20
1-2	7/8,8161E	0.645	0.620	0.666	0.145	3.20	3.20[8]	0.574	N.R.[2]	N.R.[2]
1-7	3/4,2051A	0.600	0.600	0.602	0.091	4.10	4.10	0.530	3.20	3.16
1-6	3/4,2008E	0.760	0.740	0.724	0.070	5.50	4.90	0.619	3.40	3.20
4-1	7/8,4B214	0.670	0.240	-	-	N.M.[3]	N.M.[3]	-	N.M.[3]	N.M.[3]
11-1[6]	7/8,5B403	0.710	0.600 0.110	0.620 0.129	0.150	5.00	4.35	0.620 0.129	4.00	3.47
11-2	7/8,8161B	0.729	0.630	0.720	0.173	5.13	5.0	0.657	N.R.	N.R.
11-7	3/4,2008A	0.813	0.809	0.811	0.102	6.20	5.74	0.809	6.20	5.74[8]
12-1[4]	7/8,8161C	0.607 0.465	0.518 0.360	0.585 N.M.	0.105	3.20	3.0	N.M. N.M.	3.20	3.0[8]
12-7[5]	3/4,2008D	0.590	0.375 0.256	0.375 0.259	0.100	3.90	3.5	0.375 0.259	3.90	3.5[8]

Table 7-3 (Continued)
Summary of SLB Leak Rates (2560 psid and 2405 psid) [1] and Crack Length Data

Test	Specimen	Initial Crack Lengths		Offset Tests				Zero Offset Tests		
		Total	TW	TW Length	Offset TW Length	2560 psi Leak Rate (gpm)	2405 psi Leak Rate (gpm)	TW Length	2560 psi Leak Rate (gpm)	2405 psi Leak Rate (gpm)
Bladder Pressurization Tests										
2-4	7/8,4C218	0.600	0.290	0.382	0.076	1.9	1.9	0.382	1.3	1.2
2-10	3/4,2051B	0.551	0.425	0.492	0.081	1.6	1.3	0.492	1.6	1.3
2-1	7/8,8161A	0.640	0.515	0.504	0.132	3.1	3.0	0.509	3.2	3.1
2-7	3/4,2051E	0.660	0.577	0.637	0.087	3.7	3.4	0.637	4.2	3.7
2-8	3/4,IRB-L62	0.553	0.550	-	-	N.M.[3]	N.M.[3]	-	N.M.[3]	N.M.[3]
1-1	7/8,8161G	0.626	0.620	0.595	0.147	2.4	2.2	0.595	3.5	3.2
1-2	7/8,8161E	0.645	0.620	0.668	0.085	2.8	2.6	0.666	2.7	2.5
1-7	3/4,2051A	0.600	0.600	0.613	0.100	3.3	3.0	0.613	3.2	2.9
1-6	3/4,2008E	0.760	0.740	0.726	0.070	5.0	4.5	0.726	4.8	4.3
4-1	7/8,4B214	0.670	0.240	0.606	0.112	4.2		0.606	2.5	
11-1[6]	7/8,5B403	0.710	0.600 0.110	0.754	0.154	5.0	4.5	0.754	5.0	4.5
11-2	7/8,8161B	0.729	0.630	0.707	0.150	5.3	5.0	0.707	4.9	4.3
11-7	3/4,2008A	0.813	0.809	0.811	0.100	6.2	5.8	0.811	5.7	5.2
12-1[4]	7/8,8161C	0.607 0.465	0.518 0.360	0.630 0.411	0.151	5.7	5.6	0.629 0.411	5.7	5.6
12-7[5]	3/4,2008D	0.590	0.375 0.256	0.726	0.100	3.3	3.0	0.726	3.2	2.9

Table 7-3 (Continued)
Summary of SLB Leak Rates (2560 psid and 2405 psid) [1] and Crack Length Data

Notes:

(1) Approximate leak rates at 2560 psid and 2405 psid based on linear extrapolation of log leak rate vs ΔP plots.

(2) N.R. - Estimate not reliable due to low pressure tested in zero offset condition or absence of crack to TSP interaction at lower pressures

(3) N.M. - Not Measured. Test not performed.

(4) Specimen has two throughwall cracks 90° apart.

(5) Specimen has two parallel throughwall cracks separated by a circumferential ligament 0.012" at the crack tips

(6) Specimen has two coplanar axial cracks separated by a ligament.

(7) Pressure applicable to DCPP based on PORV setpoint (2335 psig) plus 3% uncertainty

(8) Data trend is the same with increasing Δp for zero-offset, freespan and offset tests.

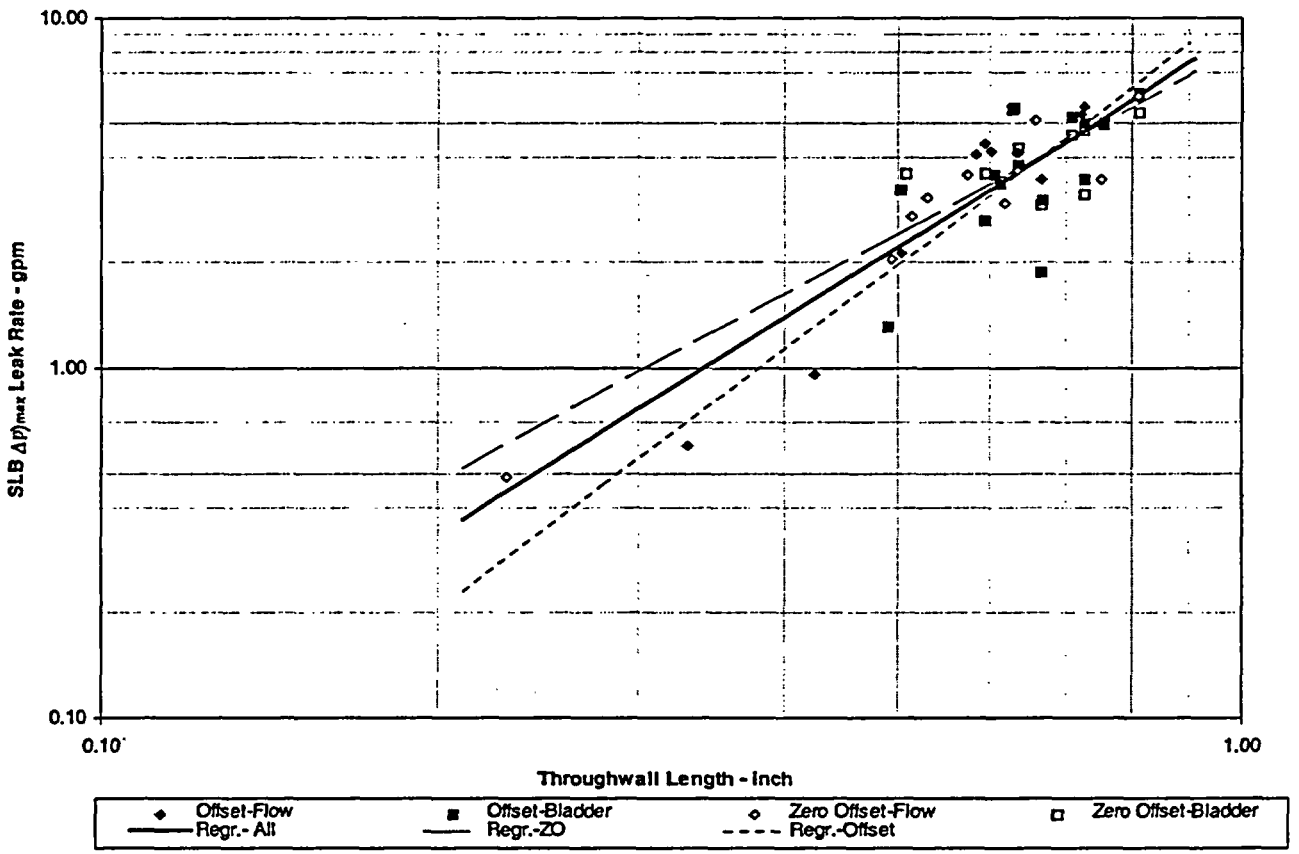

Figure 7-1
Comparison of Offset Leak Rates and Zero-Offset Leak Rates for IRBs

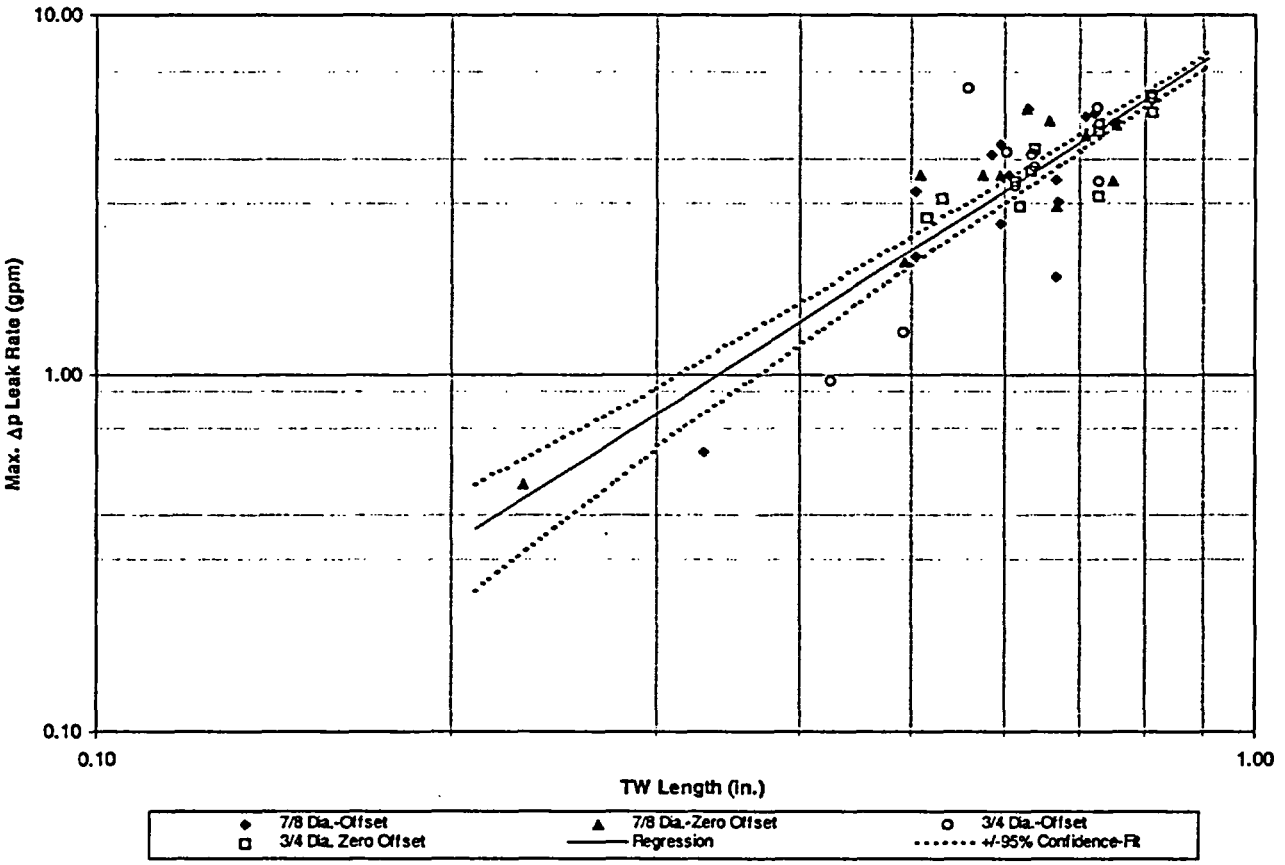

Figure 7-2
Applicability of Measured Leak Rate for 3/4" and 7/8" Diameter Tubing;
Correlation of IRB Leak Rate with Throughwall Crack Length for
Zero-Offset and Offset Tests;
(Flow Pressurization and Bladder Pressurization Included)

8.0 ANALYSIS METHODS FOR TUBE BURST AND LEAKAGE WITH LIMITED TSP DISPLACEMENTS

The purpose of this section is to address the likelihood of tube burst and the total potential leak rate from tube indications that are at least partially restrained from bursting by the presence of the TSP. The information contained herein is essentially that presented in References 1 and 2 for other plants, revised to reflect some of the information developed to respond to the NRC staff requests for additional information (RAIs) regarding the Reference 1 and 2 reports, and to include consideration of SG tubes with a nominal diameter of 7/8 inch instead of 3/4 inch. Finally, the discussion was expanded to address issues raised by the NRC staff relative to the extended application (more than one cycle of operation) of a higher voltage limit acceptance criterion as discussed in Reference 3. Specific discussions have been added regarding:

1. Combining the probability of axial burst and axial tensile failure.
2. Combining the predicted leak rates from the locked TSP indications with that from the non-locked TSP indications.

Since the TSPs do not undergo any displacement relative to indications developed within the upper and lower planes of the TSPs during normal operation, tube burst at pressures less than three times the normal operating differential pressure is obviated by the presence of the TSP, see Appendix A of References 4 and 5 for example. Therefore, the requirement of Regulatory Guide (RG) 1.121, Reference 6, for the resistance to burst relative to three times the normal operating differential pressure, $3 \cdot \Delta P$, is inherently met. Thus, the considerations documented in this section are limited to determining the margin against tube burst and the method to account for the leak rate from such indications during a postulated Steam Line Break (SLB) event.

There are multiple modes of failure that can be classified as burst. An axial burst consists of a splitting of the tube parallel to the axis of the tube and is caused by hoop stresses due to internal pressure. An axial tensile failure, or tensile failure, consists of separating the tube into two parts through a cutting plane perpendicular to the tube axis, i.e., a Guillotine break. The latter failure mode is caused by the unbalanced pressure load at the U-bend usually referred to as the end cap load. The total probability of burst of a tube with ODSCC at TSP elevations is the sum of the probability of axial burst plus the probability of tensile failure. The latter probability is negligible in SGs where the ODSCC ARC of Reference 7 have been applied and only the probability of axial burst is reported. Omission of consideration of the probability of tensile failure has also been approved by the NRC for application when a single cycle of operation with increased ARC limits is planned, Reference 3. It was specifically noted in granting that approval that the probability of axial burst and tensile failure should be combined for applications involving more than one cycle of operation, ostensibly to address the larger allowable degradation limit.

The evaluation of the burst pressure of degraded tubes and the associated probability of axial burst is contained in Sections 8.1 through 8.5. A discussion of the probability of tensile failure is provided in Section 8.6, and the joint probability of axial burst or tensile failure is discussed in Section 8.7.

The various failure modes also affect the potential leak rate from degraded tubes during a postulated MSLB event. Large indications that would burst if not constrained by the presence of the TSP could deform such that the leak rate would be significantly greater than predicted from the free span model that

is used for tubes that are not predicted to burst. These are referred to as indications restrained from burst (IRB) and assigned a bounding large leak rate as discussed in Section 7. Moreover, an axial burst or tensile failure would likely result in a leak rate larger than that from the rest of the indications in the SG combined. The treatment of the leak rate from tube indications located wholly or partially within the TSP is discussed in Sections 8.8 and 8.9. The determination of the total leak rate from all indications, including the treatment of those for which axial burst or tensile failure is possible, is discussed in Section 8.10.

8.1 GENERAL DESCRIPTION OF BURST PRESSURE ANALYSIS METHODS

The essentials of the analyses consist of consideration of correlations of the burst pressure of throughwall cracks relative to crack length and the burst pressure of ODSCC TSP indications relative to the NDE ECT amplitude, i.e., the bobbin voltage. The concern for the potential of tube rupture during a SLB is based on the consideration that the pressure gradient in the SG will cause the TSPs to deform out of plane and expose TSP intersection tube ODSCC indications such that they behave as free-span indications without the constraint of the TSP. The evaluation of the likelihood of tube rupture, i.e., the probability of burst (PoB), is based on the calculated deformations of the plates to determine the magnitude of potential exposure, the correlation of the burst pressure of tubes with free-span ODSCC indications to bobbin voltage, and the correlation of the burst pressure of tubes with free-span axial cracks to crack length.

Increased ODSCC ARC are to be applied to row and column locations where the TSP undergoes relatively minor displacements, say ≤ 0.15", during a SLB initiated from either normal operating or hot standby conditions. Since the thickness of the TSP is 3/4", it is unrealistic to treat each indication as though it would be fully exposed during a SLB. In this case the expected burst pressure can be calculated by considering a throughwall crack which is exposed by an amount equal to the deformation of the plate. The PoB for such a crack can be calculated using the correlation of the burst pressure to the crack length, adjusted as necessary to account for the constraint from the TSP. For larger deformations the PoB is calculated as the larger of the values obtained by using both correlations developed for predicting the burst pressures, i.e., as a function of bobbin or crack length. The rationale for this is that while the PoB may increase significantly for longer throughwall cracks, the actual PoB would be limited by that for a free-span ODSCC indication which can be predicted from the bobbin amplitude. The following Sections of this report present information on the free-span burst pressures for tubes with axial throughwall cracks, Section 8.2, the effect of the radial constraint afforded by the TSP on the burst pressure, Section 8.3, the probability of burst of tubes with free-span throughwall axial cracks, Section 8.4, and the effect of the TSP on the probability of burst of indications located within the TSP hole during normal operation, but which may become partially exposed during a postulated SLB event, Section 8.5.

8.2 BURST PRESSURE VERSUS THROUGHWALL CRACK LENGTH CORRELATION

Since an essential part of the methodology involves the correlation of the burst pressure to the potentially exposed crack length, it is appropriate to first consider the relationship of the burst pressure to crack length for a free-span indication. This relationship forms the basis for estimating the probability of burst as a function of the exposed crack length, i.e., in subsequent sections the relationship of burst to exposed crack length is developed relative to the free-span correlation.

Analysis of burst test data for a variety of tube sizes, Reference 8 indicates a strong correlation between the burst pressure, P_b, and the throughwall crack length, a, using an exponential relationship, i.e.,

$$P_b = \frac{(S_Y + S_U)t}{R_m}\left[0.0613 + 0.536\, e^{-0.278\lambda}\right], \tag{8.1}$$

where t and R_m are the thickness and the mean radius of the tube, and S_Y and S_U are the yield and ultimate tensile strength of the tube material. The term in brackets is usually referred to as the normalized or non-dimensionalized burst pressure, P_N, i.e.,

$$P_N = \frac{P_B r_m}{2S_f t}. \tag{8.2}$$

Thus, P_N is the ratio of the maximum Tresca stress intensity (taking the average compressive stress in the tube to be $P_B/2$), to twice the flow stress, S_f, of the material, taken as $\frac{1}{2}(S_Y+S_U)$ for Alloy 600. The exponent term, λ, is referred to as the normalized crack length, where,

$$\lambda = \frac{a}{\sqrt{R_m t}}. \tag{8.3}$$

The coefficients of equation 8.1 were found by performing a non-linear regression of P_N on λ, i.e.,

$$P_N = g_1 + g_2 e^{g_3 \lambda}. \tag{8.4}$$

The index of determination of the regression was found to be 99.1% with a standard error of the normalized predicted burst pressure of 0.0176. The p values for each of the coefficients was significantly less than 0.1%. The distribution of the residuals was found to be approximately normal. A plot of the resulting relation corresponding to the form of equation 8.1 is provided on Figure 8-1 for 7/8" diameter tubes with a nominal flow stress of 68.8 ksi, the average of the Westinghouse database for tubes at 650°F. Also shown on Figure 8-1 is the regression curve adjusted for lower 95%/95% tolerance limit material properties at 650°F. It is noted that equation 8.1 yields estimates of the critical crack length for burst during SLB of 0.89 inch for a SLB differential pressure of 2405 psi, and 0.69 and 0.63 inch for a margin of 1.4 times the SLB differential pressure for a tube with nominal and lower tolerance limit (LTL) material properties respectively at 650°F. These results imply that the limiting throughwall indication equal to the TSP thickness of 0.75 inch would not burst at SLB conditions, and that the probability of burst for an indication that extends only about 0.15 inch beyond the TSP surface will be extremely low.

8.3 BURST PRESSURE VS. CRACK LENGTH FOR CRACKS EXTENDING OUTSIDE TSPS

Using the results from the correlation analysis of Section 8.2, the probability of burst for tubes with free-span throughwall axial cracks can be calculated as discussed in Section 8.4. Moreover, the calculation can be modified to estimate the probability of burst of tube/TSP indications that extend partially outside of the

TSP due to movement of the TSP during a postulated SLB event. The calculation of the probability of burst for such indications is discussed in Section 8.5.

For tubes in which a portion of the length of the crack, i.e., indication, is restrained in the radial and circumferential directions, i.e., as would exist within a hole in a TSP, the burst pressure correlates with the exposed crack length. This is because the local condition for burst is the achievement of a critical opening of the crack at the crack tip. The critical crack tip opening displacement (CTOD) for throughwall cracks in thin walled tubing is on the order of the thickness of the tube, i.e., about 40 to 45 mils. In essence, the clearance between the OD of the tube and the ID of a TSP hole is not sufficient to permit the achievement of the critical CTOD for the end of the crack within the TSP at the pressures which would lead to the burst of cracks of significant length.[1] Hence, within the TSP, the crack would not be expected to extend in length beyond that associated with less-than-critical blunting of the crack tip. If the clearance between the inside of the TSP hole and the tube approaches zero, there can be no CTOD at that end of the crack and the strength of the cracked tube is slightly increased. If the clearance between the tube and the inside of the TSP is significant, the crack flanks may open and the crack would be expected to behave as though it were slightly longer than the exposed length. Finally, if the clearance is between the two extremes, the burst pressure may be slightly elevated or depressed depending on the value of the clearance.

In order to address the effect of the TSP on the burst pressure, a series of burst tests were performed to quantify the effect of the clearance between the tube and the TSP hole. A description of the burst test specimens is provided in Section 8.3.1. Because an essential feature of the testing program was the presence of the TSP collar and the diametral clearance between the tube and the hole in the TSP, an evaluation was performed to identify the range of clearances that might be expected in Westinghouse fabricated SGs. This is documented in the Section 8.3.2. The results from the testing are discussed in Section 8.3.3. Section 8.3.4 repeats the discussion of the potential effect of the proximity of the tube U-bend on burst behavior which was included in Reference 2 in response to an NRC staff RAI for application of elevated ARC at another plant.

8.3.1 Description of Burst Tests

To evaluate the strengthening effect of the constraint afforded by the TSP, several low energy (hydraulic as opposed to pneumatic) burst tests were performed to provide a direct comparison between the free-span burst strength and the TSP constrained burst strength. The question of whether or not high-energy tests were performed was raised by the NRC staff in reviewing the application of elevated ARC as documented in Reference 1. For example, pneumatic testing results in the internal pressure being relatively constant for a short time following the initial tearing of the crack ends. This is contrasted to hydraulic testing where the pressure decreases drastically once a leak is achieved. Since the key objective of the testing was to identify the pressure at which unstable crack extension initiates, the use of a high energy facility is not necessary. It is not necessary to ascertain by test whether or not crack extension will continue after the initial burst pressure is reached because it is explicitly assumed that crack extension will continue after initiation because of the essentially constant source of pressurized water in the SG. Considerations of free-span burst as described in Section 8.2 have not involved assumptions regarding the

[1] Specimens with 3/4" long cracks, entirely confined with the TSP exhibit burst pressures well above 8500 psi.

nature of the tube opening following the initiation of rupture. The results from a constrained burst test would be expected to be considerably different from results from free-span tests. The flanks of the crack are not free to deform significantly in the constrained case (contact with the TSP hole would be expected at about one-half of the burst pressure), and the crack behaves like a shorter crack with an attendant much lower probability of burst, and hence lower probability of unstable extension.

The tube specimens were lined with a flexible plastic tube, also referred to as a bladder, prior to testing. The OD of the bladder was reinforced with a small, low strength, 2 mils thick, lubricated brass foil shim to prevent extrusion of the bladder prior to achieving the burst pressure of the tube. A 3/4" thick collar was slipped over the tube at the elevation of the cracks prior to pressurization to simulate the presence of the TSP. Once the crack tips start to extend and the flanks open significantly, the pressure in the pressurizing medium is released and no further energy is supplied. Although the results reported on Figure 8-2, discussed in Section 8.3.3, were not from tests performed in a high-energy test facility, examination of the specimens revealed that the failed surfaces at the ends of the cracks formed an angle of approximately 45° with the exterior and interior surfaces of the tube. This is similar to the failed surfaces resulting from test cases where the tearing has continued as a result of being in a high-energy test situation, References 9, 10, and 11. Thus, initiation results are independent, as they should be, of considering the burst to occur in a high or low-energy loading configuration.

8.3.2 Tube Support Plate Hole Diameter Distribution

Prior to conducting the tests (originally for 3/4" diameter tubes as reported in Reference 1), the TSP hole size to be used to simulate conservative field conditions had to be determined. Specific data relating to the as-built dimensions of the TSP holes in Model D SGs were not available and information was developed to indirectly support the selection of the collar inside diameters for the burst test program described in Reference 1. Similar information was developed regarding the as-fabricated dimensions of the TSP holes in Model 51 SGs. The Model 51 TSP drawings indicate a tolerance for the tube hole size of [ ]^{a,c,e}, with a reference dimension of [ ]^{a,c,e}. It may be concluded that the drill size used for the Model 51 TSPs was a [ ]^{a,c,e} diameter bit. Random sampling data from TSP holes drilled for another model SG indicated that the average hole diameter is [ ]^{a,c,e} larger than the drill size, and that the standard deviation of the hole diameter is [ ]^{a,c,e} mils. A sample of hole diameters in the tubesheet of a Model 51F SG, a later Westinghouse model, were found to have a standard deviation of [ ]^{a,c,e} mils. Based on the average and standard deviation of the sample data, holes drilled with a [ ]^{a,c,e} diameter drill would be expected to have a 95% confidence upper bound of [ ]^{a,c,e}, or clearances ranging from [ ]^{a,c,e} mils.

The burst tests were conducted with diametral clearances ranging from [ ]^{a,c,e} mils. The tests were originally performed for initial applications of a limited TSP displacement ARC criterion value associated with Model D SGs which had a nominal TSP hole diameter that was larger than the minimum on the drawing. Although it was thought to be unlikely that a non-standard drill size would have been used for the manufacture of the SGs, the upper bound of the range of clearances to be tested was increased to account for the potential that special sized drill bits were fabricated for the TSP hole drilling operations.

8.3.3 Evaluation of the Burst Test Data

The results from the tests are summarized in Table 8-3 for clearances from zero to 13 mils, Series 1, and in Table 8-4 for clearances from 21 to 23 mils, Series 2 tests. The results are also illustrated on Figure 8-2. Also illustrated are the results from previous testing of 0.75" long slotted tubes tested with the slot entirely contained within the TSP simulating collar, Reference 4. For the latter tests the diametral clearance ranged from 27 to 30 mils. Free-span burst tests were performed for a range of throughwall crack lengths, simulated by narrow EDM slits, from 0.15" to 0.70". The total crack length was always 0.70" for the TSP-confined tube tests, and exposure of the crack beyond the TSP boundary ranged from 0.15" to 0.50". The presence of the TSP was simulated by a round collar which was sized to provide a radial stiffness equal to the average radial stiffness of the TSP. The diametral clearance between the tube and the TSP hole ranged from [ ]^{a,c,e} mils, or about [ ]^{a,c,e} mils on the circumference for the series of tests performed.

The results from the tests employing the smaller gap of 11 to 13 mils, listed in Table 8-1 and illustrated on Figure 8-2, verify the expectation that the burst pressure for a long crack with a portion of the crack constrained by the TSP would be similar to that of a free-span crack with a total length equal to the exposed length of the constrained crack. Hence, the throughwall burst pressure correlation may be used to evaluate the probability of burst of exposed cracks as a function of the length exposed if the diametral clearance between the tube and the hole in the TSP in the SG is small, i.e., on the order of 13 mils or less. The dented and packed TSP crevices at DCPP lead to the expectation that the actual diametral clearances are on the order of zero mils. It would be expected that the strengthening due to the TSP constraint would be significant for the larger clearances, but not as significant as for the small clearance range. In other words, the burst pressure would be expected to be slightly less than that for free-span cracks with a total length equal to the exposed length of the constrained test specimens. The results from the larger gap tests, [ ]^{a,c,e} mils, listed in Table 8-2 and also illustrated on Figure 8-2, confirm this supposition. Over the range of exposure of interest, the effect of the larger clearance is to diminish the burst pressure as predicted using the free-span crack expression, equation 8.1, by about [ ]^{a,c,e} for 7/8" diameter tubes.

The data used to obtain the adjustment factor are illustrated as solid black circles on Figure 8-2. A total of twelve (12) data points were available for the analysis, however, the adjustment factor was obtained as the average for the six (6) data points located farthest below the predicted burst curve for the specimens with the maximum slit exposure (0.3 to 0.5 inch). Since the form of the adjustment was chosen to be a constant, the average factor is the same as would be obtained from a least squares solution. The use of a censored database is considered to be conservative since the range of interest is for exposures of about 0.1 to 0.3", i.e., the actual reduction in strength would be expected to be smaller than that used for smaller TSP displacements. The data illustrate that no adjustment is really necessary for exposures in the range of ~0.1 to ~0.2" and that only a slight adjustment is necessary for exposures of ~0.2 to ~0.3". Thus, the selection of the data used for the determination of the adjustment factor essentially bounds the data in the range of interest. Since the use of an adjustment factor of [ ]^{a,c,e} psi is conservative, no further testing was performed or planned.

8.3.4 Influence of Proximity of the Tube U-Bend on the Burst Pressure

The following information was developed in response to a NRC staff request for additional information with respect to the application of the increased ARC criterion value discussed in Reference 1. The discussion is intended to be identical to that of Reference 2 except for the elevation dimension specific to Model 51 SGs instead of that for Model E SGs. The tangent point of the U-bend with the straight leg of tubing occurs at an elevation of about 3.33" above the top of the uppermost TSP. The effects of local residual stresses from the forming operation, i.e., resulting in ovality and non-uniform cold working of the material, would affect the tube over a length of about 0.3" from the tangent point. Surface stresses from the original tube straightening operation would be relieved by any blunting of the crack tip. Overall, the load in the tube is tensile in the axial and hoop directions. The tensile stress in the axial direction tends to reduce the size of the plastic zone at the crack tip, thus increasing its resistance to fracture from the hoop stress.

Due to separation of the tangent point from the uppermost TSP, the manufacturing process for the U-bend has no significant influence on the burst capability of the tube at the TSP. In general, burst tests have shown higher burst pressures for the bent U-bend tube sections than for straight sections due to the cold working and curvature of the tube.

8.4 SLB BURST PROBABILITY AS A FUNCTION OF THROUGHWALL CRACK LENGTH

A generalized form of equation 8.1 can be written as,

$$P_B = \left(\frac{2t}{R_m}\right) P_N S_f \tag{8.5}$$

Equation 8.5 may be used to estimate the probability of burst based on the variance of the estimate of P_N about the regression equation and the variance of S_f from a large database of measured properties of tubing installed in Westinghouse steam generators. An unbiased estimate of the variance, V, of P_B is given by,

$$\mathrm{V}(P_B) = \left(\frac{2t}{R_m}\right)^2 \left[P_N^2\, \mathrm{V}(S_f) + S_f^2\, \mathrm{V}(P_N) - \mathrm{V}(S_f)\, \mathrm{V}(P_N)\right]. \tag{8.6}$$

The standard deviation of the burst pressure, σ_P, is taken as the square root of $\mathrm{V}(P_B)$. If P_A is an actual burst pressure, it is assumed that the statistic,

$$t = \frac{(P_B - P_A)}{\sigma_P}, \tag{8.7}$$

is distributed as a Student's t distribution with degrees of freedom equal to the degrees of freedom ([ ][8]) used for the regression of P_N on λ.

Taking P_A equal to the SLB pressure, a t variate is calculated from equation 8.7. The probability of randomly obtaining a t variate as large at that obtained is then calculated from the cumulative Student's t distribution, this is the same as the probability of burst (PoB) during a postulated SLB for a tube with a throughwall crack length of a. A plot of probability of burst as a function of crack length using this approach is provided on Figure 8-3.

In actuality, the distribution of P_B does not follow a Student's t distribution in that the distribution is not symmetric. The third moment of the burst pressure distribution, M_3, is related to the means and variances, V, of the normalized burst pressure and the flow stress as,

$$M_3(P_B) \propto P_N^2 S_N^2 V(P_N) V(S_f). \tag{8.8}$$

Since each of the terms in equation 8.6 is positive, M_3 will also be positive. Hence the distribution of the product of the normalized burst pressure and the flow stress will be skewed right, i.e., with a higher tail for larger burst pressures. Therefore, the prediction of burst probabilities based on equation 8.5 would be expected to be conservative. In addition, the degree of conservatism would be expected to increase with decreasing probability of burst, i.e., for shorter crack lengths. Monte Carlo simulations of the burst pressures have resulted in distributions which appear close to the form of a Student's t distribution, but which have a longer tail in the higher burst pressure range, i.e., they are skewed right, confirming the analytical expectation. Hence, the use of equation 8.7 to estimate burst probabilities is expected to be conservative. Comparison of individual 95% upper bound Monte Carlo results with predictions from equation 8.7 indicate a small level of conservatism for high probabilities of burst, e.g., PoB greater than 0.1, and an order of magnitude difference for low probabilities of burst, e.g., on the order of 10^{-6}, see Figure 8-3.

The above equations apply to calculating the PoB for a single throughwall crack or indication. For multiple indications the PoB of one or more of those indications is found as one minus the probability that none of them burst. The probability of no burst, or survival, for any single indication is one minus the PoB, thus the probability of burst of one or more of m indications is given as,

$$\text{PoB (m indications)} = 1 - \prod_{k=1}^{m} (1 - \text{PoB}_k) < \sum_{k=1}^{m} \text{PoB}_k \,, \tag{8.9}$$

where PoB_k is the probability of burst of the k^{th} indication. In practice, the indications are segregated into crack length bins with all indications in one bin considered to have the length of the upper bound of the bin. Thus, the PoB for all indications in the same bin is the same. By multiple application of equation 8.9, the PoB of one or more of all of the indications in the n bins is,

$$\text{PoB}\,(n \text{ bins}) < \sum_{i=1}^{n} r_i \cdot \text{PoB}_i \,, \tag{8.10}$$

where r_i is the number of indications in bin i and PoB_i is now the probability of burst for an indication in the i^{th} bin.

It is admitted that this practice omits direct consideration of the uncertainties of the parameters of the regression equation. However, formation of the normalized burst pressures from the test data includes an uncertainty of the material properties of the test specimens. Thus, the variance of an actual P_N about its predicted P_N includes a contribution from the variation of material properties associated with repeated measurements of tensile specimens from the same tube. This, combined with the observation that equation 8.7 yields conservative results relative to Monte Carlo simulations, see Figure 8-3, is judged to outweigh the effect of omitting the uncertainty in the estimate of the coefficients.

In effect, the calculation of the probability of burst of an indication as a function of the bobbin amplitude of the indication is performed in accordance with the guidelines of Reference 7. Parameter uncertainties are explicitly included in the Monte Carlo simulations "using the correlation between burst pressure and voltage." The details of the methods employed in performing the calculations are provided in Reference 13.

For a single indication extending outside of a TSP intersection, the deterministic calculation includes consideration of the uncertainties in the parameters. The effective variance of a predicted normalized burst pressure about the regression curve is,

$$V(P_N) = s^2\left(1 + \{f_0\}^T \left[F^T F\right]^{-1} \{f_0\}\right) \tag{8.11}$$

where s is the standard error of the regression, $\{f_0\}$ is the coefficient derivative vector and $[F^T F]^{-1}$ is the normalized covariance matrix. The term containing the covariance matrix accounts for the variance of the coefficients of the regression equation.

The above discussion that refers to the omission of consideration of uncertainties in the parameters, is with respect to the effect on the *combined probability of burst as a function of crack length* of all of the indications in the SG, not on the probability of burst of any one indication. For this calculation, it is considered that the use of the deterministic estimate of the probability of burst is justified because the individual calculated probabilities of burst are an order of magnitude higher than obtained from Monte Carlo simulations, the number of intersections with indications is overestimated by at least an order of magnitude, and the assumption that the maximum TSP displacement occurs at all intersections in the SG hot leg likely overestimates the number of indications exposed to that displacement by two orders of magnitude. Thus, the effect of simulating uncertainties in the parameters would have to be sufficient to result in a change in the probability of burst of about four orders of magnitude to increase it above the values stated. The simple fact is that the probability of burst of an indication which is exposed on the order of 0.1 to 0.3" is extremely small. The development of a Monte Carlo code to simulate the distribution of indications over the TSPs, the distribution of indications at a TSP over the area of the TSP, and the distribution of indication lengths in order to simulate a distribution of exposed lengths, in addition to simulating the parameters of the correlation and the material properties is not justified in light of the very low probabilities obtained from the deterministic estimation.

8.5 MODELING FOR BURST PROBABILITY WITH TSP DISPLACEMENTS

One model was considered for the evaluation of the burst probability given the relative displacements of the TSPs during a postulated SLB. This model is based solely on the TSP displacements and estimates the

PoB by assuming every intersection to have a throughwall crack equal to the thickness of the TSP. Thus, every intersection is considered to have a throughwall crack exposed by the magnitude of the displacement at each intersection. The prediction of the PoB of a single indication can be estimated using the methods described in Section 8.4, however, in this case the predicted burst pressure for nominal material would be reduced by a pressure shift value, P_S, of [ ]^{a,c,e}, i.e., the value of the t distribution variate would be calculated as,

$$t = \frac{[(P_B - P_S) - P_A]}{\sigma_p}, \tag{8.12}$$

instead of using equation 8.7. This approach implicitly assumes that the standard error of the burst pressure based on performing many tests would be the same as that obtained from the testing of free-span cracks. Given the large database from the free-span burst tests, this is not an unreasonable assumption.

A more realistic estimate of the PoB could be obtained by considering only the estimated number of indications and the spatial distribution of those indications in a steam generator. Furthermore, assessment of the PoB of a tube at SLB conditions for limited TSP displacement only requires an estimate of the probability of a large indication occurring at the corners of the TSP where the TSP displacements are significant.

In Section 8.3, it was shown that the burst pressure of a throughwall indication extending outside the TSP has a burst pressure almost equal to the burst pressure for a free span crack at the length extending outside the TSP. Thus, the length of crack remaining within the TSP does not significantly affect the burst pressure. Similarly, the burst probability for TSP displacements with postulated throughwall cracks can be calculated as that associated with a crack length equal to the TSP displacement. This assumes that the throughwall part of a crack is located at the edge of the plate rather than, as more commonly found in pulled tubes, near the center of the TSP. Alternately, it can be postulated that there is a throughwall crack equal to the TSP thickness and the burst probability for this indication is the same as the crack length exposed by the TSP displacement.

A very conservative assumption to define a goal for limited TSP displacement is to assume that all intersections at all hot leg TSPs 1–4 (excluding hot leg TSPs 5–7 and all cold leg TSPs, which are covered by the 2V ARC) have throughwall crack lengths at least equal to the TSP displacements. This assumption is applied to develop the allowable limits on TSP displacement so that the proposed ARC are generic and envelop any possible tube degradation.

Even under the above bounding assumption on postulated tube degradation, it is desirable that the associated tube burst probability be small compared to acceptable levels. Then, if multiple ARCs are applied, the hot leg indications at TSPs 1–4 will have a negligible contribution to the tube burst probability. The most conservative guideline for an acceptable burst probability is the value of 10^{-2} given in the NRC generic letter, Reference 7. If this value is exceeded, the generic letter requires that the higher burst probability be reported to the NRC and that an assessment be performed of the significance of the result. If the burst probability for limited TSP displacement under postulated SLB conditions is then $< 10^{-5}$, the TSP indications would contribute <0.1%, i.e., 10^{-2} divided by 1,000, to the NRC reporting level. This 10^{-5} value was the starting point for developing a limited TSP displacement burst probability

requirement based on sensitivity analyses given in Section 10. By applying the tube burst probability as a function of throughwall crack length, as developed in Section 8.4, and the bounding assumption of throughwall cracks at all intersections in hot leg TSPs 1–4, tube burst probabilities can be developed as a function of TSP displacements. The tube burst probabilities are developed in Section 10 for the postulated 13,552 indications for the hot leg TSPs 1–4 with 3,388 tube intersections at each plate. For simplicity, and because the individual burst probabilities are so small, the burst probabilities are calculated as the number of TSP intersections times the single tube burst probability for a throughwall crack equal to the displacement.

8.6 POTENTIAL FOR TENSILE FAILURE OF INDICATIONS AT TSP INTERSECTIONS

The structural limit that determines tube repair limits for free-span indications is based on satisfying RG 1.121 margins for burst of a tube. With the limited displacements of the lower TSPs demonstrated by the analysis in Section 5, the constraint of the TSP reduces the tube burst probability to negligible levels and tube repair limits are not required to prevent axial tube burst. For the small TSP displacements and the expected tube degradation, the need for tube repair is dictated by the need to satisfy allowable SLB leakage limits. However, at some level of cellular or IGA corrosion, it becomes possible for the axial loads resulting from the pressure differential across the tube to result in axial tensile severing of the tube. This tensile load requirement establishes the applicable structural limit for tube expansion based on limited TSP displacement. Section 6.3 of Reference 4 provides a detailed discussion, based on the information contained in Reference 1, of the evaluation of resistance to axial tensile tearing based on the percent degraded area of the tube section. Section 6.3 of Reference 5 provides an update of the Reference 4 information based on the evaluation of additional test data. A description of the tensile tests is provided herein in Section 8.6.1.

It is noted that the bobbin coil voltage is being used to assess the potential for a SG tube to fail circumferentially. An inherent assumption in the methodology is that there is a significant axial component in the SG tube flaw such that is can be detected with the bobbin coil because the bobbin coil is relatively insensitive to circumferentially oriented cracks in SG tubes. The degradation morphology that has been found in pulled tubes for ODSCC at TSP intersections is dominantly axial SCC with varying extent of cellular patches including the absence of cellular corrosion. Cellular corrosion is a combination of axial and oblique angle cracks that form small cells of undegraded tubing within the crack pattern. The patterns of cellular corrosion have been characterized by radial grinds from the tube surface through the tube wall. The axial cracks are consistently deeper than the oblique cracks. That is, as the radial grinds progress through the wall, the crack pattern changes from cellular to multiple axial micro-cracks with the oblique cracks typically less than 50% to 60% of the tube wall when the axial crack are near throughwall. The oblique cracks in the cellular pattern are typically $< 90°$ (i.e., not circumferential) and the bobbin coil voltage responds to both the axial and oblique cracks.

It can be noted that the bobbin voltage responds primarily to the deepest and longest axial cracks. In correlating bobbin voltage with the axial tensile capability of the tube, it is assumed that the cellular pattern will increase in circumferential extent in some close proportion to the length and depth of the dominant axial cracks. Since this is not generally the case, it can be expected that the spread in the correlation (range of tensile force capability at a given voltage) will be significant and greater than that

found for the axial burst pressure correlation with voltage. Cellular corrosion can generally be seen with modest magnification on the OD of the specimen following the axial burst test since the pressure tends to expand the tube diameter and increase the visibility of the tube degradation. The absence of cellular corrosion to eliminate the tensile test can be identified in this manner although the final criterion for inclusion in the tensile force correlation would be based on metallographic specimens.

The conclusion from the Reference 5 evaluation of the data for 3/4" diameter tubes was that the probability of rupture of a single indication with an amplitude of 10V during a postulated SLB event at 2560 psi is $< 3 \cdot 10^{-7}$, and that the overall structural limit for axial separation during a postulated SLB event is significantly greater than 100V. The corresponding probability for a SLB pressure of 2405 psi is $2 \cdot 10^{-7}$. The analysis of Reference 5 was repeated to provide a relationship for use with for nominal 7/8" diameter tubes by accounting for the larger area presented to the SLB pressure and the difference in material properties. The correlating expression for the rupture force, F_R, as a function of the bobbin amplitude is,

$$F_R = a_0 + a_1 \log(Volts), \tag{8-1}$$

and is illustrated on Figure 8-5. The axial force acting on the indication is taken as the end cap load due to the pressure difference, i.e., pressure times the cross section area of the tube. A complete discussion of the axial tensile tearing correlation is provided in Section 6.3 of both References 4 and 5. The results of the regression analysis to obtain the coefficients in the Equation are provided in Table 8-5. These replace the values given in Table 6-9 of Reference 5. The results of calculations of the probability of rupture as a function of indication amplitude are illustrated on Figure 8-6. The probability of rupture of a single indication with an amplitude of 10V at a SLB differential pressure of 2405 psi is $1 \cdot 10^{-7}$, and the overall structural limit for axial separation at $3 \cdot \Delta P$ is well in excess of 100V.

Moreover, all indications with an amplitude of ≤ 4V would be expected to have significant margin to burst relative to the RG $3 \cdot \Delta P$ limit during normal operation.

8.6.1 Performance of the Tensile Tests

The axial tensile tests are performed following the axial burst testing of the specimens. The burst tested specimens are typically about 10 inch long sections of steam generator tubing with the TSP crevice regions centered in the sections (the location of the axial burst opening) and with Swagelok fittings attached to each end of the sections. Simply pulling a burst tested specimen using its attached Swagelok fittings would not work, as the local stresses associated with the Swagelok ferrule would be the source of the tensile fracture. In order to bypass the stresses concentrated at the ferrules, the Swagelok fittings are welded onto the tube above the ferrules using a buttering type weld with a non-uniform weld front that would diffuse local stresses at the weld front. A tensile test gripper mandrel (metal plug) small enough to pass through the compressed Swagelok ferrule regions of the tube is also utilized.

The burst tested specimens are then tensile tested following guidelines in Section 6.9.1 and Figure 11 of ASTM E8, Reference 14. The snug-fitting metal plugs are inserted far enough into the ends of the specimens to permit the testing machine jaws to grip the specimen properly. The plugs do not extend into the gage length portion of the specimens, which is 4 inches long with the burst opening centered in the gage lengths. The specimens are then pulled at a crosshead speed of 0.05 inch per minute and the load to

failure recorded on the load-time recorder chart. Only the loads to failure from the tensile tests are considered meaningful for determining the residual cross sectional area.

8.7 MODELING PROBABILITY OF BURST AND PROBABILITY OF AXIAL TENSILE FAILURE

The purpose of this discussion is to address Summary item (c) of Section 2.5 of Reference 3. The specific NRC concern is with regard to consideration of the potential for axial tensile failure of degraded tubes in addition to the consideration of the potential for axial burst. The NRC staff noted that a licensee requesting long-term implementation of a higher voltage ARC proposing to use the locked TSP model should address a means of combining the axial burst and axial tensile failure conditional probabilities. The background for this request is based on information presented in the ODSCC ARC documents regarding the axial tearing strength of tubes with cellular corrosion based on a correlation of the remaining cross section area (CSA) as a function of the bobbin amplitude of the TSP ODSCC. The conclusion expressed from an analysis of current data in Reference 5 was that the structural limit for axial separation during a postulated SLB event, with or without the requisite factor-of-safety, was greater than 100V. The same conclusion is evident relative to tensile failure at three times the normal operating pressure differential. Moreover, it was noted that the probability of axial separation of a single indication with amplitudes of 4 and 10V is $3.2 \cdot 10^{-8}$ and $1 \cdot 10^{-7}$ respectively. The probability of a tensile failure of one or more tubes during a postulated SLB event would be on the order of 0.001 if a 10V indication existed at all 13,522 intersections subject to the 4V ARC limit.

A summary of the simulation requirements for POB is provided in Table 8-1. The parameters of the correlation of the tensile rupture force as a function of the common logarithm of the bobbin amplitude to be used in the simulation are provided in Table 8-5. Modeling of the potential for axial tensile failure during a postulated SLB event is to be performed in accordance with the requirements given in References 7 and 13. The techniques used should include simulation of the uncertainties in the parameters as is done for the burst pressure as a function of bobbin amplitude.

8.8 SLB LEAK RATES BASED ON ASSUMED FREE SPAN INDICATIONS

A discussion of the methods employed to evaluate the leak rate from tubes during a postulated SLB is given in Reference 12. A linear model relating the common logarithm of the leak rate from a tube at SLB conditions to the common logarithm of the bobbin amplitude of an ODSCC indication is used, Reference 12. The relationship was developed and verified to be valid in accord with the requirements of the NRC generic letter, Reference 7. The use of the model to develop EOC total SG leak rates by appropriately simulating the parametric uncertainties is also described in Reference 13, and are also in accord with the requirements of the NRC generic letter. The data and the results of the analyses are discussed in a later section relative to the potential leak rate from indications at TSP elevations.

8.9 SLB LEAK RATE ANALYSES FOR OVER PRESSURIZED TUBES

This section describes the results of a Westinghouse analysis for SLB leak rates from an over pressurized tube which expands within the TSP until the crack flanks contact the ID of the TSP drilled hole. The term over pressure refers to the fact that burst would be expected if the indication were located in the free span

portion of the tube. The indications is also referred to as an indication restrained from burst. The test program and data to support the analyses are described in detail in Section 7 of this report.

Several models for predicting leakage under postulated accident conditions were developed. The models include the methodology that is used for calculating the primary-to-secondary leakage under postulated accident conditions, i.e., how the SG tube leakage from the hot leg TSPs 1–4 was calculated, and how it was combined with the SG tube leakage from other TSPs.

The objective of demonstrating limited TSP displacements under postulated SLB conditions is to allow the voltage limits of the alternate plugging criteria to increase without increasing the probability of a free-span burst of a tube. However, the probability of occurrence of indications with a higher PoB if they were free-span indications is increased. Thus, even though constrained, the probability of occurrence of indications which could experience increased crack flank deflections, referred to as over pressurization, is increased. Hence, it is appropriate to modify the prediction methodology to account for the leak rate from potentially over pressurized tubes. The standard ARC leak rate prediction methodology, described in detail in Reference 12, was only slightly modified to deal with additional leakage from IRBs.

The SG tube leakage from the hot leg side indications at TSPs 1–4 is calculated using a modification of the free span leakage methodology of the Westinghouse methods report, Reference 12, which is in concert with the guidelines provided in Reference 7. This method involves Monte Carlo simulation of the distribution of indications, uncertainties in the measurement of the indications, the growth of the indications, etc. A modification to the methodology used for the calculations has been effected which increases the leak rate for hot leg indications which are simulated as being restrained from bursting (designated as IRBs), i.e., TSPs 1–4. If the simulation of the burst pressure results in a value which is less than the differential pressure during a postulated SLB, indicating a probability of burst (PoB) of one instead of zero, the probability of leak (POL) of the indication is set to unity and the leak rate from that indication, Q_{IRB}, is assumed to be 5.0 gpm[2], see Section 7. All indications simulated to be IRBs are assigned the bounding leak rate regardless of the bobbin amplitude of the indication. If the indication is predicted to not burst, the probability of leak is found from the logistic correlation of the POL to the common logarithm of the bobbin amplitude. A random uniform deviate is then generated to determine if the indication leaks, i.e., the POL is either zero or one. If the indication leaks, the leak rate is calculated from the correlation of the common logarithm of the leak rate to the common logarithm of the bobbin amplitude.

The simulation is conservative in that the estimated leak rate obtained from the correlation is used even if it exceeds the bounding leak rate for an IRB. Thus, the SG total leak rate, Q, obtained from one simulation of the SG, with n indications in service, is given by,

$$Q_{SG\ Total} = \sum_{i}^{n} \left[\mathrm{PoB} \cdot Q_{IRB} + (1 - \mathrm{PoB}) \cdot \mathrm{POL} \cdot 10^{\beta_3 + \beta_4 \log(V_i) + Z_i \beta_5} \right], \qquad (8.13)$$

where: β_3 = the simulated population intercept of the leak rate on volts relation,

[2] An upper bound value from leak testing of indications that were deformed by internal pressurization to simulate an attempted burst within the TSP. The value corresponds to a differential pressure of 2405 psi.

β_4 = the simulated population slope of the relation,

β_5 = the simulated population standard deviation of the leak rate predictions,

Z_i = is a random normal deviate,

PoB = the probability of burst for each indication, either zero or one, and,

POL = the probability of leak for each indication, either zero or one as described in Reference 13.

The estimated EOC total leak rate for a SG is calculated as a 95% confidence bound on 95% of the possible population of leak rates based on the results of many, i.e., greater than 100,000, Monte Carlo simulations of the total leak rate.

The total leak rate from all of the indications in the SG is calculated and retained. The 95% confidence bound on the total leak rate would then be found using the ordered array of total leak rates from all of the simulations of the SG as described in Reference 13.

8.10 TOTAL LEAK RATE FOR COMBINED TSP CONDITIONS

The estimate of the total leak rate from the ODSCC indications in the SG tubes at TSP elevations has been based on adding the individual 95th percentile simulated results from the free span and restrained TSP calculations for prior applications of the ODSCC ARC when a plugging limit above the Reference 7 specified value has been specifically approved by the NRC. In order to address the concern expressed in Reference 3, Section 2.5, Summary item (f), an approach that directly simulates the 95th percentile of the joint population is needed. The detailed simulations required for the determination of the total leak rate are listed in Table 8-2.

The potential sources of leakage from degraded tubes at locations that are not in locked TSPs are the standard ODSCC ARC consideration of the crack opening as a function of pressure, axial burst of an exposed crack, and axial tensile failure of a degraded tube. The latter two sources of leakage have been traditionally excluded from specific simulation because the total probability of burst or tensile failure events has been extremely small. Indeed, for non-locked TSPs the probability remains small and the probability of a tensile failure of the tube is almost nonexistent. The potential leak rate from a single burst or tensile failure is relatively large, e.g., > 100 gpm. It is the recommendation of this report that a value of 100 gpm be used as the leak rate for indications predicted to burst or rupture during a postulated SLB event. The 100 gpm leak rate applies to the "Not Locked – Axial Burst Leak Rate" and the "Locked TSPs – Tensile Failure Leak Rate" in Table 8-2.

The specific value of a large leak rate, e.g., 100 gpm, is not meaningful to the prediction of the 95th percentile as long as the number of affected tubes is small, which is a requirement relative to the probability of burst. The true effect of predicted large individual leak rates is to effectively increase the total leak rate percentile relative to the values predicted when a burst or tensile failure does not occur. For example, the 95th percentile total leak rate at a 95% confidence level is the 95,114th ordered value from 100,000 simulations. A simulated burst will result in the total leak rate for that simulation of the SG being larger than that for all simulations where a burst has not been predicted to occur. Thus, that total leak rate would be 100,000th ordered value of the simulated total leak rates and the value that would have been at 95,115 had a burst not been predicted to occur becomes the new 95th percentile. Likewise, the 95,116th

value that would have been simulated without a burst occurring will become the new 95,114th value if two bursts are predicted to occur in 100,000 simulations of the SG indications.

Since the total probability of burst is limited to less than 0.01 at 95% confidence, the actual number of SG simulations in which a tube burst is predicted to occur is limited to 948 of 100,000. A 95% upper confidence limit for 948 events in 100,000 simulations is 1000 or 1%. Thus, a conservative and practical upper bound for the total leak rate is the 96,062nd ordered value of the total leak rates if 100,000 simulations are performed. It should be noted that the likelihood of burst is correlated to the likelihood of a large leak occurring since both increase with bobbin amplitude. Thus, it would be expected that the SG simulations with the largest leak rates when the potential for burst is not explicitly included in the leak rate predictions are also the simulations that are most likely to include burst-associated leak rates when the potential for burst is included. This simply means that the top 5% of the simulations with the largest leak rates are likely to be those where tube bursts are predicted to occur. Any burst prediction associated with an ordered leak rate simulation number greater than 95,114 does not affect the placement of the lower ranked leak rate and does not affect the 95th percentile total leak rate. This follows from the fact that the occurrence of a burst at any leak rate simulation level can only affect the placement of leak rate values above it.

8.11 CONCLUSIONS

A conservative estimate of the probability of burst of one or more indications in a SG during a postulated SLB event indicates a likelihood of burst less than that required in Reference 7. The probability of an axial separation of a tube, i.e., becoming circumferentially severed, during a postulated SLB event is very small, e.g., several orders of magnitude less than required for implementation of an ARC. However, the simulation of the probability of burst for the application of the elevated ARC voltage limit will include the joint probability of axial burst for indications at non-locked TSP elevations and tensile failure of the tubes that are locked. The probability of burst of indications in tubes that are not within locked TSPs will continue to be simulated in accordance with the requirements of the Generic Letter, Reference 7. The probability of tensile failure of tubes that are not locked is negligible.

The methodology of accounting for the leak rate from tube indications restrained from burst, i.e., over pressurized tubes, is in concert with the results from the IRB leak rate tests. Since the bounding leak rate from the tests is used in the simulations regardless of indication size, the methodology is conservative relative to the actual leak rate expectations should a SLB event occur. In addition, a large leak rate of 100 gpm will be applied for indications predicted to burst as free-span indications at non-locked TSP elevations or predicted to experience a tensile failure at locked TSP elevations. The leak rates will be applied such that the total leak rate includes the joint probability of all of the potential modes of failure considered, see Table 8-2.

8.12 REFERENCES

1. WCAP-14273 (Proprietary), "Technical Support for Alternate Plugging Criteria with Tube Expansion at Tube Support Plate Intersections for Braidwood 1 and Byron 1 Model D4 Steam Generators," Westinghouse Electric Company, Madison, PA (February 1995).

2. WCAP-15163 (Proprietary), Revision 1, "Technical Support for Implementing High Voltage Alternate Repair Criteria at Hot Leg Limited Displacement TSP Intersections for South Texas Plant Unit 2, Model E Steam Generator," Westinghouse Electric Company, Madison, PA (March 1999).

3. NRC Letter, "South Texas Project (STP), Unit 2 – Issuance of Amendment Revising the Technical Specifications to Implement 3-Volt Alternate Repair Criteria for Steam Generator Tube Repair (TAC No. MA8271)," Thadani, Mohan, US NRC, Washington, DC (March 8, 2001).

4. EPRI NP-7480-L (EPRI licensed material), Addendum 1, "Steam Generator Tubing Outside Diameter Stress Corrosion Cracking at Tube Support Plates Database for Alternate Repair Limits, 1996 Database Update," EPRI, Palo Alta CA (November 1996).

5. EPRI NP-7480-L (EPRI licensed material), Addendum 2, "Steam Generator Tubing Outside Diameter Stress Corrosion Cracking at Tube Support Plates Database for Alternate Repair Limits, 1998 Database Update," EPRI, Palo Alto, CA (April 1998).

6. Regulatory Guide 1.121 (Draft), "Bases for Plugging Degraded PWR Steam Generator Tubes," United States Nuclear Regulatory Commission, Washington, DC (August 1976).

7. Generic Letter (GL) 95-05, "Voltage-Based Repair Criteria for Westinghouse Steam Generator Tubes Affected by Outside Diameter Stress Corrosion Cracking," United States Nuclear Regulatory Commission, Washington, DC (August 3, 1995).

8. SG-95-03-10, "Burst Pressure Correlation for Steam Generator Tubes with Throughwall Axial Cracks," Westinghouse Electric Company, Madison, PA, for the EPRI, Palo Alto, CA (February 1995).

9. Nadai, A., *Theory of Flow and Fracture of Solids*, Second Edition, McGraw-Hill Book Company, New York (1950).

10. Davis, E. A., "The Effect of Size and Stored Energy on the Fracture of Tubular Specimens," Journal of Applied Mechanics, Vol. 15, American Society of Mechanical Engineers, New York, NY (September 1948).

11. Hernalsteen, P., "The Influence of Testing Conditions on Burst-Pressure Assessment for Inconel Tubing," International Journal of Pressure Vessels and Piping, Vol. 52 (1992).

12. EPRI NP-7480-L (EPRI licensed material), Volume 2, Revision 1, "Steam Generator Tubing Outside Diameter Stress Corrosion Cracking at Tube Support Plates - Database for Alternate Repair Limits, Volume 2: 3/4 Inch Diameter Tubing," EPRI, Palo Alto, CA (August 1996).

13. WCAP-14277, Revision 1, "SLB Leak Rate and Tube Burst Probability Analysis Methods for ODSCC at TSP Intersections," Westinghouse Electric Company, Madison, PA (January 1995).

14. ASTM E-8, "Standard Methods of Tension Testing of Metallic Materials," American Society for Testing and Materials (ASTM), Philadelphia, PA, USA (Published Annually).

Table 8-1
Monte Carlo Simulations for
Probability of Burst Calculations

Tube-to-TSP Condition	Axial Burst Simulation	Tensile Failure Simulation
Not Locked	Y	N(1)
Locked TSPs	N(2)	Y

Notes:
1. The probability of tensile rupture for tubes plugged at traditional GL 95-05 limits is so small that it makes no meaningful contribution to the overall POB.
2. The potential for axial burst is obviated by the presence of the TSP.

Table 8-2
Monte Carlo Simulations for
Leak Rate Calculations

Tube-to-TSP Conditions	Free Span Leak Rate	Axial Burst Leak Rate	IRB Leak Rate	Tensile Failure Leak Rate
Not Locked	Y	Y	N(1)	N(2)
Locked TSPs	Y	N(3)	Y	Y

Notes:
1. IRBs are not associated with non-locked TSPs.
2. The probability of tensile rupture for tubes plugged at traditional limits is so small that it makes no meaningful contribution to the overall leak rate.
3. The potential for a leak rate associated with an axial burst is obviated by the presence of the TSP.

Table 8-3
Burst Pressure as a Function of Crack Length and Crack Extension Outside of the TSP
Series 1

Specimen Identification	Slit (Crack) Length (inch)	TSP Hole Clearance (inch)	Slit Extension Out of TSP (inch)	Burst Pressure (ksi)
TSP3-1-015-1	0.149	N/A	Free Span	9.130
TSP3-1-015-2	0.149	N/A	Free Span	8.710
TSP3-1-015-3	0.149	N/A	Free Span	8.350
TSP3-1-030-1	0.298	N/A	Free Span	6.800
TSP3-1-030-2	0.301	N/A	Free Span	6.300
TSP3-1-030-3	0.299	N/A	Free Span	6.220
TSP3-1-050-1	0.502	N/A	Free Span	4.200
TSP3-1-050-2	0.501	N/A	Free Span	4.500
TSP3-1-050-3	0.500	N/A	Free Span	4.320
TSP3-1-070-1	0.700	N/A	Free Span	3.250
TSP3-1-070-2	0.700	N/A	Free Span	3.160
TSP3-1-070-3	0.699	N/A	Free Span	3.210
TSP3-2-070-1	0.700	0.013	0.150	8.980
TSP3-2-070-2	0.700	0.013	0.150	9.160
TSP3-2-070-3	0.699	0.013	0.150	8.870
TSP3-3-070-1	0.699	0.012	0.300	6.600
TSP3-3-070-2	0.698	0.013	0.300	6.250
TSP3-3-070-3	0.700	0.013	0.300	6.290
TSP3-4-070-1	0.702	0.011	0.500	4.500
TSP3-4-070-2	0.700	0.011	0.500	4.600
TSP3-4-070-3	0.699	0.012	0.500	4.200
Tube Material: HT 1797 for 3/4" tubes.				

Table 8-4
Burst Pressure as a Function of Crack Length and Crack Extension Outside of the TSP
Series 2

Specimen Identification	Slit (Crack) Length (inch)	TSP Hole Clearance (inch)	Slit Extension Out of TSP (inch)	Burst Pressure (ksi)
TSP3-6-070-1	0.699	0.021	0.150	8.100
TSP3-6-070-2	0.700	0.021	0.150	8.580
TSP3-6-070-3	0.699	0.021	0.300	6.090
TSP3-7-070-1	0.700	0.019	0.300	6.070
TSP3-7-070-2	0.700	0.021	0.500	3.800
TSP3-7-070-3	0.699	0.022	0.500	3.820
TSP7-2-070-1	0.701	0.022	0.150	8.970
TSP7-2-070-2	0.702	0.023	0.150	9.310
TSP7-3-070-1	0.700	0.023	0.300	6.780
TSP7-3-070-2	0.700	0.023	0.300	7.100
TSP7-4-070-1	0.700	0.021	0.500	4.880
TSP7-4-070-2	0.701	0.023	0.500	5.000
Tube Material: HT 1797 for 3/4" tubes and HT 1282 for 7/8" tubes.				

Table 8-5
Regression Analysis of Axial Rupture Force
on Log Bobbin Amplitude for 7/8" Diameter Tubes

a,c

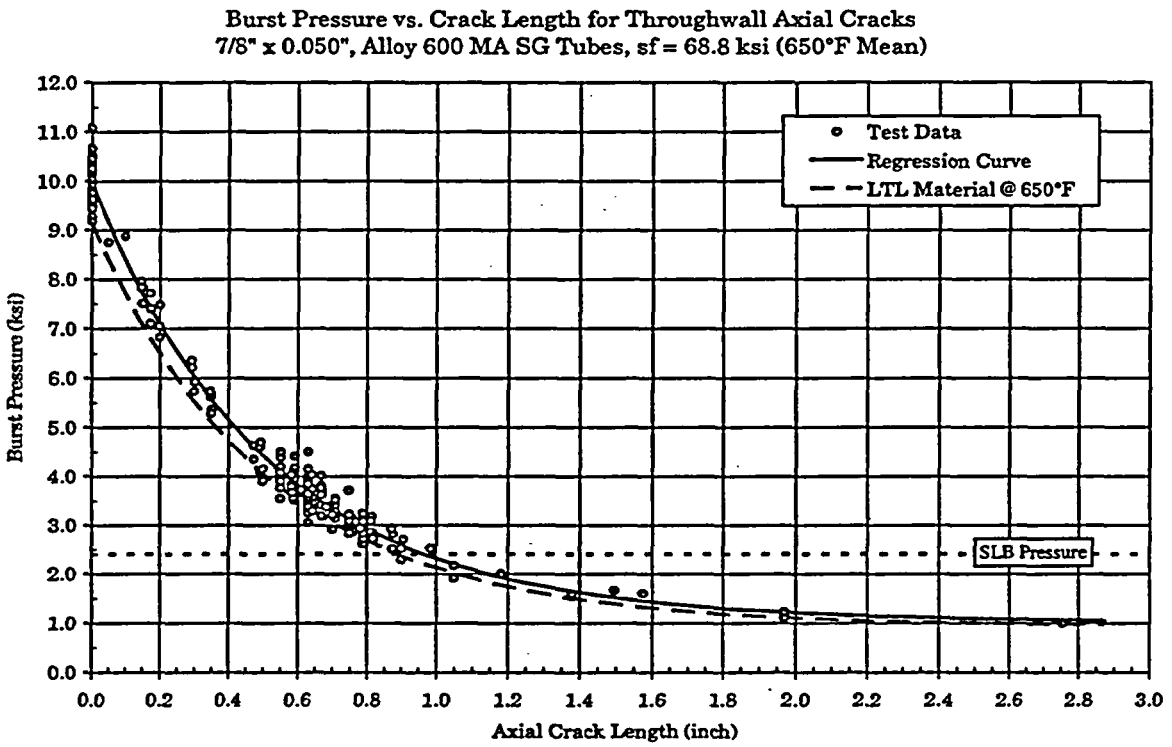

Figure 8-1: Burst pressure as a function of throughwall crack length

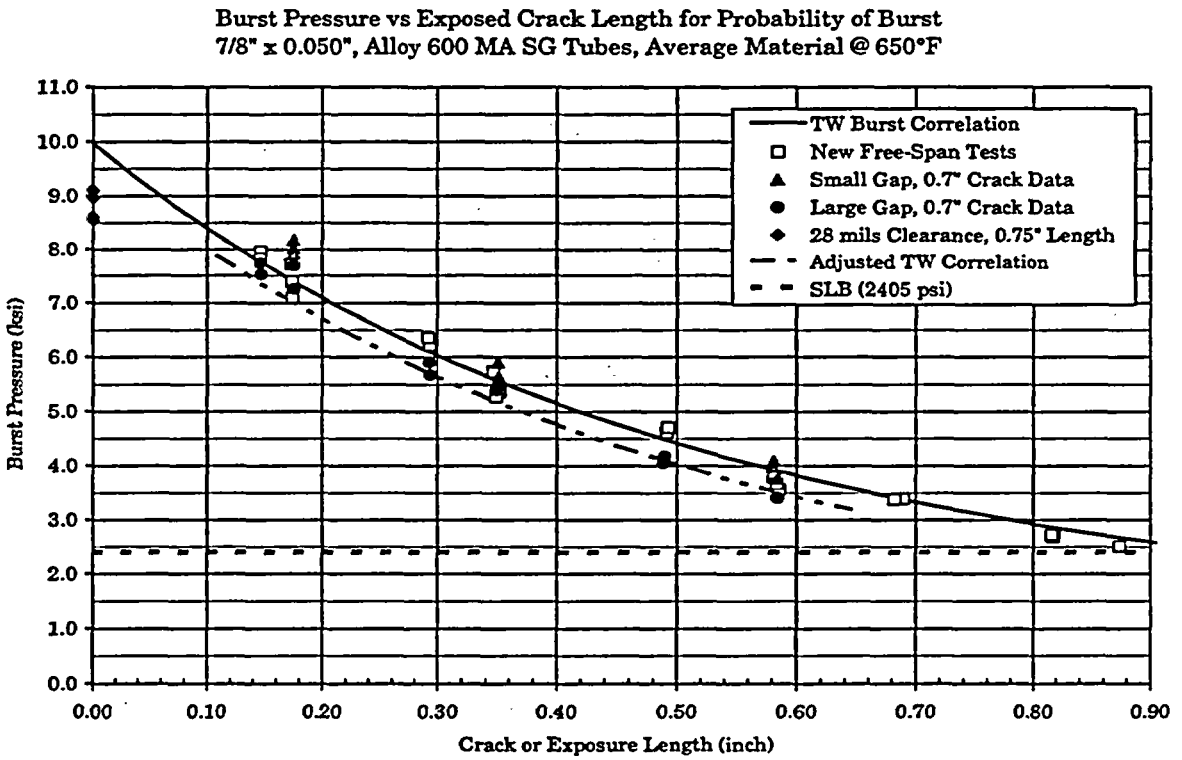

Figure 8-2: Burst pressure for throughwall cracks in TSPs

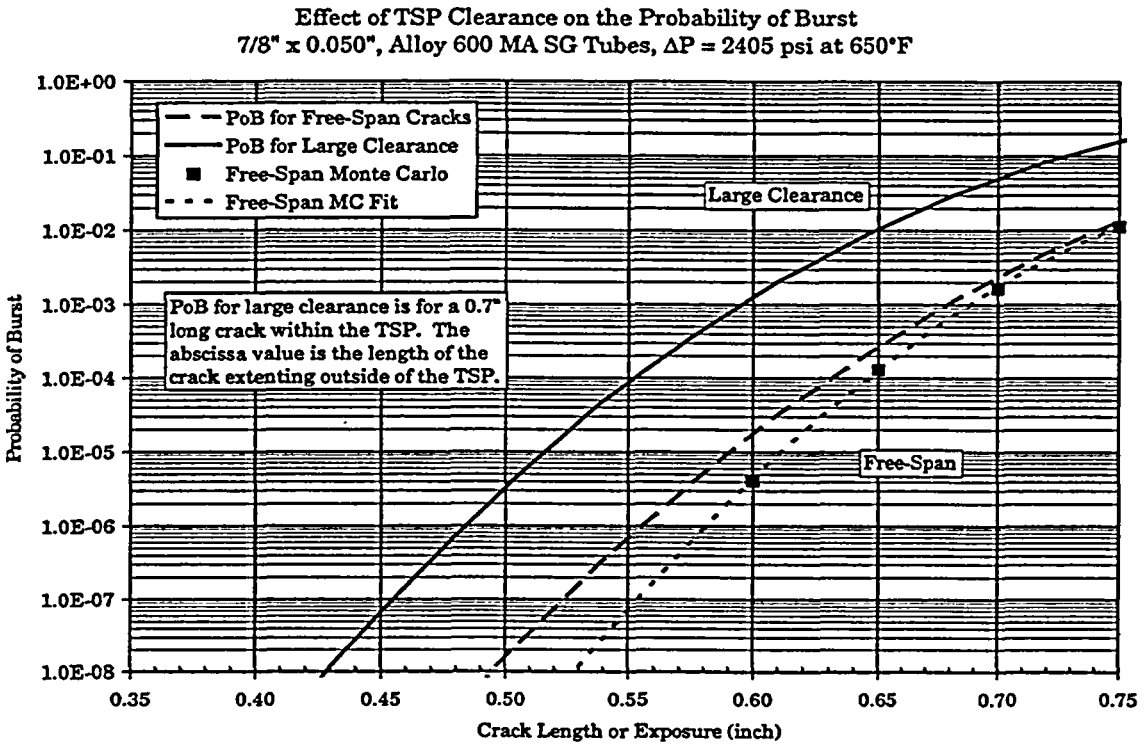

Figure 8-3: Probability of burst as a function of crack length

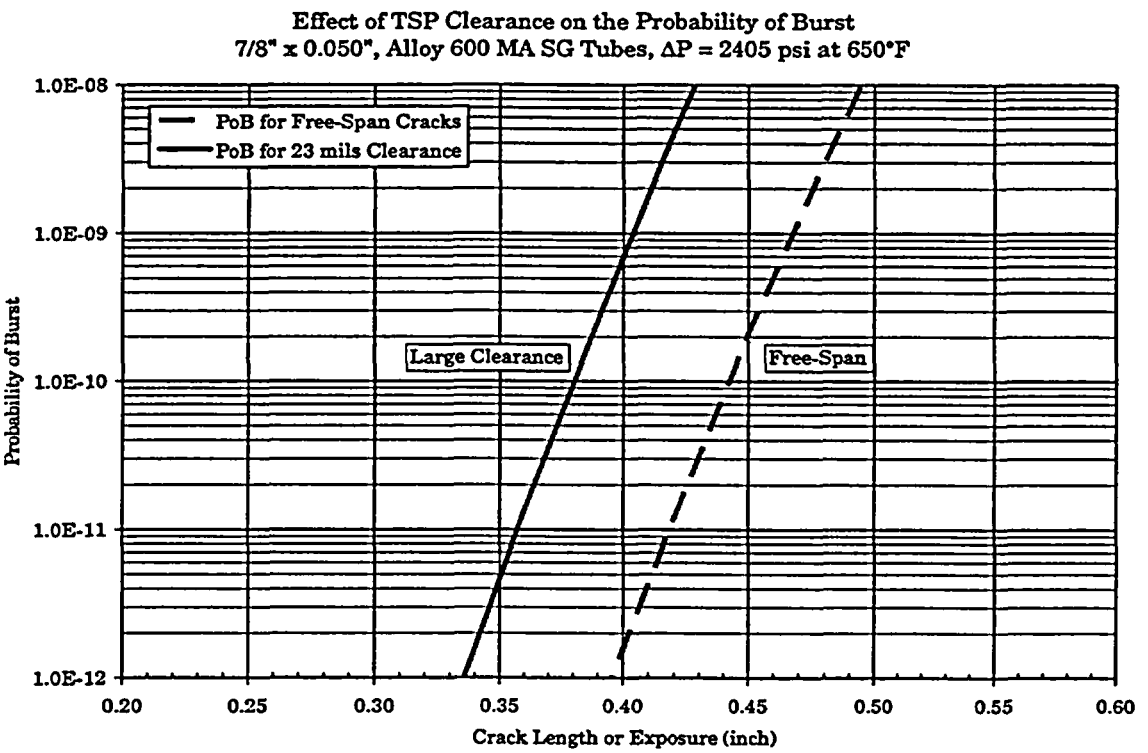

Figure 8-4: Probability of burst for relatively short cracks

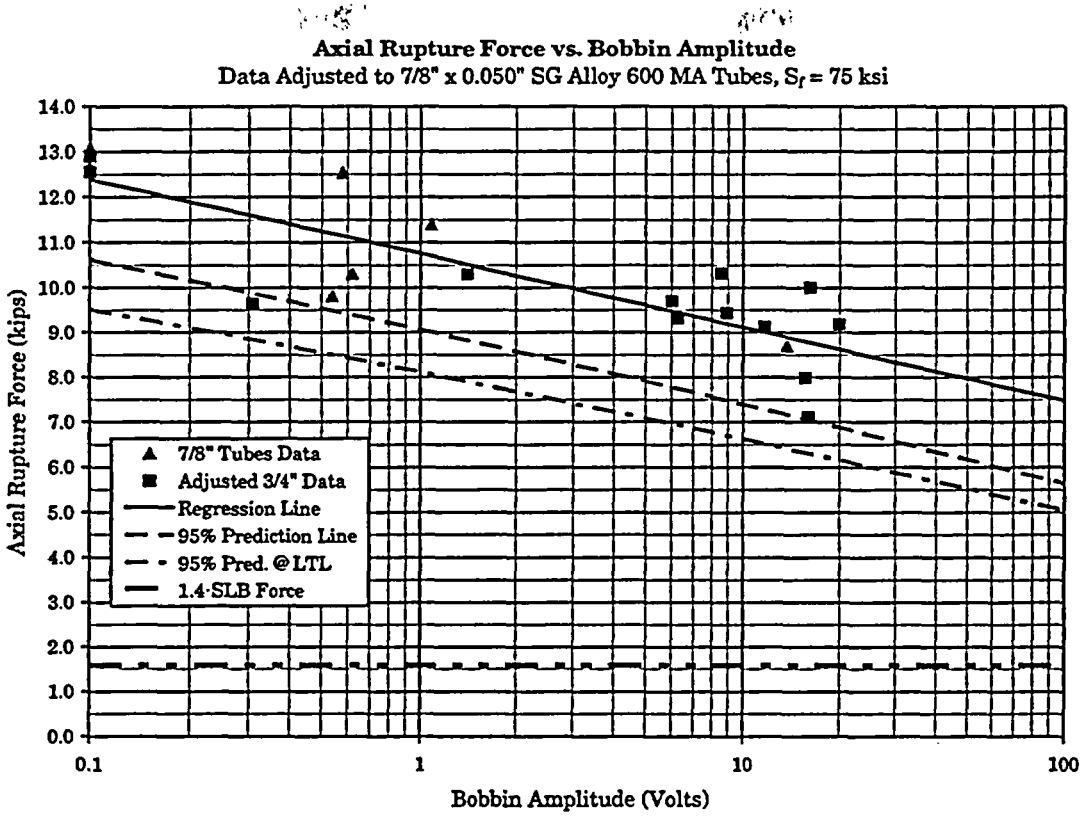

Figure 8-5: Axial Rupture Force Correlation

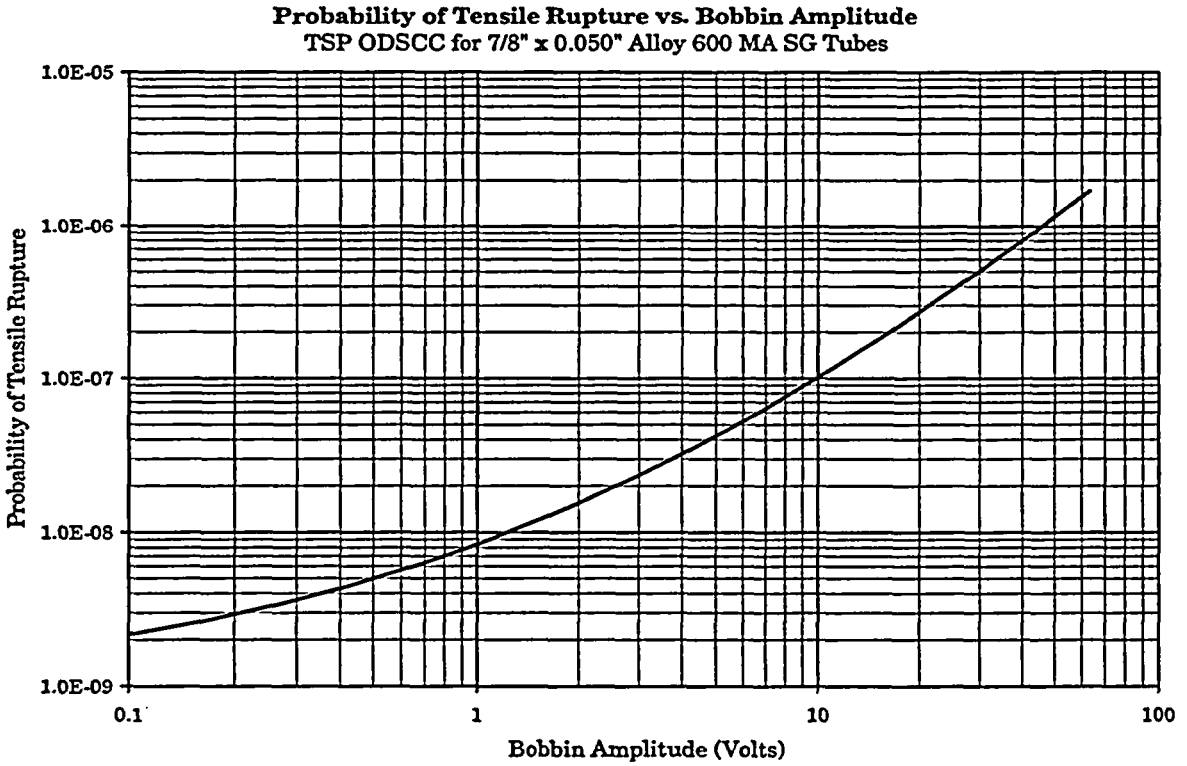

Figure 8-6: Axial Rupture Probability

9.0 STEAM GENERATOR INTERNALS INSPECTION PLAN

9.1 INTRODUCTION

The DCPP limited TSP displacement ARC relies on ODSCC indications remaining within the bounds of the tube support plates (TSPs) during a SLB event. Analyses have been performed to determine the loads placed on each TSP and the resulting displacements during such events. The analysis takes credit for specific steam generator internal components to provide a load path that limits TSP displacement.

To ensure that the load path components are not degraded to the level that they can no longer perform their intended function, DCPP has developed a steam generator internals inspection program that will be implemented prior to, or during, the outage in which the ARC will be implemented. This program contains specific inspection logic, scope, inspection method, and acceptance criteria.

The inspection logic includes 1) identifying the most significant load carrying components, 2) reviewing the industry experience, 3) establishing the most plausible degradation mechanism associated with these components, and 4) evaluating existing steam generator access openings and available inspection techniques to view these critical components.

9.2 STEAM GENERATOR INTERNALS INDUSTRY EXPERIENCE

Information Notice (IN) 96-09 and IN 96-09, Supplement 1 have been issued by the NRC to alert operating PWRs of various damage seen in the steam generator internals at foreign PWR facilities. Subsequently, the NRC issued GL 97-06 which requires licensees to document inspection plans, including scope frequency, methods and equipment for inspecting the SGs for the damage mechanisms discussed in IN 96-09 and GL 97-06.

The damage mechanisms reported, included, 1) wastage of the uppermost support plate caused by the misapplication of a chemical cleaning process, 2) broken tube support plate ligaments near both a radial seismic restraint and anti-rotation key at the upper most, and sometimes at the next lower tube support plate, and 3) wastage of tube support plate ligaments not associated with chemical cleaning. In addition to the tube support plate damage, wrapper drop and cracking of the wrapper above the original upper support have been observed at a foreign PWR facility. An evaluation of the probable causes of these foreign experiences is contained in EPRI Document GC-109558, Steam Generator Internals Degradation: Modes of Degradation Detected in EDF Units, which has been distributed to the NRC by NEI.

Steam generator internal inspections have been performed in preheater steam generators at three sites in support of limited TSP displacement ARCs. The inspections included extensive visual inspection of the top tube support plate in one steam generator at each site. Emphasis was placed on determining if degradation similar to that seen in the EDF units was present. No degradation was seen. Visual inspection was performed on eight (8) of the ten (10) tierod nuts in one of the four steam generators at two sites. The nuts were found to be tight against the top support plate with no degradation seen.

Eddy current inspection was performed on all four (4) steam generators, at each site, in the area of the anti-rotational devices at the top tube support plate for identification of cracked TSP ligaments. In

addition, eddy current inspection of the patch plate area in all four (4) steam generators, at each site, was performed. No degradation was noted.

Approximately five (5) wedges and eighty-nine (89) support bars were visual inspected at each site. No degradation was noted.

Verification that the wrapper had not shifted was performed for each steam generator at each site by assuring there were no obstructions when inserting the sludge lance equipment through the wrapper openings. No shift in the wrapper location was noted.

9.3 MODEL 51 STEAM GENERATOR INTERNAL SUPPORT STRUCTURE

The general layout of the DCPP steam generators is shown in Figure 9-1. The feedwater enters the SG through the inlet nozzle/feedring and down through the wrapper to shell downcomer to the top of the tubesheet. The SG tubes pass through the various carbon steel plates which are drilled to provide lateral support to the tubes and contain circulation holes through which water/steam passes through the tube bundle. The tube support plates are supported vertically using tierods/spacers and support bars welded to the wrapper and TSP. In-plane supports are provided by wedges located around the circumference of each plate. The wedges are welded to the wrapper and TSP. Their tapered design provides additional resistance to upward movement, in addition to in-plane support.

9.3.1 Tierod and Spacer Pipe Geometry

All of the plates are supported by a total of five tierods/spacers with one located at the center of the SG and four located on the periphery of the TSP near row 32. They are threaded into the tubesheet and extend continuously through the tube bundle assembly to the top tube support plate where a nut is attached. The nut is welded to the top surface of the top tube support plate. Around the outside of the tierods are spacer pipes that are located between each of the support plates. The length is equal to the span between the two plates separated by the pipe. This serves to keep the plates separated and to provide interior supports to the plates. For the central tierod, the spacers are welded to each of the TSPs, with the exception of the spacer between the tubesheet and first TSP, which is not welded to the tubesheet. For the spacers located at the periphery of the TSPs, there are no rigid links between the spacers and the support plates.

9.3.2 TSP Wedges and Support Bars

A schematic of the wedges and support bars are shown in Figure 9-2. The support bars are located below each plate and are welded to the wrapper and support plate.

Wedges are used between the tube support plates and the wrapper to help attain an integrated alignment of the tubes with the support plates and to provide in-plane support. Wedges are installed on the periphery of the plates as illustrated in Figure 9-2. The wedges are welded to both the wrapper and support plates.

9.4 DEGRADATION ASSESSMENT

The DCPP SG TSPs and structure load path are composed of carbon steel components. Corrosion fatigue and stress corrosion cracking (SCC) are the two plausible mechanisms that can cause active degradation of the welds in the carbon-steel load path components. Since active stresses and variations in stress are low in these components, corrosion fatigue (initiation and propagation) is unlikely. Environmental effects have been observed in corrosion fatigue tests of carbon and low alloy steels in high temperature water. However, high cycle stresses and/or oxygen levels are needed for these effects to be substantial. These conditions do not exist based on the DCPP operating conditions.

The temperature, environment and chemistry are essentially the same for all TSP support bars, hot leg and cold leg. Environment changes from the top to bottom of the steam generator are primarily increases in void fraction as a function of elevation in the steam generator while temperature is nearly constant at the secondary water saturation temperature. Denting at TSP intersections was arrested after the first cycle of operation, which limited the denting such that hourglass distortion of the TSPs has not been found in the DCPP SGs. Due to the limited denting and TSP distortion, denting is not expected to increase loads on the TSP wedges and support bars. Thus, all TSP wedges and support bars (above and below the TSP at the hot and cold legs) are equally susceptible to the same induced degradation. Similarly, manufacturing differences between wedges and bars are negligible.

Therefore, for the purpose of inspection, any carbon steel component identified in the TSP load path, represents an adequate sample for integrity verification. Any weld on any support bar, wedge, or tierod is a random weld and an acceptable sample for developing an inspection plan for determining the likelihood of a cracked weld. This permits the inspection sampling-plan to be based on the inspection of any TSP load support weld, either hot or cold leg, while applying the results of the inspection to the most critical hot leg welds.

9.5 DCPP STEAM GENERATOR INTERNALS INSPECTION RESULTS THROUGH 2003

Based on inspections performed to date at DCPP and in the domestic industry, no load path component degradation with the exception of TSP ligament cracking has been observed in Westinghouse fabricated steam generators with denting the same or less than that found at DCPP. DCPP has performed a variety of secondary side inspections of Unit 1 and Unit 2 steam generators during past refueling outages. No load path degradation was observed during any of these inspections although minor TSP cracking and loss of ligaments has been detected by eddy current. These inspections included routine refueling outage eddy current inspection of the carbon steel TSPs for ligament cracking and 1R8 visual inspection of Unit 1 plates, wedges, tierods/spacers, support bars and wrappers. The results of these inspections are summarized in Tables 9-1 and 9-2.

The eddy current inspections have identified several hundred TSP ligament indications, mostly in Unit 1. The majority of the indications are traceable to preservice inspection, indicating they are not service induced degradation. Some of the indications are associated with patch plate seam welds and others are associated with missing ligaments as verified by visual inspections conducted in 1R8. Westinghouse has concluded that the missing DCPP TSP ligaments observed during the 1R8 visual inspections are related to suspected TSP drilled hole manufacturing anomalies. The TSP manufacturing practices employed at

the time that the DCPP team generators were produced used a stacked drilling procedure. Several TSPs were clamped together and drilled simultaneously. A review of the ligament indication locations indicates distinct location patterns, indicative of manufacturing anomalies of the automatic drilling equipment. The 1R8 visual examination of some of these locations also confirmed that they did not appear to be service induced degradation. None of the ligament gap sizes have approached the 146 degree acceptance limit for tube plugging (the largest gap to date is about 120 degrees based on Plus Point). No tube wear at intersections with TSP ligament indications has been detected.

9.6 DCPP STEAM GENERATOR INTERNALS INSPECTION PLAN BEYOND 2003

To further assure the integrity of the load path components in the DCPP steam generators, additional inspections through available access openings will be performed in upcoming refueling outages. The purpose of the inspections is to provide adequate confidence that the required structural load path to support a limited TSP displacement ARC for the SGs is not degraded. The tube support plates transmit the load to the surrounding support structures. The integrity of this load path can be verified, although degradation of the base materials and welds due to SCC, corrosion, erosion or fatigue is not considered likely. Visual inspection will emphasize the lower TSP regions where most ODSCC indications have occurred. The structural integrity of the uppermost plate relative to critical load carrying features will be determined. The extent of these inspections will be based on existing accessibility, risk of "sticking" visual probes, radiation exposure and outage schedule.

Existing shell openings in the DCPP steam generators are located below the first tube support plate and in the steam drum. Two secondary side openings exist for direct access to the tube bundle in each steam generator, with both located below the first tube support plate. The two remaining openings are the secondary side manways located in the upper steam drum. The only access to the bundle from the manways is through the primary separator swirl vanes. The geometry of the Model 51 steam generator along with tooling limitations constrain the extent of hot leg in-bundle or periphery inspections that can be performed. Table 9-3 identifies the location of the available inspection openings.

Continued eddy current inspections of TSPs will be performed in a manner consistent with prior inspections. The plan is to perform a 20% +Point inspection of existing baseline indications and 100% +Point inspection of all new bobbin suspect ligament crack (SLC) indications. The term existing baseline indications includes all prior +Point confirmed TSP ligament crack indications (LIC) and ligament gap indications (LIG). Marginal calls not confirmed in later +Point inspections may be excluded from the baseline indications. If an active degradation is detected by the 20% sample inspection, +Point shall be expanded to a 100% baseline inspection. Active degradation is defined as service-induced TSP ligament erosion-corrosion and/or cracking.

A visual inspection of the wrapper and tierods / spacers will be performed in each steam generator during the outage TSP locking is implemented in both Units 1 and 2 and in every following outage (until replacement of the SGs) as shown in Table 9-4. In addition, sample visual inspections will be performed of the wedges, support bars, TSPs, tierod nuts and their associated welds in one steam generator as identified in Table 9-5 during the twelfth Unit 1 refueling outage. These inspections, along with results from previous inspections (Tables 9-1 and 9-2) are adequate to verify the structural integrity of the load path components.

Table 9-1
DCPP Unit 1 SG Internals Inspection Results

Load Path Component	Inspection Date - Extent & Method	Results
Tube Support Plates	1R8 – Visual inspection of 10 TSP Legs (6 HL/4CL) in SG 1-1 and SG 1-2	59 SLC indications inspected. Observations of 18 misdrilled TSP holes resulting in missing TSP ligaments. Excellent correlation with Plus Point prediction of missing ligament. No signs of service-induced TSP ligament erosion-corrosion or cracking were found during the visual inspections.
	1R8 – 100% Bobbin coil inspection for SLC indication, 100% Plus Point inspection of bobbin SLC indications.	225 indications confirmed by Plus Point, 116 of which had a ligament gap.
	1R9 – 100% bobbin coil inspection for SLC, 100% Plus Point inspection of new bobbin indications, 20% Plus Point inspection of baseline indications in each SG.	14 new indications confirmed by Plus Point, 3 of which had a ligament gap.
	1R9 – Visual inspection of SG 1-1 from third flowslot at 6 TSPs	No degradation detected.
	1R10 – 100% bobbin coil inspection for SLC, 100% Plus Point inspection of new bobbin indications, 100% Plus Point inspection of baseline indications in SGs 1-1 and 1-3.	1 new indication confirmed by Plus Point
	1R10 – Visual inspection of SG 1-3 at three TSP elevations at lane between column 49 and 22.	No degradation detected.
	1R11 – 100% bobbin coil inspection for SLC, 100% Plus Point inspection of new bobbin indications, 100% Plus Point inspection of baseline indications in SGS 1-1 and 1-4.	5 new indications confirmed by Plus Point, 1 of which had a ligament gap.
Wrapper	1R8 – Visual of SG1-1 at TSP 7H as well as wrapper seam welds	No degradation detected Based on 1R8 visual exams and based on no interference while inserting sludge lance equipment during every refueling outage.
Wedges	1R8 – Inspected a sample of wedges and welds at 6 HL and 4 CL TSPs in SGs 1-1 and 1-2	No degradation detected.

Table 9-2
DCPP Unit 2 SG Internals Inspection Results

Load Path Component	Inspection Date - Extent - Method	Results
Tube Support Plates	2R6 – Visual exam in SG 2-2 for Upper Support Plate, Annulus, and In-Bundle Inspections.	No degradation detected.
	2R8 – 100% bobbin coil inspection for SLC, 100% Plus Point inspection of bobbin SLC indications, 100% Plus Point inspection of bobbin indications identified during screening of 2R6 bobbin data.	45 indications confirmed by Plus Point, 1 of which had a ligament gap. 1R8 data bound 2R8 data, so no visual inspection done.
	2R9 – Visual exam of SG 2-1 at three TSP elevations during Upper Bundle In-Bundle Inspections.	No degradation detected.
	2R9 – 100% bobbin coil inspection for SLC, 100% Plus Point inspection of new bobbin SLC indications, 20% Plus Point inspection of baseline indications in SGs 2-1 and 2-2.	3 new indications confirmed by Plus Point.
	2R10 – 100% bobbin coil inspection for SLC, 100% Plus Point inspection of new bobbin indications, 20% Plus Point inspection of baseline indications in SGs 2-3 and 2-4.	2 new indications confirmed by Plus Point, of which 1 had a ligament gap.
	2R11 –100% bobbin coil inspection for SLC, 100% Plus Point inspection of new bobbin SLC indications, 20% Plus Point inspection of baseline indications.	19 new indications confirmed by Plus Point, of which 1 had a ligament gap (majority of new indications located at 7th TSP and detected as part of 100% U-bend Plus Point inspection).
Wrapper	None	No degradation detected based on no interference while inserting sludge lance equipment during every refueling outage.
Wedges	None	None

Table 9-3
DCPP Steam Generator Inspection Port Description

Size	Description	Location From Main Support Pads	Bolting
6.00 Dia	Secondary Handhole	82" above MSP	8 BOLTS 1.00" x 3.25" – 8-UN-2A
6.00 Dia	Secondary Handhole	82" above MSP	8 BOLTS 1.00" x 3.25" – 8-UN-2A
16.00 Dia	Secondary Manway	672" above MSP	20 BOLTS 1.25" x 5.00" – 8-UN-2A
16.00 Dia	Secondary Manway	672" above MSP	20 BOLTS 1.25" x 5.00" – 8-UN-2A

Table 9-4
Inspections to be Performed in All Steam Generators

Load Path Component	Inspection Method	Planned Inspection	Acceptance Criteria	Inspection Access
Tierods and Spacers	Visual	TTS	Not severed	Through sludge lance ports (secondary handhole)
TSPs	Eddy Current	20% Baseline Indications and new indications with Plus Point and 100% Bobbin	146 degrees ligament gap	Low frequency bobbin - auto analysis - plus point characterization
Wrapper	Visual	Lower shell and wrapper	Insert sludge lance equipment.	Through secondary handhole.

Table 9-5
Visual Inspections to be Performed in One Steam Generator

Load Path Component	Inspection Method	Planned Inspection	Acceptance Criteria	Inspection Access
Tierods and Spacers	Visual	Sample of tierods and spacers at three TSPs	Spacers not degraded. No distortion and in proper alignment.	Secondary Handhole
TSPs	Visual	Sample portion of three TSPs	No service-induced degradation detected.	Secondary Handhole
Wedges	Visual	Sample of wedges at three TSPs	Wedge present – weld not cracked	Secondary Handhole
TSP Support Bars	Visual	Sample of TSP support bars and welds at three TSPs	Support bar present – weld not cracked	Secondary Handhole
Tie Rod Nuts	Visual	Sample of tierod nuts on top of TSP 7	Nut tight against top TSP – weld not cracked	Secondary Manway

a,c

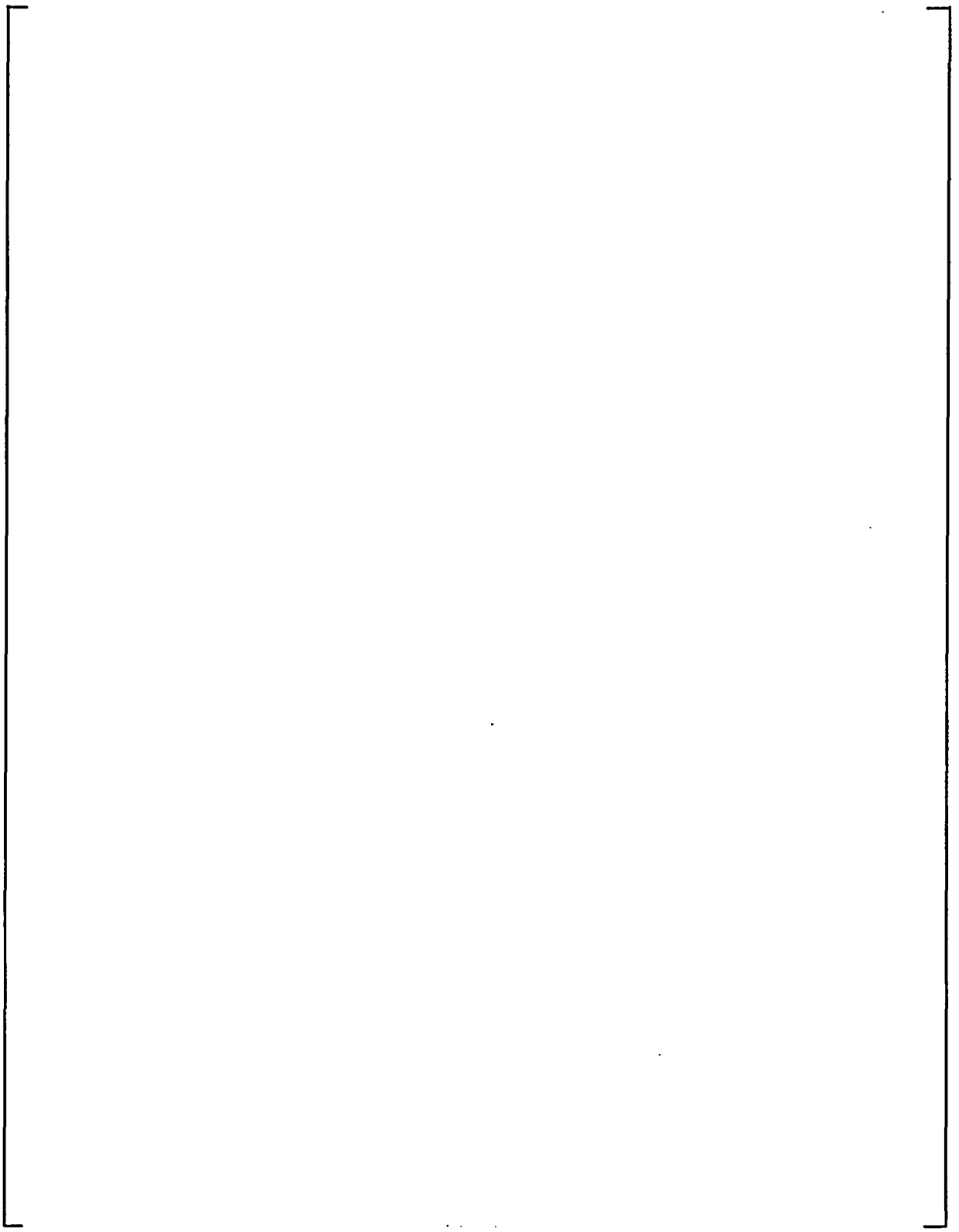

Figure 9-1
Model 51 Steam Generator Layout

a,c

Figure 9-2
Model 51 TSP Wedge and Support Bar Configurations

10.0 LOCKED TSP ALTERNATE REPAIR CRITERIA FOR DIABLO CANYON UNITS 1 AND 2

This section integrates the results of the prior sections of this report to develop the alternate repair criteria at hot leg TSP intersections with displacements less than 0.15", specifically TSPs 1-4. The general approach, design requirements, performance summary and recommended alternate repair criteria are provided in this section for the Diablo Canyon (DCPP) Units 1 and 2 SGs. Tube repair limits for the hot leg TSPs 5-7 and all cold leg TSP intersections are based on NRC Generic Letter 95-05 (Reference 1) and the current DCPP SG 2 volt ARC.

Mechanical locking of the TSPs by performing tube expansion at selected hot leg TSP intersections will be performed to ensure a locking mechanism is provided for the TSPs even though it has been shown in Reference 4 that the DCPP dented and packed tube to TSP crevices lead to tube to TSP contact forces sufficient to prevent significant TSP displacements in a SLB event. In fact, the DCPP crevice conditions would be able to prevent TSP displacement even if less than one percent of the TSPs (same percentage as will be expanded) have the expected contact forces. Reference 4 also shows that leakage would be negligible with the dented and packed crevices due to constraints on opening of the cracks with no tube to TSP gap. Despite the presence of the packed TSP condition at DCPP, the mechanical locking for TSPs 1-4 is provided under the very conservative assumptions of 100% open crevices to define the tube expansion requirements and that the crevices are open near the upper end of the original SG design clearances for leakage analyses.

In Section 2.5 of the safety evaluation (Reference 2) for the South Texas-2 locked TSP ARC, the NRC identified six items that should be addressed before approval of the ARC for more than one cycle of operation. The six items and the sections of this report that address the items are:

Item		Section
a)	The long term integrity and inspection of the SG internals, including the TSPs	10.5.2
b)	The long term integrity and inspection plans of the expanded tubes	10.5.3
c)	Combining the conditional probability of axial burst and axial tensile failures	10.6.1
d)	The long term acceptability of the IRB leakage estimates	10.2.2
e)	The effects on burst pressure of multiple indications extending outside the TSP	10.2.1
f)	The methodology for combining the leakage estimates from the free span model and locked TSP model	10.6.2

Sections 10.1 to 10.3 describe the general approach, allowable TSP displacements and functional requirements for the ARC. Sections 10.3 to 10.6 develop the tube repair limits, the inspection requirements and the SLB analysis requirements. A summary of the tube repair criteria is given in Section 10.7.

10.1 GENERAL APPROACH TO TUBE REPAIR CRITERIA

The approach applied to developing the tube repair criteria is based on a) developing minimum requirements and, b) demonstrating by analysis that the SG response to the limiting loading conditions conservatively meets the minimum requirements. The general approach can be described as follows:

- Ensure that TSP displacements are less than or equal to 0.15 inches to reduce the tube burst probability to negligible levels
  - The tube burst probability at 0.15 inch TSP displacement is negligible compared to the NRC GL 95-05 reporting guideline of 10^{-2} even with the bounding assumption that all hot leg TSPs 1-4 intersections have exposed throughwall indications equal to the limiting TSP displacement which results from a postulated SLB event.
  - An incremental cumulative tube burst probability requirement of 10^{-5} is a negligible change to the total tube burst probability.
  - A TSP displacement of 0.40 inch (Table 10-1) is acceptable to obtain a tube burst probability of 10^{-5}, conservatively assuming that all TSPs 1-4 intersections are equally displaced by this distance during a postulated SLB event.
- Conservatively apply a factor of 1.5 margin on the RELAP5 TSP hydraulic loads
  - A factor of 1.5 applied to the RELAP5 loads envelopes collective uncertainties in RELAP5 analyses (Section 4).
- Ensure that the TSP displacements are less than, or equal to, the limiting displacement for utilizing the existing leak rate test results for indications restricted from burst (IRBs) as discussed in Section 7
  - A TSP displacement of 0.21 inch is acceptable for application of IRB leak test results.
  - For DCPP, this displacement guideline is more limiting than the acceptable displacement to meet incremental burst probability objectives, and is the requirement that limits application of the ARC to TSPs 1-4.
- Demonstrate, by structural TSP displacement analyses, that the TSPs 1-4 displacements due to a postulated SLB event are less than the 0.40 inch limit for a negligible burst probability and the more limiting 0.21 inch acceptance limit for application of the IRB leak rate data
  - Conservatively limit TSPs 1-4 displacement to a design goal of ≤ 0.15 inch by expanding selected tubes at the TSPs to "lock" the tubes to the TSPs. The design goal of ≤ 0.15 inch displacements provides margin against the 0.21 inch IRB acceptance limit for the low likelihood of a failure at a TSP expansion.

- It is shown in Section 6 that the goal of ≤ 0.15 inch TSP displacement is satisfied by TSPs 1-4 during a postulated SLB event initiated from hot standby conditions (i.e., the limiting transient).

10.2 ALLOWABLE TSP DISPLACEMENTS

10.2.1 Allowable TSP Displacements for Acceptable Tube Burst Probability

In Section 8.3, it is shown that the burst pressure of a throughwall indication extending outside the TSP is approximately equal to the burst pressure for a free span crack equal to the length of the crack extending outside the TSP. Thus, the length of crack remaining within the TSP does not meaningfully affect the burst pressure. Similarly, the burst probability for limited TSP displacements with postulated throughwall cracks can be calculated as that associated with a crack length equal to the TSP displacement. This assumes that the throughwall part of a crack is located at the edge of the TSP rather than, as more commonly found from pulled tubes, near the center of the TSP. Alternately, it can be postulated that there is a throughwall crack equal to the TSP thickness and the SLB burst probability for this indication is the same as the crack length exposed by the TSP displacement during the postulated SLB event.

The most conservative possible approach to define requirements for TSP displacement is to assume that all intersections at hot leg TSPs 1-4 have throughwall crack lengths at least equal to the TSP displacements, and that these throughwall crack lengths are located at the edge of the TSP. This assumption is applied to develop the allowable limits on TSP displacements so that the design is generic and envelopes any possible tube degradation, thus eliminating the need for tube burst probability calculations for indications at hot leg TSP intersections. Even under the above bounding assumption on postulated tube degradation, it is desirable that the associated tube burst probability be very small compared to acceptable levels. For the multiple ARCs applied for the DCPP SGs, the hot leg indications at TSPs will have a negligible contribution to the tube burst probability. The most conservative guideline for an acceptable burst probability is the 10^{-2} reporting threshold given in NRC GL 95-05. If the burst probability for the limited displacement case is assumed to be $<10^{-5}$, the TSP indications would contribute < 0.1% to the reporting level established by GL 95-05. This 10^{-5} value is the design requirement for the burst probability with limited displacement based on sensitivity analyses given below.

By applying the tube burst probability as a function of throughwall crack length, as developed in Section 8.5, and the bounding assumption of throughwall cracks at hot leg TSPs 1-4 intersections, tube burst probabilities can be developed as a function of TSP displacements. The tube burst probabilities are developed in Table 10-1 for the postulated 13,552 indications for the 4 hot leg TSPs with 3388 tube intersections at each plate. Burst probabilities are given in Table 10-1 for the conservative assumption of uniform TSP displacements at all tube intersections. The burst probabilities are approximately equal to the number of TSP intersections times the single tube burst probability for a throughwall crack equal to the displacement.

Since multiple combinations of non-uniform TSP displacements are difficult to include in a generic assessment, an assumption of uniform TSP displacement during a postulated SLB event is applied to develop a limiting displacement requirement. Although the analysis of Section 6 shows that uniform

TSP displacements are not realistic due to the varying locations of TSP supports, this assumption leads to a minimum allowable TSP displacement. For burst probabilities of 10^{-3}, 10^{-4} and 10^{-5}, the acceptable SLB TSP displacements are 0.45, 0.42 and 0.40 inch, respectively. For the design requirement of a 10^{-5} contribution to the burst probability from the TSPs 1-4 displacements, the acceptable SLB TSP displacement is 0.40 inch.

South Texas NRC SER Item (e) Relating to Effects on Burst of Multiple Indications

The safety evaluation (Reference 2) for the South Texas-2 locked TSP ARC reflects a concern (item e of Section 10.0) regarding the potential effects on the burst pressure of multiple indications extending outside the TSP in a SLB event. The concern is that many closely spaced axial cracks may result in a reduction in the tube burst pressure. The ARC database includes burst pressures for closely spaced axial indications with no apparent reduction in the burst pressure of the limiting indication. Whatever effects closely spaced indications may have on the burst pressure is included in the ARC burst pressure correlation. For example, DCCP-2 pulled tube R35C57 had a secondary 100% throughwall crack (throughwall length not determined), 0.55 inch long only 10° from the burst crack which was also throughwall for 0.217 inch and 0.519 inch long. The measured burst pressure of 5,961 psi is slightly higher than that calculated (5,500 psi) from the destructive exam profile of the burst indication and is consistent with the ARC burst pressure correlation. Many burst tests have been performed for closely spaced cracks including EDM notch simulations to demonstrate that the limiting indication bursts as an isolated crack with negligible reduction in burst pressure. In addition, for the limited locked TSP displacement of 0.15 inch, the burst margins for an exposed, assumed throughwall crack are so large (7490 psi nominal burst pressure) that any effects of closely spaced indications would still leave large margins against burst at $3\Delta P_{NO}$.

10.2.2 Allowable TSP Displacement for SLB Leakage Considerations

Although an indication inside the TSP cannot burst, the flanks of a crack that could burst at SLB conditions can open up within the confines of the TSP, a condition for which a bounding leak rate was developed based on the assumption that the TSP would displace during a postulated SLB event. This condition has been labeled as an indication restricted from burst, or an IRB. Conceptually, the IRB leak rate can vary with TSP displacement that exposes part of the throughwall crack. A leak test program was performed to determine a leak rate that would conservatively envelop the leak rate from an IRB. This test program and results are described in Section 7.

For DCPP, the applicable SLB pressure differential is 2405 psi, based on the PORVs for pressure relief. At this pressure differential, the bounding IRB leak rate is 5.0 gpm (Section 7). The IRB leak rate, as compared to the much larger leak rate from a freespan burst, is dependent upon the ID of the TSP hole limiting the crack opening at or near the center of the crack. The assumption of open tube to TSP crevices for the crack opening constraint applied to develop the IRB leak rate leads to a limit on TSP displacement. It is shown in Section 7 that a maximum TSP displacement of 0.21 inch is acceptable for utilizing the bounding IRB leak rate of 5.0 gpm. For conservatism, the design goal for maximum TSP displacement is set at 0.15 inch to provide a conservative margin on the IRB leak rate application. Thus, the goal displacement, 0.15 inch, is conservative relative to both the acceptable displacement 0.21 inch for applicability of the IRB leak rate, and the acceptable displacement, 0.40 inch, for the limiting tube burst probability of 10^{-5}.

South Texas NRC SER Item (d) Relating to Long Term Acceptability of the IRB Leakage Estimates

The safety evaluation (Reference 2) for the South Texas-2 locked TSP ARC reflects a concern (item d of Section 10.0) regarding the long term acceptability of the IRB leakage estimates. The NRC staff's concerns were: 1) the potential for multiple throughwall cracks to develop near the edges of the TSPs over the long term; 2) the staff's continuing review of the leakage adjustment procedure to MSLB conditions; 3) apparent anomalies in some of the laboratory data supporting the 5.0 gpm leak rate estimate; and 4) a review of industry data on this matter.

The concern relative to multiple throughwall cracks near the TSP edges is addressed first in this assessment. The IRB leak rate applies to indications that might burst at SLB conditions within an open tube to TSP crevice. Only the limiting indication would burst such as to leak at the IRB leak rate. Any remaining throughwall indications would not burst and would leak at rates typical of the ARC SLB leak rate database, which are generally negligible compared to the 5.0 gpm bounding IRB leak rate. In addition, the potential for multiple throughwall indications being exposed by the 0.15" TSP displacement is very small as the throughwall lengths are generally located near the center of the TSP. Of 20 throughwall indications on pulled tubes with 1 to 21 volt indications for which sufficient data are available to obtain the location of the edge of the throughwall length relative to the edge of the TSP, only 1 throughwall length was within 0.15 inch of the edge of the TSP and 15 were > 0.2 inch from the edge of the TSP. DCPP-2 pulled tubes R44C45 (21.5 volt indication) and R35C57 (5.09 volt indication) had throughwall lengths of 0.374 and 0.217 inch, respectively, with the throughwall lengths approximately centered at the middle of the TSP. The throughwall lengths for both indications were more than 0.15 inch from the edge of the TSP and would not have been exposed in a SLB event. Consequently, the potential for multiple throughwall cracks to develop near the edges of the TSP is very small and, even if they would occur, only the limiting indication would burst at the IRB leak rate with relatively small free span leak rates from the other indications. The acceptability of the IRB leak rate would not be impacted under the assumption of multiple throughwall indications.

Leakage adjustments to SLB conditions are applied for the IRB leak rate data in Section 7 only to perform modest adjustments of the hot test data to reference temperature and primary/secondary pressure (15 psig secondary side pressure) conditions at the test pressure differential. All IRB leak tests contributing to defining the bounding IRB leak rate were performed at elevated temperatures including near SLB conditions. No cold to hot leak rate adjustments affect the IRB leak rate evaluation. The overall test program included some cold tests to validate the adjustment procedure for cold to reference SLB adjustments. The hot test results were in good agreement with the adjusted cold test results to support applicability of the leak rate adjustment procedure for other applications. The validity of the larger cold to hot adjustments supports the adequacy of the modest adjustments applied to hot test results used to obtain IRB leak rates. It is concluded that uncertainties on the bounding IRB leak rate due to the adjustment procedure are negligible for this application based on all applied tests performed at hot conditions and the leak rate adjustment adequacy demonstrated for the larger cold to hot adjustments.

It is not clear as to what "apparent anomalies in some of the laboratory data supporting the 5.0 gpm leak rate estimate" are referred to in the SER. Section 7 describes the bases for excluding the only three tests with leak rates exceeding the bounding IRB value of 5 gpm at 2405 psi. These included a test sensitivity performed for a non-prototypic laser cut specimen, a test with a throughwall crack longer than the support plate thickness, and a second high bladder pressurization test that non-prototypically opened a

secondary crack in the specimen. Except for the excluded tests, the bounding 5.0 gpm value is the largest found in any test at 2405 psi conditions. Variability of test results should be expected for this type of test due to the wide range of total and throughwall crack lengths included in the program. As discussed in Section 7, the bounding IRB value is primarily based on test results for cracks with initial throughwall lengths of 0.694 and 0.717 inch based on post-test fractography measurements (from Reference 5, slightly different than in-process measured 0.630 and 0.740 inch reported in Section 7). These throughwall lengths exceed any ARC pulled tube to date and any expected at DCPP following implementation of the increased voltage ARC. Selection of the largest leak rate from all prototypic tests can be expected to bound the test variability that might be interpreted as anomalies.

Item 4) of the SER concern is related to "a review of industry data on this matter". The extensive test program undertaken through EPRI to develop the IRB leak rate data are the only known tests for this type of leakage phenomena. Therefore, no response can be provided for this NRC concern.

It should be noted that the planned application of the IRB leak rate data to the DCPP SG conditions is unrealistically conservative. The tests were performed for maximum tube to TSP diametral clearances of 25 mils. The dented and packed crevices at DCPP would prevent any significant crack opening and prevent leak rates approaching the IRB numbers. However, the IRB leak rate of 5.0 gpm will be retained to eliminate the need for development of a more appropriate, smaller leak rate.

10.3 OVERALL TSP LIMITED DISPLACEMENT ARC FUNCTIONAL REQUIREMENTS

The general approach described above has led to the overall functional requirements given in Table 10-2. The bases for each requirement are also given in the tables. The tube burst probability analyses supporting the 0.40 inch TSP displacement requirement are given above in Section 10.2.1. The TSP displacement limit for application of the IRB leak rate test results is 0.21 inch (Section 10.2.2). While limiting TSP displacements to 0.40 inch is adequate to achieve a negligible tube burst probability of 10^{-5} and a 0.21 limit is acceptable for application of the IRB leak rate results, the design goal is to obtain a maximum TSP displacement of 0.15 inch.

The TSP displacement analyses in Section 5 define the tube expansion requirements to limit the maximum TSP displacement to $\leq$ 0.15 inch at all hot leg tube locations on TSPs 1-4. The tube expansion requirements are defined in Table 5-20. Overall, it is concluded that acceptable TSP displacements under limiting postulated SLB loading are achieved for TSPs 1-4 to effectively reduce tube burst probabilities to negligible levels and to apply the bounding IRB leak rate even when conservative (factor of 1.5 on RELAP5 loads) loads are applied.

10.4 TUBE REPAIR LIMITS FOR DCPP UNITS 1 AND 2

Tube repair limits are required for ODSCC indications at the hot leg TSPs and at the cold leg TSPs. At DCPP, indications at hot leg TSPs 5-7 and at cold leg TSP intersections have been small and have not challenged burst and leakage requirements. Therefore, for the hot leg TSPs 5-7 and the cold leg TSPs, it is adequate and conservative to apply the GL 95-05 ARC for ODSCC at TSPs, which are based on the assumption of free span indications at SLB conditions. The GL 95-05 criteria are the recommended repair criteria for ODSCC indications at these TSP intersections. The repair limit for these indications is

2.0 volt for RPC confirmed indications. GL 95-05 requires the upper voltage repair limit applied to RPC NDD indications to be updated on an outage-by-outage basis to the latest database, correlations and growth information. Bobbin indications >2.0 volt and below the upper voltage repair limit that are not confirmed by RPC inspection may be left in service.

Since the small maximum displacement at TSPs 1-4 during a postulated SLB event reduces the tube burst probability to negligible levels ($< 10^{-5}$), independent of the degree of ODSCC at these hot leg TSP intersections (the intersections are assumed to have throughwall indications), tube repair limits for axial tube burst are not required. Tube repair at TSPs 1-4 is primarily required only as necessary to maintain SLB leakage within acceptable limits. The structural limit for the hot leg TSP intersections and the full ARC repair limit for limited displacement of the TSPs is addressed below. Allowable SLB leakage limits developed in other reports for DCPP are not affected by the locked TSP ARC so additional limits are not developed in this report. As developed in Section 8.6, a structural limit for axial tensile tearing of cellular and IGA indications applies at very high voltages with limited TSP displacements. This structural limit appears to be in excess of 100 volts. Even if a factor of two reduction is applied for growth and NDE allowances (factor of about 1.5 to 1.75 is typical), the full ARC repair limit would be about 50 volts. For conservatism in defining the ARC repair limit for limited TSP displacement, a tube repair limit of > 4.0 volts is conservatively applied for hot leg TSP indications at the DCPP SGs. Bobbin indications > 4.0 volts are repaired independent of RPC (or equivalent probe) confirmation. The increase of 2 volts from 2.0 to 4.0 volts for the locked TSP ARC is consistent with the 2 volt increase (1.0 to 3.0 volts) applied to NRC approved locked TSP ARCs for plants with ¾ inch diameter tubing.

The technical data of this report support a high degree of conservatism in the 4.0 volt repair limit for ODSCC at hot leg TSPs 1-4 intersections.

10.5 INSPECTION REQUIREMENTS

10.5.1 Active Tube Inspection Requirements

The GL 95-05 requirements applied for the 2.0 volt ARC eddy current inspections also apply for implementation of the limited displacement ARC. However, the inspection threshold for RPC confirmation of bobbin indications is adjusted for the increased repair limits. RPC inspection of bobbin indications greater than the 4.0 volt repair limit with a sample inspection of a minimum of 100 intersections summed over all SGs below the 4.0 volt repair limit will be applied at hot leg TSPs 1-4 intersections. The GL 95-05 2.0 volt RPC inspection threshold is applied for the 2.0 volt repair limit at hot leg TSPs 5-7 intersections and at cold leg TSP intersections.

If one or more ODSCC indications at TSP intersections are found in the NDE inspection to extend beyond the edge of the TSP, the indications shall be evaluated for significance to safety and risk and the results reported to the NRC prior to restart.

The inspection of active tubes adjacent to expanded tubes shall include a bobbin coil examination for cracked TSP ligaments at expanded tube TSP intersections. If a cracked ligament indication is found and confirmed by +Point inspection as a cracked or missing ligament section, the potential implications on TSP displacements shall be assessed and documented in the ODSCC 90 day report. It is expected that a few cracked ligaments are acceptable due to margins provided by the dented and packed crevice

conditions. However, a significant increase in ligament cracking, such as more than two expanded tubes with TSP crack indications at the same TSP elevation, shall be evaluated for implications on TSP displacement and this evaluation reported to the NRC prior to restart.

10.5.2 SG Internals Inspection Considerations

SG internals inspections completed to date at the DCPP SGs are described in Section 9.5. These inspections included visual examinations for wrapper mispositioning in both units, a sample inspection of wedges and their welds in Unit 1, visual inspections of TSPs in two SGs of Unit 1, a visual inspection of wrapper seam welds in Unit 1 and extensive eddy current inspections for TSP cracking in both units. No degradation was detected in these inspections for the wrapper and wedges/welds. Indications of TSP cracking and missing ligaments have been detected as summarized in Tables 9-1 and 9-2. The visual inspection confirmed the adequacy of the +Point predictions of missing ligaments, which were largely due to misdrilled TSP holes.

The planned internals inspections at the outage implementing the locked TSP ARC are described in Section 9.6. A visual inspection of the wrapper, lower TSPs and lower tierod/spacer pipes will be performed in each steam generator during FOSAR inspections. Inspections for wrapper drop are performed as part of sludge lance equipment insertion in the secondary handhole. In addition, sample visual inspections will be performed of the wedges, support bars, TSPs, tierod nuts and their associated welds in one steam generator. These inspections along with results from previous inspections are adequate to verify the structural integrity of the load path components.

The minimum eddy current inspection of TSP ligaments at each scheduled outage includes 100% bobbin coil with +Point confirmation for new bobbin calls and a 20% +Point inspection of TSP ligament indications previously confirmed by +Point inspections. Tubes with identified missing TSP ligaments exceeding 146° based on +Point measurements are repaired. Additional requirements for inspections of tubes and TSPs to be expanded are given in Section 10.5.3.

As discussed in Section 9.2, visual inspections of SG internals have been performed at three plants implementing the locked TSP ARC. No degradation of load carrying components has been found in these inspections. In addition, no occurrences of wrapper drop have been found in domestic SGs. Assuming that the DCPP SG inspection of load carrying components finds no degradation at plate supports/welds and tierods, no subsequent inspections of these components is required. Eddy current inspections of TSP ligaments will be performed each outage as described above with supplemental requirements identified above in Section 10.5.1.

South Texas NRC SER Item (a) Relating to Integrity and Inspection of SG Internals

The safety evaluation (Reference 2) for the South Texas-2 locked TSP ARC reflects a concern (item a of Section 10.0) regarding the long term integrity of SG internal structural components and TSPs. As noted above, no degradation has been found in multiple inspections of the SG structural components, excluding TSP ligaments, and further inspections of these components should not be necessary assuming no degradation is found in the above noted DCPP inspection. Indications of TSP ligament cracking and missing ligaments have been found in the DCPP SGs and eddy current inspections for TSP ligament degradation will be performed each outage as described above.

10.5.3 Expanded Tube Inspection Considerations

Tubes selected for expansion will be inspected prior to performing the expansions. The selected tubes must have no circumferential indications in the WEXTEX expansion transition or W* length by +Point inspection. Any dented TSP intersections requiring expansion must be +Point inspected to confirm the absence of circumferential indications. TSP intersections with greater than five volt dents should not be selected for expansion to minimize the potential for future circumferential crack initiation. Any dents are also required to be small in order to permit insertion of the expansion mandrel and sleeve (0.740" OD) for the expansion process. TSP intersections requiring expansion must have no +Point indications of TSP ligament cracking. Limited axial cracking is permitted in the tubes to be expanded. TSP intersections requiring expansion must have bobbin coil voltages less than 2 volts for ODSCC or 3 volts for PWSCC and the indications confirmed by +Point inspection must be contained within the TSP.

The mandrel used to perform the tube expansions to lock the TSPs includes a bobbin coil probe. The probe is used to center the mandrel on the TSP and to measure the bulge diameters following the expansion process. Bobbin profilometry is used to measure the bulge sizes applying a calibration standard with prototypic expansions over the range of interest for the process. Section 6.8 provides additional details on the NDE support for the tube expansion process. If the minimum acceptable bulge size of [ ]^{a,c} is not achieved, an additional tube must be selected for expansion at the TSP elevation found to have the undersized expansions. Figures 5-37 and 5-38 identify a cluster of tube locations from which tubes may be selected for each required tube expansion.

Following the expansion process, 100% of the expanded tubes in all four SGs will be +Point inspected at the TTS. If circumferential indications are found at the TTS in the expanded tubes, the potential need to expand additional tubes will be evaluated and the results of this evaluation reported to the NRC prior to restart. This inspection would identify any previously undetected circumferential cracks that might have been opened by the expansion process.

There is no need to inspect the expanded TSP intersections for sleeve or parent tube indications during the outage the tubes are expanded. For the limited axial cracks permitted at the expanded TSP locations, the potential influence of the expansion process on the indications is acceptable as further discussed below for the South Texas NRC SER Item (b). Potentially undetected circumferential cracks at the TSP intersections would be located within the TSP or at the edge of the TSP as found for all circumferential cracks at dented TSPs in the DCPP SGs and other domestic SGs with dented TSPs. Even if the parent tube is severed within or at the edges of a TSP, there would be no meaningful influence on the effectiveness (stiffness of the tube expansion). Under another Westinghouse program, pull force tests were performed to measure the tube to sleeve joint stiffness for hydraulic expansions of a single bulge nearly identical to the TSP expansions with the parent tube severed below the expansion. The tube OD bulges tested for these expansions used low yield strength tubing (conservative compared to increased stiffness with higher yield strength as demonstrated for a few sample expansions) with bulge sizes ranging from [ ]^{a,c,e}, which included bulge sizes less than the DCPP TSP expansions. For the minimum DCPP bulge size of [ ]^{a,c,e}, the mean regression fit to the test data resulted in a joint stiffness of about [ ]^{a,c,e}, which is substantially higher than the [ ]^{a,c,e} used for the DCPP TSP displacement analyses. Since the sleeve to parent tube bulged joint stiffness is much higher than the parent tube to TSP joint stiffness, it can be concluded that severing of the parent tube within the TSP or at the edges of the TSP would not meaningfully reduce the TSP joint stiffness and

would have no affect on TSP displacements. For the bulge sizes at the TSP intersections, the expansions would not tear the sleeve or undegraded parent tube. Consequently, there is no need to inspect the sleeve or parent tube for axial or circumferential cracks following the tube expansion process.

If the SGS are not to be replaced at the outage following two complete cycles of operation after implementation of the locked TSP ARC, 20% of the TTS and expanded TSP locations in all four SGs will be +Point inspected. If circumferential indications greater than 100° are found at the TTS or above/below the tube support plate edges at TSP locations, the inspection will be expanded to 100% in any SG for which a circumferential indication >100° is found. The 100° crack size is less than the predicted near throughwall length for undetected circumferential indications left in the expanded tubes after two cycles of operation assuming active tube growth rates. If circumferential indications at the TTS or expanded TSP intersections <100° are left in the expanded tubes following the inspection after two cycles of operation, the locations with circumferential indications will be inspected at the next outage if the SGs are not replaced at this outage. If circumferential indications are found in the expanded tubes, the potential need for corrective actions will be evaluated and the results of this evaluation reported to the NRC prior to restart.

The design target range of [ ]^{a,c,e} for the expansion process leads to a low likelihood of circumferential cracking at the bulges as described in Section 6.10. As discussed above the parent tube can sever within the TSP with no influence on TSP displacements since the joint stiffness for movement of the bulged tube relative to the sleeve is much greater than the joint stiffness for movement of the TSP relative to the bulged tube. Axial cracking at the expansions also has a low likelihood of occurrence, but even if they do occur, they would not significantly affect the bulge stiffness. TSP displacements must compress or attempt to flatten the bulge for which the required forces would not be significantly influenced by an axial crack in the bulge. As described in Section 6-10, circumferential cracks at the top of the tubesheet of sufficient size to significantly influence the tube stiffness or sever the tube also have a very low likelihood of occurrence.

As documented in Reference 4, the dented and packed crevices in the DCPP SGs result in tube to TSP contact forces sufficient to prevent TSP displacement in a SLB event with substantial margins on the breakaway forces. The mechanical locking from expansions at selected TSP intersections provides TSP locking capability in addition to the TSP crevice conditions for limiting displacements in a SLB event. The numbers of tubes and expansions are selected to limit SLB TSP displacements to less than 0.15 inches assuming no additional constraint against displacement from the dented and packed crevices, i.e., the locking analysis assumes open crevices. Clearly, the crevice conditions provide sufficient margin against TSP displacements to compensate for an assumed loss of one or a few expanded tubes due to postulated separation due to circumferential cracking. The NRC review of Reference 4 (WCAP-14707) given in Reference 7 provides the following conclusion: "The primary technical concern with the approach outlined in the subject report is the relatively small database for tube-to-TSP displacement forces and leak rates under accident conditions. The staff believes this difficulty can be overcome with additional plant-specific tube pulls and laboratory leak rate testing as well as through the application of conservative margins." All leak rate analyses supporting this ARC assume open crevices with no credit for reduced leakage with packed crevices. Thus, the noted concern for accident leak rates is not applicable for this application. The application of locked TSPs for this ARC clearly provides conservative margins beyond the crevice condition locking, and thus addresses the NRC concern for margins. It would appear that the "principal technical concern" reduces to the small database for tube-to-

TSP displacement forces. Since the WCAP was issued, breakaway forces for pulled tubes cut at the TTS have been obtained from two DCPP-2 tubes including R44C45 at 2R11 and two tubes from Plant Z-2 as presented at the April 15 PG&E/NRC meeting. These breakaway force measurement results (≥ 500 lbs/intersection) are much higher than the 60 lbs required to prevent TSP displacements for a large SLB (31 lbs for a small break). In addition, a tube will be pulled at 1R12 following chemical cleaning and can be also expected to substantially exceed the force required to prevent SLB TSP displacements. These pulled tube results provide eight domestic pulled tube measurements (only three reported in WCAP-14707) for TSP intersections without reported dents. Although a limited statistical basis for breakaway forces, the pulled tube breakaway force measurements at non-dented intersections provide a high confidence level that the TSPs at DCPP would not be displaced in a SLB event when taken together with general knowledge of the behavior of dented TSP intersections. For the mechanically locked TSP ARC of this report, consideration of the locking from crevice conditions is applied only to reduce the need for more conservative expanded tube inspection and hydraulic load requirements than included in this report.

Based on the low likelihood of circumferential cracking at the expansion joints, that a severed parent tube within the TSP would have no significant effect on displacements, that axial cracks at the expansions would not significantly influence the expanded joint stiffness (discussed below) and the large margins against TSP displacement provided by the crevice conditions at DCPP, there is no need to inspect the expanded tubes at less than two cycle intervals. There may be two or three operating cycles for the DCPP SGs prior to replacement. The post-expansion +Point inspection of the expanded tubes further reduces the need for expanded tube inspections at less than two cycle intervals.

Although the likelihood of severing an expanded tube at the TTS is negligible, a stabilizer will be installed at the TTS of the expanded tubes to provide in-depth assurance that no new failure mode (damage to adjacent tubes from a severed tube) is introduced by the expansions. The TTS stabilizer may be a sleeve or cable. The sleeve incorporated in the TSP expansions also functions as a stabilizer in the low likelihood event of a severed parent tube at an expanded tube location.

South Texas NRC SER Item (b) Relating to Integrity and Inspection of Expanded Tubes

The safety evaluation (Reference 2) for the South Texas-2 locked TSP ARC reflects a concern (item b of Section 10.0) that for long term implementation of the increased voltage ARC, it would be necessary to develop an inspection plan for the expanded tubes to ensure their long term structural integrity. The associated SER discussion for this concern notes that expanding tubes at TSP intersections with a one volt (3/4" tubing) bobbin indication is acceptable for one cycle of operation, but that the expanded tube should be inspected regularly for long term application of the expanded tube with a one volt bobbin indication.

The bases for permitting expansion at an intersection with a small axial flaw is that the flaw would not be deep enough to tear at the ends within the TSP during the expansion process due to the ductility of the material and that the tear would have to extend into the bulges above and below the TSP to influence the expansion process. This point is noted in the SER with the conclusion that a small flaw in a tube within the TSP should not affect the expansion process at the bulges above and below the TSP and would not affect the load carrying capacity of the tube. This implies, although not explicitly stated, that the long term concern reflected in the SER is that a small axial crack could grow over more than one cycle to a

point that would affect the load carrying capacity of the tube (e.g., reduce the stiffness of the joint and thus permit increased TSP displacement).

As noted above, the TSP intersections to be expanded that have bobbin indications or are dented must be inspected prior to expanding the tubes to confirm the absence of circumferential cracks or axial cracks extending outside the TSP. The potential for axial cracks extending outside the TSP applies primarily to PWSCC indications at the less than five volt dents permitted at tube expansion intersections. The indications must also have bobbin coil voltages less than 2 volts for ODSCC or 3 volts for PWSCC to provide a high likelihood that the indications are not throughwall. Consequently, the potential for an existing crack to be extended by the expansion process to a throughwall indication outside the TSP is negligible. Growth of the crack to outside the TSP over subsequent operating cycles is also unlikely. In a SLB event, the hydraulic loads must push the TSP up the slope of the bulge at the TSP edges such as to compress the bulge. Consequently, even if the crack grew to be throughwall at the bulge location, there would be a negligible effect on the stiffness of the expansion joint.

10.6 SLB ANALYSIS REQUIREMENTS

Per GL 95-05, SLB leak rate and tube burst probability analyses for condition monitoring are required prior to returning to power and the results are to be included in a report to the NRC within 90 days of restart. SLB leak rates and burst probabilities obtained for the actual voltage distribution measured at the inspection (condition monitoring) are required prior to restart and the projected next EOC values (operational assessment) are required in the 90 day report. If allowable limits on leak rates and burst probability are exceeded for either the condition monitoring or operational assessment, the results are to be reported to the NRC and an assessment of the significance of the results is to be performed. For the limited displacement ARC, SLB leak rates must be calculated for the hot leg TSP indications at TSPs 1-4, and both leak rates and tube burst probability are to be calculated for cold leg TSP indications and hot leg indications at TSPs 5-7. The required SLB analyses are discussed below.

10.6.1 SLB Tube Burst Probability Analysis Requirements

The free span tube burst probability must be calculated for hot leg TSPs 5-7 and cold leg TSP indications per the requirements of GL 95-05. Analysis methods for the GL 95-05 analyses are described in Reference 2. Per NRC GL 95-05, the burst probability limit for reporting results to the NRC is $>10^{-2}$. The contribution from indications at hot leg TSPs 1-4 is negligible for both indications exposed by the limited TSP displacements and for axial tensile tearing as shown in Section 8.6. The contribution from TSPs 1-4 would be less than 10^{-5} even under the extreme assumption of exposed throughwall cracks at the design limit for every TSP intersection. Consequently, the TSPs 1-4 contribution to axial burst probability can be ignored in the burst probability analyses. Although the contribution from axial tensile tearing is expected to be insignificant, the burst probability methods of Section 8 have been revised to include this calculation as described below.

South Texas NRC SER Item (c) Related to Combining Probability of Axial Burst and Axial Tensile Failures

The safety evaluation (Reference 2) for the South Texas-2 locked TSP ARC reflects a NRC recommendation (item c of Section 10.0) that future submittals for the locked TSP burst model should address a means of combining the axial burst and the axial tensile failure conditional probabilities.

The axial burst probability of potential significance results from hot leg TSPs 5-7 and all cold leg indications. The potential for axial tensile rupture may occur when the ODSCC indications have substantial circumferential involvement from cellular corrosion, which includes oblique cracks that potentially reduce the axial tensile strength of the tube. To date, 5 tubes have been removed from DCPP Units 1 and 2 for destructive examination and ARC applications. None of these tubes have had significant cellular corrosion including the recent 5.09 and 21.5 volt indications removed at 2R11. Consequently, tensile tearing tests have not been performed for the DCPP pulled tubes. The data for the ARC correlation of axial rupture force versus bobbin voltage (latest data in Addendum 2 of ARC database) were obtained using only indications with large cellular patches. The use of tensile tearing for indications without cellular corrosion would distort the correlation by including results that are essentially independent of bobbin voltage. Application of the tensile tearing correlation to obtain the associated rupture probability implicitly assumes that all bobbin voltage indications have cellular corrosion.

Although cellular corrosion does not appear to be present to a significant extent at DCPP, the burst probability for axial tensile tearing will be calculated for TSPs 1-4 for which the higher ARC repair limit is applied. Including this analysis assumes cellular corrosion will occur at DCPP with the higher voltage repair limit. Upon implementation of the limited TSP displacement ARC at DCPP, the axial tensile tearing rupture probability for TSPs 1-4 will be combined with the freespan burst probability for axial ODSCC indications at hot leg TSPs 5-7 and all cold leg indications as described in Section 8. This revision to the burst probability analysis methods will be implemented to resolve this NRC SER item.

10.6.2 SLB Leakage Analysis Requirements

The SLB leak rates for hot leg TSP indications at TSPs 1-4 are to be calculated as free span leakage using the GL 95-05 leak rate methods, if the sampled indication is not found to be a potentially overpressurized indication. For indications that are found to be potentially overpressurized indications, the bounding leak rate for indications restricted from burst (IRB) is applied. Free span leak rate methods must be applied for the cold leg TSP indications and hot leg indications at plates 5 through 7. The free span leak rates are based on the EPRI methodology for correlating probability of leakage and SLB leak rates with bobbin voltage. Acceptable methods (References 3 and 6) are modified in Section 8 to resolve a NRC SER item as described below.

As noted above, in addition to the free span leak rates, the leak rate analyses for hot leg TSP indications at plates 1-4 include the potential leakage from overpressurized indications within the TSP. Under the assumption of open tube to TSP crevices, an indication predicted to burst as a free span indication could have the crack open up significantly more than the crack opening that occurred in the free span SLB leak rate measurements for a similar voltage indication. The probability that a crack will open up to the limits of the tube to TSP gap is equivalent to the probability of free span burst. The analysis methods for the

overpressurized condition are given in Section 8.9. The overpressurized condition leak rates are obtained from the probability of free span burst and a bounding leak rate (IRB bounding leak rate) for the overpressurized condition.

South Texas NRC SER Item (f) Related to Combining Leakage from Free Span and Locked TSP Models

The safety evaluation (Reference 2) for the South Texas-2 locked TSP ARC reflects a concern (item f of Section 10.0) regarding methods for combining the conditional probability of leakage estimates from the free span model and locked TSP model. For the South Texas-2 ARC, the 95% probability leak rates from the IRB model at locked TSPs was added to the 95% probability leak rates from the free span model. The SER notes that the NRC staff was evaluating the need for a long term approach that combines the leakage estimates from the freespan model and locked TSP model, including a contribution from ODSCC indications that burst under the free span model, prior to ordering the total leakage values to define the 95% probability leakage.

The leakage analysis methods to be used by DCPP for the locked TSP ARC are described in Section 8.10. The methods combine the leak rates for the locked hot leg TSPs 1-4 with the freespan leak rates for hot leg TSPs 5-7 and all cold leg TSPs to define the 95% confidence SLB leak rate. The locked TSP leak rates are calculated including the assignment of the bounding IRB leak rate for Monte Carlo samples predicted to burst at SLB conditions, and an assignment of a large leak rate to indications predicted to have an axial tensile rupture. For the free span model, the GL 95-05 methods, as implemented per the guidelines of Reference 5, are modified to assign a large leak rate to Monte Carlo samples predicted to burst at SLB conditions. The assigned large leak rate of 100 gpm is similar to that associated with burst of a free span axial indication. This change is made to resolve the above noted SER item although the results of applying the methods change is expected to have an insignificant effect on the total leak rate. The assignment of a large leak rate to a Monte Carlo burst is only significant when the predicted free span burst probability is notably higher than the NRC reporting limit of 10^{-2} such as approaching $5x10^{-2}$ so as to influence the upper 5% of the leak rate distribution. While this condition may occur for the locked TSPs with a higher voltage repair limit, burst probabilities near 10^{-2} are not expected for indications subject to the two volt ARC repair limit.

Upon implementation of the limited TSP displacement ARC at DCPP, the modified SLB leak rate analysis methods of Section 8 will be implemented to resolve this NRC SER item.

10.7 SUMMARY OF DCPP ARC AT TSPS

This section provides a summary of the alternate tube repair criteria (ARC), as developed above, to be applied at DCPP tube support plates, including plates 1-4 with limited SLB displacement. This summary includes the tube repair limits, general inspection requirements at inspections following TSP locking, SLB leak rate and tube burst probability analysis requirements. SLB analysis methodology is summarized in Section 10.6 and described in detail in Section 8. The tube expansions required to support the ARC are defined in Table 5-20.

DCPP Tube Repair Limits

- For hot leg TSP indications at plates 1-4, axial ODSCC bobbin indications > 4.0 volts shall be repaired independent of RPC confirmation.

- The tube repair requirements for the NRC licensed 2.0 volt repair limit at DCPP per GL 95-05 continue to apply for implementation of the limited TSP displacement ARC with the modification that the 2.0 volt repair limit applies only to axial ODSCC indications at hot leg plates 5-7 and at cold leg TSP intersections.

If the projected operational assessment SLB leak rates exceed the DCPP allowable limits, bobbin indications ≤ 4 volts may be preventively repaired to obtain leak rates below the allowable limit.

General Inspection Requirements

The tube inspection requirements for the NRC licensed 2.0 volt repair limit at DCPP per GL 95-05 continue to apply for implementation of the limited TSP displacement ARC with the following modifications:

- All bobbin flaw indications exceeding 4.0 volts for hot leg TSP intersections at plates 1-4 shall be RPC (or equivalent probe) inspected. In addition, a minimum of 100 hot leg TSP intersections at plates 1-4 with bobbin voltages less than or equal to 4.0 volts shall be RPC inspected. The RPC data shall be evaluated to confirm responses typical of ODSCC within the confines of the TSP.

- If one or more ODSCC indications at TSP intersections are found in the NDE inspection to extend beyond the edge of the TSP, the indications shall be evaluated for significance to safety and risk and the results reported to the NRC prior to restart.

The minimum eddy current inspection of TSP ligaments at each scheduled outage shall include 100% bobbin coil with +Point confirmation for new bobbin calls and a 20% +Point inspection of TSP ligament indications previously confirmed by +Point inspections. The inspection of active tubes adjacent to expanded tubes shall include a bobbin coil examination for cracked TSP ligaments at expanded tube TSP intersections. If a cracked ligament indication is found and confirmed by +Point inspection as a cracked or missing ligament section, the potential implications on TSP displacements shall be assessed and documented in the ODSCC 90 day report. However, a significant increase in ligament cracking at the expanded TSP intersections, such as more than two indications at the same TSP elevation, shall be evaluated for implications on TSP displacement and this evaluation reported to the NRC prior to restart.

Expanded Tube Inspection Requirements

Following the expansion process, 100% of the expanded tubes in all four SGs shall be +Point inspected at the TTS. If circumferential indications are found at the TTS in the expanded tubes, the potential need to expand additional tubes will be evaluated and the results of this evaluation reported to the NRC prior to restart.

If the SGS are not to be replaced at the outage following two complete cycles of operation after implementation of the locked TSP ARC, 20% of the TTS and expanded TSP locations in all four SGs will be +Point inspected. If circumferential indications greater than 100° are found at the TTS or above/below the tube support plate edges at TSP locations, the inspection will be expanded to 100% in any SG for which a circumferential indication > 100° is found. The 100° crack size is less than the predicted near throughwall length for undetected circumferential indications left in the expanded tubes after two cycles of operation. If circumferential indications are found in the expanded tubes, the potential need for corrective actions will be evaluated and the results of this evaluation reported to the NRC prior to restart.

The bases supporting the above inspection plan are provided in Section 10.5.3.

SLB Leak Rate and Tube Burst Probability Analyses

The SLB leakage and burst requirements for the NRC licensed 2.0 volt repair limit at DCPP per GL 95-05 continue to apply for implementation of the limited TSP displacement ARC with the following modifications:

- SLB leak rates based on combining the locked TSP and free span model results, as described in Section 10.6.2, shall be added to the SLB leak rates from all other DCPP ARCs and shall be less than the DCPP allowable SLB leakage limits for constrained indications.

- The SLB tube burst probability for cold leg TSP intersections and hot leg intersections at plates 5-7 when combined with the tube rupture probability for TSPs 1-4 shall be compared to the reporting value of 10^{-2}.

Conservatisms for the DCPP Limited TSP Displacement ARC

The DCPP ARC has been very conservatively developed as summarized in Table 10-3. In particular, mechanical locking of the TSPs is a backup to locking provided by dented and packed TSPs. The packed crevices are adequate to prevent tube burst and limit leakage to negligible values as described in Reference 4. Since the IRB bounding leak rate was developed for open crevices, the IRB leak rate of 5 gpm is extremely conservative.

10.8 REFERENCES

1. NRC GL 95-05, "Voltage Based Repair Criteria for Westinghouse Steam Generator Tubes Affected by Outside Diameter Stress Corrosion Cracking", August 1995.

2. Letter Mohan C. Thadani, NRC, to William T. Cottle, "STP Nuclear Operating Company; South Texas Project (STP) Unit 2 – Issuance of Amendment Revising the Technical Specifications to Implement 3-volt Alternate Repair Criteria for Steam Generator Tube Repair (TAC No. MA8271)", March 8, 2001.

3. WCAP-14277; "SLB Leak Rate and Tube Burst Probability Analysis Methods for ODSCC at TSP Intersections (Revision 1)", December 1996.

4. WCAP-14707, "Model 51 Steam Generator Limited Tube Support Plate Displacement Analysis for Dented or Packed Tube to Tube Support Plate Crevices", August 1996.

5. TR-107625, "SG Indications Restricted from Burst (IRB) Leak Test Report", EPRI Final Report, September 1998.

6. NP-7480-L, Addendum 5, 2002 Database Update, "Steam Generator Tubing Outside Diameter Stress Corrosion Cracking at Tube Support Plates Database for Alternate Repair Limits", EPRI Report, October 2002.

7. Letter from Steven D. Bloom, NRC to Gregory M. Rueger, PG&E, "NRC Staff Review of WCAP-14707/14708, Model 51 Steam Generator Limited Tube Support Plate Displacement Analysis for Dented or Packed Tube-to-Tube Support Plate Crevices – Diablo Canyon Power Plant, Units 1 and 2 (TAC Nos. M99011 and M99012)", January 18, 2000.

Table 10-1
Allowable Model 51 SLB TSP Displacements for
Acceptable SLB Tube Burst Probability

No. Hot Leg TSP Intersections	Assumed SLB TSP Displacement	Burst Probability Per Indication	Total SLB Tube Burst Probability[1]
Uniform TSP Displacements at All TSPs and Tube Locations			
13,552	0.45"	7.4×10^{-8}	1.0×10^{-3}
13,552	0.42"	7.4×10^{-9}	1.0×10^{-4}
13,552	0.40"	7.4×10^{-10}	1.0×10^{-5}
13,552	0.15" [2]	$< 10^{-15}$	$< 10^{-10}$
1	0.59"	1.0×10^{-3}	
1	0.64"	1.0×10^{-2}	

Notes:

1. Burst probability estimates very conservatively postulate that all hot leg TSPs 1-4 intersections have a throughwall crack length equal to, or greater than, the SLB TSP displacement. The tip of the throughwall crack length is assumed to be at the edge of the TSP.
2. Maximum limiting TSP displacement by design.

Table 10-2
Summary Requirements for TSP Limited Displacement ARC Application

Requirement	Rationale
TSP displacements and tube expansion process design loads shall be based on a factor of 1.5 margin on RELAP5 hydraulic loads.	Provides a conservative margin against load uncertainties based on RELAP5 analyses.
Tube expansions at selected TSP intersections under the assumption of open tube to TSP crevices to "lock" the TSPs and limit displacements at TSPs 1-4 intersections.	Provides defense in depth to limit TSP displacements since dented and packed tube to TSP crevices without expansions have been shown to prevent SLB TSP displacements in WCAP-14707 (Reference 4).
The maximum TSP displacement under a postulated SLB event shall be: 1. Less than 0.40 inch to limit tube burst probability, and 2. Less than 0.21 inch for application of IRB leak test bounding leak rate results	1. Results in a tube burst probability $<10^{-5}$, even under the extremely conservative assumption of throughwall cracks at all hot leg TSPs 1-4 intersections. 2. Justifies use of the bounding IRB leak rate test results that include offsets up to 0.21 inches.
As a design goal for implementing the locked TSP ARC, the maximum TSP displacement under a postulated SLB event shall be less than 0.15 inch.	1. Provides a conservative margin for application of IRB bounding leak rate test results. 2. Provides a tube burst probability of $<10^{-10}$, even under the extremely conservative assumption of throughwall cracks at all hot leg TSPs 1-4 intersections.

Table 10-3
Summary of Conservatism in the Application of the Limited TSP Displacement ARC

Issue	Conservatism Identified
Tube Expansions at Selected TSP Intersections.	Dented and packed tube to TSP crevices without expansions have been shown to prevent SLB TSP displacements in WCAP-14707 (Reference 4). The DCPP crevice conditions would prevent TSP displacement even if only about 1% (percent of tubes expanded) of the TSPs have the expected contact forces.
Hydraulic Loads for TSP Displacements	For displacement and stress analyses, RELAP5 hydraulic loads on TSPs were increased by factor of 1.5 to envelope modeling uncertainties.
TSP Displacements	TSP displacements are limited by design to 0.15" compared to the acceptable 0.40" required to limit tube burst probability to 10^{-5}, and compared to the 0.21" required for application of the IRB bounding leak rate.
Burst Probability Estimate	1. All hot leg TSPs 1-4 are assumed to have a throughwall indication equal to, or greater than, the maximum TSP displacement, with the tip of the indication located at the edge of the TSP. 2. The displacement of each TSP is assumed to be the maximum displacement for that TSP for all tube intersections.
SLB Leakage	1. SLB leakage is based on a bounding IRB leak rate for indications predicted to burst under free span conditions and free span leakage for indications not predicted to burst under free span conditions. 2. IRB bounding leak rate very conservatively assumes open crevice conditions with maximum tube to TSP hole clearance even though the DCPP SGs have dented and packed crevices that would prevent crack opening inside the TSP and limit leakage to negligible levels (Reference 4). Also demonstrated by in situ testing of throughwall indications at the 2R11 outage.
Tube Repair Limit	Although axial tensile rupture data support a much higher repair limit, the tube repair limit is very conservatively set at 4 volts.